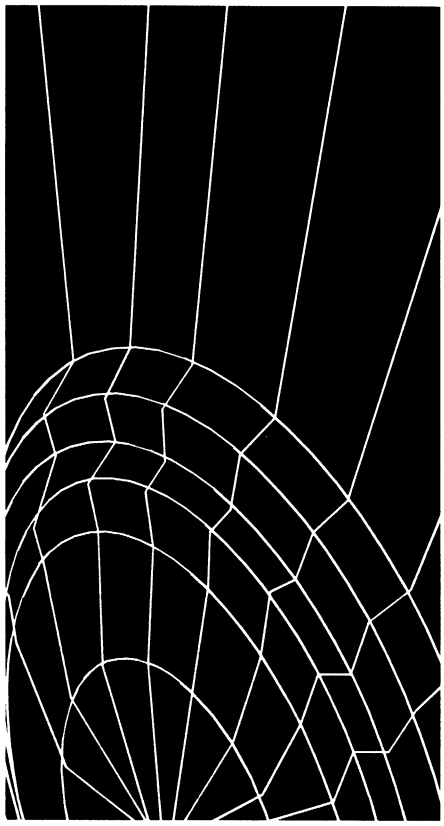

MARC

Analysis
Research
Corporation

MARC

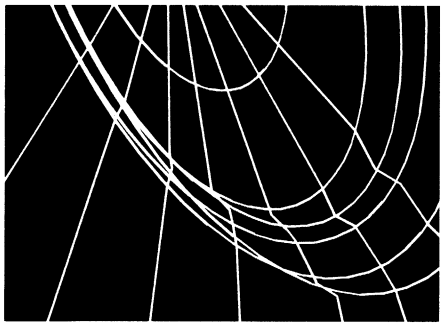

Volume E

Demonstration Problems

Version K7

MARC Analysis Research Corporation
260 Sheridan Avenue, Suite 309
Palo Alto, CA 94306 USA

Phone: (650) 329-6800
FAX: (650) 323-5892

Document Title: **MARC Volume E: Demonstration Problems, Part II, Version K7**
Part Number: RF-3018-07.II
Revision Date: June, 1998

Proprietary Notice

Restricted Rights Notice

Trademarks

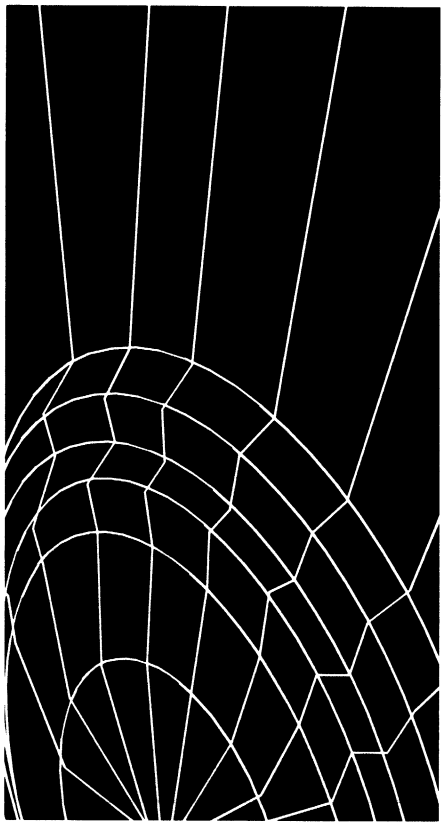

MARC

Analysis
Research
Corporation

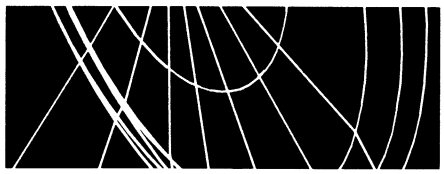

Volume E

Demonstration Problems

Version K7

Part II

- Plasticity and Creep
- Large Displacement

Part II

Volume E: Demonstration Problems

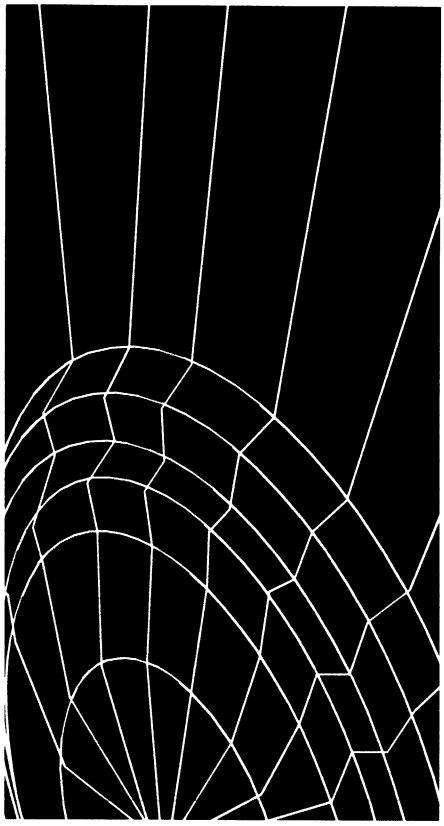

MARC

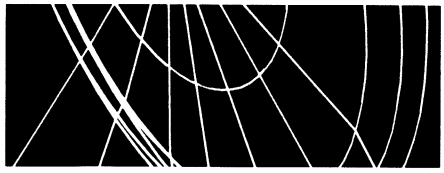

Volume E

Demonstration Problems

Version K7

MARC
Analysis
Research
Corporation

Chapter 3
Plasticity and Creep

3 Plasticity And Creep Contents

3 Plasticity and Creep List of Figures

Figure **Page**

Figure **Page**

Figure **Page**

Figure **Page**

Figure **Page**

3 Plasticity and Creep List of Tables

3 Plasticity and Creep

MARC contains an extensive material library. A discussion on the use of these capabilities is found in *Volume A: User Information*. In this chapter, material nonlinearity often exhibited in metals is demonstrated. Material nonlinearity associated with rubber or polymer materials can be found in Chapter 7. The capabilities demonstrated here can be summarized as:

Variable load paths

- Proportional loads
- Nonproportional loads

Choice of yield functions

- von Mises
- Drucker-Prager, Mohr-Coulomb
- Gurson
- Shima

Strain magnitude

- Infinitesimal plasticity
- Finite strain plasticity

Strain hardening

- Limit Analysis
- Isotropic hardening
- Kinematic hardening

Rate effects

- Deviatoric creep
- Volumetric swelling
- ORNL

Compiled in this chapter are a number of solved problems. Table 3-1 summarizes the element type and options used in these demonstration problems.

Table 3-1 Nonlinear Material Demonstration Problems

Problem Number	Element Type(s)	Parameters	Model Definition	History Definition	User Subroutines	Problem Description
3.1	4	TIE SCALE SHELL TRAN SHELL SECT	WORK HARD CONTROL FXORD SHELL TRAN TYING, 2, 6, & 100	AUTO LOAD PROPORTIONAL	—	Combines tension and torsion of a thin-walled cylinder
3.2	67	SCALE	TYING, 1 & 3 WORK HARD CONTROL	AUTO LOAD PROPORTIONAL	—	Combines tension and torsion of a thick-walled cylinder.
3.3	11 115	SCALE	MESH2D CONTROL	AUTO LOAD PROPORTIONAL	IMPD	Limit load analysis of bar.
3.4	16	SCALE SHELL SECT	WORK HARD CONTROL	AUTO LOAD PROPORTIONAL	UFORMS	Bending of prismatic beam.
3.5	15	THERMAL SHELL SECT	UFXORD TRANSFORMATION THERMAL LOAD WORK HARD TEMPERATURE EFFECT CONTROL INITIAL STATE	AUTO THERM CHANGE STATE	WKSLP UFXORD	Hemispherical shell under thermal expansion.
3.6	50	SCALE SHELL SECT	DEFINE CONTROL	AUTO LOAD PROPORTIONAL	ANPLAS	Bending of square plate, simple supported, pressure load.
3.7	10	SCALE	CONTROL RESTART	AUTO LOAD PROPORTIONAL	—	Elastic-plastic analysis of a thick cylinder
3.8	27	SCALE J-INT	J INTEGRAL WORK HARD CONTROL	PROPORTIONAL	WKSLP	Double edge notch specimen under axial tension.
3.9	11	SCALE	OPTIMIZE, 2 CONTROL	AUTO LOAD PROPORTIONAL	—	Mises Mohr-Coulomb example.
3.10	26	SCALE	WORK HARD CONTROL OPTIMIZE, 2	AUTO LOAD PROPORTIONAL	—	Plate with hole.
3.11	28	SCALE THERMAL	TYING, 1 WORK HARD CONTROL RESTART	AUTO THERM CHANGE STATE PROPORTIONAL	—	Axisymmetric bar in combined tension and thermal expansion.

Table 3-1 Nonlinear Material Demonstration Problems (Continued)

Problem Number	Element Type(s)	Parameters	Model Definition	History Definition	User Subroutines	Problem Description
3.12	10	CREEP SCALE	CREEP CONTROL	AUTO CREEP	CRPLAW	Creep ring.
3.13	25	THERMAL STATE VARS CREEP	THERMAL LOADS SPRINGS CREEP CONTROL	AUTO CREEP	VSWELL CREDE	Beam under axial thermal gradient.
3.14	16	CREEP SHELL SECT	CONTROL CREEP	DISP CHANGE AUTO CREEP	—	Creep bending of prismatic beam.
3.15	26	POST CREEP ACCUM BUC	OPTIMIZE, 2 CONTROL CREEP	AUTO CREEP CREEP INCREMEN T EXTRAPOLATE	—	Creep of a square plate with central hole.
3.16	15	LARGE DISP SHELL SECT BUCKLE	UFXORD TRANSFORMATION WORK HARD CONTROL	AUTO LOAD PROPORTIONAL BUCKLE	UFXORD	Plastic buckling of externally pressurized hemispherical dome.
3.17	72	SHELL SECT LARGE DISP	UFXORD	AUTO LOAD PROPORTIONAL	UFXORD	Shell roof with nonlinearities.
3.18	15 12	LARGE DISP UPDATE FINITE SHELL SECT MATERIAL	WORK HARD TYING, 102 CONTROL GAP DATA	AUTO LOAD DISP CHANGE	—	Olson cup test.
3.19	10 116	LARGE DISP UPDATE FINITE	WORK HARD CONTROL UDUMP	AUTO LOAD PROPORTIONAL	IMPD	Compression of an axisymmetric member, height reduction 20%.
3.20	16	LARGE DISP FOLLOW FOR SHELL TRAN UPDATE FINITE	CONN GENER WORK HARD CONTROL NODE FILL SHELL TRAN	AUTO LOAD PROPORTIONAL	—	Bending of beam into semicircle.
3.21	10 116	UPDATE LARGE DISP FINITE	WORK HARD UDUMP	AUTO LOAD PROPORTIONAL	IMPD	Necking of a cylindrical bar.
3.22	42 28	ALIAS HEAT CREEP THERMAL	INITIAL TEMP CONTROL FILMS TYING, 1 CREEP INITIAL STATE	TRANSIENT AUTO THERM CHANGE STATE AUTO CREEP	FILM CRPLAW	Combined thermal, elastic-plastic, and creep analysis.

Table 3-1 Nonlinear Material Demonstration Problems (Continued)

Problem Number	Element Type(s)	Parameters	Model Definition	History Definition	User Subroutines	Problem Description
3.23	75	SHELL SECT LARGE DISP PROCESSOR	POST CONTROL	AUTO INCREMENT	UFXORD	Analysis of a shell roof with material and geometric nonlinearity. Demonstrate adaptive load control.
3.24	41 26	HEAT CREEP	INITIAL TEMP FIXED TEMP FILMS INITIAL STATE CREEP	TRANSIENT AUTO THERM CREEP CHANGE STATE	CRPLAW	Uncoupled thermal creep stress analysis of a pressure vessel.
3.25	11	LARGE DISP UPDATE FOLLOW FOR	POWDER RELATIVE DENSITY DENSITY EFFECTS	TIME STEP AUTO LOAD	—	Hot isostatic pressing of a can demonstrates powder model.
3.26	28	LARGE DISP UPDATE FOLLOW FOR COUPLE	DEFINE POWDER WORK HARD RELATIVE DENSITY TEMP EFFECTS DENSITY EFFECTS FIXED TEMP FORCDT	TRANSIENT	FORCDT	Hot isostatic pressing coupled analysis.
3.27	54	UPDATE FINITE LARGE DISP	DEFINE UFXORD WORK HARD DAMAGE	DISP CHANGE AUTO LOAD	UFXORD	Shear band development, Gurson damage model.
3.28	55	UPDATE FINITE LARGE DISP	DEFINE WORK HARD DAMAGE	DISP CHANGE AUTO LOAD	—	Notched Specimen, Gurson damage model.
3.29	10	CREEP	CREEP	AUTO CREEP	—	Creep ring – implicit procedure.
3.30	18 75	R-P FLOW ISTRESS	CONTACT WORK HARD	AUTO LOAD MOTION CHANGE	WKSLP UINSTR	Deep drawing by a spherical punch.
3.31	11	LARGE DISP UPDATE	CONTACT CONTACT TABLE	AUTO LOAD DISP CHANGE DIST LOADS	—	Formation of geological strata.
3.32	11 18 75	R-P FLOW FOLLOW FOR	CONTACT	AUTO LOAD	UINSTR URPFLO PLOTV	Superplastic forming of a strip.
3.33	26	PLASTICITY	WORK HARD	AUTO STEP DISP CHANGE	—	Large strain stretching of plate with hole.

Table 3-1 Nonlinear Material Demonstration Problems (Continued)

Problem Number	Element Type(s)	Parameters	Model Definition	History Definition	User Subroutines	Problem Description
3.34	18	PLASTICITY FOLLOW FOR	WORK HARD	AUTO LOAD DIST LOADS	—	Inflation of thin cylinder.
3.35	11	PLASTICITY	WORK HARD	AUTO LOAD POINT LOAD PROPORTIONAL	—	Large bending of a cantilever beam.
3.36	7	PLASTICITY	WORK HARD	AUTO LOAD DISP CHANGE	—	Large strain stretching of plate with hole.
3.37	11	PLASTICITY	—	AUTO LOAD DISP CHANGE	—	Elastic, closed loop deformation path.
3.38	3	PLASTICITY	WORK HARD	AUTO LOAD DISP CHANGE	—	Test rotational invarience.

3.1 Combined Tension and Torsion of a Thin-walled Cylinder

A thin-walled cylinder of 1 inch radius and 10 inches length is extended 1% of its original length ($\lambda = l/l_0 = 1.01$) and then twisted so that the twist per unit original length ($\psi = \theta/l_0$) is 0.02. The material is elastic-plastic with isotropic hardening. This is the default option of MARC. This example demonstrates the ability of MARC to analyze small strain elastic-plastic problems.

Element

Element type 4, a curved quadrilateral thin shell, is used. This is a very accurate element for analyzing regular curved shells. Elements 22, 72, or 75 are easier to use.

Model

The cylinder is divided into four elements with ten nodes. As θ^1 and θ^2 must be continuous, the cylinder is modeled with a joint at angular coordinates (θ) 0 and 360 degrees. This joint is closed with use of TYING. The geometry and finite element mesh are shown in Figure 3.1-1. The nodal point input is θ, Z, and R. Since R is constant, it needs to be given only for the first nodal point. Type 4 of the FXORD option is then used to generate the complete coordinate set required by the elements in the program. One end of the cylinder is assumed fixed; the other end is under the combined action of tension and torsion.

Geometry

The cylinder thickness is 0.01 in. and is assigned in EGEOM1 of this option.

Shell Transformation

This option allows transformation of the even-numbered nodes from the global to a local direction. It facilitates the application of tension and torsion loading at the Z = 10 end in the POINT LOAD option. In particular, the degrees of freedom are transformed such that they are in the plane of the shell or normal to it at each node.

Tying

Three types of tying constraints are imposed in this example. The tying type 2 ties the second degree of freedom between node 2 and nodes 4, 6, and 8 for tensile load. The tying type 6 ties the sixth degree of freedom between node 2 and nodes 4, 6, and 8 for torsion load. The tying type 100 ties all degrees of freedom between node 1 and node 9, and between node 2 and node 10, joining together the shell boundaries at angular coordinates (θ) 0° and 360°.

Boundary Conditions

The cylinder is fixed against rotation and displacement at the Z = 0 end. Four sets of boundary conditions are necessary. Movement in the θ_2 direction is continuously zero $\left(\frac{\partial u}{\partial \theta_2} = \frac{\partial v}{\partial \theta_2} = w = 0\right)$. Also, movement tangent to the shell surface is zero $\left(\frac{\partial w}{\partial \theta_1} = 0\right)$ for nodes 1, 3, 5 and 7, $\frac{\partial u}{\partial \theta_1} = 0$ for nodes 1 and 5).

Material Properties

Values for Young's modulus, Poisson's ratio, and initial yield stress used here are 10.0×10^6 psi, 0.3 and 20,000 psi, respectively.

Work Hard

The single workhardening slope of 20.0×10^5 psi starts at zero plastic strain.

Loading

Axial tension is first applied to the second degree of freedom of node 2 in nine steps. At this increment, the maximum stress is 32,790 psi and the total plastic strain is 63.85×10^{-4}. The load is scaled to reach the yield surface in the first step. Subsequently, a torsion is applied to the sixth degree of freedom of node 2 in eight steps. The final maximum Mises' stress intensity is 51,300 psi with a plastic strain of 0.0168.

Results

The results show the cylinder is stretched axially to an extension of (λ) 1.00967 and the axial tension is 2044.4 pounds in nine steps. The cylinder is then twisted to ratio (ψ) 0.0204 and the torsion is 10 49.6 in-lb. in eight steps. The plastic strains are only 1.5% and the final stress is much less than the workhardening modulus; therefore, small strain theory is acceptable for this analysis. The PRINT CHOICE option is used to limit the printout to shell layers 2, 5, and 8.

Parameters, Options, and Subroutines Summary

Example e3x1.dat:

Parameter	Model Definition Options	History Definition Options
ELEMENTS	CONNECTIVITY	AUTO LOAD
END	CONTROL	CONTINUE
SCALE	COORDINATES	POINT LOAD
SHELL SECT	END OPTION	PROPORTIONAL INCREMENT
SIZING	FIXED DISP	
TITLE	FXORD	
	GEOMETRY	
	ISOTROPIC	
	POINT LOAD	
	PRINT CHOICE	
	SHELL TRANFORMATIONS	
	TYING	
	WORK HARD	

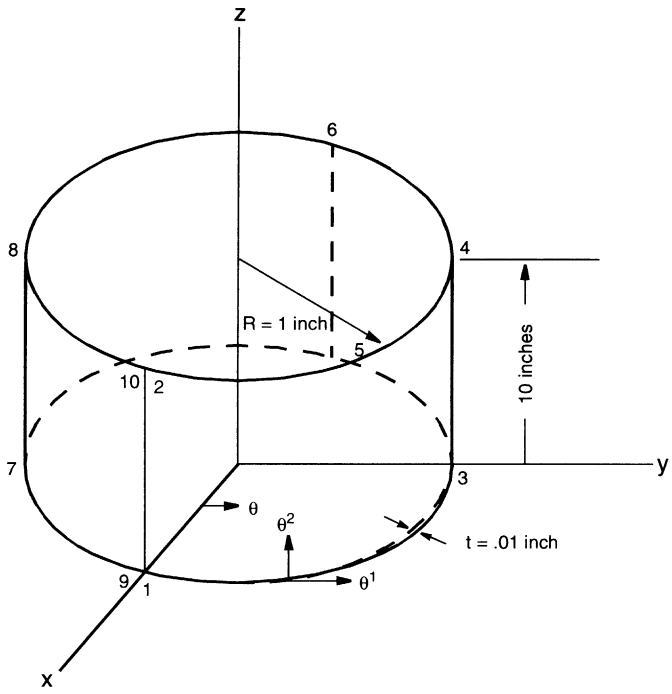

Figure 3.1-1 Thin Walled Cylinder and Mesh

3.2 Combined Tension and Torsion of a Thick-walled Cylinder

A thick-walled cylinder of 1 inch length, 2 inches outer radius, and 1 inch inner radius is extended 1% of its original length ($\lambda = l/l_o = 1.01$) and then twisted so that the twist per unit original length ($\psi = \theta/l_o$) is 1%. The material is elastic-plastic with kinematic hardening. This example demonstrates the ability of the program to analyze small strain elastic-plastic problems with kinematic hardening and change of loading conditions. The RESTART option is also demonstrated.

Element

Element type 67 is an axisymmetric 8-node distorted quadrilateral including a twist mode of deformation.

Model

The cylinder has been divided into five elements through the thickness with a total of 28 nodes. The mesh is shown in Figure 3.2-1.

Geometry

This option is not required for this element.

Tying

The displacements in Z and θ direction at the free (Z = 1) end are made the same by tying the first and third degrees of freedom of all nodes at this end to node 3. TYING types 1 and 3 are used for this purpose. This simulates a generalized plane-strain condition.

Boundary Conditions

The cylinder is fixed against rotation (θ) and displacement (Z) at the built-in end (Z = 0).

Material Properties

Values for Young's modulus, Poisson's ratio, and yield stress used here are 10.0×10^6 psi, 0.3 and 20,000 psi, respectively.

Workhard

The workhardening curve is specified with two primary workhardening slopes and breakpoints. The first workhardening slope is 2.0×10^6 psi. The second workhardening slope of 0.5×10^6 psi starts at a plastic strain of 1.0×10^{-2}. This is depicted in Figure 3.2-2.

Loading

An end load is applied axially to the cylinder through the first degree of freedom of node 3 in nine steps. Subsequently, an eight-step torsion load is applied in the third degree of freedom of node 3.

Restart

The analysis has been made in two runs using the RESTART option. The increment 0 loading is scaled to initiate yielding in the most highly stressed element. In the first run, the elastic-plastic solution due to tension is obtained in increments 0 through 8. The plastic strain is 30.64% at increment 8. Restart data is written to file 8 and is saved. The restart file is used for the second run, which starts at increment 8. In this run, torsion is applied in increments 9 through 17. The total plastic strain at increment 17 is 1.28%. The equivalent stress is 39,000 psi in this increment.

Results

The results show the cylinder is stretched axially to a strain of 0.68%, creating an axial load of 309,129 pounds. The cylinder is then twisted by an angular ratio (ψ) of 0.00779. The resultant twisting moment is 180,000 inches-pound. The displacement history is shown in Figure 3.2-3.

Parameters, Options, and Subroutines Summary

Example e3x2a.dat:

Parameter	Model Definition Options	History Definition Options
ELEMENTS	CONNECTIVITY	AUTO LOAD
END	CONTROL	CONTINUE
SCALE	COORDINATES	PROPORTIONAL INCREMENT
SIZING	END OPTION	
TITLE	FIXED DISP	
	ISOTROPIC	
	POINT LOAD	
	PRINT CHOICE	
	RESTART	
	WORK HARD	

Example e3x2b.dat:

Parameter Options	Model Definition Options	History Definition Options
ELEMENT	CONNECTIVITY	AUTO LOAD
END	CONTROL	CONTINUE
SCALE	COORDINATE	POINT LOAD
SIZING	END OPTION	PROPORTIONAL INCREMENT
TITLE	FIXED DISP	
	ISOTROPIC	
	POINT LOAD	
	PRINT CHOICE	
	RESTART	
	WORK HARD	

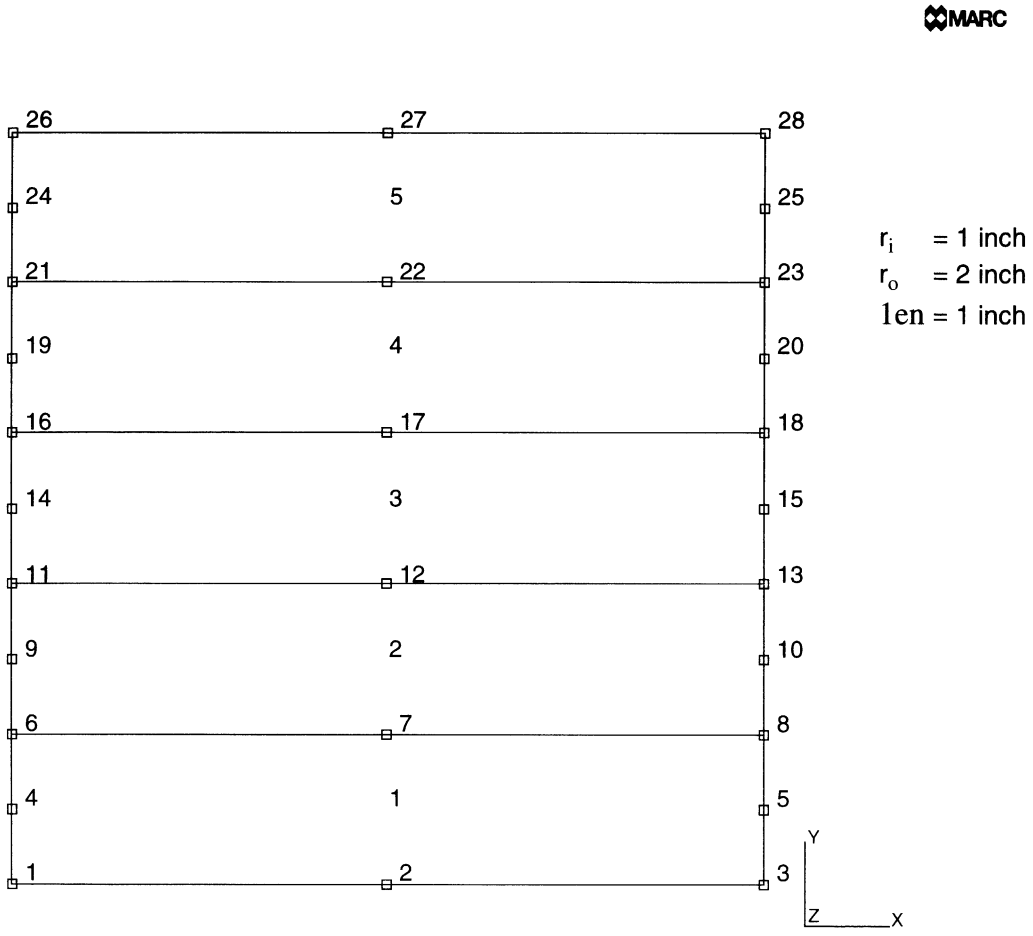

Figure 3.2-1 Thick Walled Cylinder and Mesh

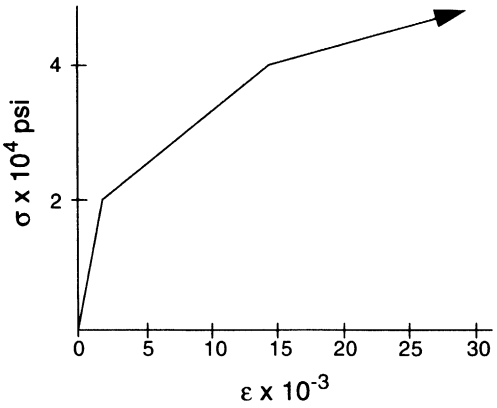

Figure 3.2-2 Stress-Strain Curve

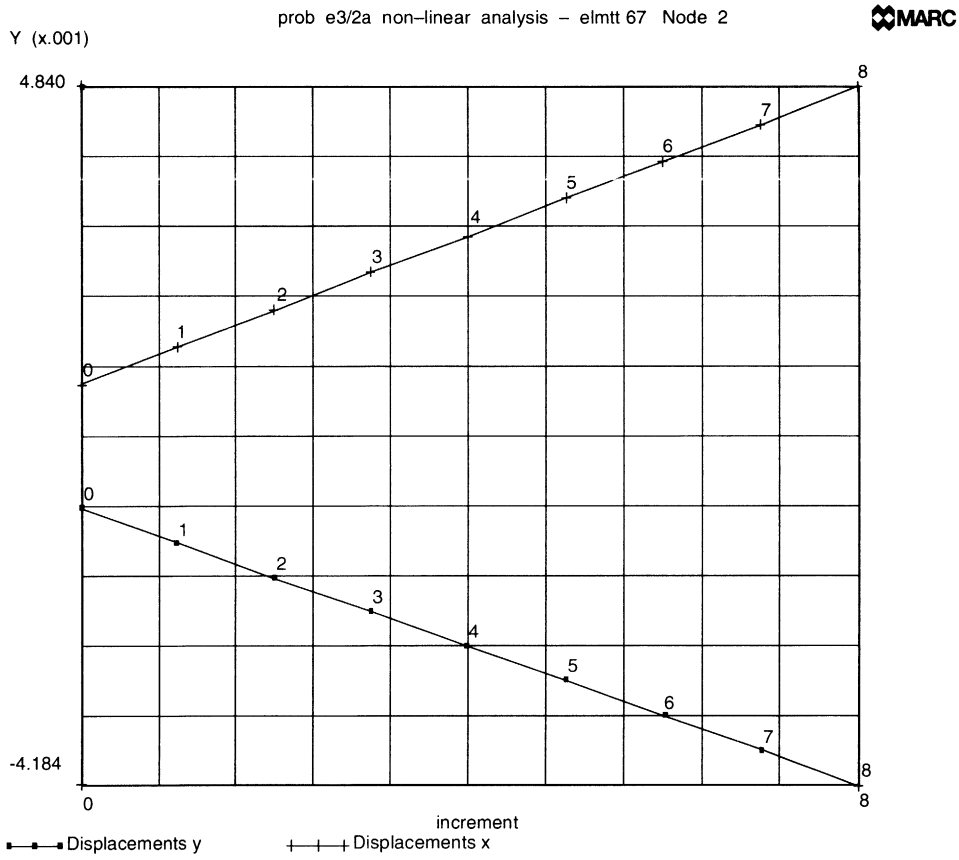

Figure 3.2-3 Displacement History at Inner Radius

3.3 Limit Load Analysis

The compression of a layer between two rigid plates is studied in this problem and compared to theoretical results.

This problem is modeled using the two techniques summarized below.

Data Set	Element Type(s)	Number of Elements	Number of Nodes
e3x3	11	24	35
e3x3b	115	24	35

Elements

The solution is obtained using first order isoparametric quadrilateral elements for plane strain, element types 11 and 115, respectively. Type 115 is similar to type 11; however, it uses reduced integration with hourglass control.

Model

The plate dimensions are 4 inches wide by 40 inches high, where ($-h < x < h$) and ($-l < y < l$), $h = 2$ and $l = 20$. Due to symmetry, only one-quarter of the layer is modeled, namely ($0 < x < h$ and $0 < y < l$). Figure 3.3-1 shows the mesh that is used for both element types.

Geometry

The strip has a thickness of 1 inch given in the first field (EGEOM1). To obtain the constant volumetric strain formulation, (EGEOM2) is set to unity. This is applied to all elements of type 11. This has no effect for element type 115 because the element does not lock.

Material Properties

The material for all elements is treated as an elastic perfectly-plastic material, with Young's modulus of 10.0 E+06 psi, Poisson's ratio (ν) of 0.3, and a yield strength of 20,000 psi.

Boundary Conditions

The symmetry conditions require that all nodes along the $x = 0$ axis have their horizontal displacements constrained to zero, and all nodes along the $y = 0$ axis have their vertical displacements constrained to zero.

Load History

The x-displacement enforced across the x = h surface during increment 0 is -0.003, and the y-displacement is enforced to be zero. Ten load steps with a PROPORTIONAL INCREMENT of 0.5 follow. Another sequence of ten load steps with a proportionality factor of 3 is added, for a total of 20 increments resulting in a total displacement of -0.063.

Results

The analytical slip-line solution was found by Prandtl for a rigid-plastic material and published in *Foundations of the Theory of Plasticity*, Kachanov, North Holland Publishing, Amsterdam, 1971. The stresses in a plate are expressed as follows:

$$- \sigma_{xx}(x,y) = p + k\,[\, y/h - 2\,(1 - x^2/h^2)^{1/2}]$$

$$- \sigma_{yy}(x,y) = p + k\, y/h$$

$$- \sigma_{xy}(x,y) = k\, x/h$$

and the limit load is found as:

$$P = -kl(\, l/h + \pi)$$

Where p is the surrounding pressure, and the yield condition is:

$$k^2 = 1/4\,(\sigma_{xx} - \sigma_{yy})^2 + \sigma_{xy}^2.$$

The relationship between k and the von Mises yield strength, Y, for plane strain conditions becomes:

$$3\,k^2 = Y^2.$$

Contour plots for the of stress are shown in Figure 3.3-2 and Figure 3.3-3. Comparing the predictions of maximum shear to the analytical values shows:

Component	Analytical	Type 11	Type 115
$- \sigma_{xy} =$	11,541 psi	11,770 psi	11,540 psi

A user-written subroutine, IMPD, was written to sum the reactions at the nodes where the displacements are prescribed to determine the load-deflection curve shown in Figure 3.3-4. The curve clearly shows that a limit load has been reached. The last several increments show no increase in loading, indicating a steady state plastic flow condition. Comparison of the limit load becomes:

$- P =$ 1,512,000 lbf (Slip-line solution)
1,665,000 lbf (Element type 11)
1,754,000 lbf (Element type 115)

The value of the limit load predicted by element type 11 is closer to theoretical than element type 115.

Computationally, it is interesting to note that, during the analysis, the singularity ratio was reduced by a factor of five.

Parameters, Options, and Subroutines Summary

Example e3x3.dat:

Parameters	Model Definition Options	History Definition Options
END	CONNECTIVITY	AUTO LOAD
SIZING	CONTROL	CONTINUE
TITLE	COORDINATES	PROPORTIONAL INCREMENT
	DEFINE	
	END OPTION	
	FIXED DISP	
	GEOMETRY	
	ISOTROPIC	
	POST	
	PRINT CHOICE	
	UDUMP	

User subroutine in u3x3.f

IMPD

Example e3x3b.dat:

Parameters	Model Definition Options	History Definition Options
ALIAS	CONNECTIVITY	AUTO LOAD
ELEMENTS	CONTROL	CONTINUE
END	COORDINATES	PROPORTIONAL INCREMENT
FINITE	DEFINE	
LARGE DISP	END OPTION	
SIZING	FIXED DISP	
TITLE	GEOMETRY	
UPDATE	ISOTROPIC	
	POST	
	PRINT CHOICE	
	UDUMP	

User subroutine in u3x3b.f:

IMPD

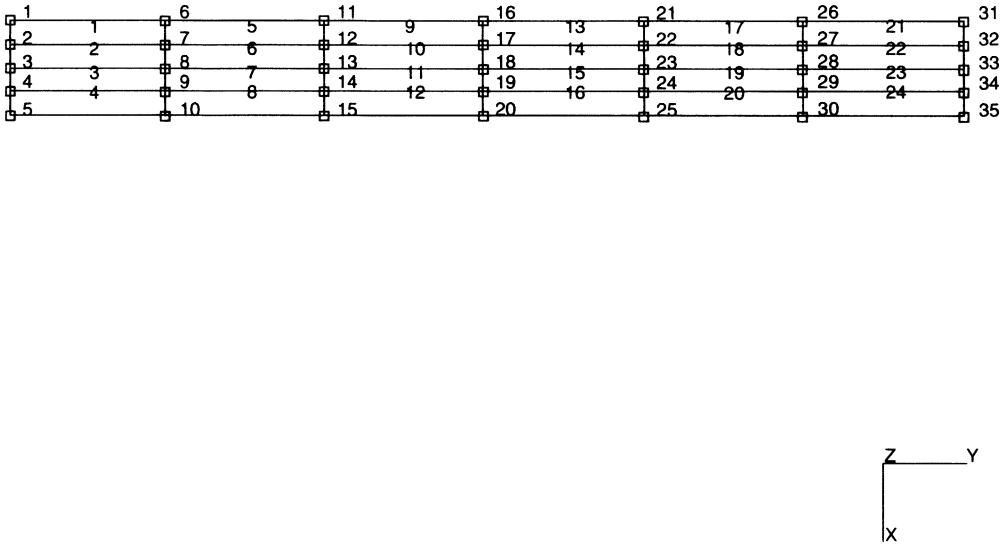

Figure 3.3-1 Finite Element Mesh

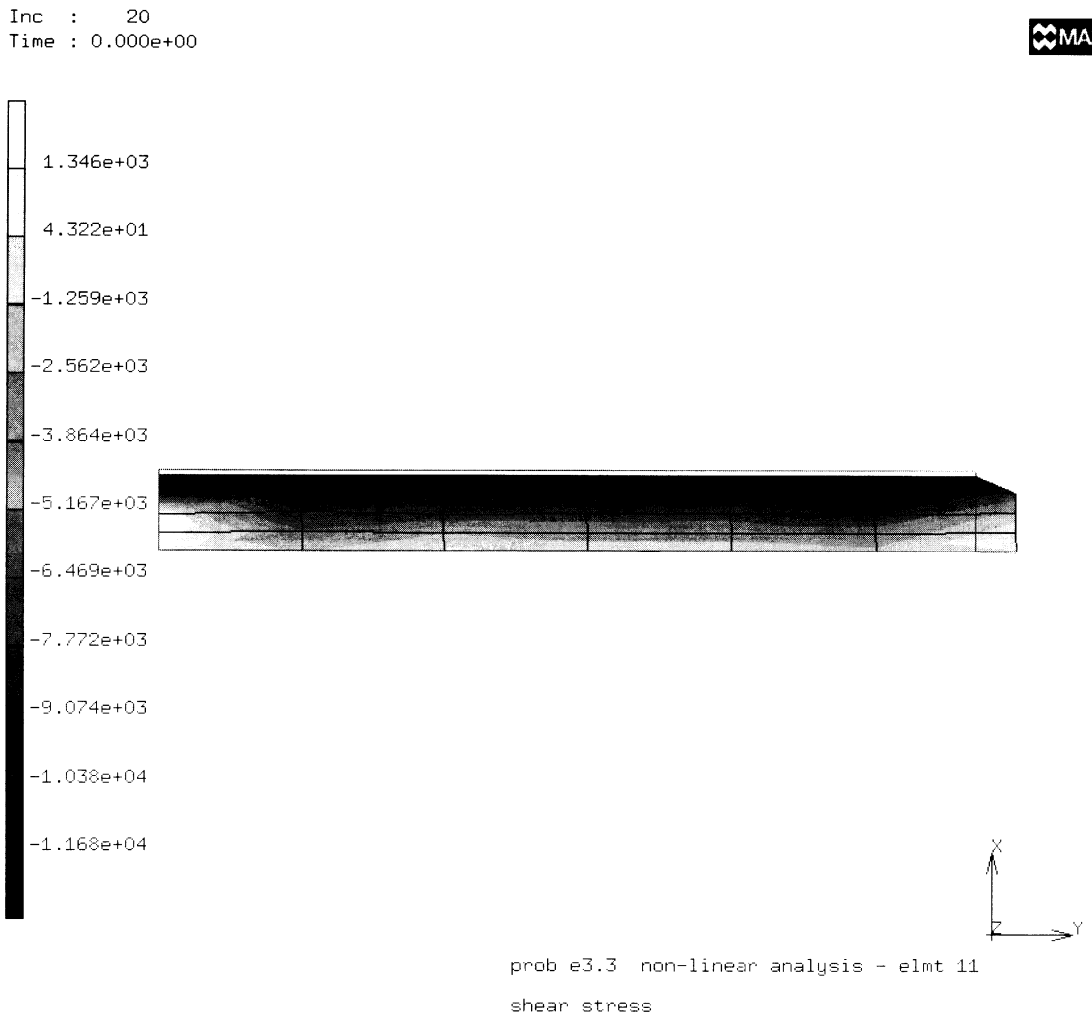

Figure 3.3-2 σ_{xy} Contour Element 11

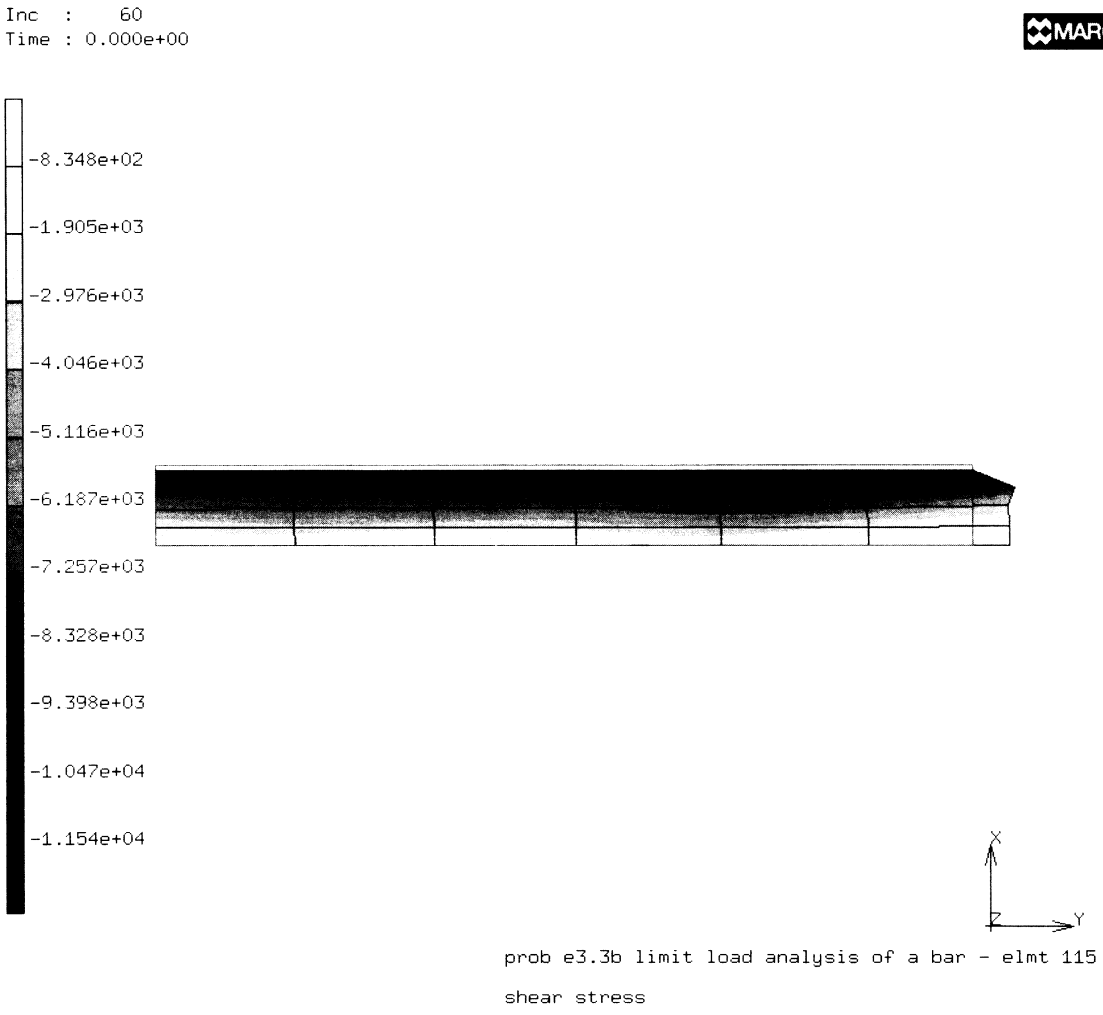

Figure 3.3-3 σ_{xy} Contour Element 115

Displacement (in.)	Element 11	Element 115
0.0	0.0	0.0
3.00E-03	3.96824E-01	3.96262E-01
6.00E-03	7.26945E-01	7.28464E-01
9.00E-03	9.22769E-01	9.25604E-01
1.20E-02	1.09504E+00	1.09972E+00
1.50E-02	1.24589E+00	1.25424E+00
1.80E-02	1.37297E+00	1.38484E+00
2.10E-02	1.47581E+00	1.49313E+00
2.40E-02	1.55544E+00	1.57812E+00
2.70E-02	1.61131E+00	1.63987E+00
3.00E-02	1.64520E+00	1.68006E+00
3.30E-02	1.65915E+00	1.70095E+00
3.90E-02	1.66661E+00	1.72789E+00
4.80E-02	1.66520E+00	1.74967E+00
4.98E-02	1.66517E+00	1.75428E+00

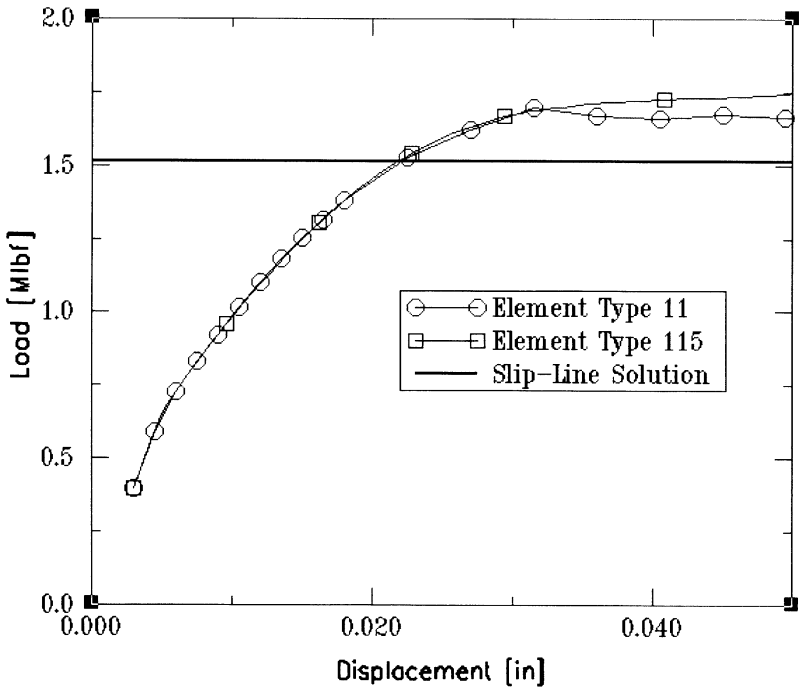

Figure 3.3-4 Load-Displacement Curve

3.4 Bending of Prismatic Beam

A prismatic beam is loaded into the elastic-plastic range by an end moment. Subsequently, the loading direction is reversed. The material follows the ORNL recommended constitutive theories. This problem demonstrates nonproportional loading for an elastic-plastic analysis.

Element

Element type 16 is a 2-node curved beam element.

Model

One end of the beam is fixed; the other end is subjected to a moment. There are four elements and five nodes for a total of 20 degrees of freedom (see Figure 3.4-1). The length of the beam is 100 inches.

Geometry

The beam height is taken to be 10.0 inches and is specified as EGEOM1. The beam width is 1.0 inches and is specified as EGEOM2. Seven layers are used for integration through the height of the beam (SHELL SECT option).

Boundary Conditions

One end of the beam is fixed against displacement (u = v = 0) and rotation ($\frac{dv}{ds} = 0$), simulating a cantilevered beam.

Material Properties

The material is elastic-plastic. The ORNL constitutive theory is used; consequently kinematic hardening is automatically invoked by the program. The ORNL theory is flagged through the ISOTROPIC option. Values for Young's modulus, Poisson's ratio, first and second yield stresses used here are 10.0×10^6 psi, 0.3, 20,000 psi, and 22,000 psi, respectively.

Work Hard

The primary workhardening slope is 3.0×10^5 psi. The initial secondary workhardening slope is $10. \times 10^5$ psi. The subsequent secondary workhardening slope of 3.0×10^5 psi starts at a plastic strain of 1%.

Loading

An end moment is applied in the fourth degree of freedom of node 5 in 13 steps. The moment is then reversed in direction and is incremented for 25 steps.

Results

The results show that the program is capable of treating problems involving loading paths with reversal of plastic deformation. The end moment is scaled to reach yield stress in element 4 and proportionally incremented to 160% of the moment to first yield in 12 steps. All seven layers of beam element 1 have developed plastic strain. The maximum effective plastic strain is around 1%. The end moment is then reversed with a small negative scaling factor (-0.05). Once elastic response is established, a large step can be taken using a scaling factor of 40. Twenty-four more steps are used to bring the reversed moment to about the same maximum in the opposite direction. The reversed maximum effective plastic strain is around 0.35%. The moment-rotation diagram is shown in Figure 3.4-2. The residual stress distribution for zero applied moment after first loading is shown in Figure 3.4-3. The reverse plastic flow starts at a moment of -0.1833×10^6 in-lb. This is 55% of the load to first yield in the original, undeformed beam. The PRINT CHOICE option is used to restrict the output to layer 2 of element 1 only.

Parameters, Options, and Subroutines Summary

Example e3x4.dat:

Parameters	Model Definition Options	History Definition Options
ELEMENTS	CONNECTIVITY	AUTO LOAD
END	CONTROL	CONTINUE
SCALE	COORDINATES	PROPORTIONAL INCREMENT
SHELL SECT	DEFINE	
SIZING	END OPTION	
TITLE	FIXED DISP	
	GEOMETRY	
	ISOTROPIC	
	POINT LOAD	
	POST	
	PRINT CHOICE	
	WORK HARD	

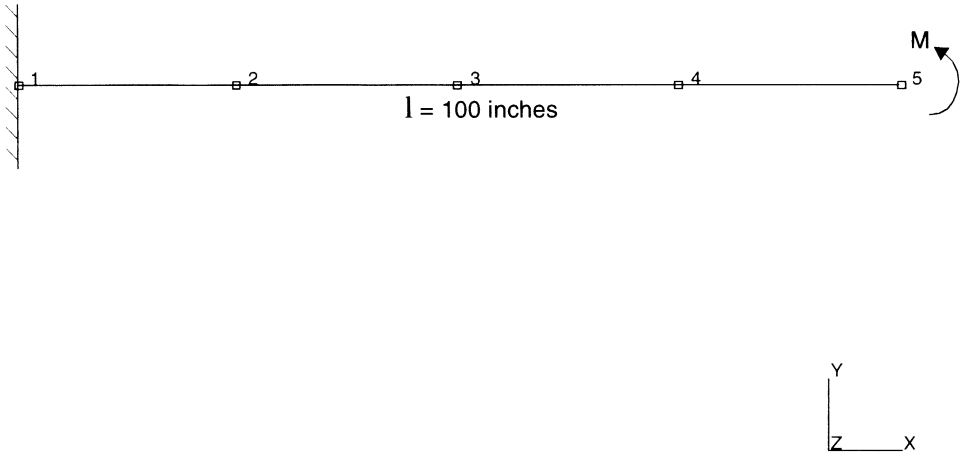

Figure 3.4-1 Prismatic Beam Model and Mesh

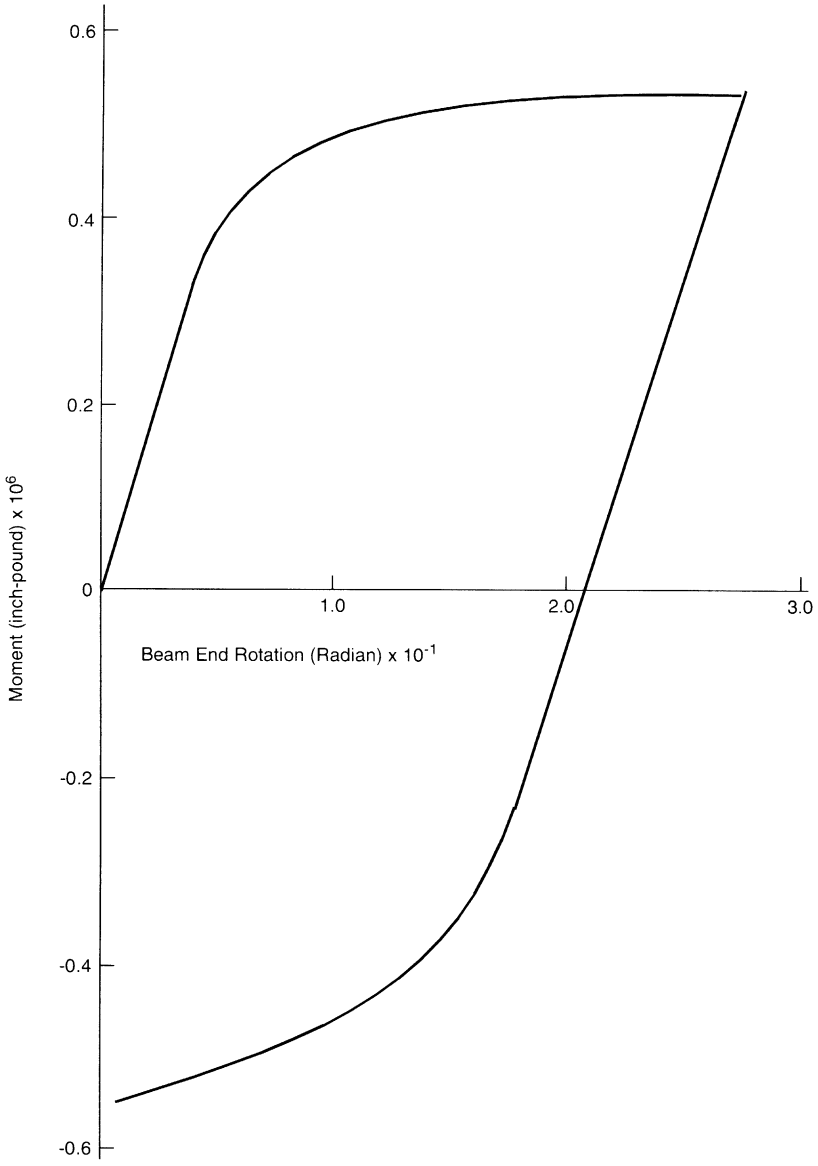

Figure 3.4-2 Moment-Rotation Diagram

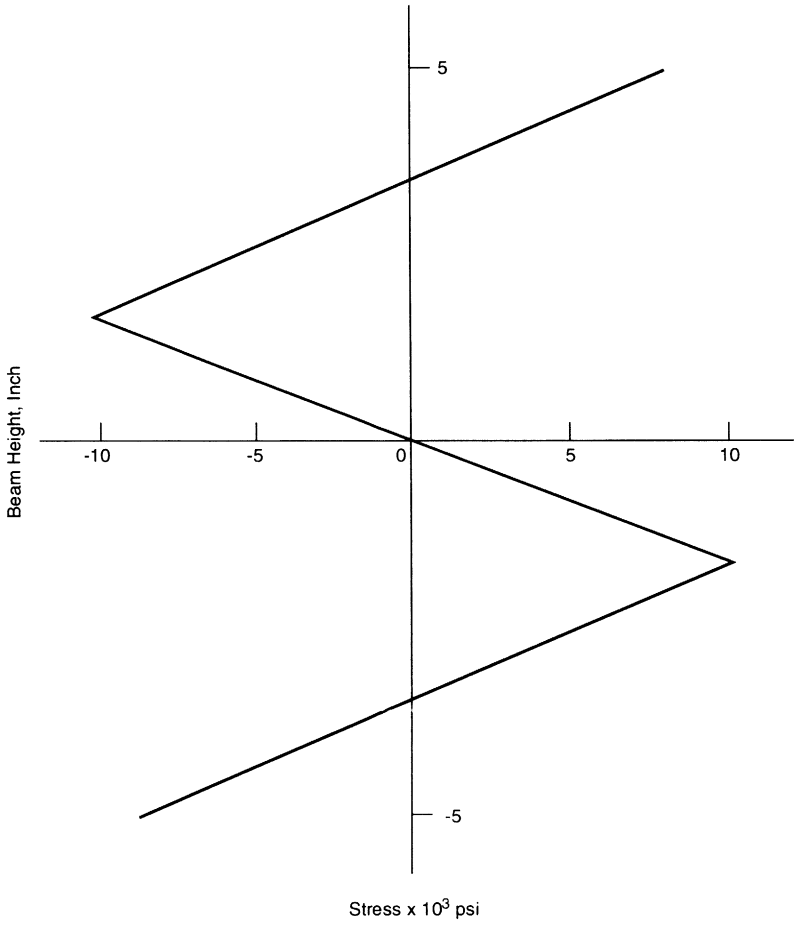

Figure 3.4-3 Residual Stress Distribution for Zero Moment

3.5 Hemispherical Shell under Thermal Expansion

A hemispherical shell under uniform thermal load is analyzed. The temperatures are prescribed and elastic-plastic stress and strain are computed.

Element

Element type 15, a 2-node axisymmetric thin shell, is used.

Model

The geometry of the hemisphere and the mesh is shown in Figure 3.5-1. A 90° cross section is referenced with respect to an R-Z global coordinate system. The shell has been divided into eight elements with nine nodes.

Geometry

The shell thickness is 2.0 inches and specified as EGEOM1 of this option. Five layers are used for integration through the shell cross section as prescribed in the SHELL SECT option.

Boundary Conditions

Fixed boundary conditions are specified at node 9 $\left(u = v = \frac{du}{ds} = 0\right)$. Symmetry boundary conditions are specified at node 1 $\left(v = \frac{du}{ds} = 0\right)$.

Transformation

Nodes 2 through 9 have been transformed to a new local coordinate system. Boundary conditions at node 9 are input in the transformed system such that at each node the displacements are given as radial and tangential.

Material Properties

The material is assumed to be elastic-plastic with strain hardening. The elastic properties are considered to be independent of temperature. The yield stress decreases with temperature to a value of zero at 2000°F. Values for Young's modulus, Poisson's ratio, coefficient of thermal expansion, initial temperature, and yield stress used here are 10.0 x 10^6 psi, 0.3, 1.0 x 10^{-6} in/in/°F, 70°F, and 20,000 psi, respectively.

UFXORD

User subroutine UFXORD is used to generate a full set of five coordinates required for element type 15.

Work Hard

The user subroutine WKSLP is used to generate the current yield stress and the corresponding workhardening slope. The workhardening curve is shown in Figure 3.5-2.

Loading

A uniform temperature of 800°F is applied to all elements. The temperature is then proportionally incremented 100°F for 11 steps.

Temperature Effects

The initial yield stress decreases 10 psi for each increase in temperature of 1°F above 70°F.

Results

Temperature is increased to 1970°F by increment 11; plastic strain at layer 1 of integration point 3 of element 8 is 0.29. The total displacement due to thermal expansion for node 1 is 0.224 inches. The resultant displacement is shown in Figure 3.5-3. The PRINT CHOICE option is used to restrict printout to layers 1 through 3.

The highest stressed element is element 8, which is at the fixed boundary. This boundary condition is quite severe and a more accurate solution would have been obtained if mesh refinement would have been used in this region. Initial yield can be predicted by assuming that a small region near this boundary is constrained. Then,

$$\sigma_{11} = \sigma_{22} = E\alpha\Delta T \qquad \sigma_{33} = 0$$

$$\bar{\sigma} = \sqrt{\frac{3}{2}S_{ij}S_{ij}} = E\alpha\Delta T$$

$Y(T) = \bar{\sigma}$ at yield, so

$$(20000 - 10\Delta T = 10.0 \times 10^{6} \times 1.0 \times 10^{-6}\Delta T)$$

$$\Delta T = 1000°F$$

Hence, yield should occur in increment 2, as it does.

Parameters, Options, and Subroutines Summary

Example e3x5.dat:

Parameters	Model Definition Options	History Definition Options
ELEMENTS	CONNECTIVITY	AUTO THERM
END	CONTROL	CHANGE STATE
NEW	DEFINE	CONTINUE
SHELL SECT	END OPTION	
SIZING	FIXED DISP	
THERMAL	GEOMETRY	
TITLE	INITIAL STATE	
	ISOTROPIC	
	PRINT CHOICE	
	TEMPERATURE EFFECTS	
	THERMAL LOADS	
	TRANSFORMATION	
	UFXORD	
	WORK HARD	

User subroutines in u3x5.f:

WKSLP
UFXORD

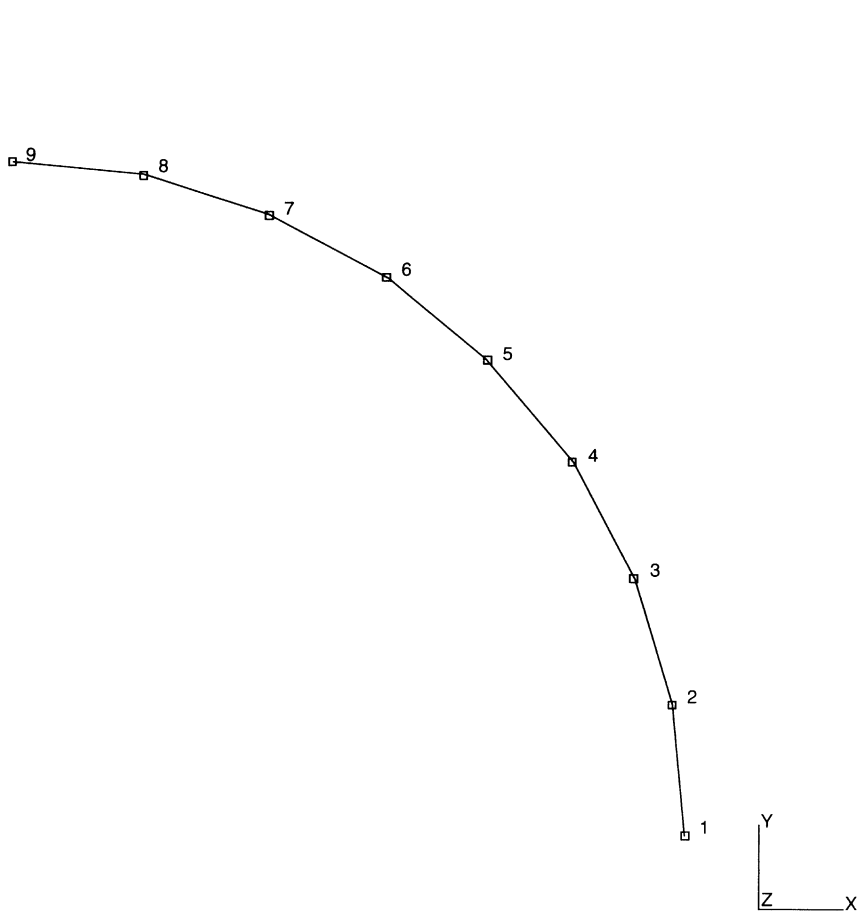

Figure 3.5-1 Hemispherical Shell and Mesh

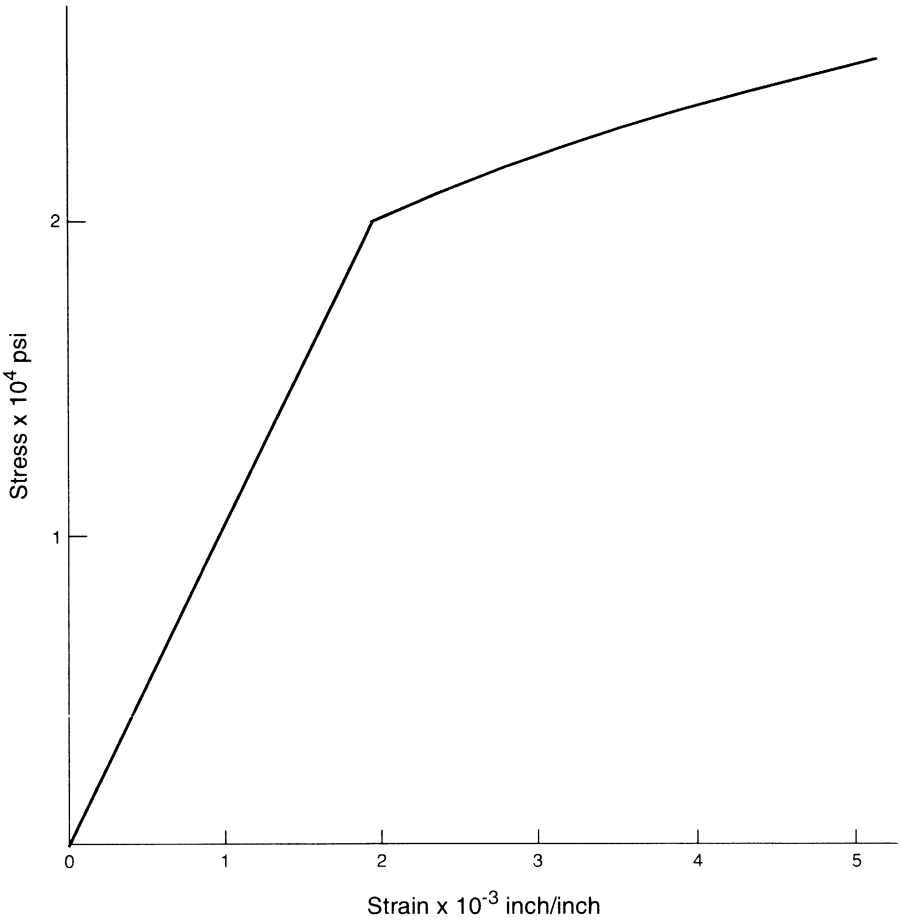

Figure 3.5-2 Workhardening Curve

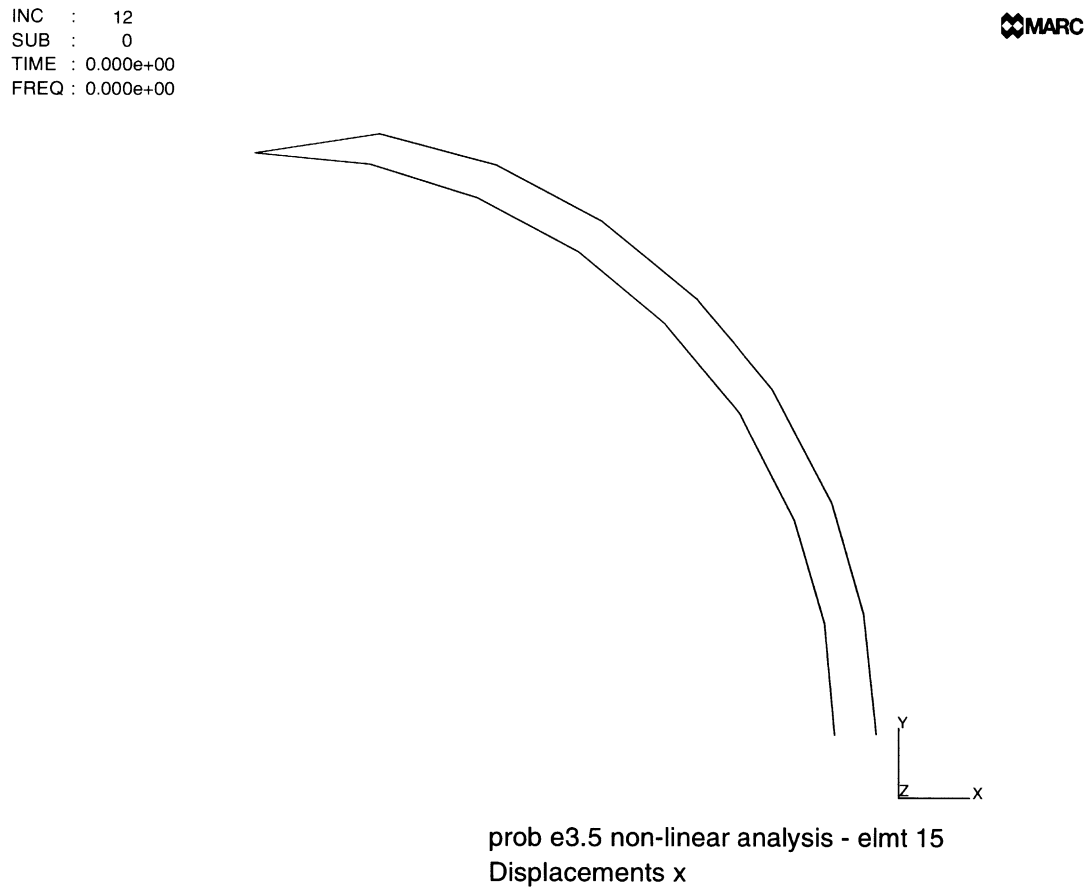

Figure 3.5-3 Displaced Mesh

3.6 Collapse Load of a Simply Supported Square Plate

In this problem, the maximum transverse load that a square plate of isotropic material can sustain is determined.

Element

Library element type 49 is a 6-node triangular thin shell element.

Model

The dimensions of the plate and the finite element mesh are shown in Figure 3.6-1. Based on symmetry considerations, only one-quarter of the plate is modeled. The mesh is composed of 32 elements and 81 nodes.

Material Properties

The material is elastic with a Young's modulus of 3.0×10^4 N/mm^2, a Poisson's ratio or 0.3, and a yield stress of 30 N/mm^2.

Geometry

The thickness of the plate is specified as 0.4 mm. Since a geometrically linear plate problem is solved, the elements can be considered as flat, which is indicated by a 1 on the fifth geometry field. In this way, computational time is reduced. In order to trigger the response in thickness directions, five layers are chosen using the SHELL SECT parameter.

Loading

A uniform pressure load of 0.02 N/mm^2 is applied. Since this load is larger than the actual collapse load, the auto increment option is used with a limited number of increments. In this way, the analysis stops if the maximum allowed number of increments is reached.

Boundary Conditions

Symmetry conditions are imposed on the edges x = 20 ($u_x = 0$, $\phi = 0$) and y = 20 ($u_y = 0$, $\phi = 0$). Notice that the rotation constraints only apply for the midside nodes. Simply supported conditions are imposed on the edges x = 0 and y = 0 ($u_z = 0$).

Results

Figure 3.6-2 shows the deflection of the central node as a function of the equivalent nodal load. The solution turns out to be in reasonable agreement with the reference solution taken from *Selected Benchmarks for Material Non-Linearity* by D. Linkens (published by NAFEMS, 1993). This reference solution, which is obtained using higher order elements is indicated in Figure 3.6-3.

Parameters, Options, and Subroutines Summary

Example e3x6.dat:

Parameters	Model Definition Options	History Definition Options
ALL POINTS	CONNECTIVITY	AUTO INCREMENT
DIST LOADS	COORDINATES	CONTINUE
ELEMENTS	DEFINE	CONTROL
END	END OPTION	DIST LOADS
SETNAME	FIXED DISP	
SIZING	GEOMETRY	
TITLE	ISOTROPIC	
	NO PRINT	
	OPTIMIZE	
	POST	
	SOLVER	

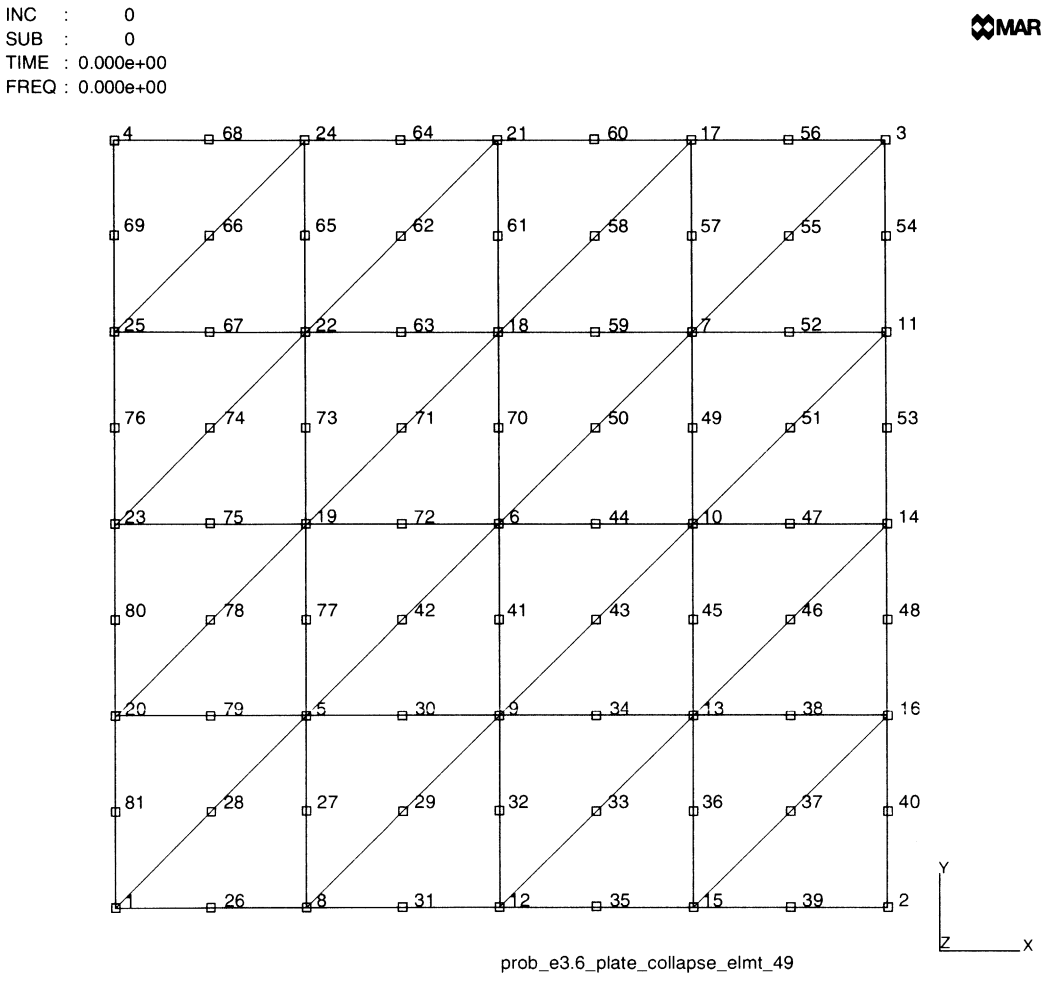

Figure 3.6-1 Square Plate and Finite Element Mesh

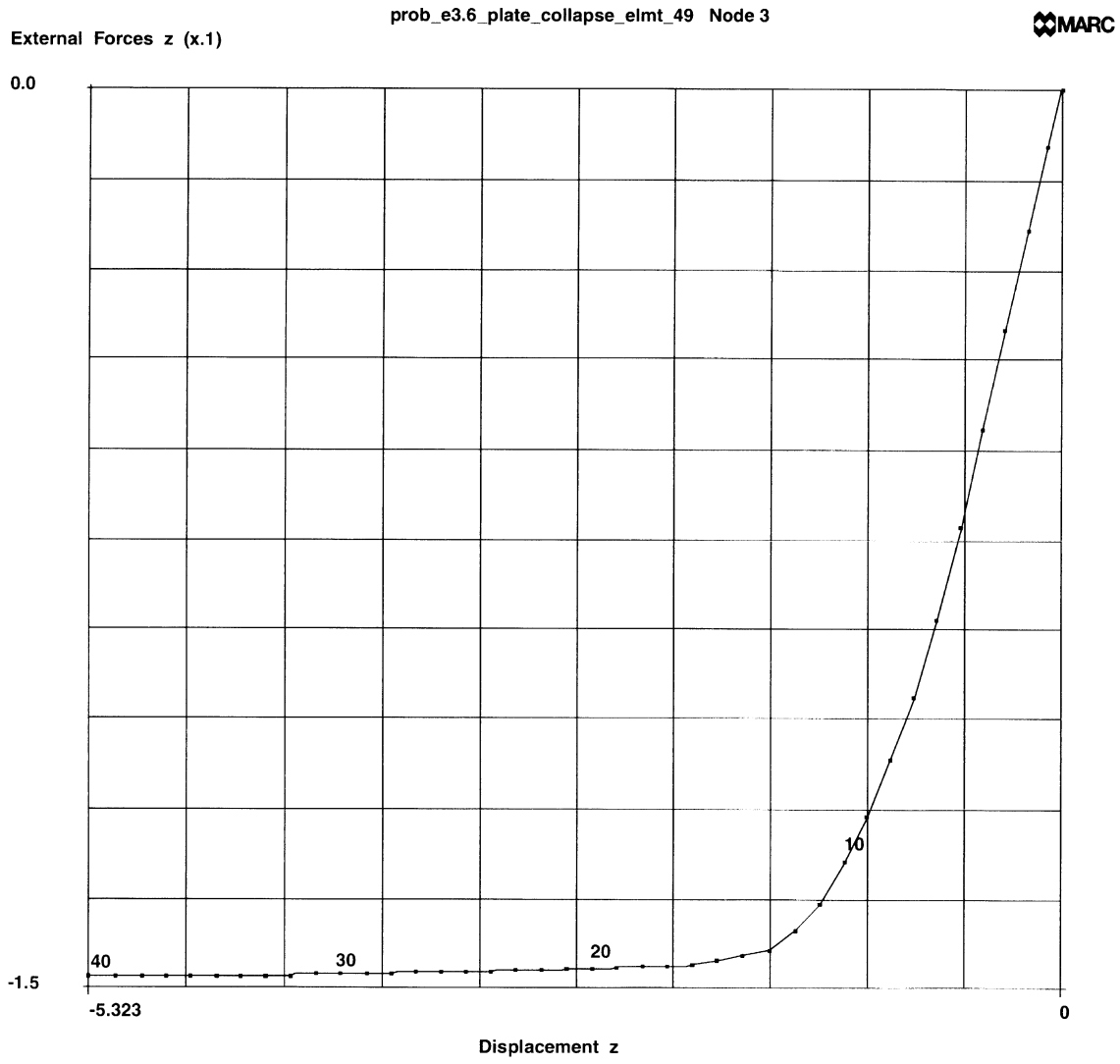

Figure 3.6-2 Central Deflection Versus Nodal Load (MARC Solution)

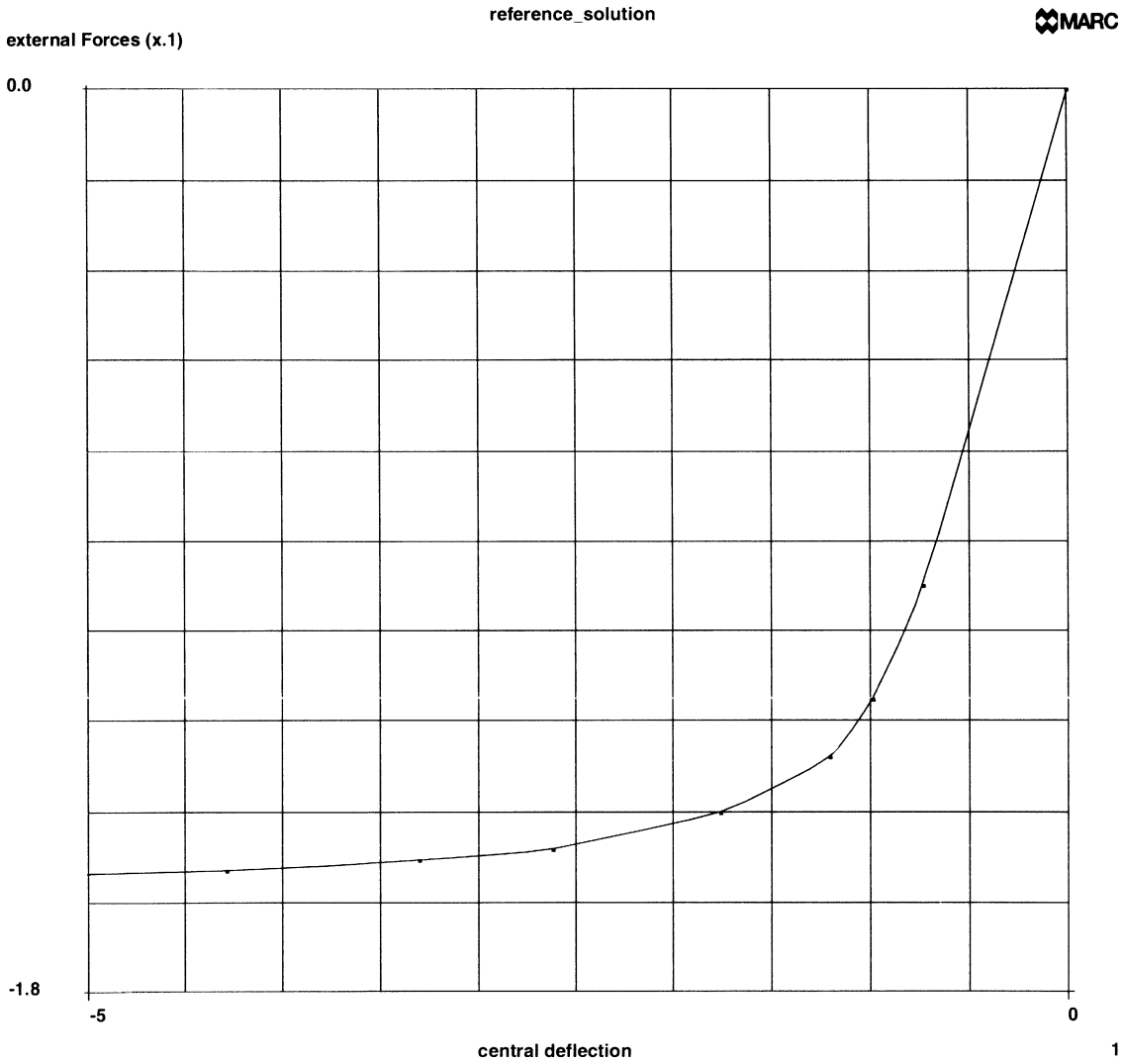

Figure 3.6-3 Central Deflection Versus Nodal Load (Reference Solution)

3.7 Elastic-Plastic Analysis of a Thick Cylinder

In this problem, a thick cylinder under the action of uniform internal pressure is loaded into the plastic region. A comparison with rigid plastic results is provided.

Element

The axisymmetric quadrilateral element, library element type 10, is used to model the wall of the cylinder. Details for this element are found in *MARC Volume B: Element Library.*

Model

Figure 3.7-1 shows the model geometry for this example. The cylinder wall has an inner radius of 1.0 inches and an outer radius of 2.0 inches.

The mesh is shown in Figure 3.7-2 and results in a model of the wall consisting of 20 elements, 42 nodes and 84 degrees of freedom.

Geometry

The geometry option is not required for this element.

Material Properties

The material data is: Young's modulus (E) of 30.0 x 10^6 psi, Poisson's ratio (v) of 0.3, and von Mises yield stress (σ_y) of 45,000 psi. The material is assumed to behave elastic-perfectly plastic; that is, no strain hardening.

Boundary Conditions

Restraint boundary conditions are imposed in the axial direction on all nodes thus allowing only radial motion of the wall. This solution corresponds to a plane strain case.

Loading

An initial uniform pressure of 19,550 psi is applied using the DIST LOAD option. To investigate the plastic effects, SCALE is used to raise this pressure to a magnitude such that the highest stressed element (element 1) in the model has an equivalent yield stress (J2) which is equal to the specified yield stress of 45,000 psi. The resulting scale factor here is 1.045 which indicates the applied pressure for increment zero is 20,430 psi.

The data before END OPTION provides the elastic solution such that the highest stressed element is at first yield of 45,000 psi and any further loading is done incrementally into the plastic region.

Control

This option specifies a maximum of 15 increments in this example and a tolerance of 15% for convergence. (Only 11 increments are provided as the input data count for the zero increment.)

Incremental Loading

The data blocks following END OPTION are used to specify the incremental load step into the plastic region. The AUTO LOAD option is used to apply two load increments of equal size and the PROPORTIONAL INCREMENT option is used to provide a scaling factor of the load step size for each application of the AUTO LOAD option.

The PROPORTIONAL INCREMENT option as used here specifies a scaling factor to be applied to the previous load step size, and the minimum number of cycles through the prediction of plastic effects (NCYCM) was set to 2 to improve solution accuracy. The scaling factor is adjusted to give the necessary small load steps to keep the solution within the desired tolerance.

The incremental loads which are applied in this example are as follows:

Increment

0 $P_0 = sp = (1.03)(19550) = 20{,}136$ psi

1 $P_1 = P_0 + \Delta P_1$: $\Delta P_1 = fsp = (0.13)(1.03)(19{,}550)$

2 $P_2 = P_0 + \Delta P_1 + \Delta P_2$: $\Delta P_2 = \Delta P_1$

3 $P_3 = P_0 + \Delta P_1 + \Delta P_0 + \Delta P_3$: $\Delta P_3 = 0.8\Delta P_2$

5 $P_5 = P_0 + \Delta P_1 + \ldots + \Delta P_5$: $\Delta P_5 = 0.7\Delta P_4$

7 $P_7 = P_0 + \Delta P_1 + \ldots + \Delta P_7$: $\Delta P_7 = 0.667\Delta P_6$

10 $P_{10} = P_0 + \Delta P_1 + \ldots + \Delta P_{10}$

$$\Delta P_{10} = \Delta P_9 = 0.5\Delta P_8 = 0.5\Delta P_7 = \ldots = 0.5(0.667)(0.7)(0.8)(0.13)\Delta p =$$

$$= 1.04052 \times 10^{-2}\,\Delta p = 488 \text{ psi}$$

If a reverse load is desired, a negative scale factor should be used only once to reverse the sign of the load step.

If a load step is applied which is too large to allow the energy change tolerance to be satisfied, MARC, in this case, cycles through the predicted displacement iteration five times. On the last try, a message indicating NO CONVERGENCE TO TOLERANCE is printed out. Then the strains and stresses corresponding to the last iteration are printed in the output, and MARC exits with an appropriate exit message.

Restart

To protect against failure to meet tolerances, use of the restart capability available in the program is recommended. The RESTART option has been used in this example. Two input decks which follow this discussion illustrate the use of RESTART. The first run creates a restart file (unit 8) and writes the necessary data to this file so that the analysis can be restarted at any increment.

The initial deck is set up to run completely through the analysis while the second is used to restart the problem at a point in the middle of the analysis. The analysis was restarted at increment 7.

In general, this specification requires the program to read the next set of load data following END OPTION to be applied as the increment 8 load set. In this case, the program already has the required load data for the increment 8 solution because of the use of the AUTO LOAD option, and it will complete the step of the option before reading the additional data after END OPTION. The data supplied after END OPTION is only enough to complete increments 9 and 10. In the third part, the restart file is read and positioned so that postprocessing plotting can be done.

Results

The results of this analysis are shown in Figure 3.7-3 through Figure 3.7-6. Comparison is made with the results of the finite difference solution given in Chapter 4 of *Theory of Perfectly Plastic Solids* by W. Prager and P. G. Hodge, Jr. (published by John Wiley and Sons, 1963).

Comparison is shown for two values of tolerance which varied from 0.5 to 0.1. The results did not vary appreciably as a function of the displacement tolerance.

The following terminology is used in Figure 3.7-4 through Figure 3.7-6:

a = inner radius

b = outer radius

ρ = radius of elastic-plastic boundary

σ_r = radial stress

$\sigma\theta$ = circumferential stress

σ_z = axial stress

Y = yield stress

$k = Y/\sqrt{3}$

The elastic-plastic boundary is shown as a function of the pressure, p, in Figure 3.7-3.

For the plane strain condition, a numerical solution obtained by finite difference methods was given in the reference. The radial stress distribution for two different positions of the elastic-plastic boundary ($\rho/a = 1.2$ and $\rho/a = 2.0$) are compared to the solution given in the reference in Figure 3.7-4. Excellent agreement is observed. The circumferential stress distribution in the partially plastic tube is similarly compared in Figure 3.7-5. A comparison of the axial stress distribution is given in Figure 3.7-6. The two solutions are seen to be in good agreement.

Parameters, Options, and Subroutines Summary

Example e3x7a.dat:

Parameters	Model Definition Options	History Definition Options
END	CONNECTIVITY	AUTO LOAD
SCALE	CONTROL	CONTINUE
SIZING	COORDINATES	PROPORTIONAL INCREMENT
TITLE	DIST LOADS	
	END OPTION	
	FIXED DISP	
	ISOTROPIC	
	PRINT CHOICE	
	RESTART	

Example e3x7b.dat:

Parameters	Model Definition Options	History Definition Options
END	CONTROL	AUTO LOAD
SCALE	DIST LOADS	CONTINUE
SIZING	END OPTION	PROPORTIONAL INCREMENT
TITLE	FIXED DISP	
	ISOTROPIC	
	PRINT CHOICE	

Example e3x7c.dat:

Parameters	Model Definition Options	History Definition Options
END	BOUNDARY CONDITIONS	CONTINUE
MESH PLOT	CONTROL	
SCALE	DIST LOADS	
SIZING	END OPTION	
	TITLE	
	ISOTROPIC	
	PRINT CHOICE	
	RESTART	

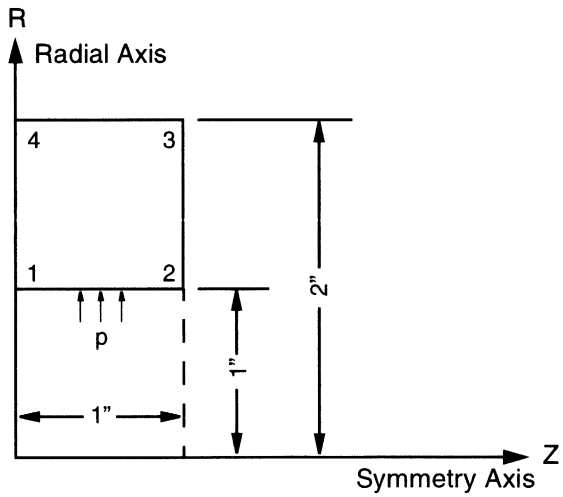

Figure 3.7-1 Cylinder Wall

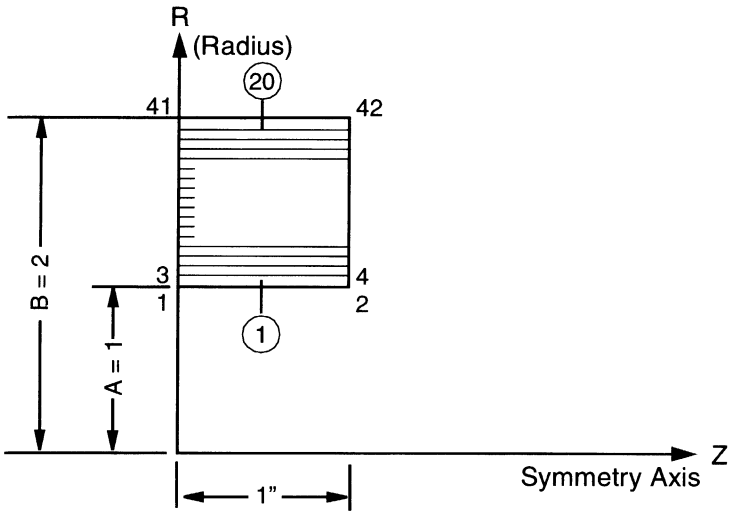

Figure 3.7-2 Cylinder Wall Generated Mesh

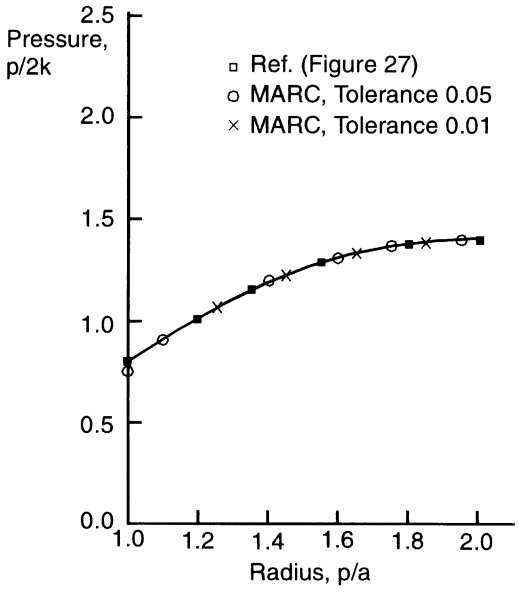

Figure 3.7-3 Pressure Versus Elastic-Plastic Boundary

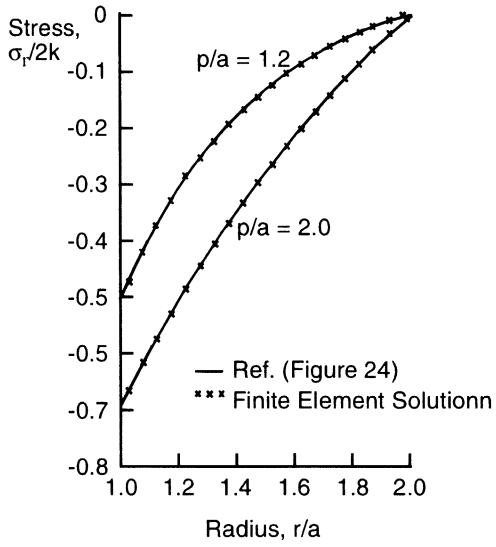

Figure 3.7-4 Radial Stress Distribution

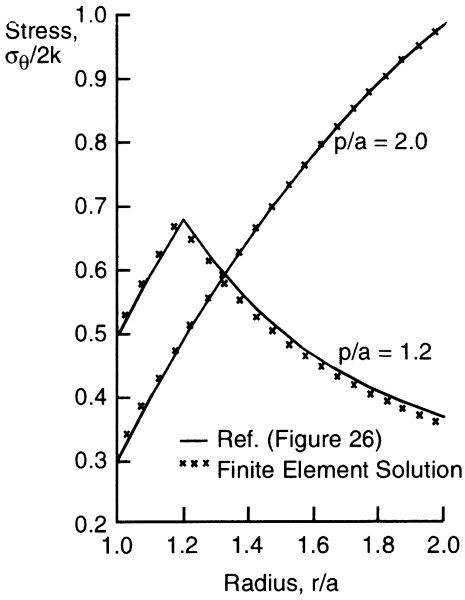

Figure 3.7-5 Circumferential Stress Distribution

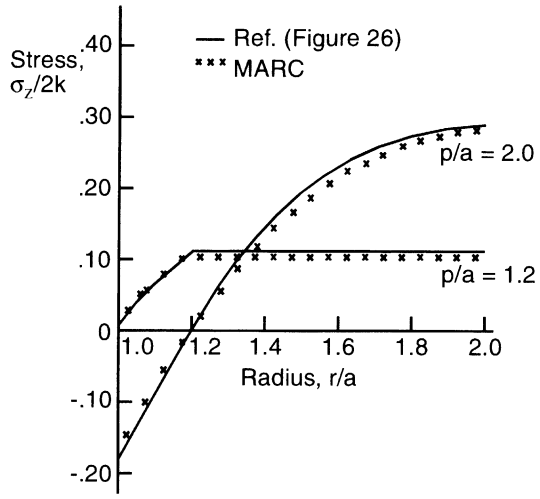

Figure 3.7-6 Axial Stress Distribution

3.8 Double-Edge Notch Specimen under Axial Tension

In this problem, the J-integral is evaluated for an elastic-plastic Double-Edge Notch (D.E.N.) specimen under axial tension. Three different paths are used for the J-integral evaluation. The variation in the value of J between the three paths indicates the accuracy of the solution.

Element

Element type 27 is an 8-node plane-strain quadrilateral.

Model

Figure 3.8-1 shows the geometry and the principal boundary nodes for the seven blocks used to define the quarter specimen. Figure 3.8-2 shows the mesh with 32 elements and 107 nodes. A second COORDINATES block is used to move the side nodes of the crack tip elements to the one-quarter points (one-quarter of the way along the sides from the crack tip to the opposite face of the element).

Geometry

The option is not required for this element as a unit thickness will be considered.

Boundary Conditions

Boundary conditions are used to enforce symmetry about the x- and y-axes.

Material Properties

The material is elastic-plastic with strain hardening. Values for Young's modulus, Poisson's ratio, and yield stress used here are 30 x 10^6 psi, 0.3 and 50.0 x 10^3 psi, respectively.

Workhard

User subroutine WKSLP is used to input the workhardening slope. The workhardening curve is shown in Figure 3.8-3. The yield surface can be expressed as:

$$\bar{\sigma}(\bar{\varepsilon}^p) = \sigma_o(1 + E\bar{\varepsilon}^p/\sigma_o)^{0.2}$$

$$\frac{\partial\bar{\sigma}}{\partial\bar{\varepsilon}^p} = 0.2\ E(1 + E\bar{\varepsilon}^p/\sigma_o)^{-0.8}$$

J-Integral

The J-integral is evaluated numerically by moving nodes within a certain ring of elements around the crack tip and measuring the change in strain energy. (This node movement represents a differential crack advance.) This mesh has three obvious "rings" of elements around the crack tip, so that three evaluations of J are provided. A differential movement of 10^{-2} is used in all three evaluations.

Loading

An initial uniform pressure of 100 psi is applied using the DIST LOAD option. The SCALE parameter is used to raise this pressure to a magnitude such that the highest stressed element (element 20 here) is at first yield. The pressure is scaled to 3,047 psi. The pressure is then incremented for five steps until the final pressure is 3,308 psi.

Results

The program provides an output of the strain energy differences. This must be normalized by the crack opening area to obtain the value of J. Since this specimen is of unit thickness, the crack opening area is Δl, where Δl is the differential crack motion. The mesh used symmetry about the crack line, so that the strain energy change in the actual specimen would be twice that printed out. These results are summarized in Table 3.8-1. It is clear that these results do demonstrate the path independence for the J-integral evaluation. A plot of the equivalent stress for increment 5 is shown in Figure 3.8-4. The plastic deformation is local to the crack tip only, occurring in elements 3, 4, 19, and 20. The PRINT CHOICE option is used to restrict the printout to those elements in the inner rings surrounding the crack tip.

Table 3.8-1 J-Integral Evaluation Results

	Move Tip Only	Move First Ring of Elements	Move Second Ring of Elements
Strain Energy Change for increment 0 (Δu)	6.220×10^{-2}	6.203×10^{-2}	6.199×10^{-2}
J-Integral $\left(\frac{2\Delta u}{\Delta l}\right)$	12.46	12.424	12.418
Strain Energy Change for increment 1 (Δu)	6.858×10^{-2}	6.839×10^{-2}	6.834×10^{-2}
J-Integral $\left(\frac{2\Delta u}{\Delta l}\right)$	13.738	13.698	13.69
Strain Energy Change for increment 2 (Δu)	7.528×10^{-2}	7.506×10^{-2}	7.501×10^{-2}
J-Integral $\left(\frac{2\Delta u}{\Delta l}\right)$	15.078	15.034	15.026
Strain Energy Change for increment 3 (Δu)	8.228×10^{-2}	8.205×10^{-2}	8.199×10^{-2}
J-Integral $\left(\frac{2\Delta u}{\Delta l}\right)$	16.482	16.434	16.424
Strain Energy Change for increment 4 (Δu)	8.960×10^{-2}	8.934×10^{-2}	8.929×10^{-2}
J-Integral $\left(\frac{2\Delta u}{\Delta l}\right)$	17.948	17.896	17.886
Strain Energy Change for increment 1 (Δu)	9.723×10^{-2}	9.695×10^{-2}	9.689×10^{-2}
J-Integral $\left(\frac{2\Delta u}{\Delta l}\right)$	19.476	19.422	19.41

Parameters, Options, and Subroutines Summary

Example e3x8.dat:

Parameters	Model Definition Options	History Definition Options
ELEMENTS	CONNECTIVITY	AUTO LOAD
END	CONTROL	CONTINUE
J-INT	COORDINATES	PROPORTIONAL INCREMENT
SCALE	DIST LOADS	
SIZING	END OPTION	
TITLE	FIXED DISP	
	ISOTROPIC	
	J-INTEGRAL	
	PRINT CHOICE	
	RESTART	
	WORK HARD	

User subroutine in u3x8.f:

WKSLP

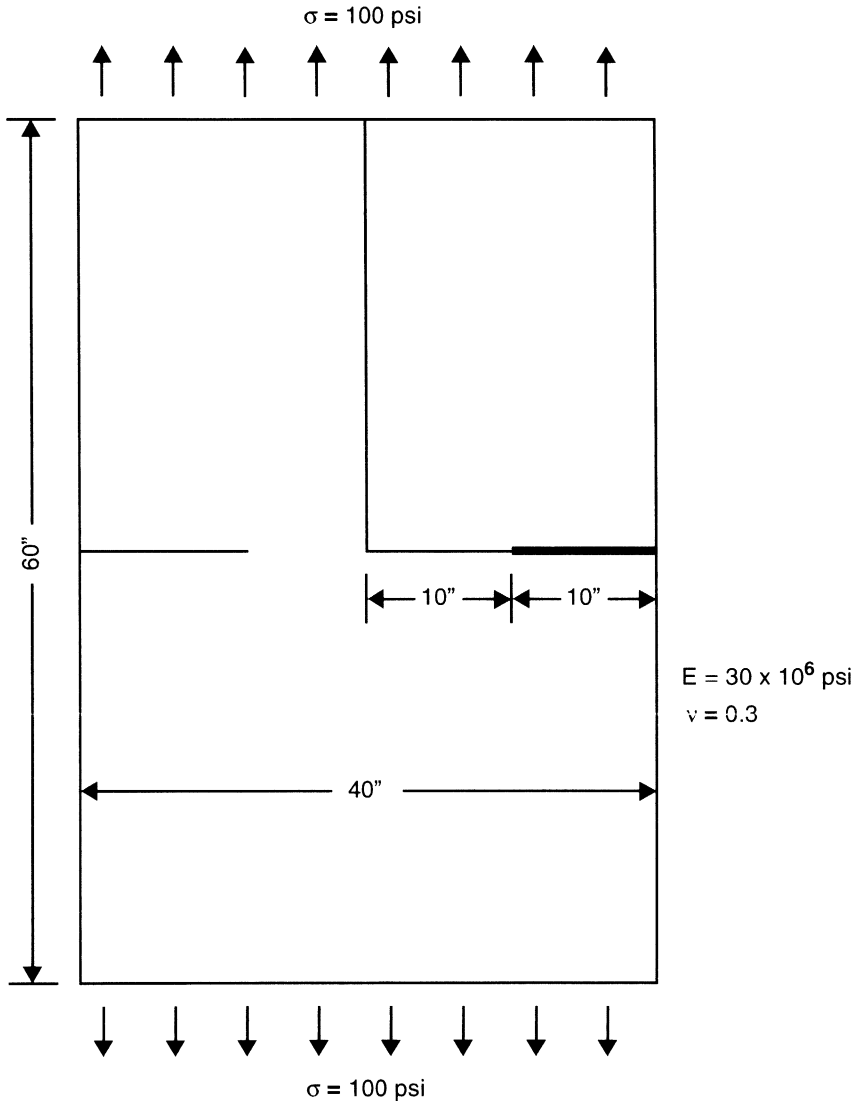

Figure 3.8-1 D.E.N. Specimen

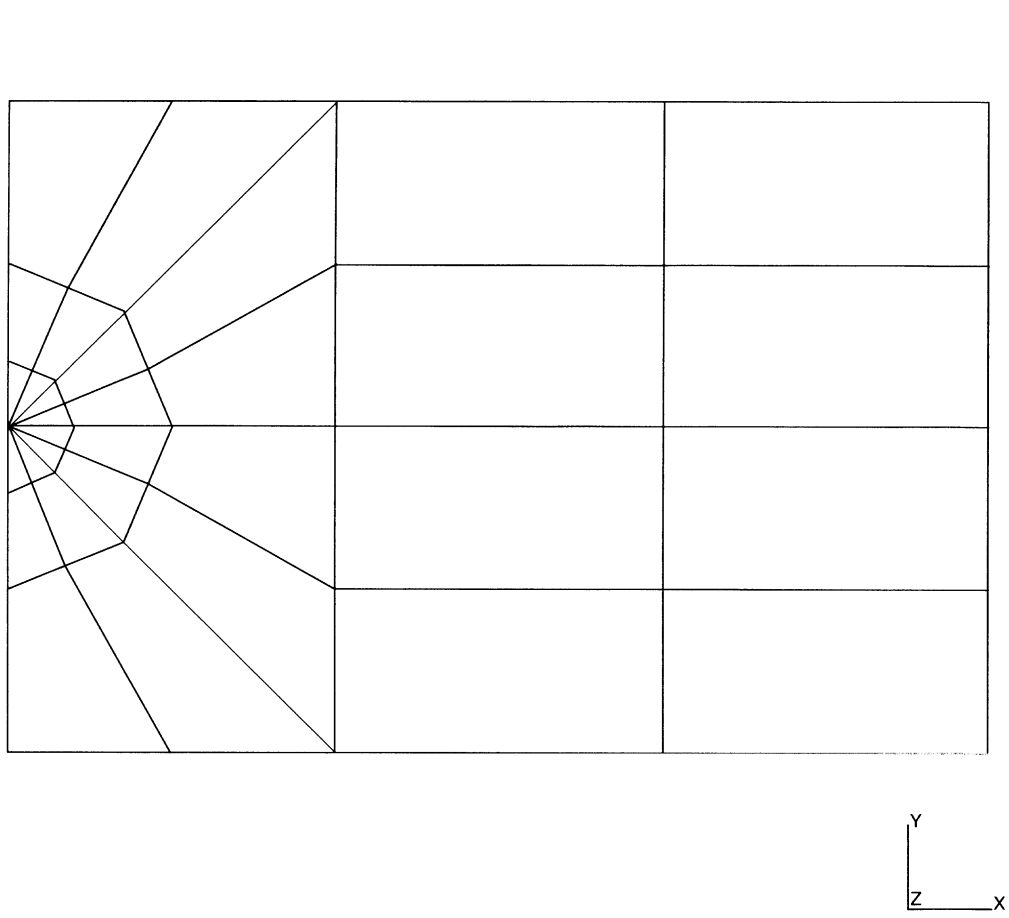

Figure 3.8-2 Mesh for D.E.N.

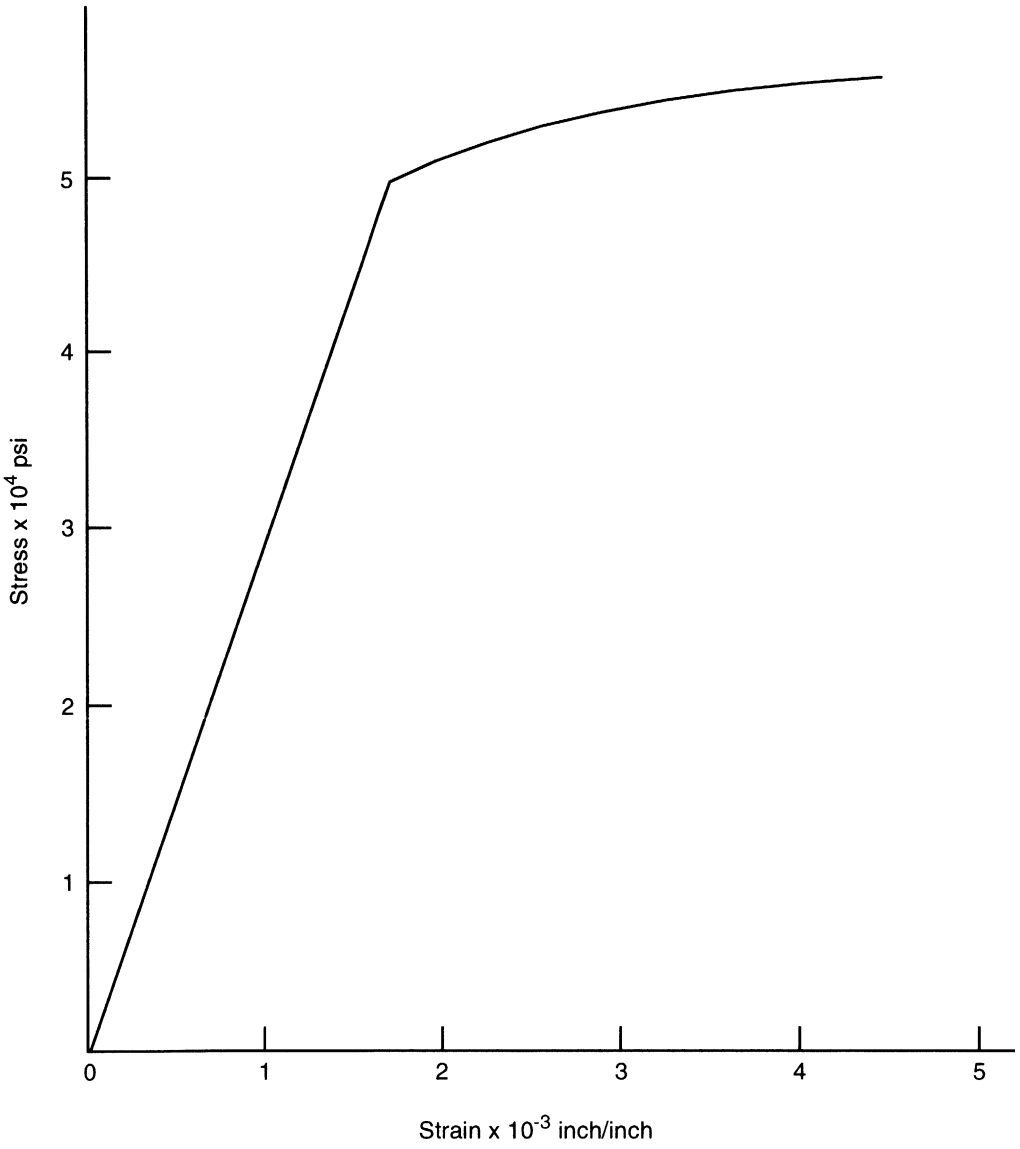

Figure 3.8-3 Workhardening Slopes

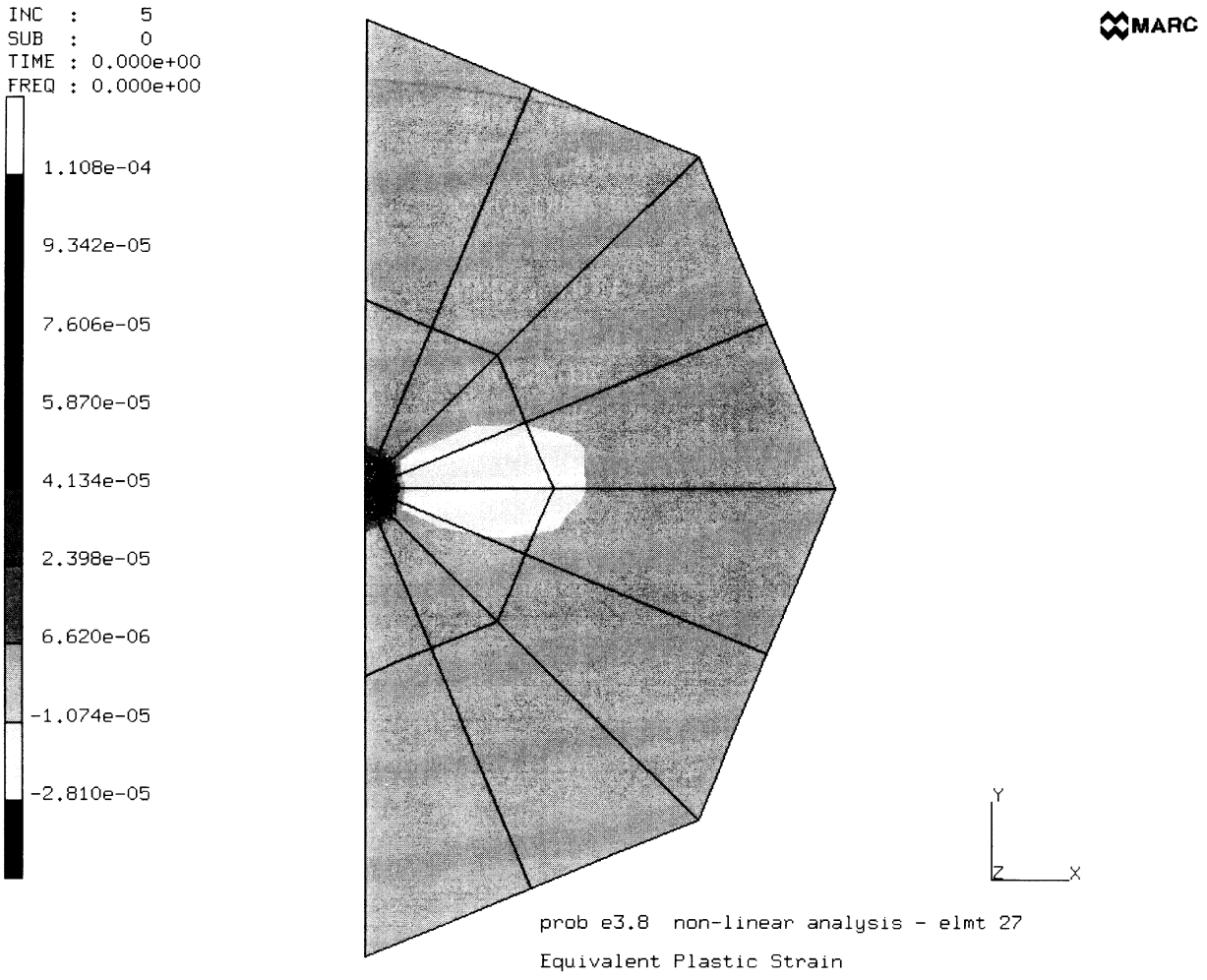

Figure 3.8-4 Equivalent Plastic Strain for Increment 5

3.9 Analysis of a Soil with a Cavity, Mohr-Coulomb Example

The availability of complex yield functions in the material library of MARC allows the modeling of many problems involving materials with hydrostatic yield dependence, such as ice, soil, and rock. A parabolic hydrostatic stress dependency is available as an alternative to the more usual linear model, so that the hydrostatic dependence of the yield function can be closely modeled over a wider range of stress. The dilatancy can be made a function of the hydrostatic stress using parabolic dependency; therefore, it is felt that this is a more straightforward approach than adopting a nonassociative flow rule (see "Theories of Plasticity and the Failure of Soil Masses" by E. H. David in *Soil Mechanics, Selected Topics*, I. K. Lee, ed., American Elsevier Publishing Co., 1968). As an example of the various yield functions, a simple structure was analyzed under small displacement assumptions and plane strain conditions.

Element

The plane-strain quadrilateral element type 11 is used in this example.

Model

The geometry of the generated mesh used is shown in Figure 3.9-1. The final model consists of 80 elements, 99 nodes, and 198 degrees of freedom.

Geometry

This option is not required for this element as a unit thickness is considered.

Boundary Conditions

A plane strain condition is assumed. The displacement boundary conditions are due to symmetry on the inner edges ($y = 0$ and $x = 0$). The zero displacement at all points on the rigid circular cutout ($x^2 + y^2 = 50$) is zero, representing a rigid inclusion.

Loading

The edge ($y = 300$) is loaded with a uniform pressure in an incremental fashion. The initial load is scaled to a condition of first yield and is proportionally incremented using the automatic load incrementation option for several steps. No other forms of load are applied.

Material Properties

The material is assumed to have elastic constants: $E = 5.0 \times 10^5$ psi and $\nu = 0.2$. Several yield surfaces were assumed:

1. von Mises material: $c = 140$ psi ($\sigma = 202$ psi).
2. Linear Mohr-Coulomb: $c = 140$ psi, $\phi = 30°$.

3. Parabolic Mohr-Coulomb: $c = 140$ psi, $\alpha = \frac{c}{\cos 30°}$.
4. Parabolic Mohr-Coulomb: $c = 140$ psi, $\alpha = c \tan 30°$.
5. Item (3) is such that the angle of friction at zero mean stress is the same as in the linear surface (2), while (4) has the same yield as (2) at zero shear. The plane-strain forms of those surfaces are shown in Figure 3.9-2. Their generalization into the (J_1 - J_2) plane is shown in Figure 3.9-3. For the present analysis only (1), (2) and (4) were used. The type of constitutive law is set in the ISOTROPIC option.

Results

Global load-displacement behavior is shown in Figure 3.9-4. Node 35 (at approximately x = 300) represents motion of the free surface in a negative x-direction.

The von Mises idealization shows first yielding at 167 psi pressure and reaches a limit load at about 230 psi pressure when all elements are in a state of plastic flow. The parabolic Mohr-Coulomb idealization yields first at 238 psi pressure. At 315 psi pressure, a sharp change in stiffness is observed. A limit load is not reached, though the stiffness is relatively low above the load.

The linear Mohr-Coulomb material shows a rather different behavior; after yielding initially at 264 psi pressure, a gradual change in stiffness occurs until, at about 400 psi pressure, all elements are flowing plastically. Above that load, the structure continues to respond with the same resistance, as the hydrostatic stress build up.

The stress fields at high load levels are shown for the various material idealizations in Figure 3.9-5 through Figure 3.9-10. Figure 3.9-5, Figure 3.9-6, and Figure 3.9-7 show σ_{yy} for von Mises, linear Mohr-Coulomb and parabolic Mohr-Coulomb respectively; the von Mises material is just below limit load at 220 psi pressure. The linear Mohr-Coulomb is in the fully plastic state at 475 psi pressure, and the parabolic is close to the fully plastic state at 327 psi pressure. These stress fields are similar for the three materials. In Figure 3.9-8 and Figure 3.9-9, the mean normal stress and deviatoric stress ($\sqrt{3J_2}$) are shown for the linear Mohr-Coulomb model in the fully plastic state (p = 475 psi). The linear relation between these stress measures is apparent. Notice the high compression just above the cutout and on the edge of the prism. The edge stress is probably due to the symmetry condition and the plain strain constant. Figure 3.9-10 shows two stress measures (mean normal and deviatoric, respectively) for the parabolic Mohr-Coulomb model close to the fully plastic state (at p = 327 psi). Here the ($\sqrt{3J_2}$) plot shows a more uniform field, since the parabola in the (J_1 - J_2) plane is considerably reduced in slope compared to the straight line at the hydro-static stress levels (see Figure 3.9-3).

Finally, in Figure 3.9-10, the contours of plastic strain are displayed. Interestingly, the peak value is somewhat above the cutout, at x = 0, y = 100.

Input Deck

The input deck is set up to do only the analysis for the parabolic Mohr-Coulomb case. Appropriate changes are necessary for the other forms discussed. The contour plots shown were obtained using Mentat.

Parameters, Options, and Subroutines Summary

Example e3x9.dat:

Parameters	Model Definition Options	History Definition Options
ELEMENTS	CONNECTIVITY	AUTO LOAD
END	CONTROL	CONTINUE
SCALE	COORDINATES	PROPORTIONAL INCREMENT
SIZING	DIST LOADS	
TITLE	END OPTION	
	FIXED DISP	
	ISOTROPIC	
	OPTIMIZE	

MARC

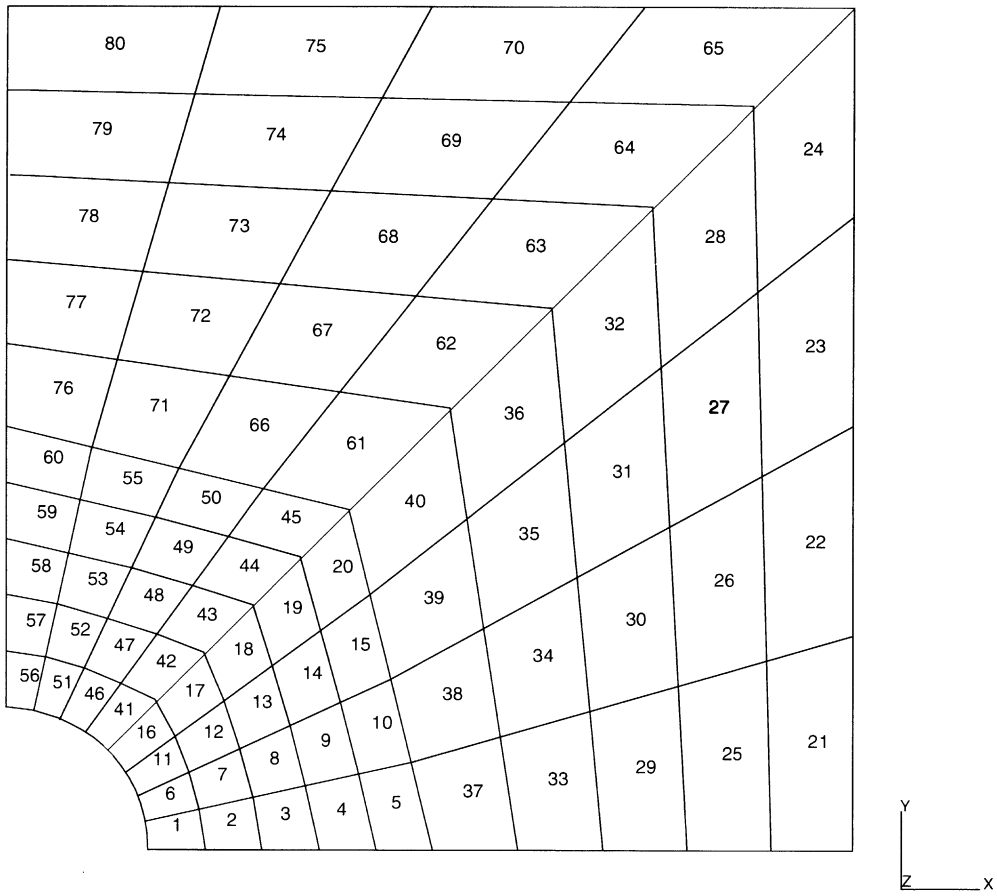

Figure 3.9-1 Simple Geometry Mesh

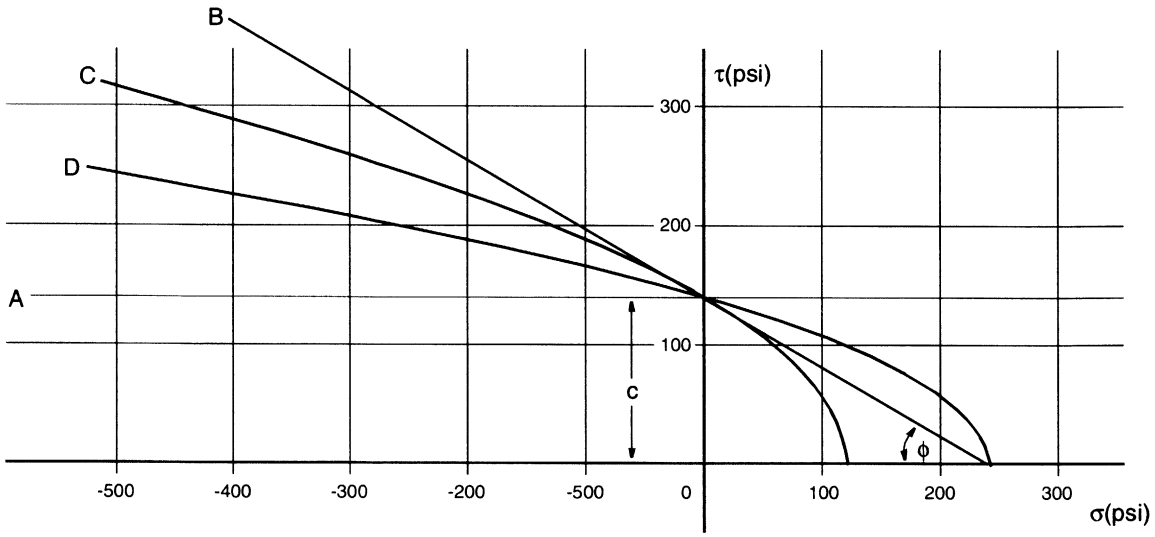

A – von Mises, c = 140 psi
B – Linear Mohr-Coulomb, c = 140 psi, f = 30°
C – Parabolic Mohr-Coulomb, c = 140 psi, $\alpha = \frac{c}{\cos 30°}$
D – Parabolic Mohr-Coulomb, c = 140 psi, $\alpha = c \tan 30°$

Figure 3.9-2 Plane Strain Yield Surfaces

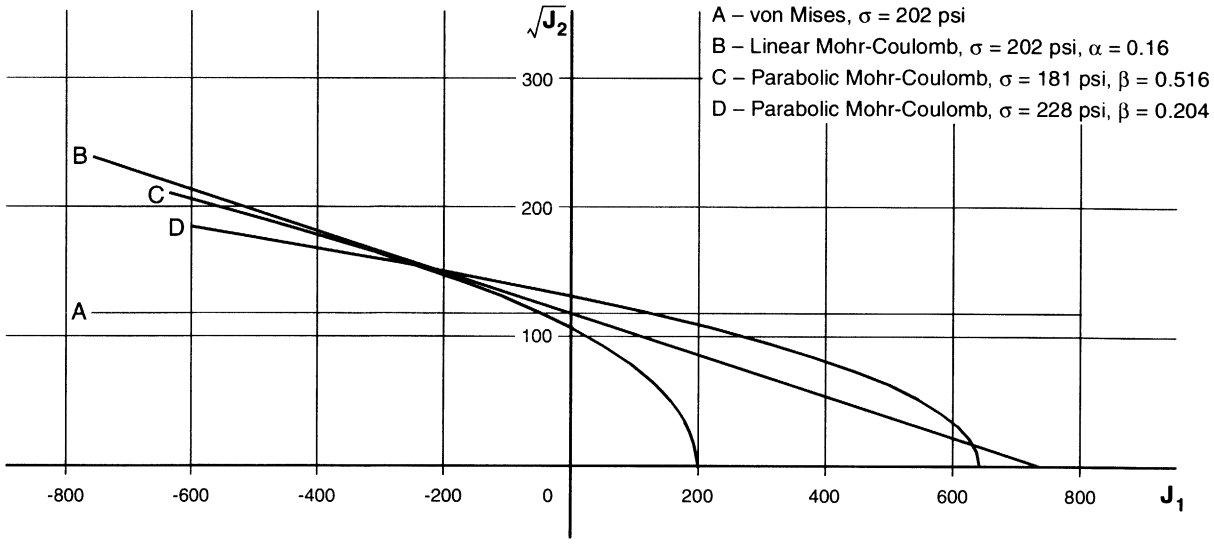

A – von Mises, σ = 202 psi
B – Linear Mohr-Coulomb, σ = 202 psi, α = 0.16
C – Parabolic Mohr-Coulomb, σ = 181 psi, β = 0.516
D – Parabolic Mohr-Coulomb, σ = 228 psi, β = 0.204

Figure 3.9-3 Yield Surfaces in $J_1 - \sqrt{J_2}$ Plane

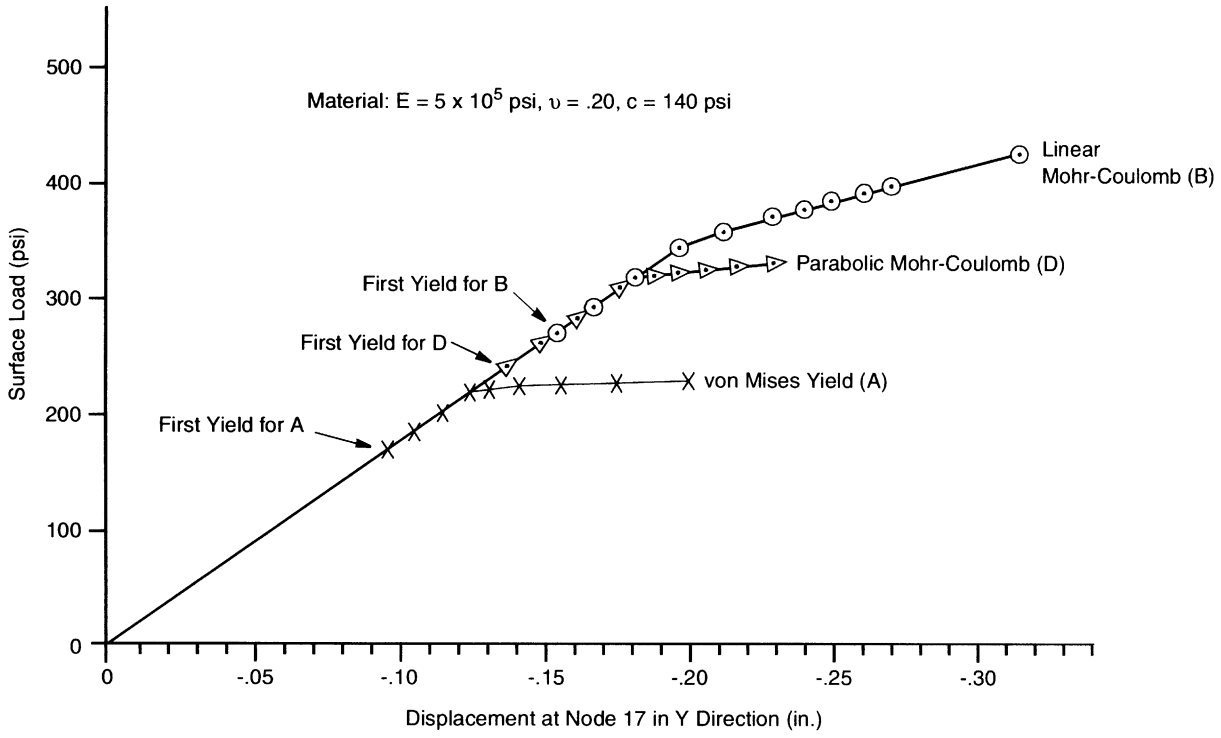

Figure 3.9-4 Global Load Displacement

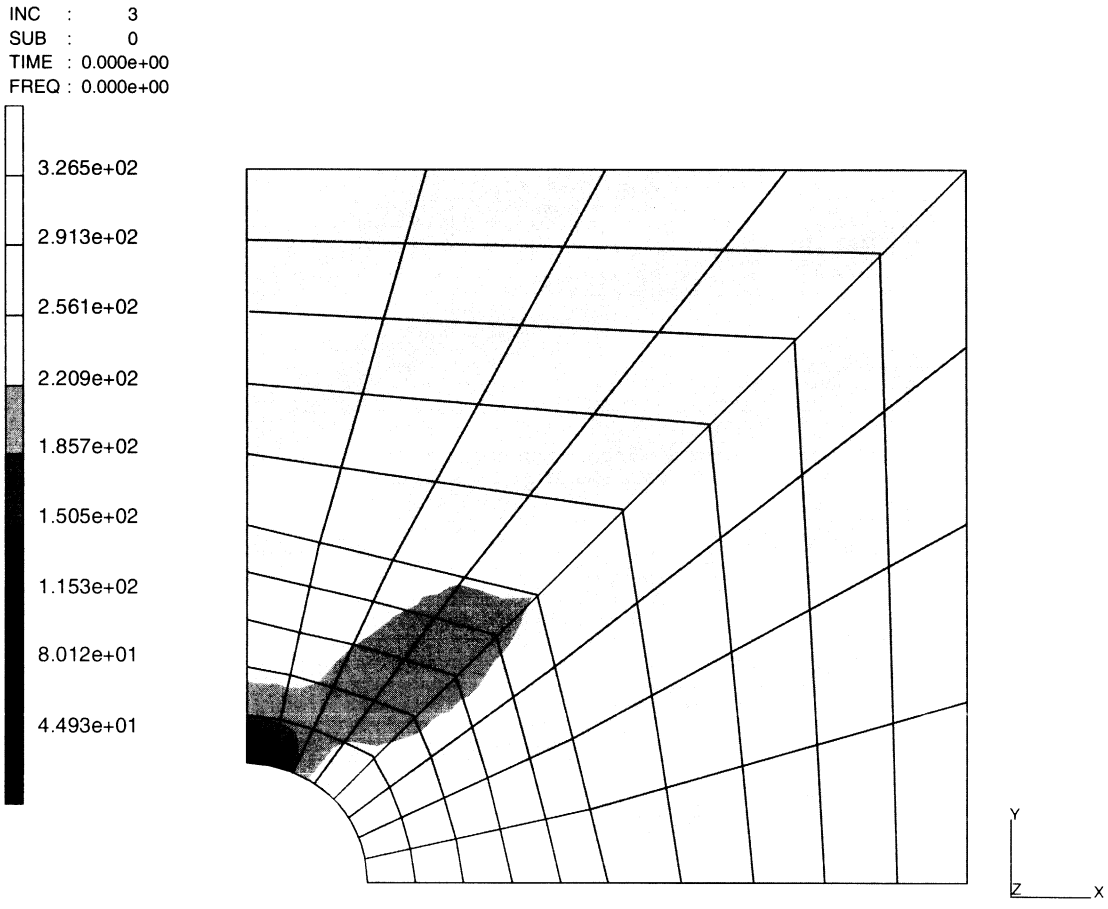

Figure 3.9-5 Equivalent Stress at 307 psi

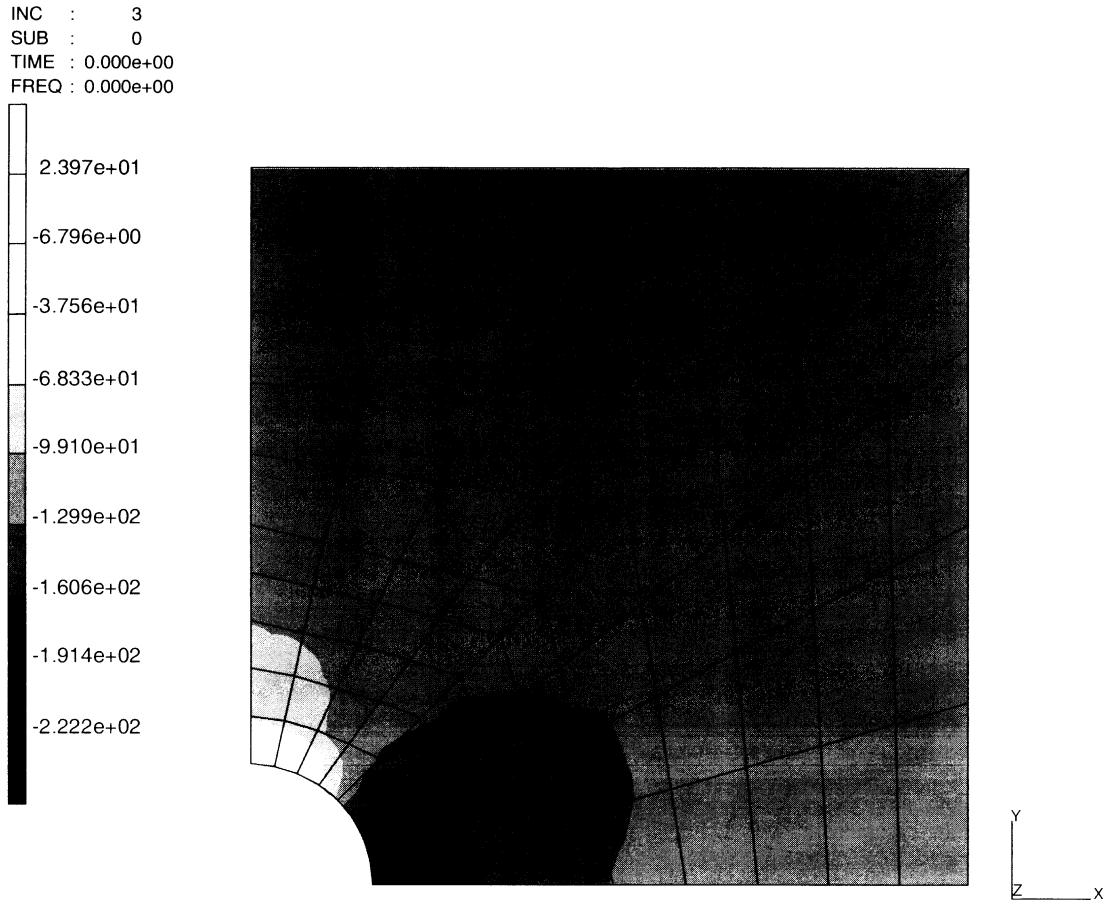

Figure 3.9-6 Mean Normal Stress at 307 psi

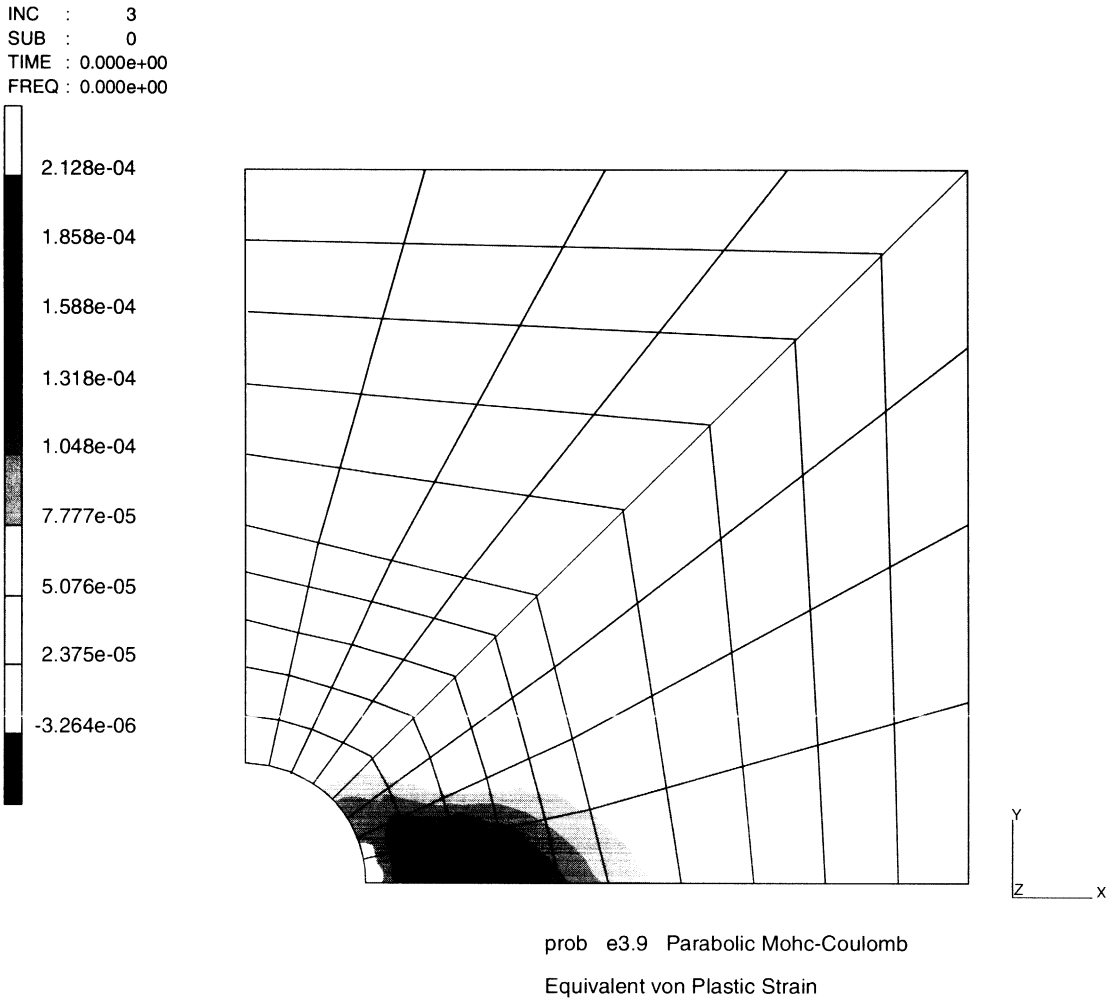

Figure 3.9-7 Equivalent Plastic Strain at 307 psi

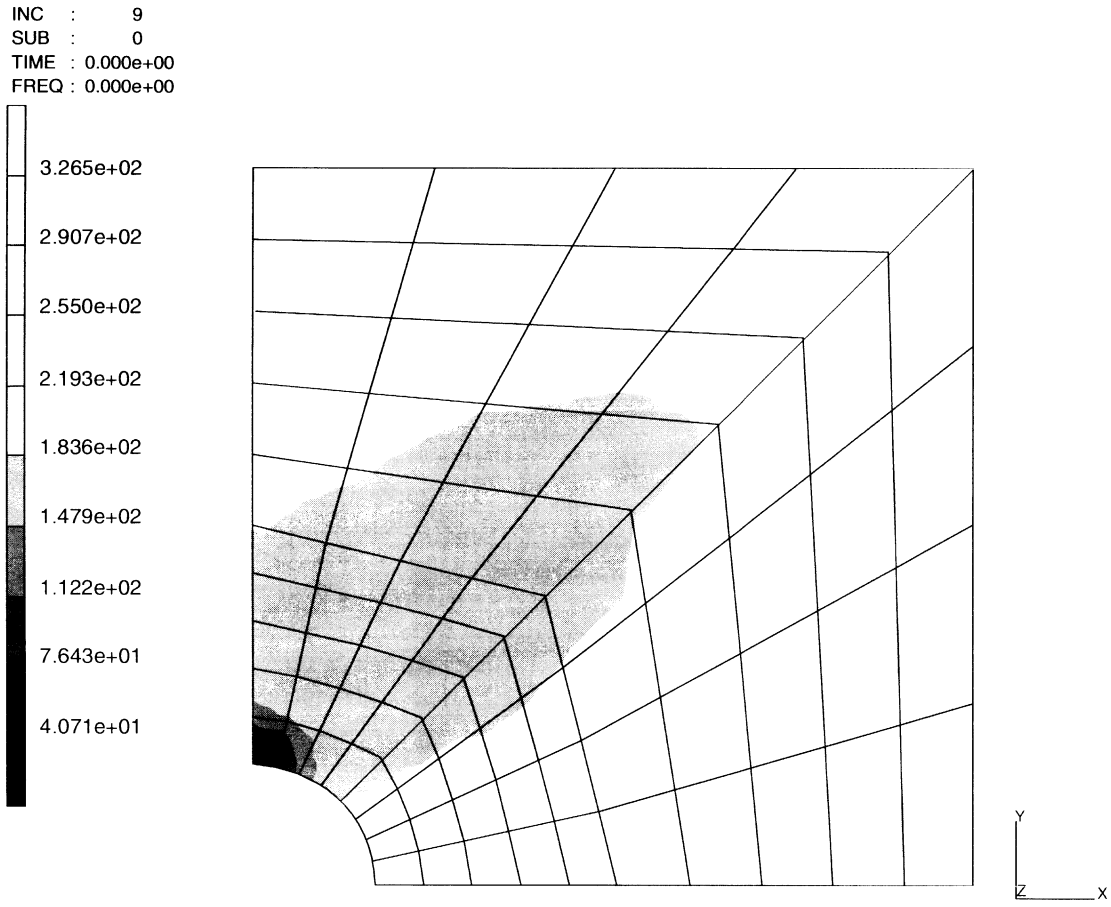

Figure 3.9-8 Equivalent von Mises Stress at 475 psi

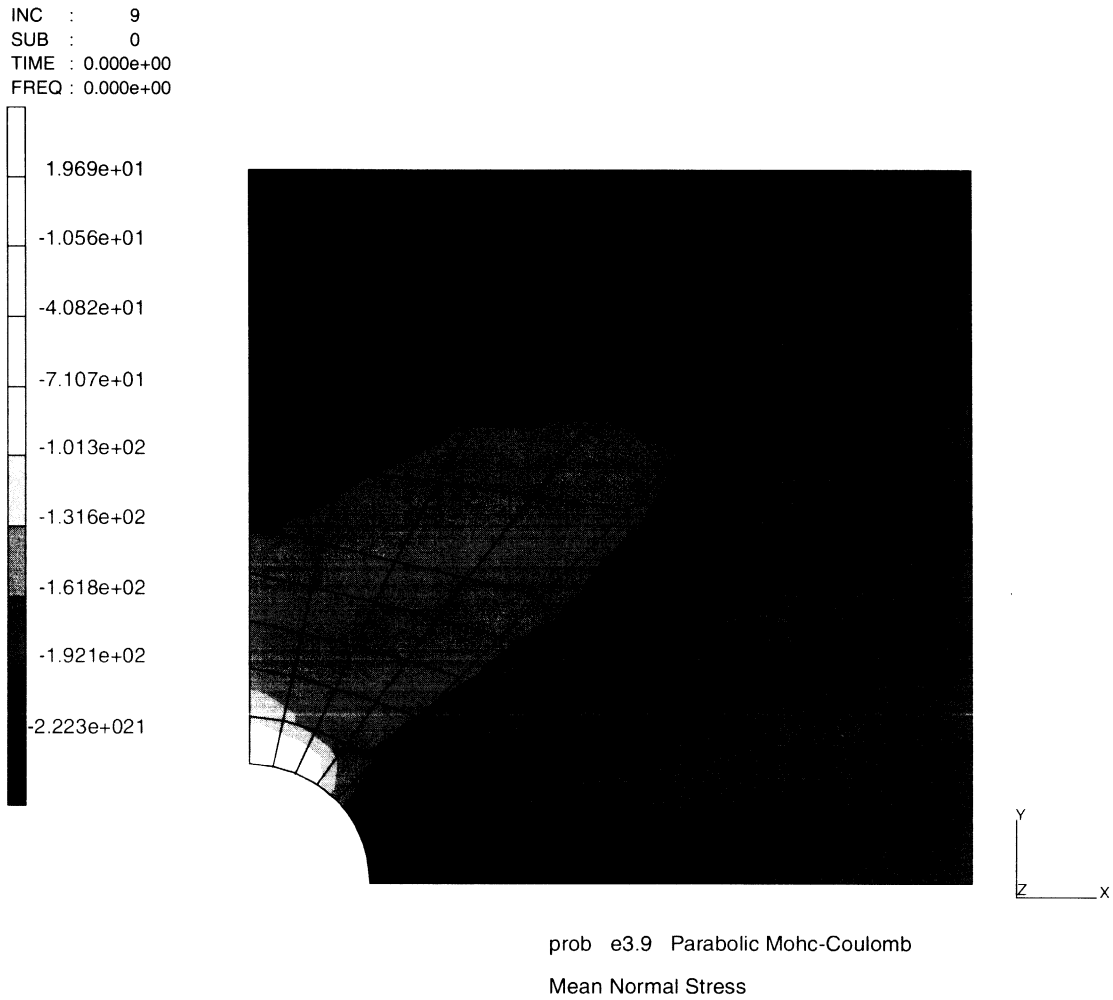

Figure 3.9-9 Mean Normal Stress at 475 psi

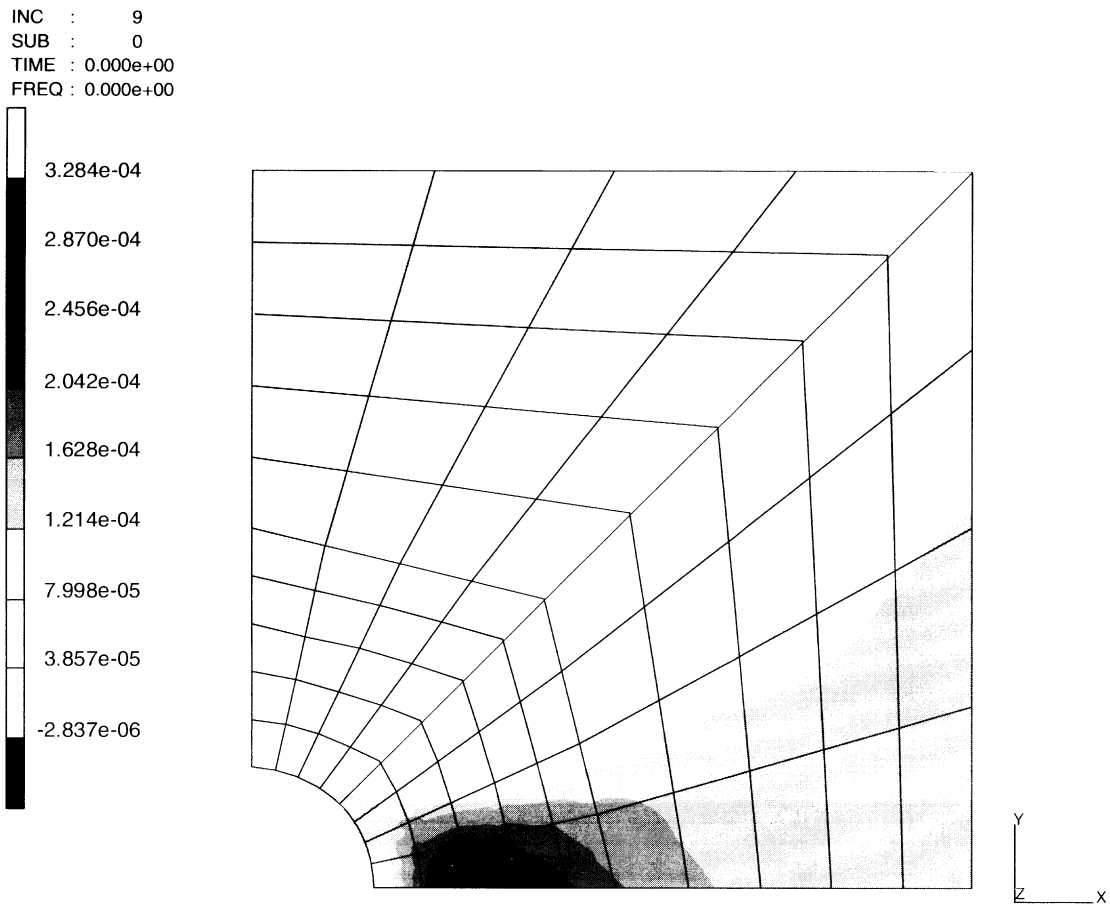

Figure 3.9-10 Equivalent Plastic Strain at 475 psi

3.10 Plate with Hole Subjected to a Cyclic Load

A plate with hole under the action of an in-plane force is loaded into an elastic-plastic range. The load is reversed until it reaches an absolute value which is the same as the initial load. The material is elastic-plastic with combined isotropic and kinematic hardening.

Element

Element 26 is an 8-node plane-stress quadrilateral.

Model

The mesh, consisting of 20 elements and 79 nodes, is shown in Figure 3.10-1.

Geometry

The thickness of the plate is specified as 1.0 in. in EGEOM1.

Boundary Condition

Boundary conditions are used to enforce symmetry about the x- and y-axes.

Material Properties

The material is elastic-plastic with combined isotropic and kinematic hardening. Values for Young's modulus, Poisson's ratio, and yield stress used here are 30×10^6 psi, 0.3, 50×10^3 psi, respectively.

Workhard

Five sets of workhardening slope and breakpoint are used to define the workhardening curve as shown in Figure 3.10-2:

First workhardening slope	$= 14.3 \times 10^6$, breakpoint = 0.
Second workhardening slope	$= 3. \times 10^6$, breakpoint = 0.7×10^{-3}
Third workhardening slope	$= 1.9 \times 10^6$, breakpoint = 1.6×10^{-3}
Fourth workhardening slope	$= 0.67 \times 10^6$, breakpoint = 2.55×10^{-3}
Fifth workhardening slope	$= 0.3 \times 10^6$, breakpoint = 3.3×10^{-3}

The final slope is used for the kinematic hardening portion of the workhardening behavior.

Loading

An initial in-plane tension is applied on the top edge of the mesh. SCALE is used to raise this tension to a magnitude such that the highest stressed element (in this case element 8) is at first yield. The tension is then incremented to 130% of load to first yield in five steps. The in-plane load is then reversed in direction and is incremented to the same absolute magnitude in 19 steps.

Optimization

The Cuthill-McKee algorithm is used to obtain a nodal bandwidth of 26 after 10 trials. The correspondence table is written to unit 1.

Results

The plate with hole reaches yield stress at a tension of 1.62×10^4 pounds. As the tension increases to 130% of yield load (2.1×10^4 pounds) in 5 increments, yielding advances from integration point 2 to 5 of element 8. The maximum effective plastic strain is around 3.3×10^{-4}. After the in-plane load is reversed in direction and incremented to the same absolute maximum in 19 steps, the maximum effective plastic strain is 2.0×10^{-4}. A contour plot of von Mises stress for increment 23 is shown in Figure 3.10-3. The displacements are shown in Figure 3.10-4. The PRINT CHOICE option is used to restrict the output to layers 2, 5, and 8 of elements 7 and 8.

Parameters, Options, and Subroutines Summary

Example e3x10.dat:

Parameters	Model Definition Options	History Definition Options
ELEMENTS	CONNECTIVITY	AUTO LOAD
END	CONTROL	CONTINUE
SCALE	COORDINATES	PROPORTIONAL INCREMENT
SIZING	DIST LOADS	
TITLE	END OPTION	
	FIXED DISP	
	GEOMETRY	
	ISOTROPIC	
	PRINT CHOICE	
	WORK HARD	

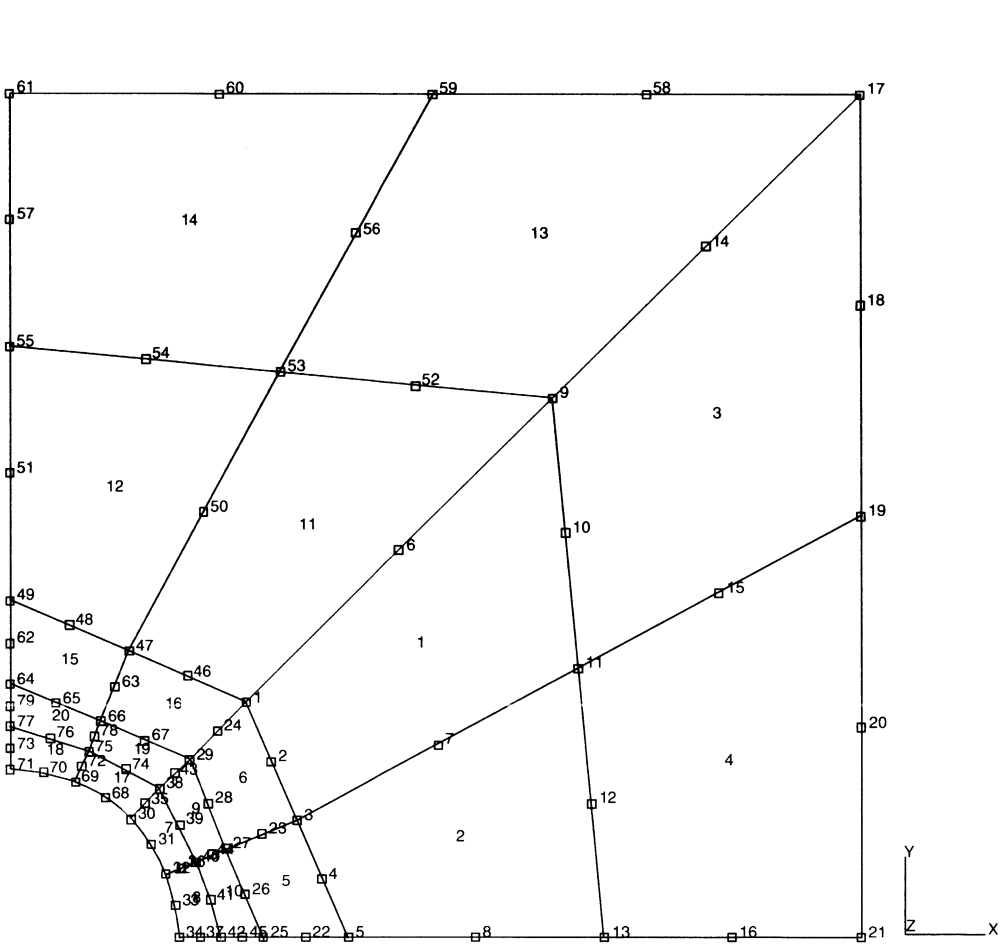

Figure 3.10-1 Mesh Layout for Plate with Hole

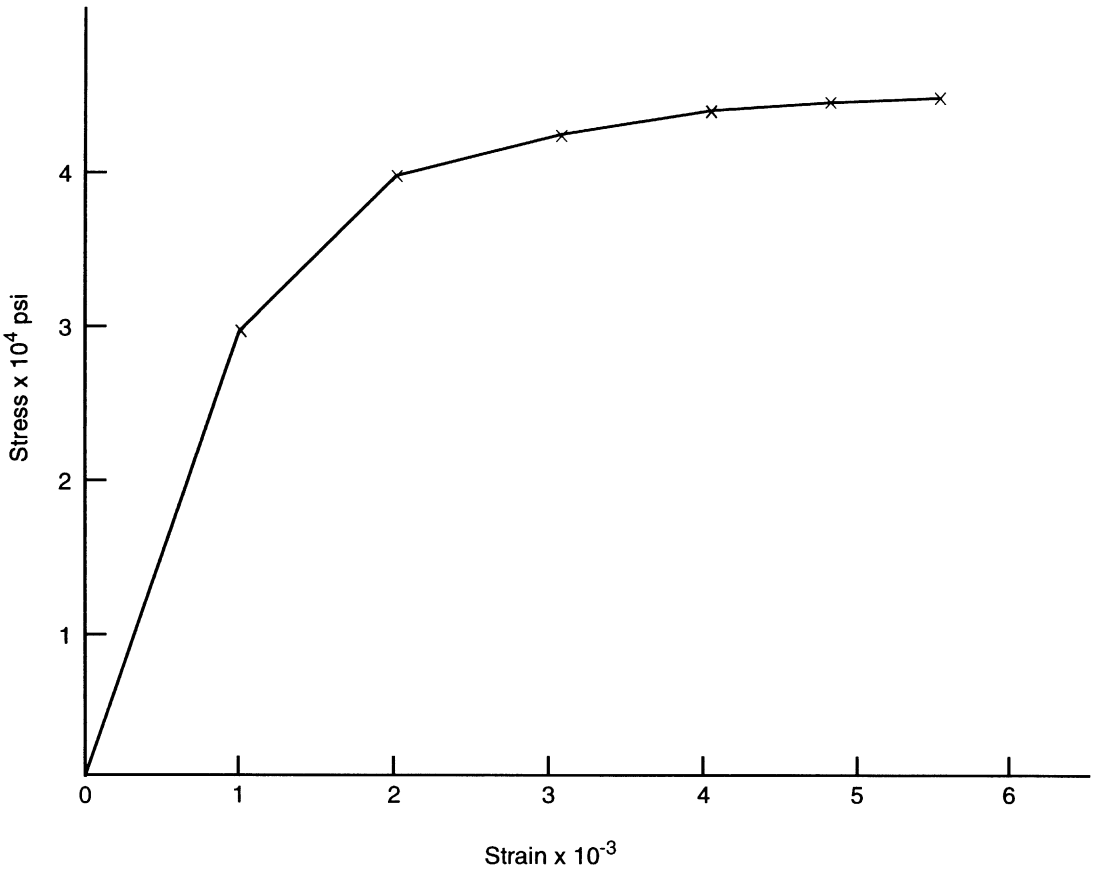

Figure 3.10-2 Workhardening Curve

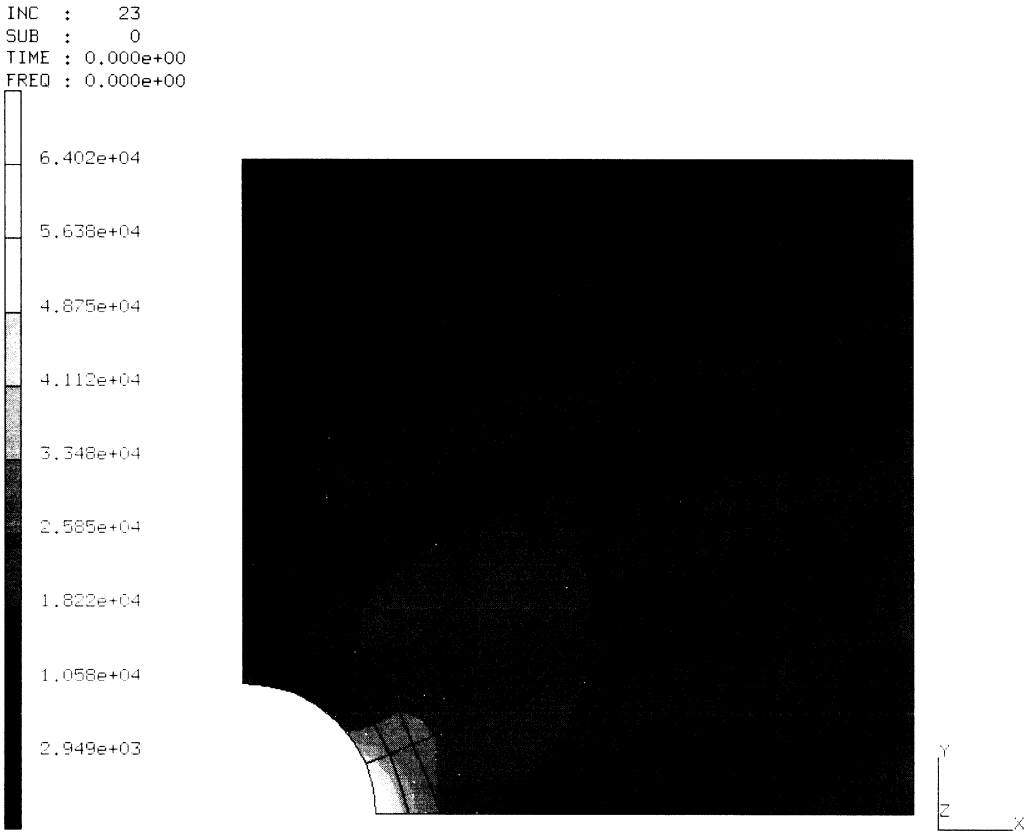

Figure 3.10-3 von Mises Stress Results

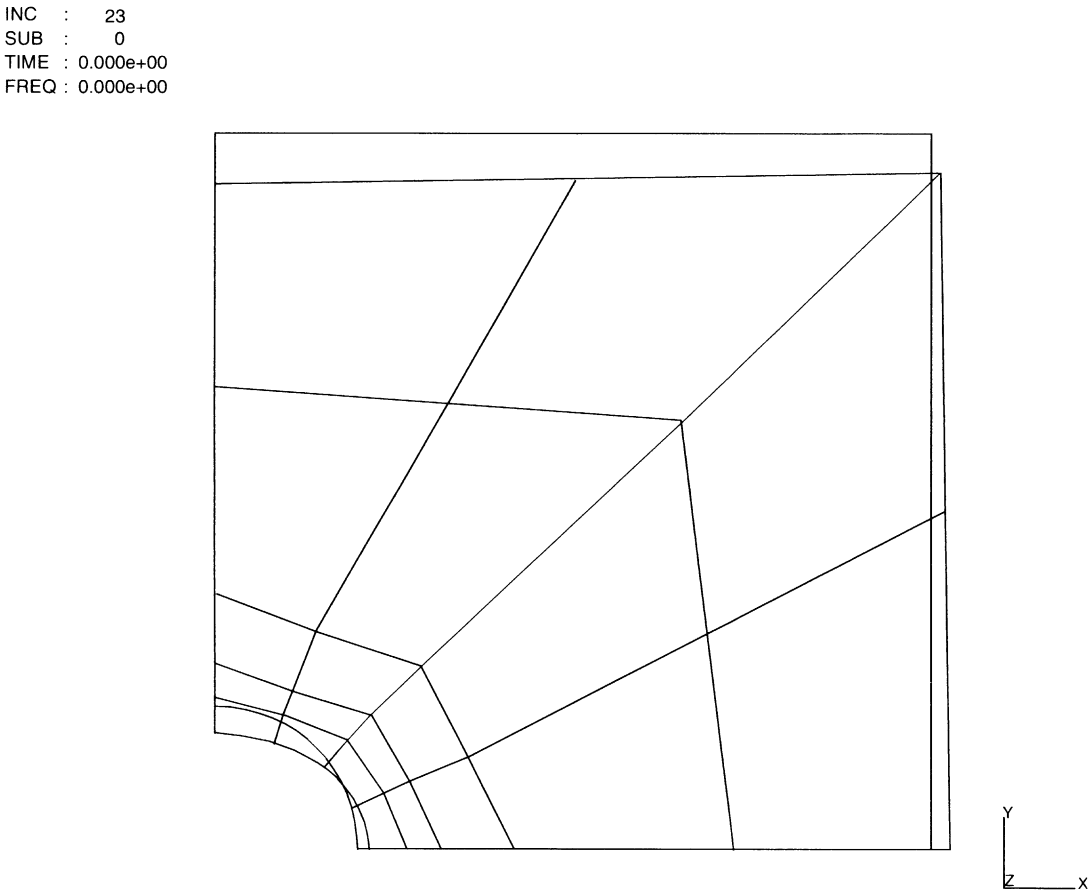

Figure 3.10-4 Displaced Mesh

3.11 Axisymmetric Bar in Combined Tension and Thermal Expansion

An axisymmetric bar under combined tension and thermal expansion is loaded into the elastic-plastic range. The bar is loaded in tension to yield, and the temperature and mechanical load are subsequently increased.

Element

Element type 28 is an 8-node distorted quadrilateral.

Model

The geometry of the bar and the mesh are shown in Figure 3.11-1. The bar is divided into five elements with 28 nodes.

Geometry

This option is not required for this element.

Tying

The same axial displacements are imposed by TYING the first degree of freedom of all nodes in the loaded face (Z = 1) to node 3, producing a generalized plane-strain condition.

Boundary Conditions

Fixed boundary conditions in the z-direction are specified at the built-in end (Z = 0).

Material Properties

The material is assumed to be elastic-plastic with isotropic strain hardening. Values for Young's modulus, Poisson's ratio, coefficient of thermal expansion and yield stress used here are 10.0×10^6 psi, 0.3, 1.0×10^{-5} in/°F, and 20,000. psi, respectively.

Work Hard

A constant workhardening slope of 30.0×10^4 psi is used.

Loading

An end load of 10,000 pounds is first applied to the bar in the direction of the first degree of freedom of node 3 using the POINT LOAD option. The load is scaled to a condition of first yield. The temperature is then increased by a total of 500° in five steps. The mechanical load is scaled by a factor of 0.15376.

Results

The bar reaches yield stress due to tension at a load of 1.57×10^5 pounds. At the maximum temperature, the plastic strain is about 0.5% and the total load is 1.68×10^6 pounds. The loading is proportional; therefore, no iteration is required for a convergent solution. The PRINT CHOICE option is used to restrict the output to shell layers 2, 5, and 8. A restart file was created at every increment. This can be used to extend the analysis or for postprocessing.

Parameters, Options, and Subroutines Summary

Example e3x11.dat:

Parameters	Model Definition Options	History Definition Options
ELEMENTS	CONNECTIVITY	AUTO THERM
END	CONTROL	CHANGE STATE
SCALE	COORDINATES	CONTINUE
SIZING	END OPTION	PROPORTIONAL INCREMENT
THERMAL	FIXED DISP	
TITLE	ISOTROPIC	
	POINT LOAD	
	PRINT CHOICE	
	RESTART	
	WORK HARD	

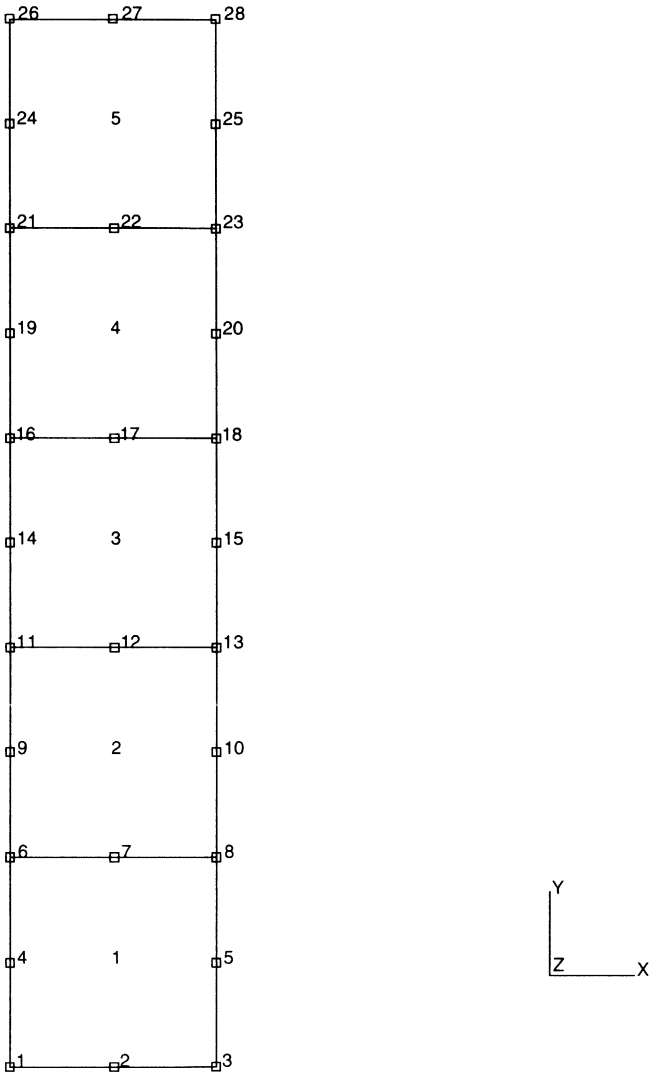

Figure 3.11-1 Axisymmetric Bar and Mesh

3.12 Creep of Thick Cylinder (Plane Strain)

A thick-walled cylinder loaded by internal pressure is analyzed using the creep analysis procedure available in MARC. This example provides you with guidelines for specifying stress and strain tolerances.

This problem is modeled using the two techniques summarized below.

Data Set	Element Type(s)	Number of Elements	Number of Nodes	Differentiating Features
e3x12	10	20	42	AUTO CREEP
e3x12b	10	20	42	AUTO STEP

Element

Element type 10, the axisymmetric quadrilateral, is used here.

Model

The geometry and mesh used are shown in Figure 3.12-1. The cylinder has an outer to inner radius ratio of 2 to 1. The mesh has 20 elements, 42 nodes and 84 degrees of freedom.

Geometry

This option is not required for this element.

Material Properties

The material data assumed for this example is: Young's modulus (E) is 30.0 x 10^6 psi, Poisson's ratio (v) is 0.3, and yield stress (σ_y) is 20,000 psi.

Loading

A uniform internal pressure of 1000 psi is applied to the inner wall of the cylinder using the DIST LOAD option. The inclusion of the SCALE parameter causes this load to be automatically scaled upward to 9081.3 psi which is the pressure load which causes the highest stress element (number 1 here) to be at a J_2 stress of 20,000 psi.

Boundary Conditions

All nodes are constrained in the axial direction such that only radial motion is allowed.

Creep

Creep analysis is flagged by use of CREEP and the conditions are set using the CREEP model definition block. The creep law used here is:

$$\dot{\varepsilon} = A\sigma^n \quad , \text{in/in-hr.}$$

where:

A is 1.075×10^{-26}

and:

n = 5.5 (where the stress is given in psi).

The exact, steady-state solution for this problem is:

$$\sigma_{zz} = \frac{p}{d}\left[\left(\frac{1}{n} - 1\right)\left(\frac{b}{r}\right)^{2/n} + 1\right]$$

$$\sigma_{rr} = \frac{p}{d}\left[\left(\frac{b}{r}\right)^{2/n} - 1\right]$$

$$\sigma_{\theta\theta} = \frac{p}{d}\left[\left(\frac{2}{n} - 1\right)\left(\frac{b}{r}\right)^{2/n} + 1\right]$$

where:

p is the internal pressure

a is the inside radius

b is the outside radius

and:

$$d = \left(\frac{b}{a}\right)^{2/n} - 1$$

The CREEP model definition option has set the fifth field to zero; therefore, the creep law has been introduced via user subroutine CRPLAW (see *MARC Volume D: User Subroutines & Special Routines).*

Creep Control Tolerances – AUTO CREEP Option

MARC runs a creep solution (under constant load conditions) via the AUTO CREEP history definition option. This option chooses time steps automatically based on a set of tolerances and controls provided by you. These are as follows:

1. Stress Change Tolerance (AUTO CREEP Model Definition Set, Line 3, Columns 11-20). This tolerance controls the allowable stress change per time step during the creep solution, as a fraction of the total stress at a point. The stress changes during the transient creep, and the creep strain rate is usually very strongly dependent on stress (in this case, the dependence is $\sigma^{5.5}$); this tolerance governs the accuracy of the transient creep response. Due to accurate track of the transient, a tight tolerance (1% or 2% stress change per time step) should be specified. If only the steady-state solution is sought, a relatively loose tolerance (10-20%) can be assigned.

2. Creep Strain Increment Per Elastic Strain (AUTO CREEP Model Definition Set, Line 3, Columns 1-10).

   MARC explicitly integrates the creep rate equation, and hence requires a stability limit. This tolerance provides that stability limit. In almost all cases, the default of 50% represents that limit, and the user need not provide any entry for this value. Figure 3.12-6 illustrates the problems that can occur if the stability limit is violated.

3. Maximum Number of Recycles for Satisfaction of Tolerances (AUTO CREEP Model Definition Set, Line 2, Columns 36-40).

   MARC chooses its own time step during AUTO CREEP based on the algorithm described below. In some cases, MARC may recycle in order to choose a time step to satisfy tolerances, but it is rare for the recycling to occur more than once per step. If excessive recycling occurs, it may be because of physical problems (such as creep buckling), bad coding of user subroutine CRPLAW, or excessive residual load correction. Excessive residual load correction occurs when the creep solution begins from a state which is not in equilibrium. This entry prevents wasted machine time by limiting the number of cycles to a prescribed value. The default of 5 cycles is reasonable in most normal cases.

4. Low Stress Cut-Off (AUTO CREEP Model Definition Set, Line 3, Columns 21-30.)

   This control avoids excessive iteration and small time steps caused by tolerance checks on elements with small round-off stress states. A simple example is a beam column in pure bending – the stress on the neutral axis will be a very small number; it would make no sense to base time step choice on satisfying tolerances at such points. The default here of 5% is satisfactory for most cases – MARC does not check those points where the stress is less than 5% of the highest stress in the structure.

5. Choice of Element For Tolerance Checking (AUTO CREEP Model Definition Set, Line 7, Columns 31-35.)

   The default option for creep tolerance checking is having all integration points in all elements checked. To save time, tolerances are checked in one selected element – this field is then used to select that element. Usually, the most highly stressed element is chosen.

Notes

All stress and strain measures used in tolerance checks are second invariants of the deviatoric state (that is, equivalent von Mises uniaxial values).

All tolerances and controls can be reset upon restart.

When a tolerance or control can be entered in two places (for example, on the CREEP or CONTROL model definition set), the values or defaults provided by the last of these options in the input deck are used.

Auto Creep

This history definition set chooses time steps according to an automatic scheme based on the tolerances described above. AUTO CREEP is designed to take advantage of diffusive characteristics of most creep solutions – rapid initial gradients which settle down with time. The algorithm is as follows:

- For a given time step Δt, a solution is obtained.
- The largest value of stress change per stress $\left|\frac{\Delta\sigma}{\sigma}\right|$ and creep strain change per elastic strain, $\left|\frac{\varepsilon^c}{\varepsilon^e}\right|$ are found. These are compared to the tolerance values set by the user, T_σ and T_ε.

- Then the value p is calculated as the bigger of $\left|\frac{\Delta\sigma}{\sigma}\right| / T_\sigma$ or $\left|\frac{\Delta\varepsilon^c}{\varepsilon^e}\right| / T_\varepsilon$.

  a. Clearly if $p > 1$, the solution is violating one of your tolerances in some part of the structure. In this case, MARC resets the time step as:

  $\Delta t_{new} = \Delta t_{old} * .8/p$

  that is, as 80% of the time step which would just allow satisfaction of the tolerances. The time increment is then repeated. Such repetition continues until tolerances are successfully satisfied, or until the maximum recycle control is exceeded – in the latter case the run is ended. Clearly, the first repeat should satisfy tolerances – if it does not, the cause could be:

  excessive residual load correction
  creep buckling – creep collapse
  bad coding in subroutine CRPLAW or VSWELL

  and appropriate action should be taken before the solution is restarted.

  b. If $p<1$ the solution is satisfactory in the sense of the user supplied tolerances. In this case, the solution is stepped forward to $t+\Delta t$ and the next time step begun. The time step used in the next increment is chosen as:

  $\Delta t_{new} = \Delta t_{old}$ if $0.8 \le p \le 1.0$

  $\Delta t_{new} = 1.25 * \Delta t_{old}$ if $0.65 \le p \le 0.8$

  $\Delta t_{new} = 1.5 * \Delta t_{old}$ if $p \ge 0.65$

The diffusive nature of the creep solution is utilized to generate a series of monotonically increasing time steps.

Results

Four solutions were found and compared to the steady-state solution as shown in Table 3.12-1 using the notation below.

1. Column A – 3% stress tolerance, 30% strain tolerance, with residual load correction.
2. Column B – 10% stress tolerance, 50% strain tolerance, with residual load correction.
3. Column C – 10% stress tolerance, 100% strain tolerance, with residual load correction.

These solutions are compared (at 20 hours) in Table 3.12-1. Graphical comparisons are drawn in Figure 3.12-2 through Figure 3.12-6.

Table 3.12-1 Creep of Thick Cylinder – Comparison of Results at 20 Hours

Stress	Location	EXACT Steady-State	A (85)†	B (48)	C (42)
σ_{zz}	inside (r=1.025)	-1372.2	-1369.2	-1375.4	-1332.8
	middle (r=1.475)	2725.1	2725.1	2725.6	2725.3
	outside (r=1.975)	5641.0	5635.9	5636.7	5638.2
σ_{rr}	inside	-8717.0	-8712.4	-8714.0	-8710.9
	middle	-3709.2	-3707.1	-3707.4	-3707.3
	outside	-145.24	-144.49	-144.56	-144.58
$\sigma_{\theta\theta}$	inside	5972.6	5974.0	5948.3	6072.8
	middle	9159.3	9158.0	9158.9	9156.4
	outside	11427.0	11424.0	11425.0	11426.0
σ	inside	12741.0	12719.0	12698.0	12803.0
	middle	11144.0	11141.0	11143.0	11140.0
	outside	10022.0	10019.0	10019.0	10020.0

†Number of steps required to reach 20 hours.

All solutions are satisfactory in the sense that monotonic convergence, with monotonic increase in time-step size, is achieved except for the strain-controlled part of the solution with 100% strain tolerance. Here the stresses oscillate. In fact, it may be shown that the strain change repeats a numerical stability criterion, and that 50% is the stability limit. The residual load correction controls the oscillation in the sense that the solution does not diverge completely. The residual load correction has little effect until a large number of steady-state increments (that is, strain-controlled increments) have been performed. At this point, it is essential for an accurate solution. The 10% stress control allows a slightly more rapid convergence to steady-state. This control is quite satisfactory, considering that it reduces the number of increments needed by 42%.

Parameters, Options, and Subroutines Summary

Example e3x12a.dat:

Parameters	Model Definition Options	History Definition Options
CREEP	CONNECTIVITY	AUTO CREEP
END	CONTROL	CONTINUE
SCALE	COORDINATES	DIST LOADS
SIZING	CREEP	
TITLE	DIST LOADS	
	ELEMENT	
	END OPTION	
	FIXED DISP	
	ISOTROPIC	
	PRINT CHOICE	

Example e3x12b.dat:

Parameters	Model Definition Options	History Definition Options
CREEP	CONNECTIVITY	AUTO STEP
END	CONTROL	CONTINUE
SCALE	COORDINATES	DIST LOADS
SIZING	CREEP	
TITLE	DIST LOADS	
	ELEMENT	
	END OPTION	
	FIXED DISP	
	ISOTROPIC	
	PRINT CHOICE	

User subroutine in u3x12.f:

CRPLAW

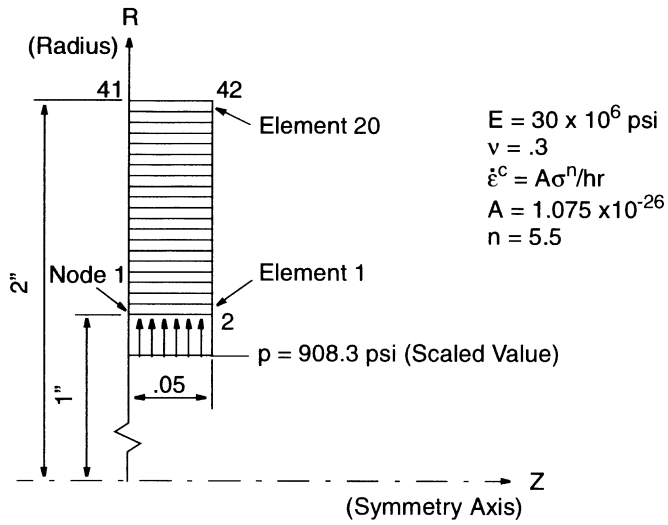

Figure 3.12-1 Thick Cylinder Geometry and Mesh

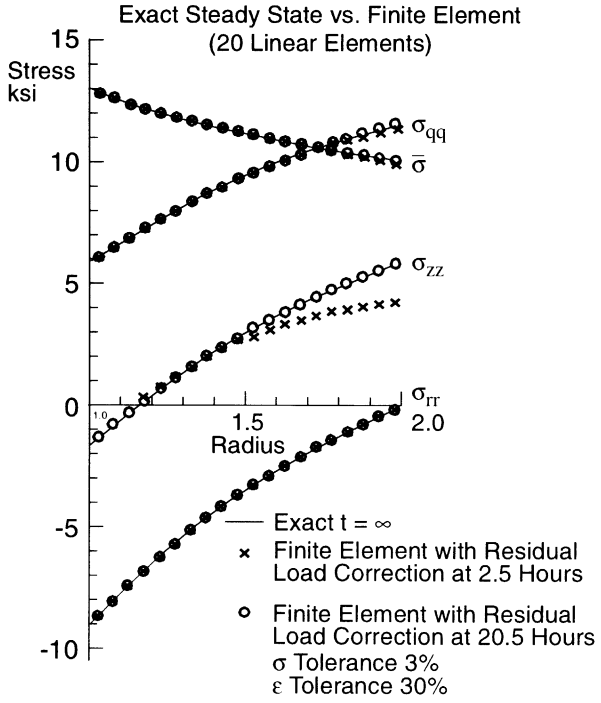

Figure 3.12-2 Creep of Thick Cylinder, Long Time Results

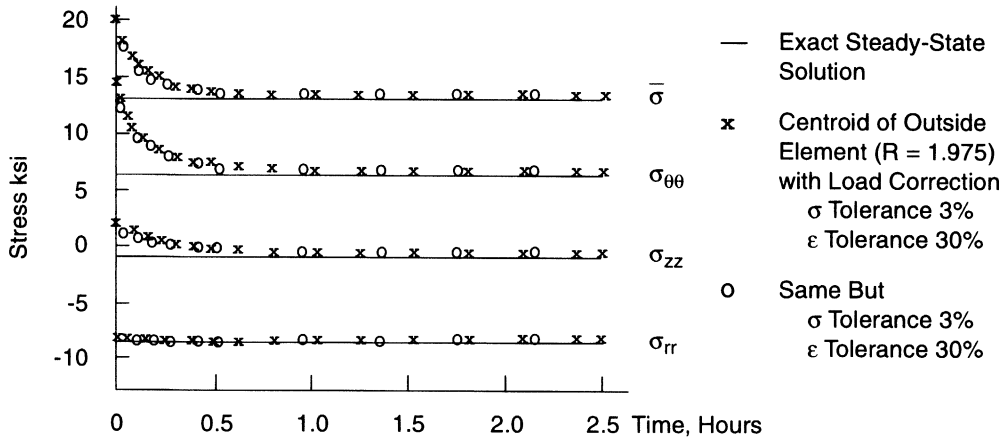

Figure 3.12-3 Creep of Thick Cylinder – Numerical Comparisons

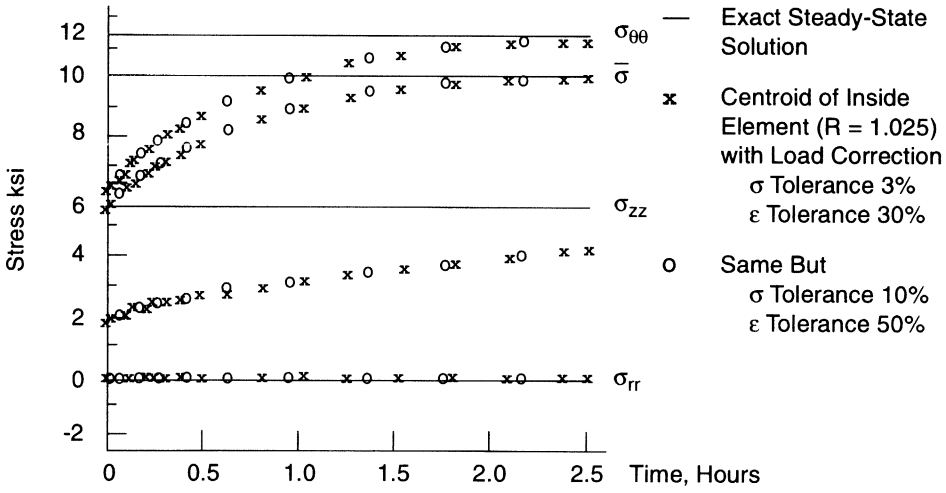

Figure 3.12-4 Creep of Thick Cylinder – Numerical Comparisons

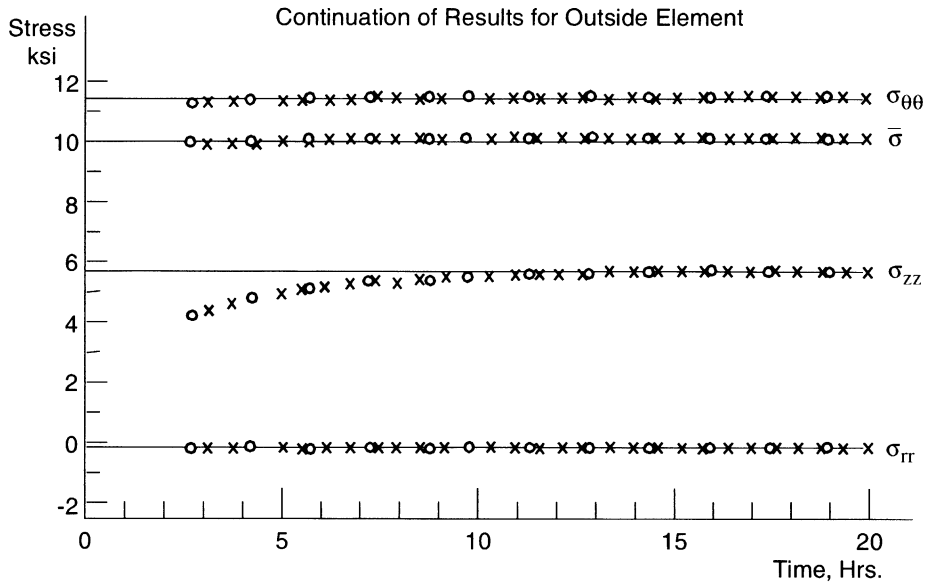

Figure 3.12-5 Creep of Thick Cylinder – Numerical Comparisons

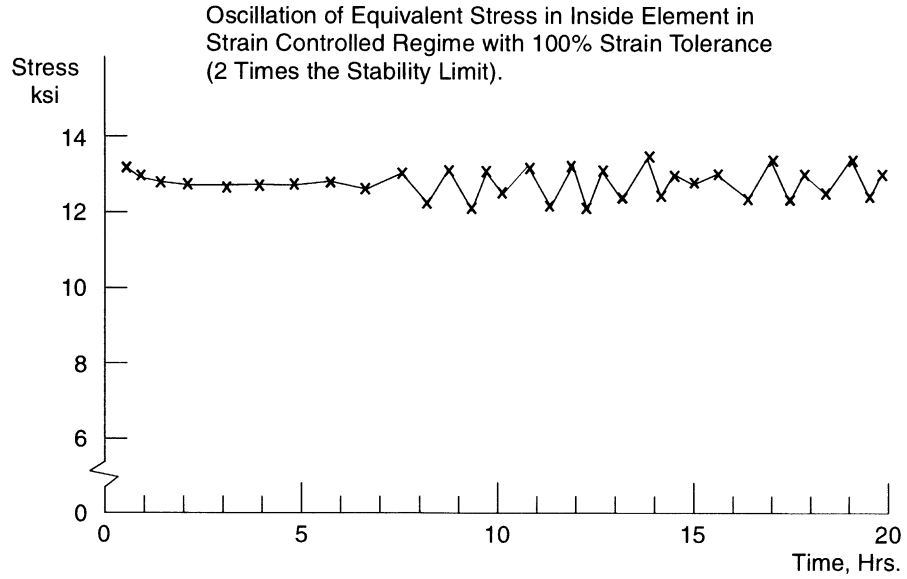

Figure 3.12-6 Creep Ring

3.13 Beam Under Axial Thermal Gradient and Radiation-induced Swelling

A hollow circular-section beam is analyzed under axial and transverse temperature gradients. It is also subject to a variable neutron flux field resulting in irradiation-induced creep swelling.

Element

In this problem, thermal gradients will result in an axial strain that varies along the length of the beam. Element type 14 only allows constant axial strain so it is not suitable here; element 25 is used instead. This is element type 14 with an additional local degree of freedom which allows nonuniform axial strain. Element type 25 is a closed-section straight beam element with no warping of the section, but including twist. The element has seven degrees of freedom per node; three displacements and three rotations in the global coordinate system and axial strain.

Model

The beam is constrained axially at its base; rotations are allowed. Reaction forces at the base and three collars are computed. Each reaction force is modeled by the use of a linear spring, one end of which is attached to the node at the base or collar point; the remaining end is attached to a fixed node. The springs are dimensionless and completely linear. There are 21 elements and 20 nodes for a total of 182 degrees of freedom (see Figure 3.13-1).

Geometry

The BEAM SECT can be used to specify a cross section other than the default (circular section) used here.

Material Properties

The material is elastic with a Young's modulus of 26.4×10^6 psi and Poisson's ratio of 0.3. The initial stress-free temperature is 400°F and the coefficient of thermal expansion is 0.96×10^{-5} in/in/°F.

Loading

Thermal gradients and neutron flux are the only loading imposed; no mechanical loads are applied.

Boundary Conditions

The beam end is fixed axially (u = o). In order to model reaction forces, the beam end and collar points are "fixed" by linear springs that are stiff enough to effectively zero the displacements.

User Subroutines

Long-term creep and swelling results are desired. Subroutine VSWELL is used. The creep law is written for 304 and 306 stainless steel. The swelling is written in accordance with ORNL recommendations.

The creep law can be expressed as:

$$\bar{\varepsilon}^{c} = A\bar{E} \bullet \bar{\sigma}(1 - \exp(-\bar{E}\phi t/B)) + C\bar{E}\phi \bullet \bar{\sigma}t$$

Differentiating:

$$\dot{\bar{\varepsilon}}^{c} = A\bar{E}\phi\bar{\sigma} \bullet \bar{E}\phi/B \bullet \exp(-\bar{E}\phi \bullet t/B) + C\bar{E}\phi \bullet \bar{\sigma}\varepsilon$$

where:

- $\bar{\varepsilon}^{c}$ is the equivalent creep strain
- t is the time (sec.)
- ϕ is the neutron density
- $\bar{E}$ is the mean neutron energy in MeV
- σ is the equivalent J_2 stress
- T is the temperature
- A = 1.7×10^{-23}
- B = 2.0×10^{20}
- C = 7.5×10^{-30}

The radiation-induced swelling strain model can be expressed as:

$$\frac{\Delta V\ \%}{V} = R\phi t + \frac{R}{\alpha}\ln\left[\frac{1 + \exp(\alpha(\tau - \phi t))}{1 + \exp\tau}\right]$$

where R, τ, α are functions of temperature. Differentiating:

$$100\dot{\varepsilon}_{ii} = R\phi - R\phi\left[\frac{\exp(\alpha(\tau - \phi t))}{(1 + \exp(\alpha(\tau - \phi t)))}\right]$$

$$R = \exp B$$

$$B = -88.5499 + 0.531072T - 1.24156 \times 10^{-3}T^2 + 1.37215 \times 10^{-6}T^3 - 6.14 \times 10^{-10}T^2$$

$$\tau = \exp[-16.7382 + 0.130532T - 3.81081 \times 10^{-4}T^4$$

To properly model the complex temperature and flux distributions for use by these subroutines, a subroutine CREDE has been written with two state variables. The first state variable is temperature; the second is the neutron flux density. Two linear gradients, in the coordinate

directions on the section, are assumed for both state variables. The four values of each variable at each node correspond to the values at the first, fifth, eighth, and thirteenth points on the section. The remaining values are determined by bilinear interpolation.

Special Considerations

The RESTART option is used, as the prediction of the number of increments that will be analyzed is difficult. The option also permits the input and output to be checked as often as each increment. When the problem is restarted, the parameters and loads can be changed. To modify the time increments specified in the AUTO CREEP option, the REAUTO model definition option would be necessary. The CONTROL option can be used to specify the number of increments in this analysis. To determine the creep increment input in the first field, second line of the AUTO CREEP option, the procedure outlined in *Volume A: Theory and User Information* was used. Briefly a "worst" case with highest stress and temperature (extracted from the elastic load case) is studied. The total strain rate is set to zero as in a relaxation test; then the initial creep strain rate and the tolerance for stress change (AUTO CREEP option, second field of the third line) are used to determine a conservative upper bound on the initial creep time step.

MARC used three Gaussian integration points per element rather than just the centroid for calculation and storage of element stresses.

The nonuniform temperature and flux information was input in the THERMAL LOADS option. A well-behaved temperature and flux variation could be generated within the CREDE subroutine, in which case the THERMAL LOAD series would consist of just the first two lines.

Results

After 4500 hours of creeping the plot of stress versus time changes from straightforward stress relaxation to an oscillation. This change is due to an increase in swelling contribution. Stress relaxation has been plotted in Figure 3.13-2.

Parameters, Options, and Subroutines Summary

Example e3x13.dat:

Parameters	Model Definition Options	History Definition Options
CREEP	CONNECTIVITY	AUTO CREEP
ELEMENTS	CONTROL	CONTINUE
END	COORDINATES	
SIZING	CREEP	
STATE VARS	END OPTION	
THERMAL	FIXED DISP	
TITLE	GEOMETRY	
	ISOTROPIC	
	PRINT CHOICE	
	RESTART	
	SPRINGS	
	THERMAL LOADS	

User subroutines in u3x13.f:

CREDE
VSWELL

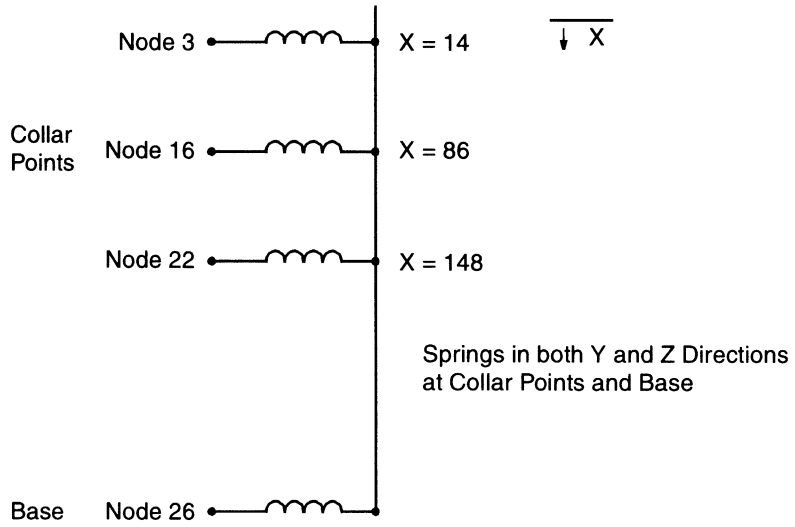

Figure 3.13-1 Beam-Spring Model

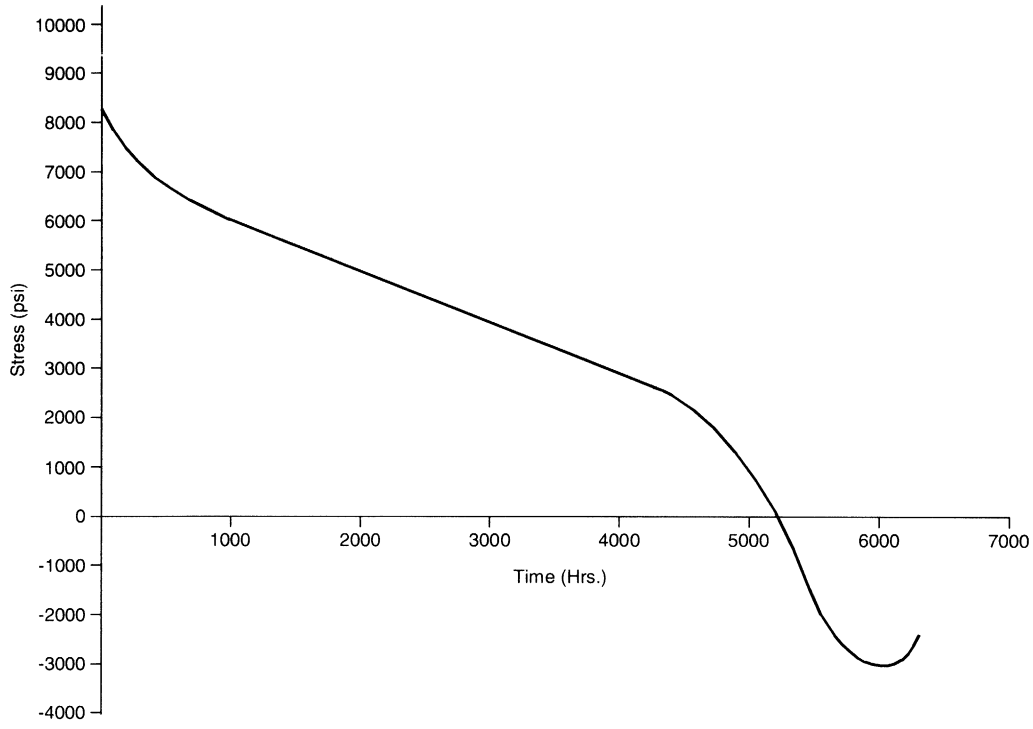

Figure 3.13-2 Transient Extreme Fiber Stress

3.14 Creep Bending of Prismatic Beam with ORNL Constitutive Equation and Load Reversal

A cantilever beam of 100 inches length, with a solid cross section of 4 inches height and 2 inches width, is subjected to a forced rotation of 1/20 radians at the free end at time zero (see Figure 3.14-1).

Due to creep, stress relaxation occurs. Subsequently, the prescribed rotation is reversed to -1/20 radians, and again stress relaxation is allowed to occur. The creep law is of the strain hardening type, and for load reversals follows the ORNL recommendation. Automatic time stepping is used in both creep periods.

Discussion of Constitutive Equation

The creep equation used in this example has the form:

$$\dot{\bar{\varepsilon}}^c = 10^{-24} f(\bar{\varepsilon}^c) \bar{\sigma}^5$$

where $f(\varepsilon^c)$ is specified through slope-breakpoint data. The MARC slope-breakpoint data assumes that at the first breakpoint the function f is equal to zero. However, for our constitutive equation it is required that f(0)=1. The first breakpoint is defined (in reality, this cannot occur) at an equivalent creep strain of -1.0, and a slope of 1.0 is entered. The function f will be 1.0 at the start of the analysis. The specified curve for positive equivalent creep strain is shown in Figure 3.14-2.

If a load reversal occurs, the ORNL rules take effect. In a uniaxial situation, these rules assume the existence of two values of the creep strain: ε^{c^+} and ε^{c^-}. For tension, ε^{c^+} is used in the calculation of $f(\varepsilon^c)$, and during tensile creep ε^{c^+} is updated. During compression, ε^{c^-} is used in the calculation of $f(\varepsilon^c)$, and ε^{c^-} is updated. After the first load reversal, ε^{c^-} is still zero and the material starts creeping as if no previous creep-strain hardening occurred. For the ORNL material relaxation of the stresses after load reversal, it starts more quickly than for a standard isotropically hardening material.

Element)

The two-dimensional cubic beam element, MARC type 16, is used in this analysis.

Model

Four elements are used in this example. The moment is constant throughout the beam; therefore, all elements will undergo the same deformation. The geometry of the mesh is shown in Figure 3.14-1.

Geometry

Beam height and width are specified in the first and second fields of the GEOMETRY option.

Material Properties

Linear elastic material behavior with Young's modulus (E) of 1 x 10^7 psi and Poisson's ratio (n) of 0.3 is specified on the ISOTROPIC option. Since no plasticity is assumed to occur, no yield stress is specified. The creep properties are specified on the CREEP model definition block. The CREEP properties were discussed before.

Boundary Conditions

Element 16 has as degrees of freedom: u, v, $\frac{du}{dv}$ and $\frac{dv}{ds}$. In this problem, the beam-axis corresponds with the x-axis, $\frac{dv}{ds}$ is equal to the rotation. Therefore, at node 1, both displacements and the rotation are suppressed, whereas at node 5 the rotation is prescribed as a nonzero value.

SHELL SECT

The SHELL SECT parameter is used to specify seven layers for integration through the thickness. Since the material does not have tangent-modulus nonlinearities, the elastic properties will be integrated exactly. The creep strain increment will be integrated with sufficient accuracy with the seven points specified.

PRINT CHOICE

In this option, output is requested at only one integration point (2) and one element (1), and nodal quantities are only printed at node 5. At the one integration point, all layers are printed, however.

Post File

A post file is written containing only the displacements and the reaction forces. This can be used by Mentat.

Creep Analysis Procedure

The AUTO CREEP option is used to analyze the first relaxation period of 200 hours. An initial time step of 100 hours is specified. MARC scales this down in order to obtain a starting value such that the tolerances are satisfied. All control parameters are set to their default values. The testing for the satisfaction of CREEP tolerances is done for element type 1 only. A zero rotation increment is specified for node 5 with the DISP CHANGE option. This is done in order to ensure

constant rotation during the creep period. A maximum number of increments in each AUTO CREEP block is 50; the total number of increments must be less than 80, as specified in the CONTROL option.

At the end of the first creep period, a rotation increment of negative-2 times the originally specified rotation is prescribed. This effectively reverses the loading. Then another creep period is started similar to the previous one.

Results

In increment zero, the elastic solution is obtained. The stress and strain in the extreme fiber of the beam are equal to 10^4 and 10^{-3} psi, respectively. With the specified creep law, this yields an initial creep strain rate of 10^{-4} hours^{-1}. If the stress change is to be less than 10% (the default on AUTO CREEP), the creep strain increment must be less than 10^{-4}. The initial time step must be less than 1. MARC selects an initial time step of 0.8. Due to the stress relaxation, the creep strain rate rapidly decreases, and MARC rapidly increases the time step. In 15 steps, the creep period of 200 hours is traversed. The last step prior to load reversal is equal to 42.7 hours. The stresses through the section before and after relaxation are shown in Figure 3.14-3. The creep strain in the extreme fibers has reached a value of 6.2×10^{-4}, and the creep strain rate has been reduced by a factor of more than 2 due to creep strain hardening.

Subsequently the load is reversed. The stresses in the extreme fibers now increase to a value of 1.622×10^4. Since the load is reversed, the ORNL creep equation predicts a creep rate as if no hardening had occurred: $\varepsilon^c = 11.23 \times 10^{-4}$ hours^1. In order to satisfy the creep tolerances, the initial time step must now be less than 0.1445 hours. MARC selects a time step of 0.1157 hours. Again, the time step rapidly increases during the creep period. Now, 20 steps are needed to cover the 200-hour period, with the time step in the last increment equal to 45 hours. The stress profiles at the beginning and the end of the increment are compared in Figure 3.14-4.

Also of interest is the variation of the bending moment in the beam during the two creep periods. For that purpose, a post file is written. Only displacement and reaction forces are written on this tape. The MARC PLOT program is then used to plot the bending moment (the reaction force at node 1, degree of freedom 4) against time. The result is shown in Figure 3.14-5. The input for the MARC PLOT can be found at the end of the input for the MARC STRESS program.

Parameters, Options, and Subroutines Summary

Example e3x14a.dat:

Parameters	Model Definition Options	History Definition Options
CREEP	CONNECTIVITY	AUTO CREEP
END	CONTROL	CONTINUE
NEW	COORDINATES	DISP CHANGE
SHELL SECT	CREEP	PRINT CHOICE
SIZING	END OPTION	
TITLE	FIXED DISP	
	GEOMETRY	
	ISOTROPIC	
	POST	

Example e3x14b.dat:

Parameters
END
TITLE
USER

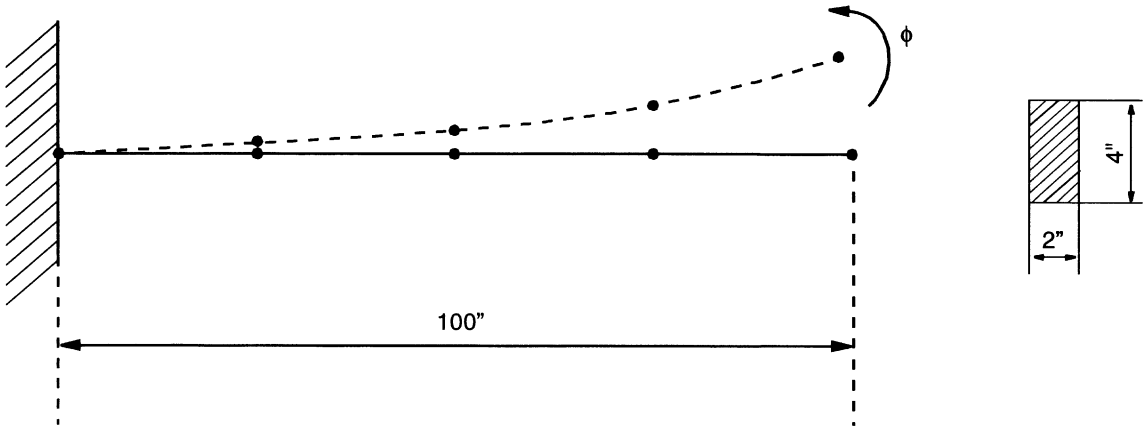

Figure 3.14-1 Geometry of Beam and Finite Element Mesh

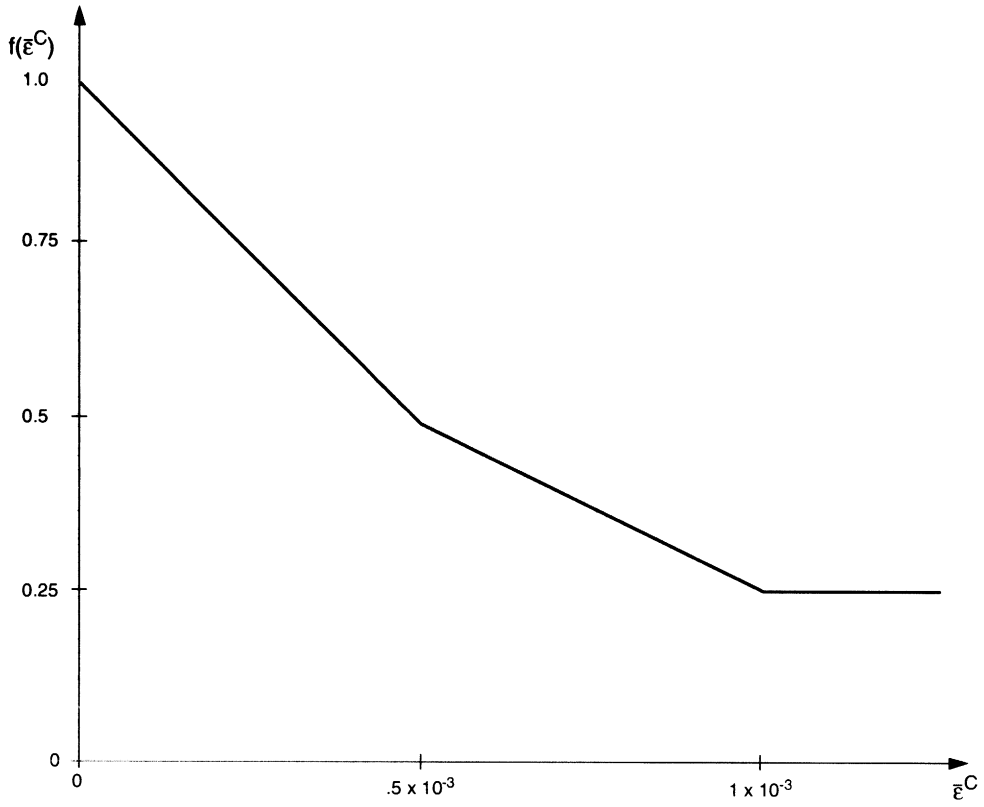

Figure 3.14-2 Creep Strain Coefficient as Function of Creep Strain

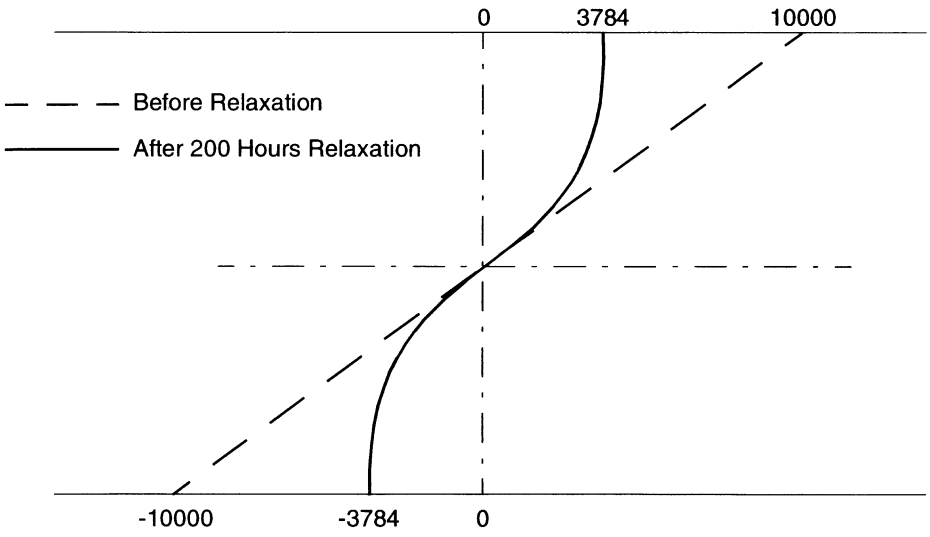

Figure 3.14-3 Stress Distribution through the Thickness before Load Reversal

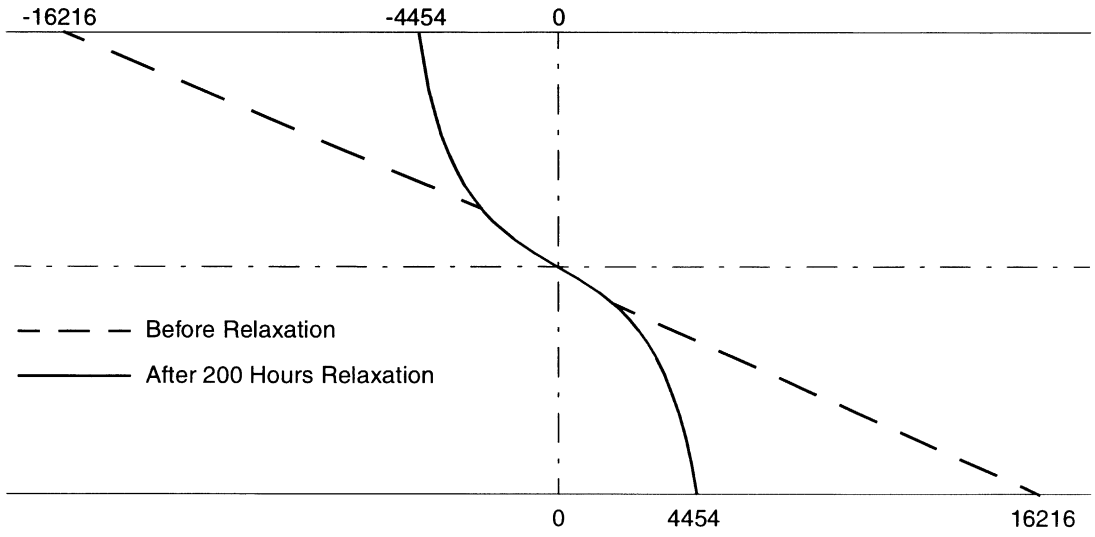

Figure 3.14-4 Stress Distribution through the Thickness after Load Reversal

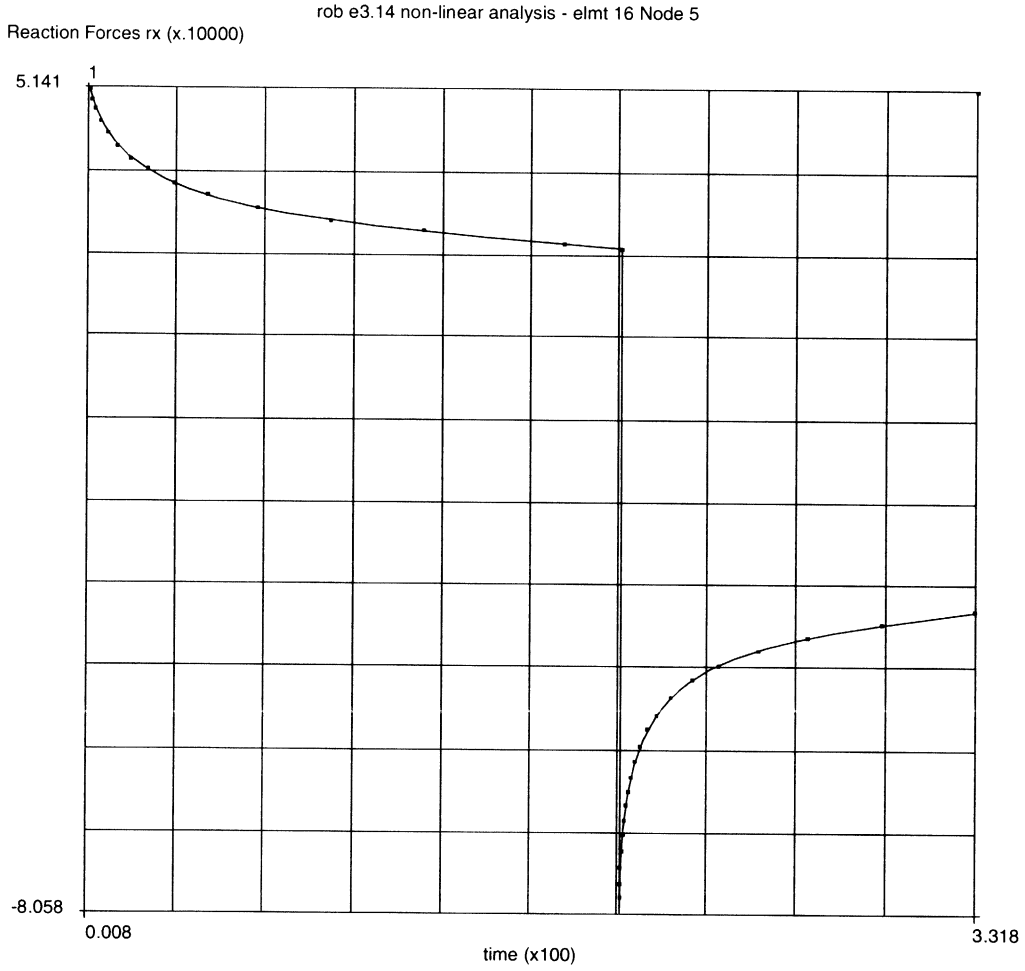

Figure 3.14-5 Relaxation Curve for Bending Moment

3.15 Creep of a Square Plate with a Central Hole using Creep Extrapolation

A square plate of 10 x 10 inches with a central hole of 1-in. radius is loaded in tension.

A state of plane stress is assumed in the plate, and the thickness of the plate is taken as 1 in.

A tensile load of 10,000 psi is applied. The plate is allowed to creep for a period of 10,000 hours. Followed by a single creep increment of 100 hours is taken, during which the strains and displacements are accumulated. Based on the accumulated strains and displacements, the solution is then extrapolated to a total creep time of 20,000 hours.

This problem is modeled using the two techniques summarized below.

Data Set	Element Type(s)	Number of Elements	Number of Nodes	Differentiating Features
e3x15	26	20	79	CREEP
e3x15b	26	20	79	Implicit Creep

Element

MARC element type 26, an 8-node quadrilateral plane stress element, is used in this analysis. Because of symmetry, only one-quarter of the plate is modeled. The mesh is shown in Figure 3.15-1.

Material Properties

The elastic properties of the material are a Young's modulus (E) of 30.E6 psi and Poisson's ratio (ν) of 0.3. The creep properties are characterized by the Power law equation: $\dot{\varepsilon}^{c} = 10^{-24}\sigma^{4}$. The elastic properties are entered through the ISOTROPIC option. The creep properties are entered through the CREEP option. Note that stress and strain changes, as used for the AUTO CREEP options, will only be monitored in element 8, where the maximum stress occurs. The CREEP parameter block flags use of the creep option.

Boundary Condition

Symmetry conditions are imposed on the two edges intersecting the central hole.

Loading

A distributed load of 10,000 psi is applied to the upper edge of the plate. For element type 26, the load type 8 is used to apply the load to the correct face of elements 13 and 14. Load type 8 is a pressure load; a negative value is entered to obtain a tensile load.

Optimization

Ten Cuthill-McKee iterations are allowed to reduce the bandwidth. The original bandwidth was equal to 67. In the third iteration, a minimum of 26 is reached. The correspondence table is written to file 1.

Post File Generation

The equivalent stress and creep strain are written on the post file. Both total displacements and reaction forces are written on the post file.

Analysis Control

All default controls are in effect. The CONTROL option is only used to increase the number of increments to more than the default of 4.

PRINT CHOICE

The PRINT CHOICE option is used to select output for element 8 and for nodes 30 through 34 and 68 through 71, which are the nodes on the edge of the hole.

Automatic Creep Analysis

The AUTO CREEP option is used for the first creep period of 10,000 hours. A time step of 1,000 hours is specified as the starting value. If necessary, MARC scales this value down to a time step which satisfies the specified stress and strain control criteria.

Strain and Displacement Accumulation

After the AUTO CREEP period is completed, accumulation of total strains, creep strains, and displacements is started with use of the ACCUMULATE option. Because storage of the accumulated values requires additional core allocation, the ACCUMULATE parameter must be included.

User Controlled Creep Analysis

The CREEP INCREMENT option is used to specify a single creep increment of 100 hours. If the CREEP INCREMENT option is invoked, the time step is not adjusted to satisfy the creep tolerances.

Strain and Displacement Extrapolation

Based on the incremental results obtained during the CREEP INCREMENT, the total strains, creep strains and displacements are extrapolated to estimate values at a total CREEP time of 20,000 hours. The EXTRAPOLATE option is used for this purpose. The extrapolation from a single increment is rather trivial; a more meaningful use of the EXTRAPOLATE option can be found in extrapolation of cyclic loading results.

Results

The results of increment 0 indicate that a maximum stress of 31,370 psi in the y-direction occurs in element 8. This corresponds to a stress concentration factor of 3.137, which is slightly higher than the factor of 3 occurring in an infinite plate. In increment 1, your selected time step of 1,000 hours yields a stress change which is almost five times higher than the maximum allowed in the CONTROL option. MARC then picks a time step of 161.2 hours, with which the tolerances are satisfied. The maximum stress change governs the time incrementation up to increment 7, where at a total creep time of 3,685 hours the strain control becomes effective. The time step rapidly stabilizes at a value of about 2,000 hours, until the end of the AUTO CREEP period is reached in increment 12. A single time step of 100 hours is taken, during which the displacements, total strains and creep strains are accumulated. The options used for this are CREEP INCREMENT and ACCUMULATE. In increment 13, the accumulated quantities are subsequently extrapolated to a time of 20,000 hours. The stress relaxation is shown in Figure 3.15-2. The creep strain history is shown in Figure 3.15-3. One can observe the creep strain at node 30 appears to be zero. As the creep strain goes as the fourth power of stress, we see that neighboring points can have substantially different amounts of creep.

Although the ACCUMULATE and EXTRAPOLATE options are primarily useful for extrapolation of cyclic loading results, they also offer some advantage in analysis of creep problems in which steady state is approached. If a long steady state phase must be analyzed, the standard explicit creep procedure still limits the maximum time step because of the existence of a stability limit. This stability limit corresponds with the default value of the strain change control set in the CONTROL option. This stability problem is absent in the EXTRAPOLATE options, however, since the stresses are not affected by extrapolation. Substantial savings in computer run time can be obtained. It should be noted, however, that extrapolation can lead to considerable errors in strains and displacements, particularly if extrapolation is done from an increment in which steady state creep had not yet been reached. Extreme care must be exercised when this option is used.

Parameters, Options, and Subroutines Summary

Example e3x15.dat:

Parameters	Model Definition Options	History Definition Options
ACCUMULATE	CONNECTIVITY	ACCUMULATE
CREEP	CONTROL	AUTO CREEP
ELEMENTS	COORDINATES	CONTINUE
END	CREEP	CREEP INCREMENT
SIZING	DIST LOADS	DIST LOADS
TITLE	END OPTION	EXTRAPOLATE
	FIXED DISP	
	GEOMETRY	
	ISOTROPIC	
	POST	
	PRINT CHOICE	

Example e3x15b.dat:

Parameters	Model Definition Options	History Definition Options
CREEP	CONNECTIVITY	AUTO LOAD
ELEMENTS	CONTROL	CONTINUE
END	COORDINATES	CREEP INCREMENT
SIZING	CREEP	DIST LOADS
TITLE	DIST LOADS	
	END OPTION	
	FIXED DISP	
	GEOMETRY	
	ISOTROPIC	
	POST	
	PRINT CHOICE	

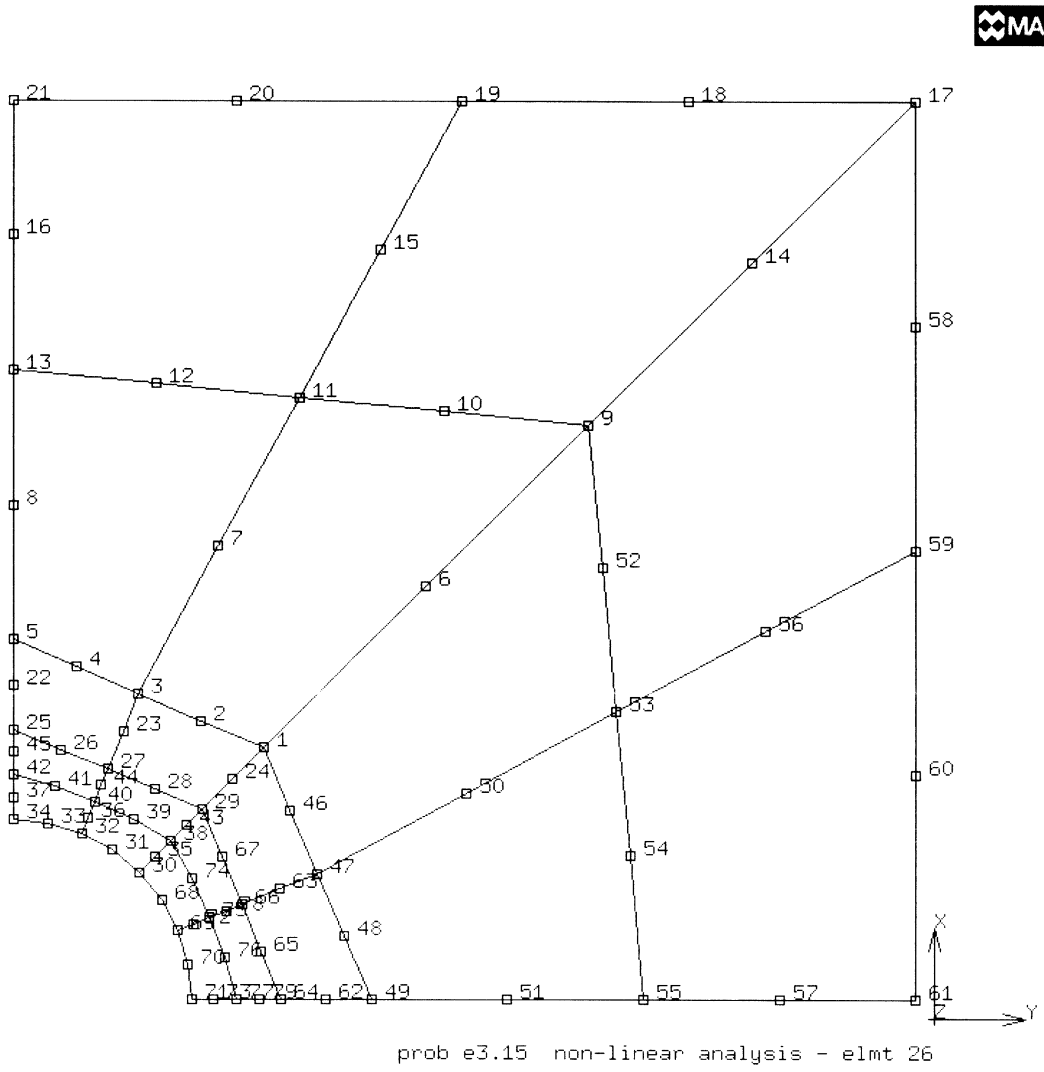

Figure 3.15-1 Mesh Layout for Plate with Hole

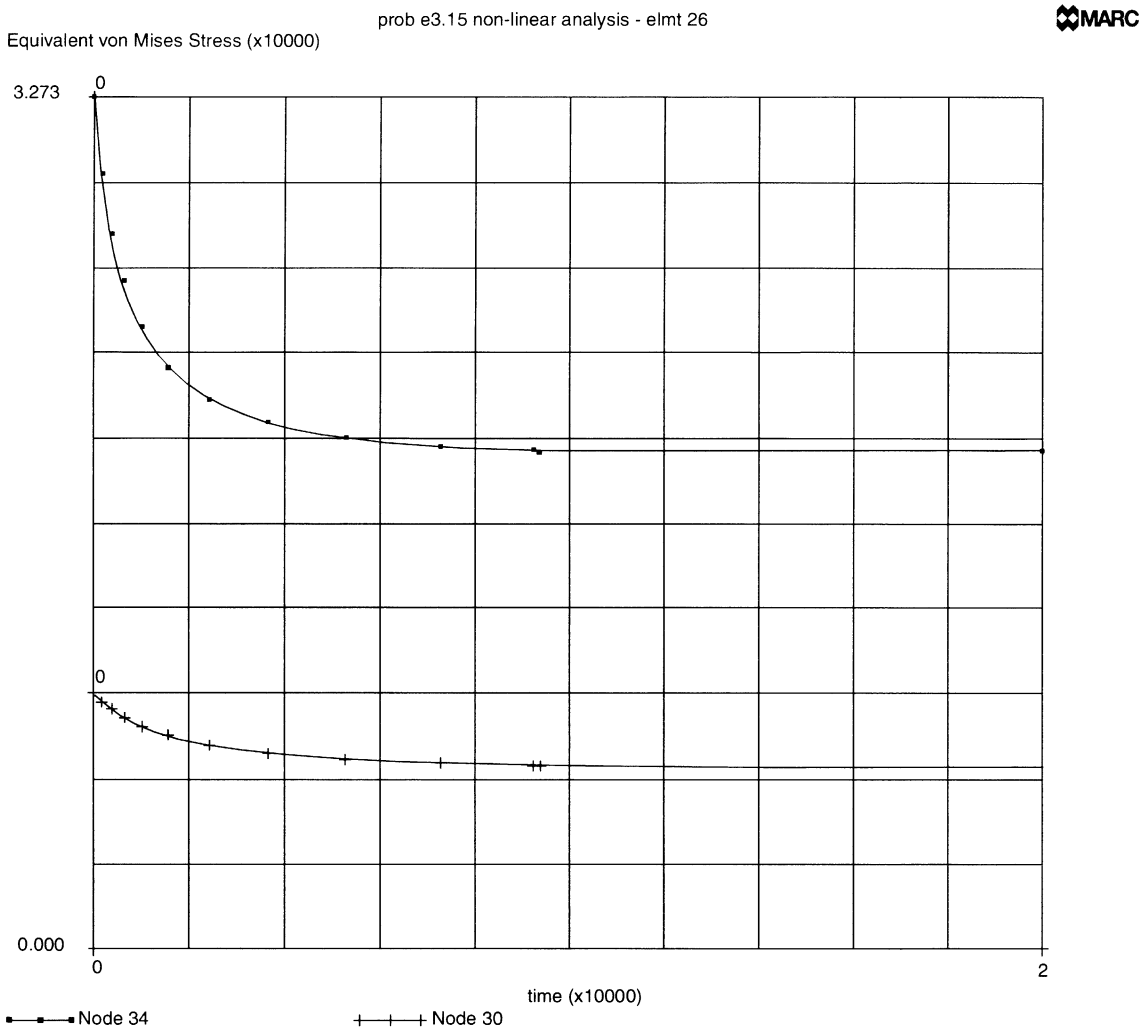

Figure 3.15-2 Stress Relaxation

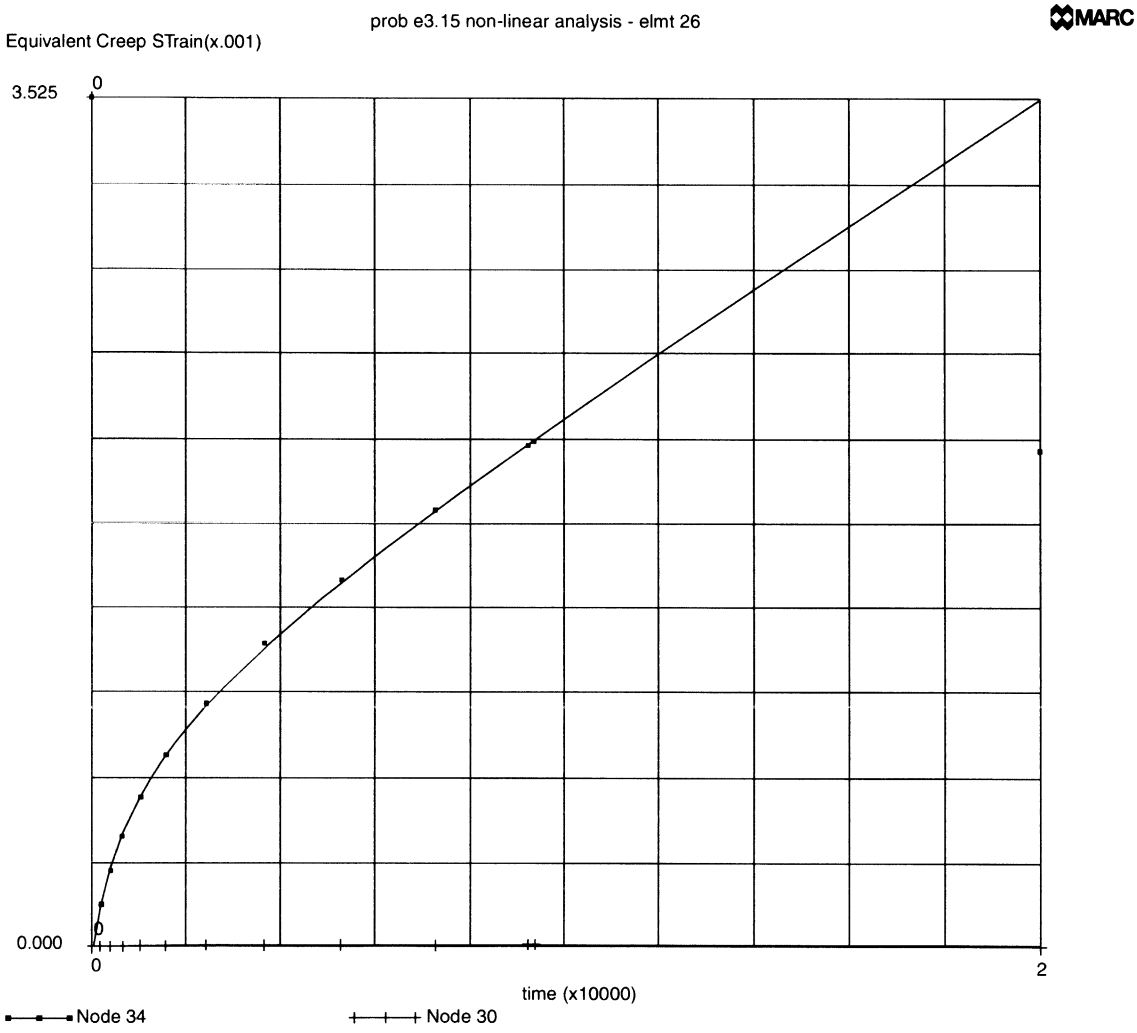

Figure 3.15-3 Creep Strain History

3.16 Plastic Buckling of an Externally Pressurized Hemispherical Dome

In this problem, MARC analyzes structures in which both geometric and material nonlinearities occur and cause collapse of the structure. The model used is a hemispherical dome with a radius of 100 inches and a thickness of 2 inches which is clamped at the edge (Figure 3.16-1). The material is elastic-plastic, with a Young's modulus of 21.8 x 10^6 psi, a Poisson's ratio of 0.32 and a yield stress of 20,000 psi.

This geometrically nonlinear problem is solved incrementally with Newton-Raphson style iteration. The analysis is continued until plastic collapse occurs. In MARC, such collapse becomes apparent either due to failure to converge in the iteration process (MARC exit 3002) or due to the stiffness matrix turning nonpositive definite (MARC exit 2004).

It is assumed that the collapse is axisymmetric, so that the problem can be analyzed with an axisymmetric finite element model. If it were likely that a nonsymmetric collapse mode would occur, the problem would have to be analyzed with a full three-dimensional shell model (using MARC element type 22, 72, or 75). Two analyses are performed. In the first analysis, the inverse power sweep method is used to extract the collapse load; while in the second analysis, the Lanczos method is used. This is controlled by the BUCKLE parameter. The properties of the dome change strongly as plasticity develops; and, hence, the results of the eigenvalue extraction vary substantially during the analysis.

This problem is modeled using the two techniques summarized below.

Data Set	Element Type(s)	Number of Elements	Number of Nodes	Differentiating Features
e3x16	15	8	9	Buckling by inverse power sweep
e3x16b	15	8	9	Buckling by Lanczos procedure

Element

Eight axisymmetric shell elements (MARC type 15) were used in this analysis. Element 15 is an element with fully cubic interpolation functions, quadratic membrane strain variation and linear curvature change variation along its length. This element yields rapid convergence and behaves very well in geometrically nonlinear situations.

Geometry

A thickness of 2.0 inches is specified in the first data field (EGEOM1) of the GEOMETRY option.

Coordinate Generation

Element type 15 requires input of higher order coordinates. For a simple shape like a dome, these coordinates are most easily generated automatically. The model definition option UFXORD and the user subroutine UFXORD are used for this purpose.

Material Properties

The elastic properties (Young's modulus, Poisson's ratio, yield stress) are specified in the ISOTROPIC option. The WORK HARD option is used to specify two slopes.

Transformations

Transformations are applied to all nodes except node 1. For all nodes, the transformed degrees of the freedom are the same:

1 = Radial displacement
2 = Tangential displacement
3 = Rotation
4 = Meridional membrane strain

This transformation is not necessary, but facilitates visual inspection of displacement vectors and buckling nodes.

Boundary Conditions

Symmetry conditions are specified for node 1, fully clamped conditions for node 9.

Loading

The DIST LOAD option is used to specify a distributed pressure load of 540 psi on all elements.

Control

Since the objective of the analysis is to calculate the collapse load, a large number of recycles (six) is allowed. Default convergence controls are used.

Stress Storage

The SHELL SECT parameter is used to specify a five-point integration through the thickness.

Geometric Nonlinearity

The LARGE DISP parameter indicates that geometrically nonlinear analysis will be performed.

Buckling

The BUCKLE parameter is included to indicate that a maximum of three buckling modes are to be extracted, with a minimum of one mode with a positive buckling load. The sixth parameter is used to activate the Lanczos method.

After increment 0 (the linear elastic increment) is carried out, the BUCKLE history definition option is used to extract the linear buckling mode. The BUCKLE option does not increment the analysis (increment number or loads). After the execution of the BUCKLE option, MARC proceeds as usual.

Load Incrementation

The AUTO LOAD and PROPORTIONAL INCREMENT options are used to increase the pressure during four increments with an increment of 10% of the applied pressure in increment 0. Subsequently, the same options are used to increase the pressure with an increment of 20% (2% of the original load) for two increments. With the PROPORTIONAL INCREMENT option, the load increment is then divided by 2, which brings the total pressure up to: 1.45 x 540 = 783 psi. A buckling mode extraction is performed to estimate the collapse mode and collapse pressure. Plots are made of deformation increment and the buckling mode. This last sequence is repeated twice, with the total pressure at the end of increment 9 equal to 793.8 psi.

Results

In increment 0, the linear elastic solution is obtained. The maximum stress of 19,720 psi occurs in element 8, integration point 3, layer 1, which is the point closest to the clamped edge. The displacement increment is shown in Figure 3.16-2. The linear elastic buckling analysis, which is subsequently carried out, yields a collapse pressure of: 19.74 x 540 = 10,660 psi. The buckling mode is shown in Figure 3.16-3, the calculated pressure is very close to the buckling pressure of a perfect sphere. For the perfect sphere, the buckling pressure (taken from Timoshenko's and Gere, *Theory of Elastic Stability*) is given by the equation:

$$P_c = \frac{2\ Et^2}{r^2\sqrt{3(1-\nu^2)}}$$

The data for this problem yields 10,628 psi from this equation. As the load is increased, the plastic flow begins to occur near the clamped edge. At the end of increment 6, plasticity occurs at all points in elements 7 and 8. The average membrane stress level is now only 2.7% under the yield stress.

In increment 6, the plasticity spreads out into element 6. The maximum plastic strain is about 0.12% and occurs at the inside of element 8. The average membrane stress is 2.1% under the yield stress.

The buckling analysis at this state yields a collapse pressure equal to the current pressure plus 158 times the pressure increment. This corresponds to a collapse pressure of 1,609 psi. The buckling mode has the same shape as the displacement increment, as follows from comparison of Figure 3.16-4 and Figure 3.16-5.

Increment 8 is applied. Plasticity spreads deeper into the model, and the average membrane stress is 1.5% under the yield stress. The buckling analysis yields a collapse pressure of current pressure plus 64 times the pressure increment, which is equal to 1,134 psi. Some differences now occur between buckling mode and displacement increment, as shown in Figure 3.16-6.

At increment 9, the pressure is 793 psi. If additional load is applied, the stiffness matrix becomes nonpositive definite.

As indicated by Table 3.16-1, the frequencies obtained by both, Inverse power sweep as well as the Lanczos method are identical.

Discussion of Results

It is clear that in this problem the dominant mode of failure is plastic collapse. Throughout most of the analysis, the geometric nonlinearities do not play a significant role. In fact, if the simple failure criterion is used that collapse occurred when the membrane stress reaches yield, a collapse pressure of

$$p_c = 2\frac{\sigma_y t}{r} = 800 \text{ psi}$$

is calculated, which is only 1% over the result obtained in the finite element analysis. It should be noted that in this demonstration problem, the step size is decreased gradually when the critical point is approached. In a practical situation, one does not know when this critical point occurs. The procedure would then be to analyze the problem first without step refinement and write a RESTART file. The analysis will still come to a point where no convergence occurs or where the matrix turns nonpositive definite. The analysis is then restarted with a smaller load step one or two increments before the critical point, and a solution with improved accuracy is obtained. This procedure can be refined as often as necessary to get the required accuracy. In the present example, two restarts would probably have been necessary in order to obtain the above results. The first run would have been with a constant pressure increment of 54 psi. The second run would have restarted at increment 4 with a pressure increment of 10.8 psi. The final run would involve a restart at increment 6 with a pressure increment of 5.4 psi. The PRINT CHOICE option is used to restrict the output to layers 1 through 3.

Table 3.16-1 Eigenvalues

	Inverse Power Sweep	Lanczos
0	19.99	19.99
2	188.7	188.2
4	122.7	122.7
6	2050.0	2050.0
7	1845.0	1845.0
8	1623.0	1623.0
9	1387.0	1387.0

Parameters, Options, and Subroutines Summary

Example e3x16a.dat and e3x16b.dat:

Parameters	Model Definition Options	History Definition Options
BUCKLE	CONTROL	AUTO LOAD
ELEMENTS	CONNECTIVITY	BUCKLE
END	DIST LOADS	CONTINUE
SHELL SECT	END OPTION	PROPORTIONAL INCREMENT
SIZING	GEOMETRY	
TRANSFORM	FIXED DISP	
	ISOTROPIC	
	PRINT CHOICE	
	TRANSFORMATION	
	WORK HARD	
	UFXORD	

User subroutine in u3x16.f:

UFXORD

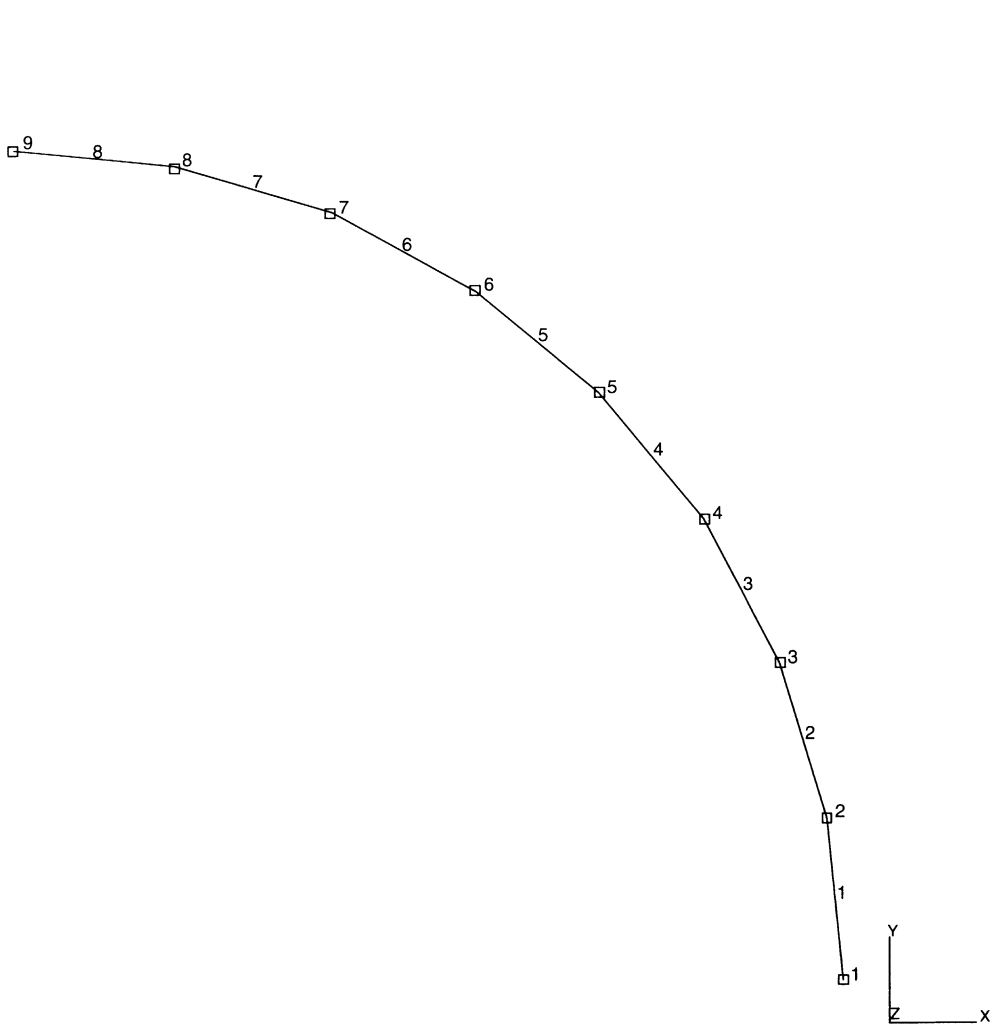

Figure 3.16-1 Geometry and Mesh

Figure 3.16-2 Buckling Mode, Increment 0

Figure 3.16-3 Buckling Mode, Increment 2

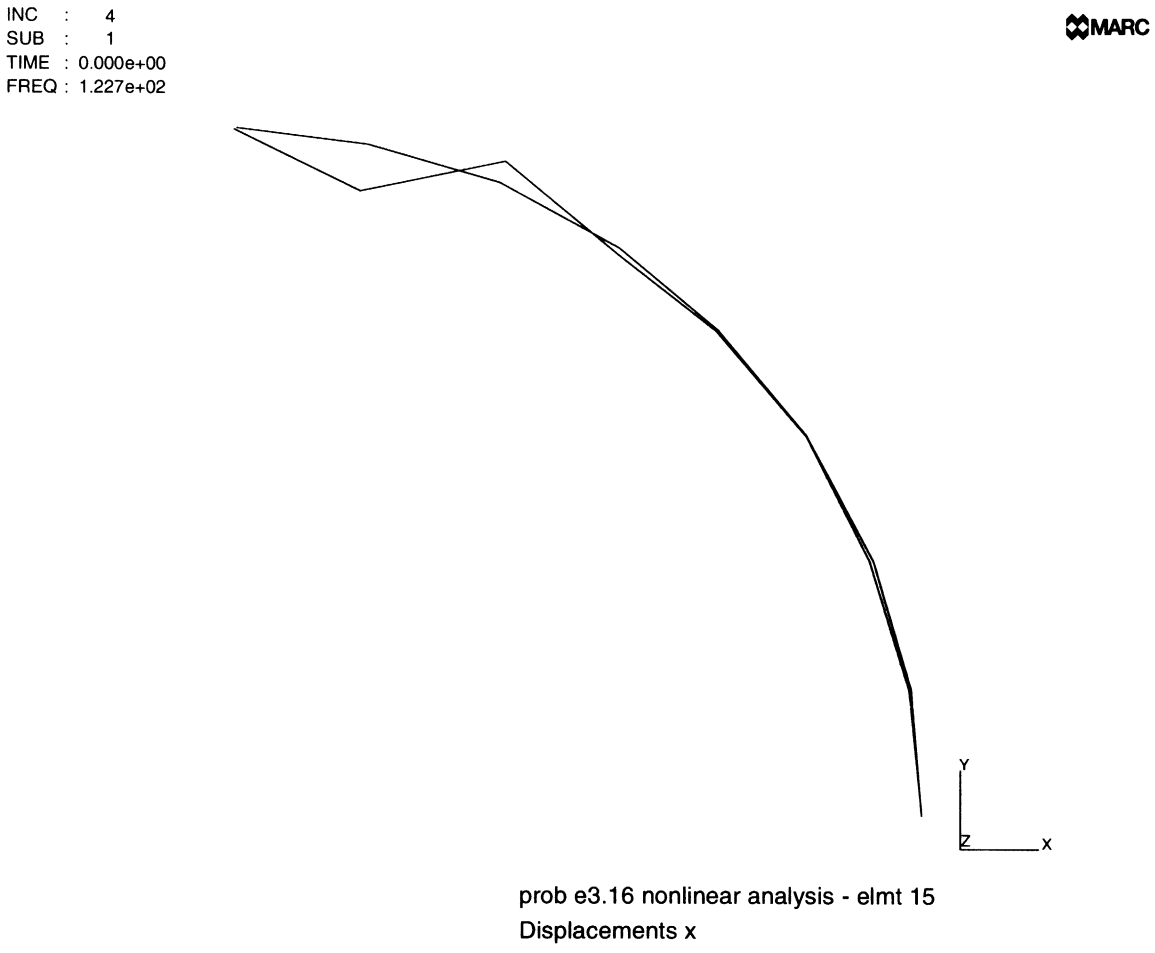

Figure 3.16-4 Buckling Mode, Increment 4

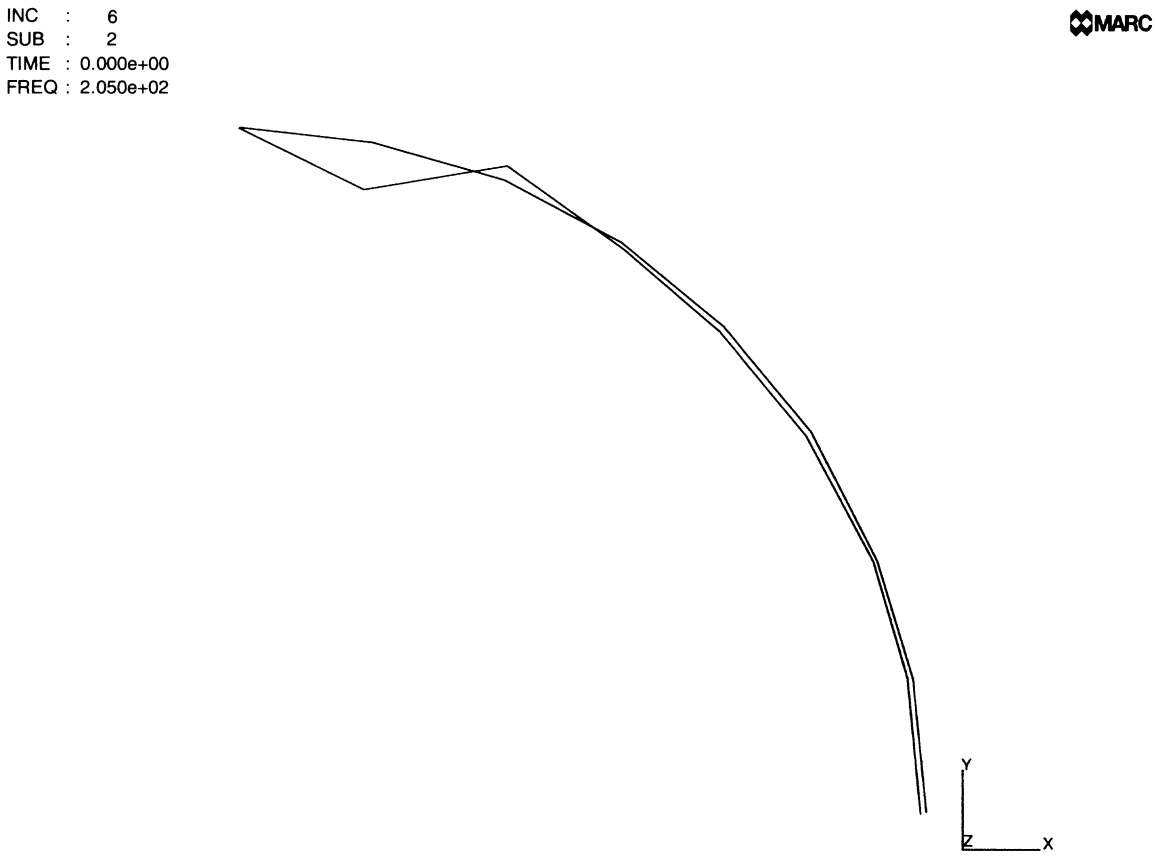

Figure 3.16-5 Second Buckling Mode, Increment 6

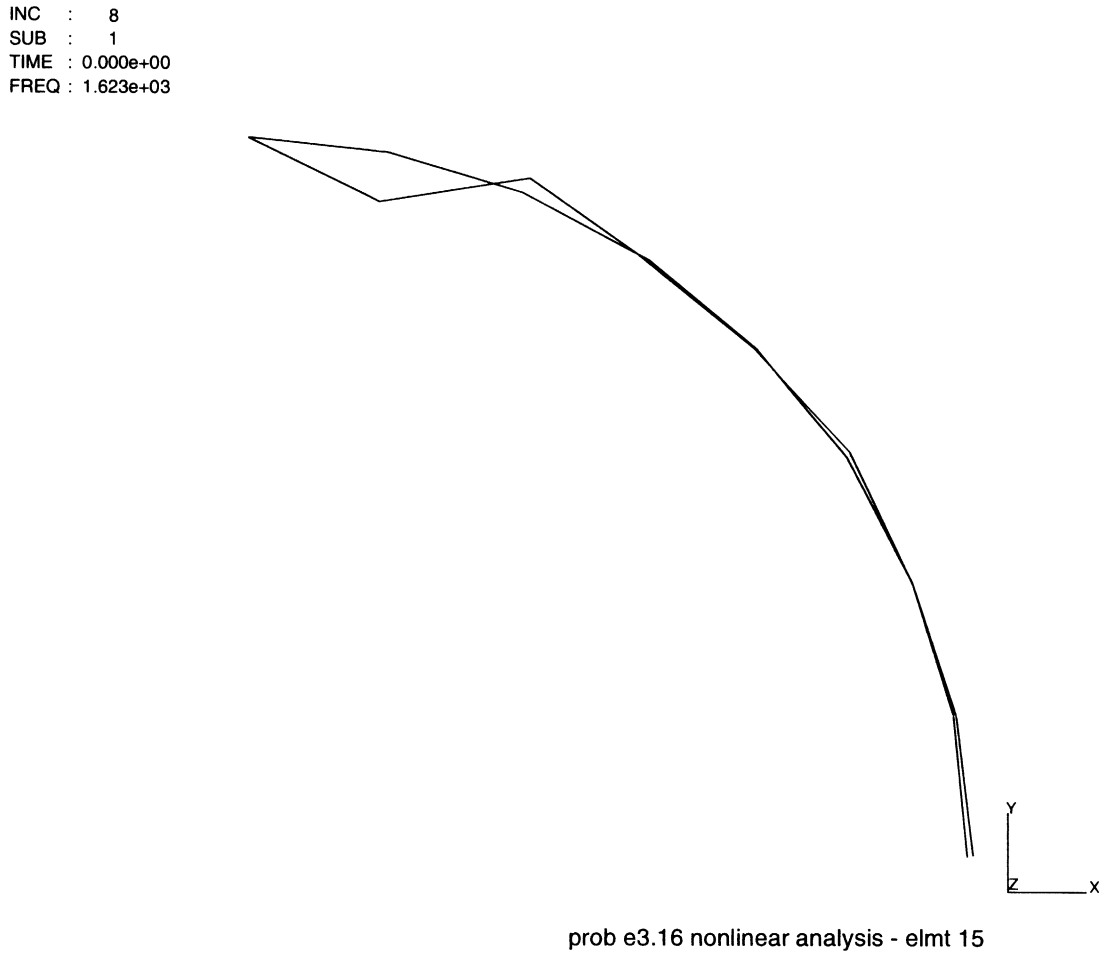

Figure 3.16-6 Second Buckling Mode, Increment 8

3.17 Shell Roof with Geometric and Material Nonlinearity

One of the standard problems for testing the performance of linear shell elements is the shell roof shown in Figure 3.17-1. The shell roof is supported at the curved edge by a rigid diaphragm. The linear solution for this problem can be compared with the analytical results obtained by Scordelis and Lo [1]. The solution for this nonlinear problem can be compared with the results of another finite element study, carried out by Kråkeland [2]. In this problem, combined geometric and material nonlinearities are considered. An elastic perfectly plastic material model is used. Young's modulus is equal to 2.1×10^4 N/mm^2 and Poisson's ratio is assumed to be zero. A gravity type load of 3.5×10^{-4} N/mm^2 (= 350 N/m^2) is applied in increment 0. In nine increments, this load is increased by a factor of 10 to a total value of 3,500 N/m^2. During this loading, geometric and material nonlinearities have a clear effect on the behavior of the structure.

Element

One quarter of the roof is modeled with 25 elements of MARC type 72. This is a noncompatible thin-shell element based on discrete Kirchhoff theory. With this element, the stiffness of a structure is not necessarily overestimated. After elimination of suppressed degrees of freedom, the finite element model has a total of 135 active degrees of freedom.

Model

The coordinates are first entered as a two-dimensional mesh, in which the first and second coordinates represent circumferential and axial coordinates of the shell roof. The UFXORD option is then used to transform these cylindrical coordinates to Cartesian coordinates.

Geometry

The thickness of 76 mm is specified with use of the GEOMETRY option.

Boundary Conditions

The diaphragm support conditions and appropriate symmetry conditions are specified with the use of the FIXED DISPLACEMENT option. With element type 72, the degrees of freedom have very clear physical significance, and the specification of boundary conditions is very simple and does not need further clarification.

Material Properties

Since no workhardening is included, all properties (Young's modulus, Poisson's ratio, and yield stress) can be specified with the ISOTROPIC option.

Loading

A distributed load of type 1 with a magnitude of 3.5×10^{-4} N/mm^2 is prescribed with the DIST LOAD option. This is a gravity type load, working in the negative z-direction.

Data Storage

The number of integration stations through the thickness of the shell is set to 5 with the SHELL SECT parameter. Because of the fact that nonlinear shell elements require storage of fairly large amounts of data, the ELSTO parameter is used to store this data out-of-core. With this procedure, more workspace is available for assembly and solution of the main system of equations.

Geometric Nonlinearity

The LARGE DISP option is included to invoke geometric nonlinear behavior. The Newton-Raphson iterative technique (default option in MARC) is used to solve the nonlinear equations.

Analysis Control

With the CONTROL option, the maximum number of load increments (including increment 0) is specified as 10. All other CONTROL parameters have the default value.

Post-Processing

In addition, a POST file is written. No element variables are written on this file. Both the total displacement and the reaction forces appear on the POST file.

Print Control

The PRINT CHOICE option is used to limit print output to one element (25) at one integration point (1) at two layers (1 and 5) and one node (96). More complete nodal data is stored on the POST file, whereas plotted information is obtained concerning the plastic strains.

Load Incrementation

Nine equal load increments are applied with the use of the AUTO LOAD option, to bring the total load up to 3.5×10^{-3} N/mm^2.

Results

The generated mesh is shown in Figure 3.17-2. The mesh generation process generates coordinates for corner nodes and midside nodes. For the midside nodes of element type 72, coordinates do not have to be specified, and the program does not utilize any coordinates generated. This is also clear from Figure 3.17-2, where the elements are plotted with straight edges.

The most interesting result of the analysis is the z-displacement of node 96; because, for this degree of freedom, results are available from the literature. In Figure 3.17-3, the results obtained in this analysis are compared with those of Kråkeland [2]. It is clear that good agreement is obtained.

The extent of plasticity is shown in Figure 3.17-4. From these plots, it is clear that plasticity in the extreme layers has spread out over a fairly large region. Nevertheless, the nonlinearity in this problem can still be considered mild. As a result, for most increments, minimal iterations are necessary to obtain a convergent solution.

References

1. A. C. Scordelis and K. S. Lo, "Computer analysis of cylindrical shells," *J. Am. Concrete Inst.*, Vol. 61 (May 1964).
2. B. Kråkeland, "Large displacement analysis of shells considering elasto-plastic and elasto-viscoplastic materials," Technical report no. 77-6, Division of Structural Mechanics, The Norwegian Institute of Technology, University of Trondheim, Norway, 1977.

Parameters, Options, and Subroutines Summary

Example e3x17.dat:

Parameters	Model Definition Options	History Definition Options
ELEMENTS	CONNECTIVITY	AUTO LOAD
END	CONTROL	CONTINUE
LARGE DISP	COORDINATES	PROPORTIONAL INCREMENT
SHELL SECT	DIST LOADS	
SIZING	END OPTION	
TITLE	FIXED DISP	
	GEOMETRY	
	ISOTROPIC	
	POST	
	PRINT CHOICE	
	UFXORD	

User subroutine in u3x17.f:

UFXORD

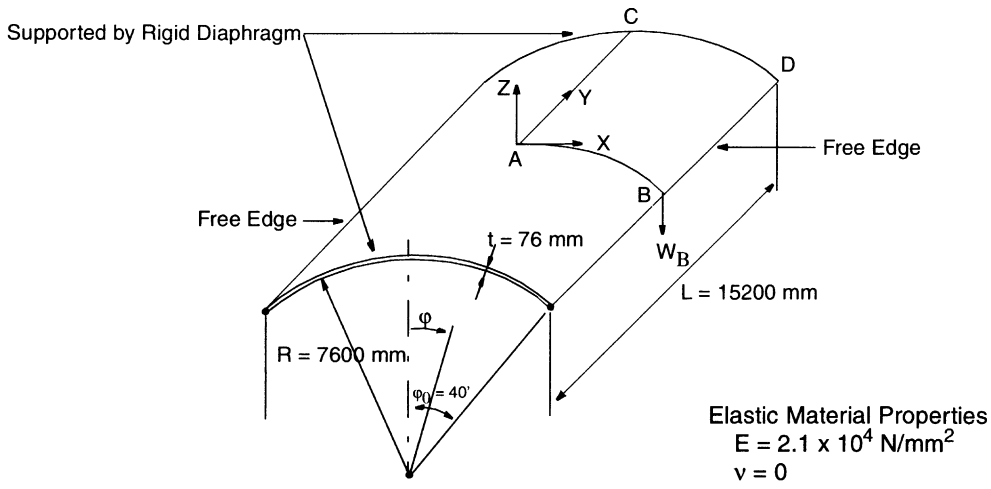

Figure 3.17-1 Shell Roof

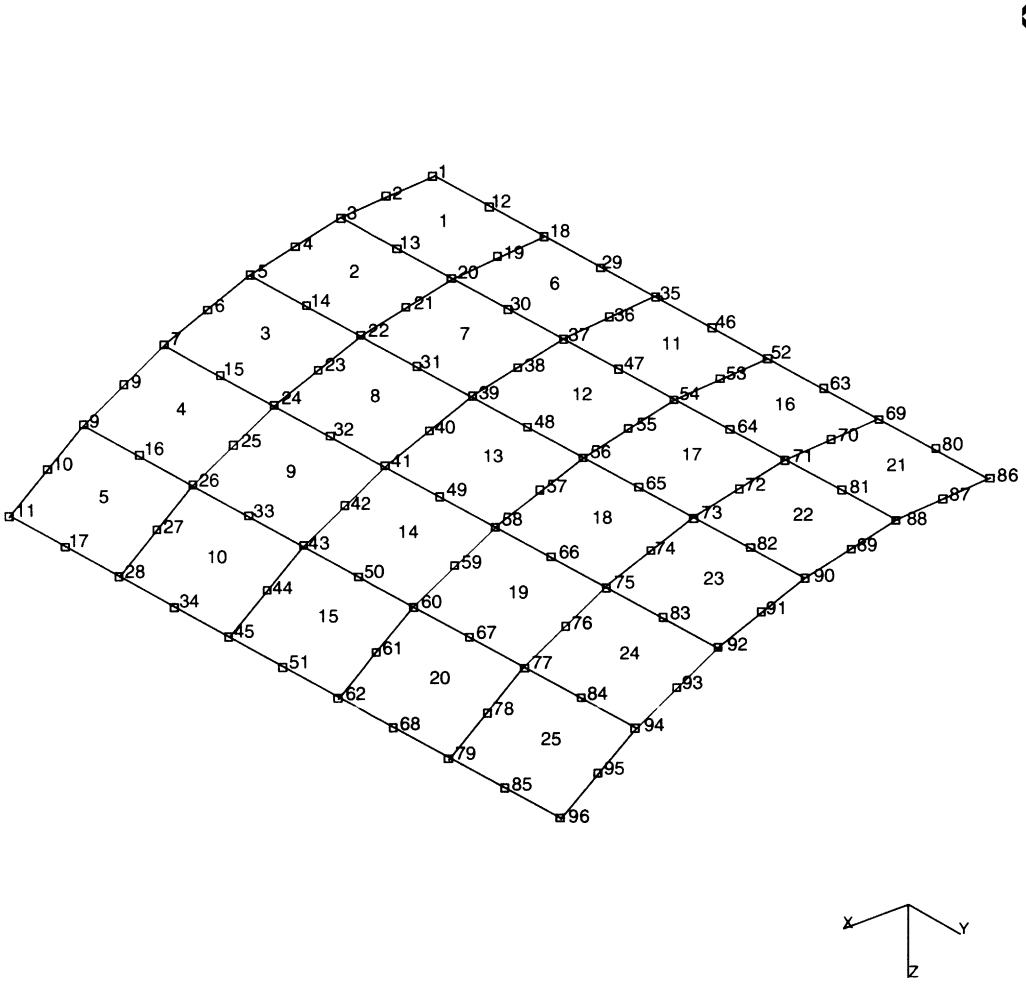

Figure 3.17-2 Mesh of Shell Roof

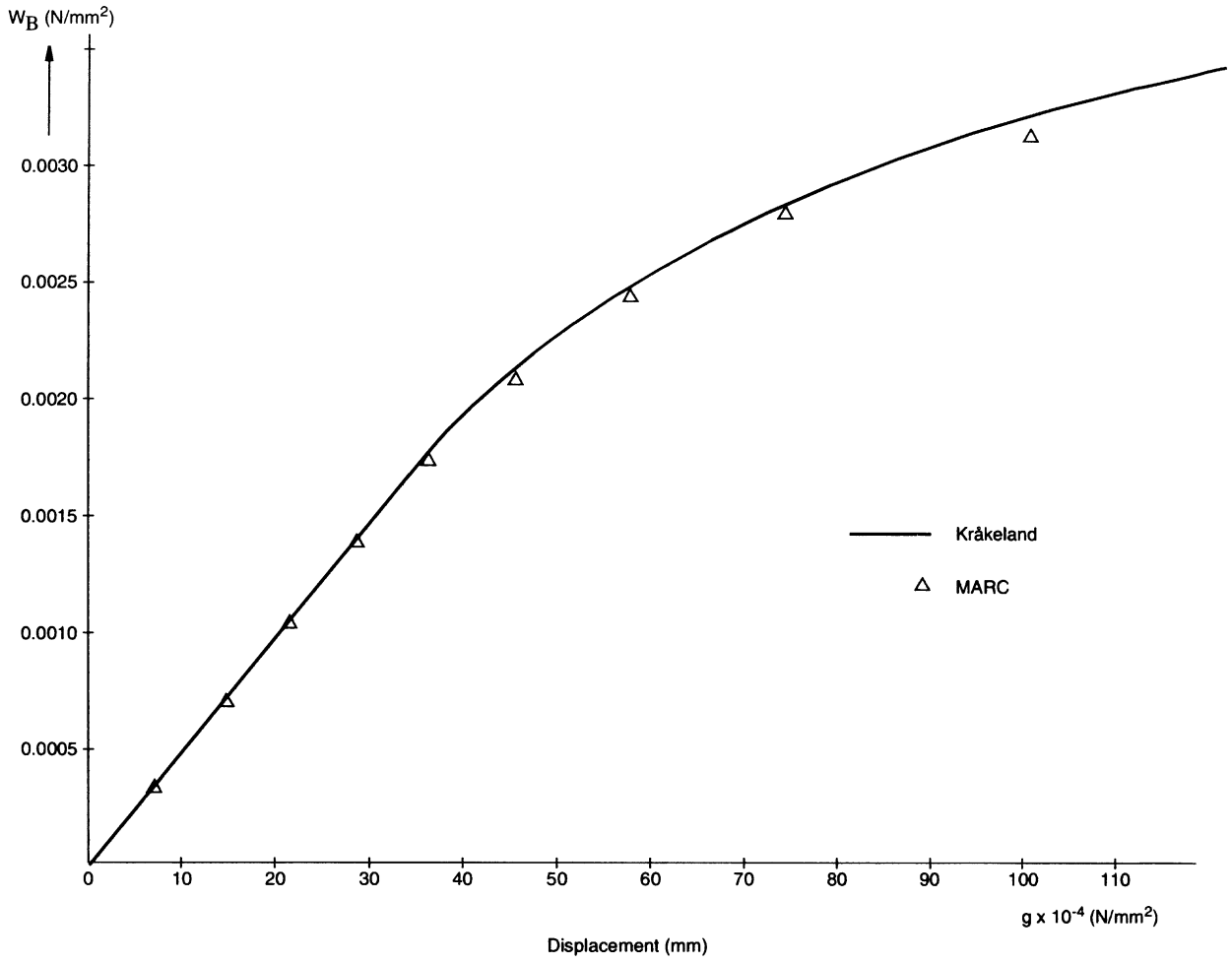

Figure 3.17-3 Load Displacement Curve, Node 96

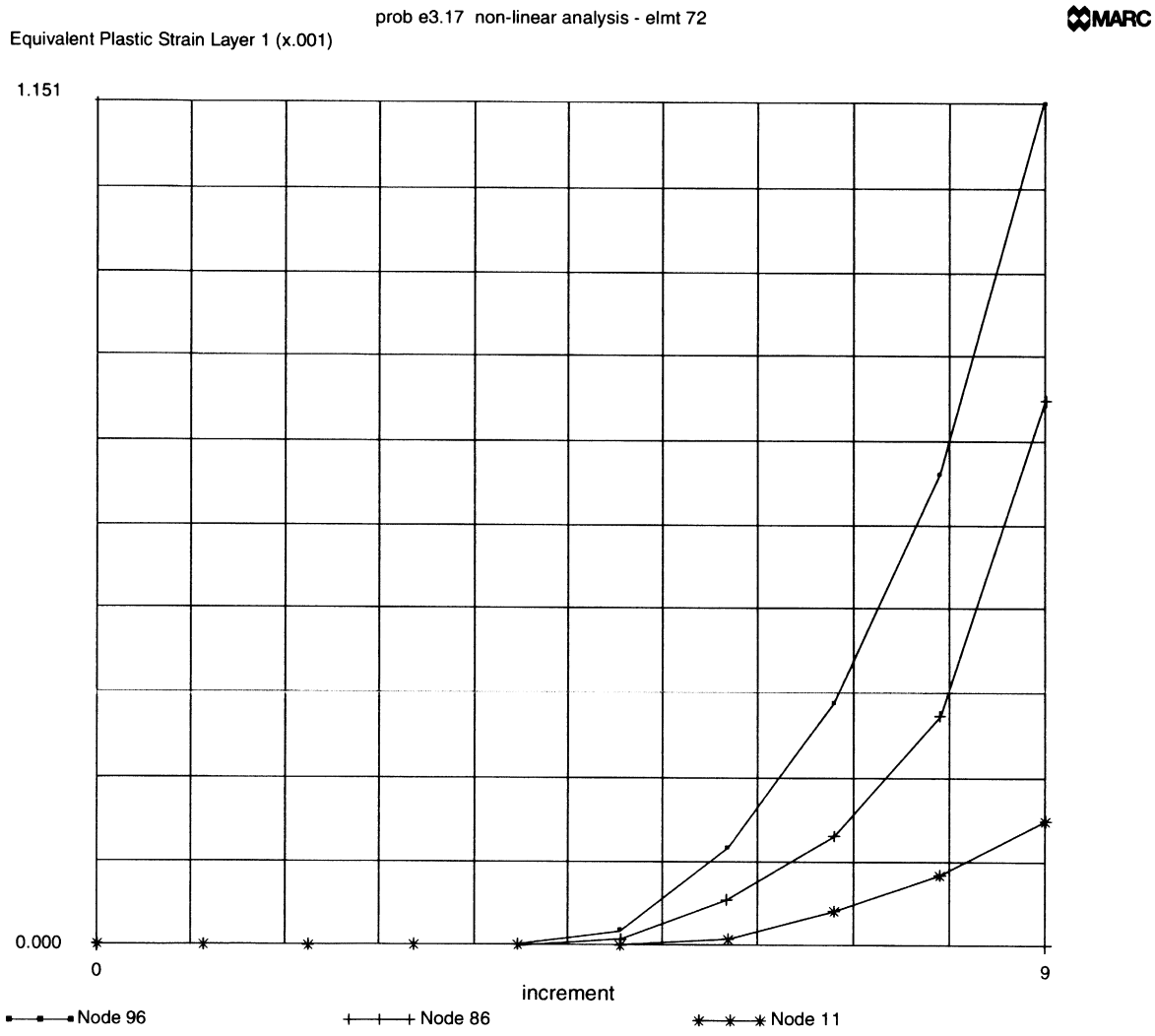

Figure 3.17-4 Equivalent Plastic Strain in Layer 1 History for Selective Nodes

3.18 Analysis of the Modified Olson Cup Test

The modified Olson Cup test is used to determine material properties of a metal for the purpose of stretch forming. In this test, a thin plate is clamped in a rigid circular die. The die has an inner radius of 1.2 inches, and the plate has a thickness of 0.04 inches. Subsequently, a rigid, hemispherical punch is forced into the plate, causing considerable plastic strain. This punch has a radius of 1 inch, and is assumed to be frictionless. A sketch of the process is shown in Figure 3.18-1.

This problem demonstrates the capability of MARC to analyze large plastic deformations in shell-like structures. It also demonstrates the use of the "true distance" gap element.

Element

The plate is modeled with 12 axisymmetric shell elements of MARC type 15. These elements all have the same length of 0.1 inch, and a thickness of 0.04 inch, which is specified with the GEOMETRY option. Gap elements of MARC type 12 are used to model the punch. One of the gap ends is attached to the shell nodes and the other end is attached to the center of the punch. Only the nodes of the shell are forced to be on the punch surface; and since the shell elements have cubic interpolation functions, it is possible that local penetration of the punch between nodes occurs. If the mesh is sufficiently refined, such local penetration will only be a source of small inaccuracies in the analysis.

Material Properties

The plate has elastic-plastic material behavior with isotropic workhardening. The Young's modulus of 1.0×10^7 psi, the Poisson's ratio of 0.3, and the initial yield stress of 3.0×10^4 psi are entered through the ISOTROPIC option. The workhardening data are entered in slope-breakpoint form with use of the WORK HARD option. The limiting yield stress of 6.13×10^4 is reached after 29.8% plastic strain. The workhardening curve is displayed in Figure 3.18-2.

Gap Data

The gaps used in this analysis use the optional true distance formulation. This is flagged in the seventh field of the GAP DATA input. The minimum separation distance between the two end nodes of the gap which represents the punch radius is 1.0 and is entered in the first field.

Boundary Conditions

Symmetry conditions are prescribed on node 1 on the axis of symmetry, whereas clamping conditions are prescribed for node 13 at the outer edge of the disk. The gap node at the center of the punch is also constrained, as well as the third degree of freedom for all end nodes of the gaps. The node at the center of the punch is later moved in the axial direction to simulate movement of the punch.

Tying

The shell nodes have four degrees of freedom: u, v, $\frac{du}{ds}$ and $\frac{dv}{ds}$. The first two agree with the u, v, w degrees of freedom of the gap element. The third degree of freedom is different, so it is not possible to use the shell nodes also as end nodes of the gap. Separate node sets are defined, and TYING type 102 is used to equate degrees of freedom 1 and 2 only.

Nonlinear Analysis Options

In order to perform a finite strain plasticity analysis, a number of parameter blocks are included. The LARGE DISP option indicates that a geometrically nonlinear analysis is to be done. The UPDATE option indicates that the stiffness formulation will be done in the updated (current) configuration. For shell elements, this makes the treatment of large rotation increments feasible. The FINITE option insures that the constitutive equations are used in appropriate invariant formulation. For shell elements, it also invokes a procedure to update the thickness of the elements due to plastic straining.

With use of the CONTROL model definition option, the maximum number of increments is set equal to 31, and the maximum number of recycles is set equal to 8. The iteration control is left on the default value of 0.1. The strain correction procedure is used to improve the convergence of this large displacement shell problem.

Data Storage Options

The SHELL SECT parameter is used to indicate that five layers will be used for integration through the shell thickness. The element data are stored out-of-core; this makes analysis with a fairly small workspace of 60,000 possible.

Output Files

The PRINT CHOICE option is used to create printed output for integration point 2, layer 1, 3, and 5 only. The POST option indicates that a post file will be written with nodal variables only. The RESTART option here indicates that at every increment the state is written to the RESTART file.

Incremental Load Specification

The DISP CHANGE option is used to prescribe a punch displacement increment of 0.025 inches. With the AUTO LOAD option, 30 of the above increments are applied. This brings the total displacement up to 0.75 inches, or three-fourths of the radius of the punch.

Results

The deformation process starts with only the center gap element closed in increment 1. In increment 2, the first two gaps are closed. In increment 3, the center gap element opens again. The center gap recloses in increment 6; the other gaps do not open up after first closure. The closing sequence is as follows:

the 3rd gap closes in increment 4;
the 4th gap closes in increment 6;
the 5th gap closes in increment 9;
the 6th gap closes in increment 13;
the 7th gap closes in increment 16;
the 8th gap closes in increment 20.

During most of the analysis one recycle is needed to obtain convergence, except in the first eight increments, when two recycles are needed. The largest number of recycles is six – needed in increment 1. Here, the overall deformation pattern is first established. The punch force versus punch displacement is shown in Figure 3.18-3. The punch force is obtained as the reaction force on node 50 in the center of the punch. The force steadily rises. The thickness in the center of element 1 reduces from 0.04 to 0.0165, whereas away from the center the thickness reduction is much smaller. In this example, the punch eventually penetrates the plate through rupture in the center of the plate.

Parameters, Options, and Subroutines Summary

Example e3x18.dat:

Parameters	Model Definition Options	History Definition Options
ELEMENTS	CONNECTIVITY	AUTO LOAD
END	CONTROL	CONTINUE
FINITE	COORDINATES	DISP CHANGE
LARGE DISP	END OPTION	
MATERIAL	FIXED DISP	
SHELL SECT	GAP DATA	
SIZING	GEOMETRY	
TITLE	ISOTROPIC	
UPDATE	POST	
	PRINT CHOICE	
	RESTART	
	TYING	
	WORK HARD	

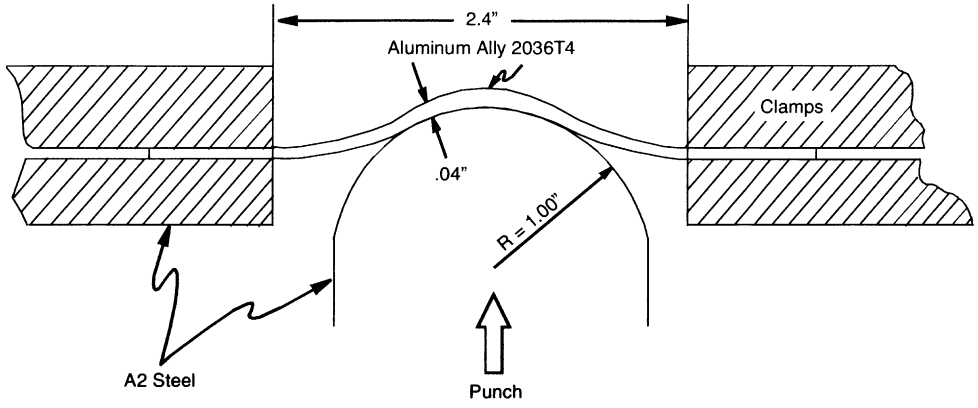

Figure 3.18-1 Modified Olsen Cup Test

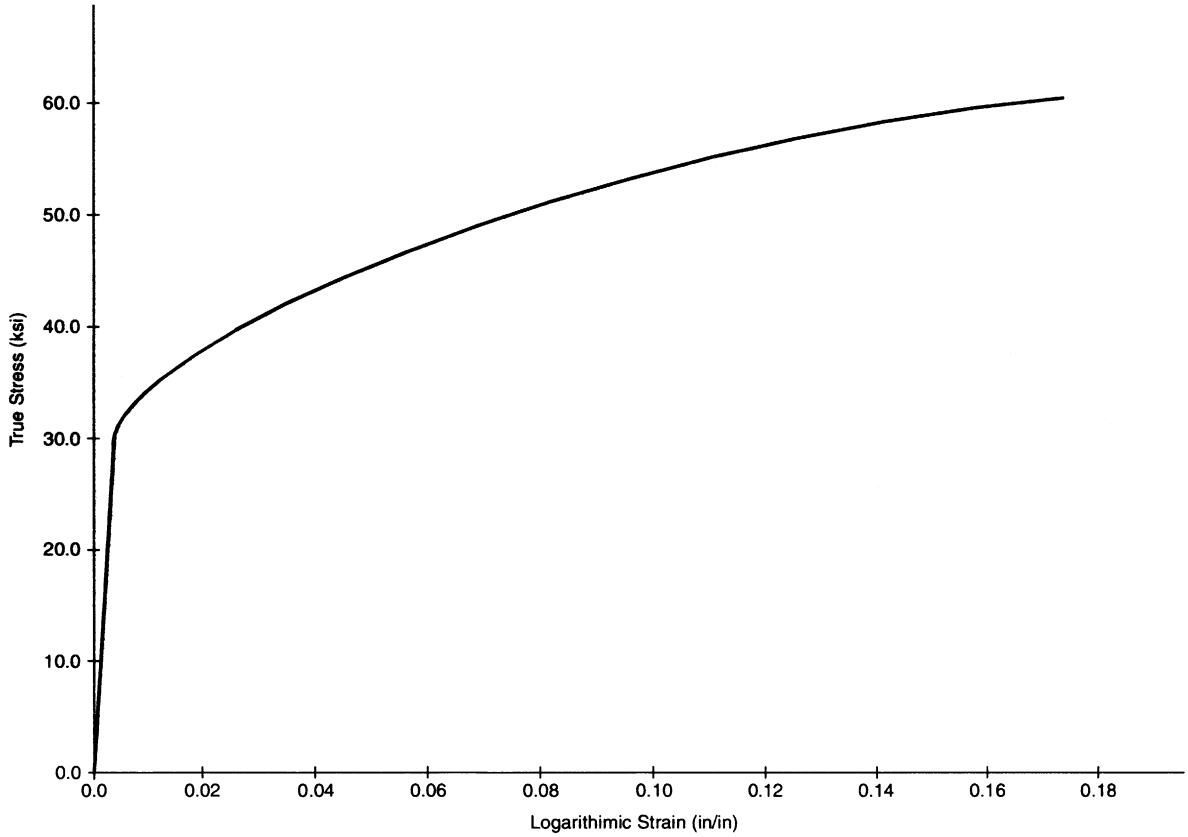

Figure 3.18-2 Tensile Stress-Strain Curve

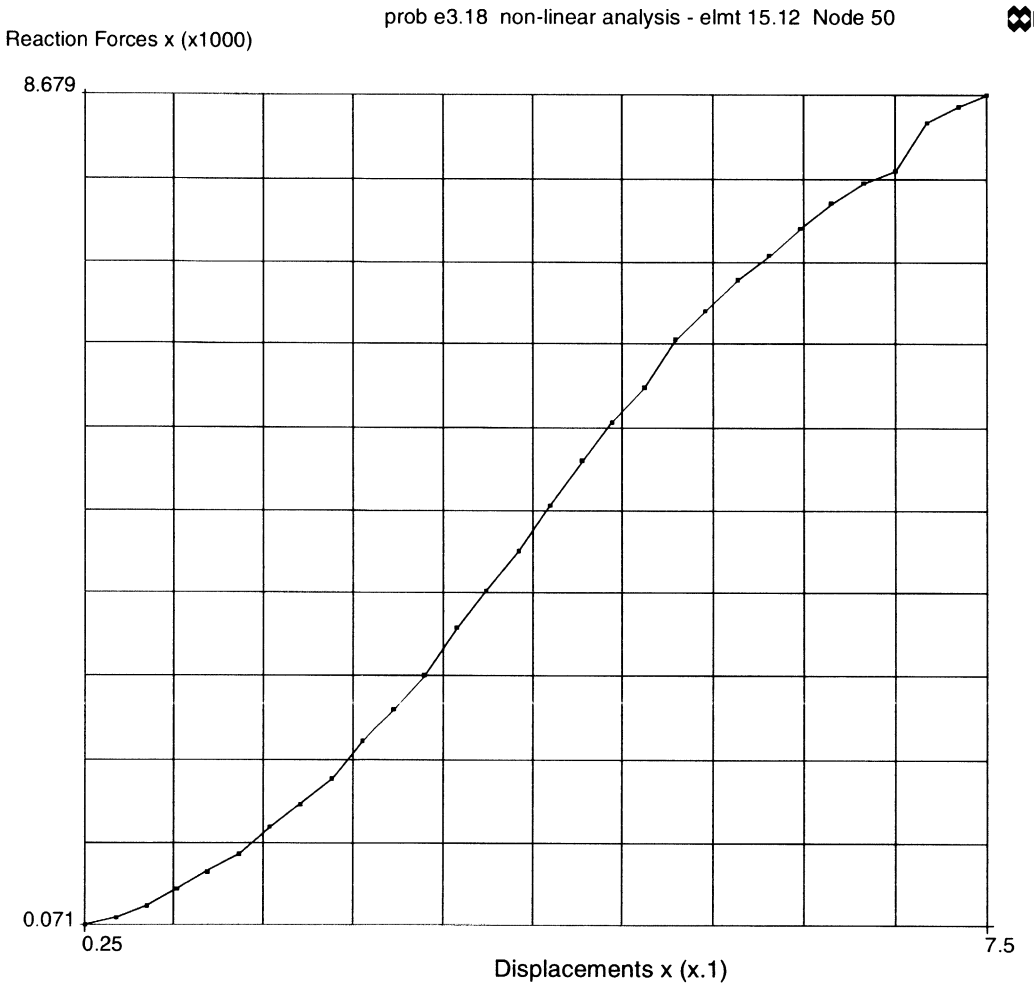

Figure 3.18-3 Load vs. Displacement

3.19 Axisymmetric Upsetting – Height Reduction 20%

An axisymmetric cylinder with a height of 8 inches and a diameter of 20 inches is compressed between two rough rigid plates. A total height reduction of 20% is obtained in 20 increments. The material is elastic-plastic with linear workhardening. The updated Lagrange and finite strain plasticity options in MARC are used to model the large-strain elastic-plastic material behavior.

This problem is modeled using the four techniques summarized below.

Data Set	Element Type(s)	Number of Elements	Number of Nodes	Differentiating Features
e3x19	10	24	35	Fully integrated element
e3x19b	116	24	35	Reduced integration hourglass element
e3x19c	116	384	425	Fine model with hourglass element
e3x19d	10	24	35	Multiplicative Decomposition (F^eF^p) Plasticity

Elements

These models are made with 4-node axisymmetric elements. Element type 10 uses full integration, while element type 116 uses reduced integration with hourglass stabilization. Because the conventional element type 10 normally locks, the constant dilatation procedure is used. This is not necessary for element type 116. When these elements are used with the F^eF^p procedure, an augmented variational principal is used, and MARC insures that the modeling of the incompressibility is accurate.

Finite Element Mesh

A mesh with 24 axisymmetric MARC type 10 and type 116 elements is used to model one-half of the cylinder. The mesh has six elements in the radial direction and four in the axial direction. Symmetry conditions are specified on the axis and the midplane of the cylinder. Sticking conditions and a prescribed compressive displacement are specified at the tool-workpiece interface. The mesh is displayed in Figure 3.19-1.

Geometry

A nonzero number is entered in the second GEOMETRY field to indicate that the elements are to be used with the constant dilatation formulation. For the F^eF^p formulation, this flag is not necessary since the incompressibility is imposed using a mixed formulation.

Property and Workhardening

The material has a Young's modulus of 10^7 psi, a Poisson's ratio of 0.3 and initial yield stress of 20,000 psi. The material is linearly workhardening with a hardening coefficient of 10^5 psi. At large strains, most materials reach a limiting stress; more sophisticated hardening behavior can be specified with either extended slope-breakpoint data or with the user subroutine WKSLP.

Geometric Nonlinearity

In the upsetting problem, large strains and rotations occur. Hence, the problem is geometrically nonlinear. The large rotations are taken care of with the LARGE DISP option; the large strain effects are taken into account with the FINITE option, which, in turn, necessitates the use of the updated Lagrange formulation (UPDATE option). In model e3x19d, the F^eF^p procedure is used which automatically activates all required options for geometric nonlinearity.

Control

A fairly coarse tolerance of 20% is specified for the iterative procedure. With only one iteration in each increment, this tolerance is easily satisfied. A restart file is written in case part of the analysis would have to be repeated with a different load step. In order to reduce the amount of printed output, only the element with the highest stress (element 24) is printed.

Load History

The displacement of the tool is prescribed. In increment 0, this displacement is 0.003 inches, which brings the stress to 46% of yield. As increment 0 is a linear elastic increment, the prescribed load was kept small. The PROPORTIONAL INCREMENT option is then used to increase the displacement increment such that the total displacement at the end of increment 1 is equal to 0.009 inches, corresponding to 0.225% height reduction. Subsequently, the displacement increment is increased to 0.034 inches. Twenty increments are applied to bring the total height reduction to 20%.

Results

The maximum stress in increment 0 (the elastic increment) occurs in element 24, integration point 3 and is equal to 9,311 psi. In the first increment, plasticity develops throughout the mesh. The von Mises stress contours after this increment (Figure 3.19-2) are in excess of the initial yield stress everywhere. No special care has to be taken to accurately follow the elastic-plastic transition. Subsequently, plastic deformation continues without giving rise to any particular problems.

The residual stress calculation indicates that the solution is somewhat in equilibrium. Compared to the reaction forces, the errors in nodal equilibrium are on the order of 1%. A total height reduction of 20% is obtained at the end of increment 22. Here, the Von Mises stress has risen to a value of 103,800 psi, as shown in the contour plot in Figure 3.19-2, for element type

10. The maximum integration point value occurs in element 24, integration point 4, and is 83,840 psi, which corresponds to a calculated plastic strain of 61.7%. This equivalent plastic strain is calculated from the strain components. The strain path is not straight, and so the calculated value differs slightly from the integrated equivalent plastic strain rate. The integrated equivalent plastic strain rate is 63.8%. The maximum stress for element type 116 is 67,090 psi (Figure 3.19-3) and is much lower because of the large element size and that this element has only one integration point per element. A new mesh is made that subdivides each of the 24 elements into 4 elements for a total of 96 elements. This model is subjected to the same loads and boundary conditions, and the stress contours are shown in Figure 3.19-4. The maximum stress for this model is 119,400 psi. Figure 3.19-6 shows the results using the F^eF^p (finite strain plasticity using multiplicative decomposition) formulation. The maximum von Mises stress is 89590 psi which is nearly midway between the full and reduced integration elements. For the axisymmetric case, the incompressibility is handled better by the mixed formulation used in the F^eF^p framework and hence it yields lower stresses. These stresses are however higher than the reduced integration, which use only one integration point for calculation of the stresses. Finally, the load deflection curve is constructed using user subroutine IMPD which determines the total load placed on the structure for each increment. The load deflection curve for this problem, as shown in Figure 3.19-5, is calculated from the total reaction forces in the plane of symmetry using subroutine IMPD. The total reaction force on the tool interface is the same. The finer mesh is slightly more flexible than the coarser models. This is reflected by a lower load required as shown in Figure 3.19-5.

The contours plotted on the deformed geometry show some perturbation in the internal mesh boundaries. This so-called hourglassing is a side effect of constant dilatation for the elements. The high bulk stiffness requires each element to retain approximately constant volume and so hourglassing type modes can develop. These modes only include deviatoric strains. This hourglassing has very little effect on the solution accuracy.

Also, the severe distortion that occurs in the fine mesh near the singularity should be remeshed using the REZONE option for more accuracy. This would prevent the mesh from becoming too distorted. Finally, the CONTACT option could be used to automatically enforce the contact constraints at the tool-workpiece interface.

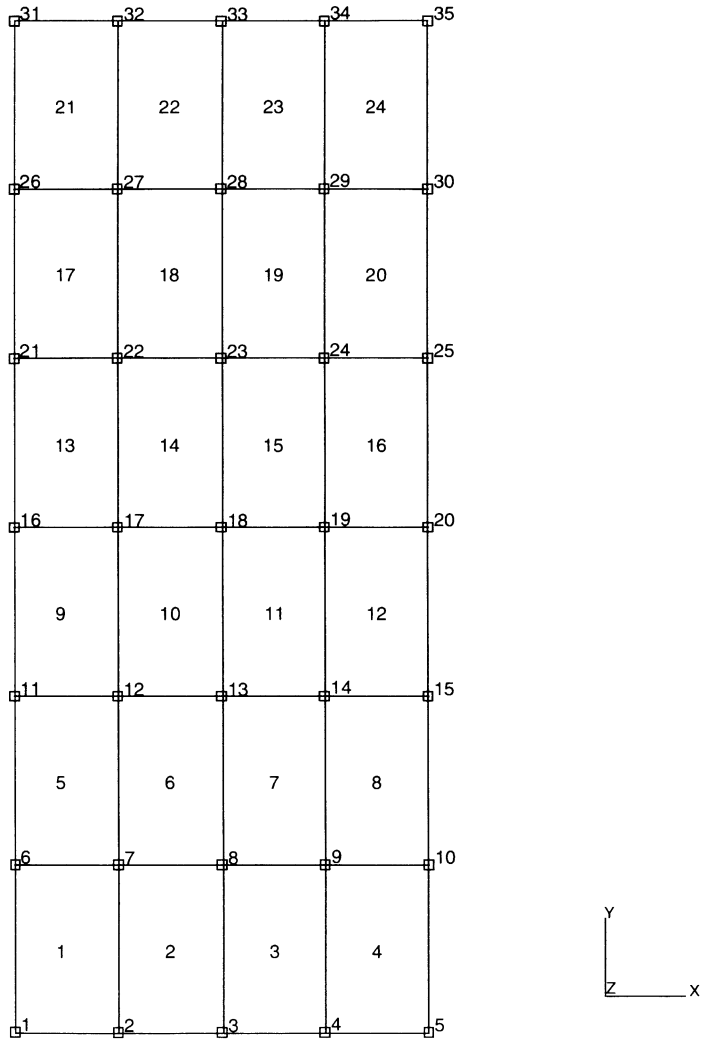

Figure 3.19-1 Model with Elements and Nodes Labeled

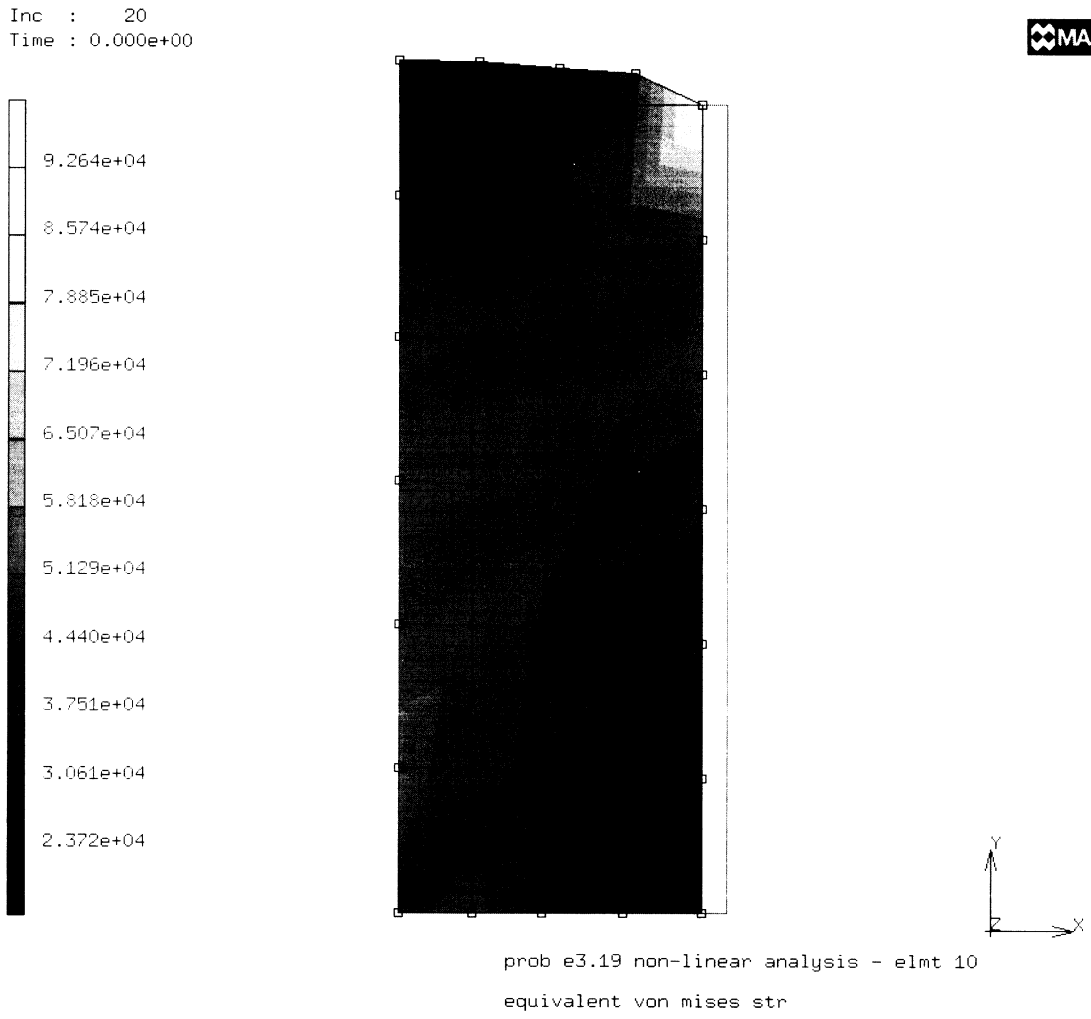

Figure 3.19-2 von Mises Stress Contours at Increment 20 Element Type 10

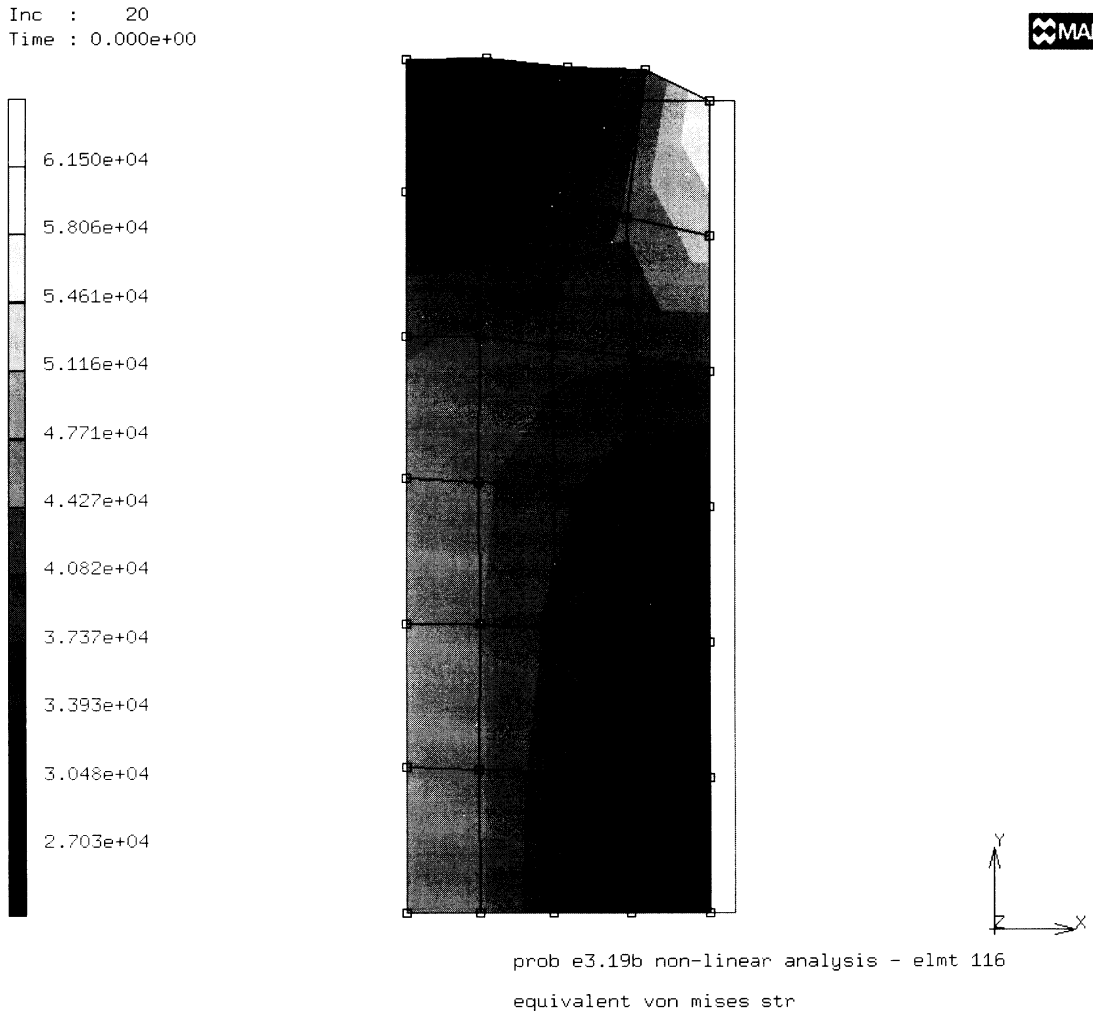

Figure 3.19-3 von Mises Stress Contours at Increment 20 Element Type 116

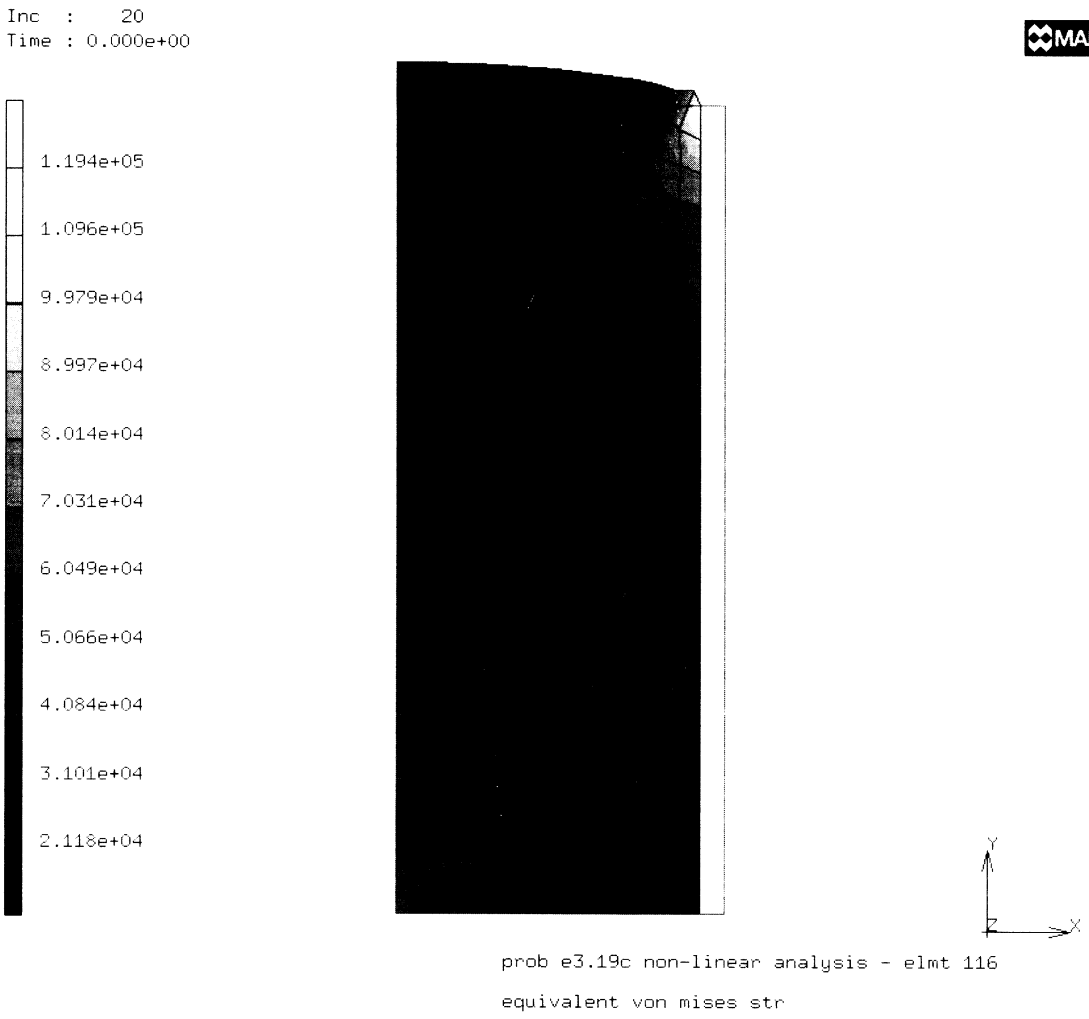

Figure 3.19-4 von Mises Stress Contours at Increment 20 Element Type 116 (Fine Mesh)

Displacement (x-1 inches)	Load (x-10**7 lbf)			
	Type 10	Type 116	Type 116 fine	Type 10, F^eF^p
0.0	0.0	0.0	0.0	
6.0E-03	5.44666E-01	5.44678E-01	5.42062E-01	
4.0E-02	9.09003E-01	9.51534E-01	8.73461E-01	
8.0E-02	9.53196E-01	9.86861E-01	9.39867E-01	
1.2E-01	1.05619E+00	1.05823E+00	1.02221E+00	
1.6E-01	1.14687E+00	1.14637E+00	1.10502E+00	
2.0E-01	1.21936E+00	1.23329E+00	1.18878E+00	
2.4E-01	1.31785E+00	1.32650E+00	1.28633E+00	
2.8E-01	1.38827E+00	1.40290E+00	1.37896E+00	
3.2E-01	1.49609E+00	1.50275E+00	1.46018E+00	
3.6E-01	1.56728E+00	1.62923E+00	1.54599E+00	
4.0E-01	1.68304E+00	1.68450E+00	1.63446E+00	
4.4E-01	1.82681E+00	1.77902E+00	1.72597E+00	
4.8E-01	1.86321E+00	1.92374E+00	1.82075E+00	
5.2E-01	1.97708E+00	1.99075E+00	1.91924E+00	
5.6E-01	2.14452E+00	2.09846E+00	2.02156E+00	
6.0E-01	2.28568E+00	2.26072E+00	2.12789E+00	
6.4E-01	2.40272E+00	2.41074E+00	2.23832E+00	
6.8E-01	2.52240E+00	2.53974E+00	2.35296E+00	
7.2E-01	2.65395E+00	2.66853E+00	2.47188E+00	
7.6E-01	2.79495E+00	2.80702E+00	2.59501E+00	
8.0E-01	2.94241E+00	2.95548E+00	2.72212E+00	

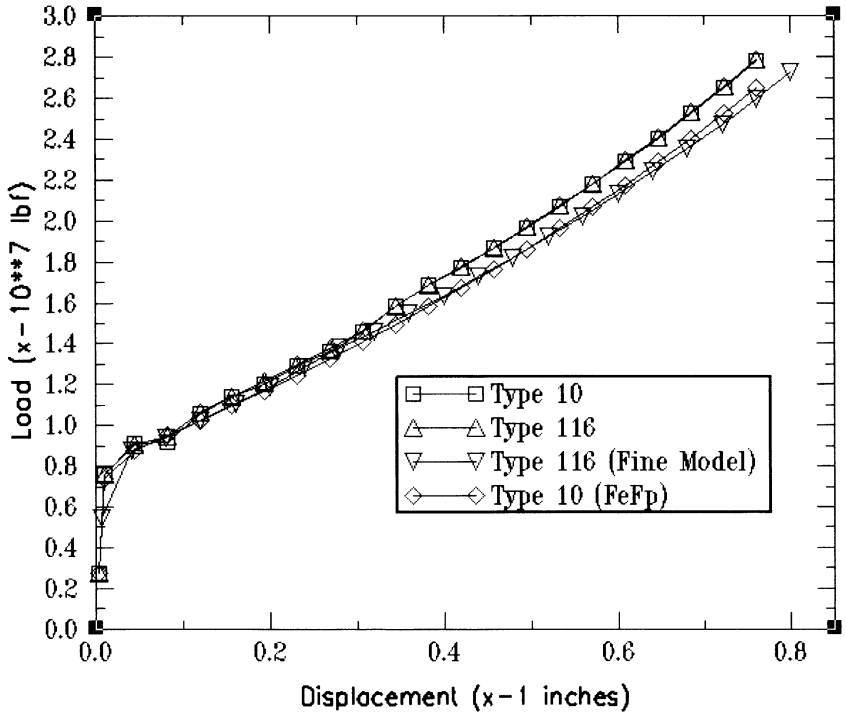

Figure 3.19-5 von Mises Stress Contours at Increment 20, Element Type 10, F^eF^p Formulation

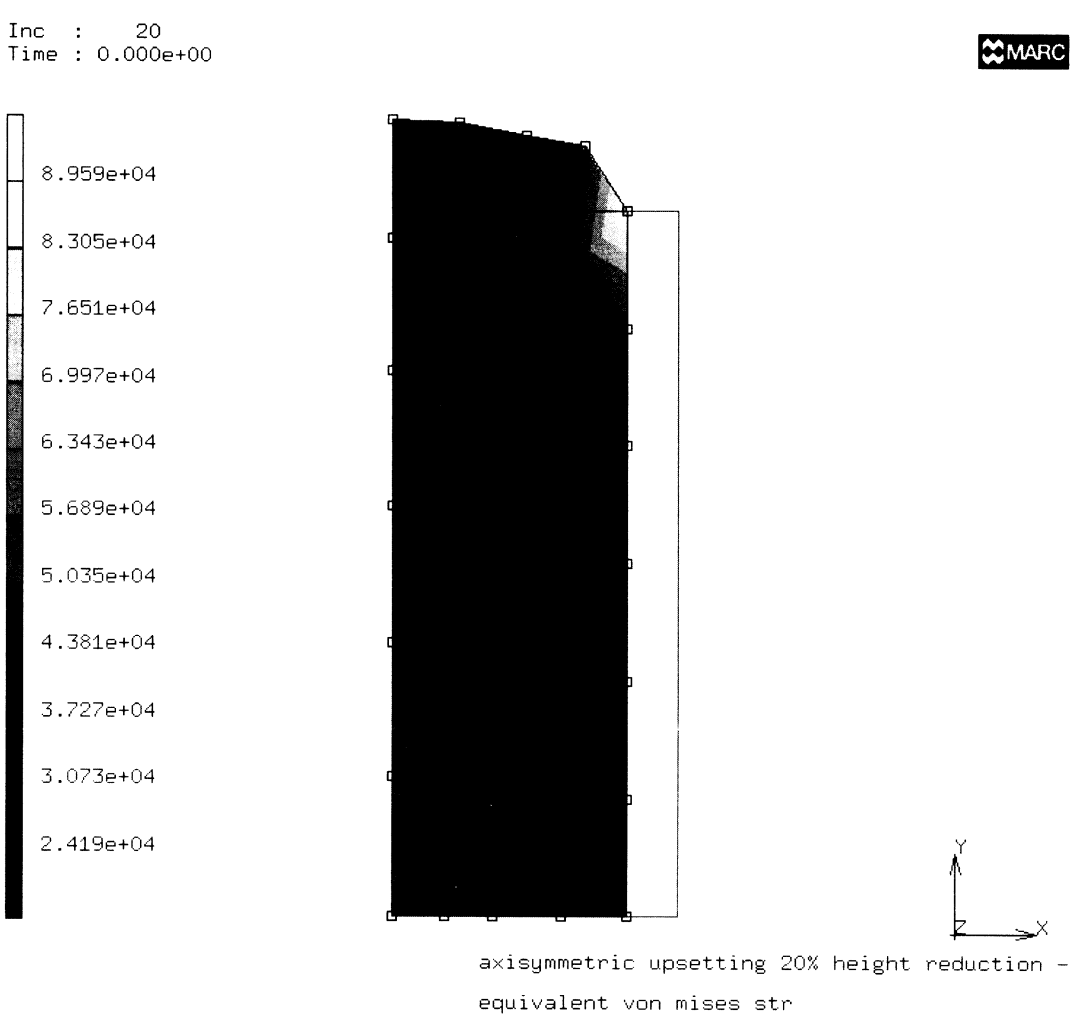

Figure 3.19-6 Load Displacement Curve

3.20 Plastic Bending of a Straight Beam into a Semicircle

A straight two-dimensional cantilever beam is subjected to a prescribed end rotation. The beam deforms plastically into a semicircle, and has a length of 20 inches and square cross section of 1 square inch. After a prescribed rotation of 90°, the end is released and the beam springs back elastically to a permanently deformed state.

Element

A 10-element mesh of MARC element type 16 models the beam. This is a two-dimensional beam element with fully cubic interpolation functions. This element type is particularly suited for problems in which geometrically nonlinear effects are important. Only one element (number 1) and two nodes (numbers 1 and 11) are specified directly. The connectivity and coordinates of the remaining elements and nodes are generated with the CONN GENER and NODE FILL options, respectively. The element type 16 has a rectangular cross section. In this problem, the GEOMETRY option is used to specify both height and width equal to 1 in. Seven-point integration through the height of the beam is specified with the SHELL SECT parameter.

Material Properties

The elastic properties are specified with the ISOTROPIC option. Young's modulus is equal to 10^7 psi and Poisson's ratio is equal to 0.33. The initial yield stress of 20,000 psi is also specified with the ISOTROPIC option. The remaining part of the stress-strain curve is specified with the WORK HARD option. The initial workhardening slope is equal to 238,029 psi, up to a plastic strain of 0.196%, which corresponds to a stress of 20,466 psi. Subsequently, the workhardening slope is equal to 97,515 psi, up to a plastic strain of 5.671%, or 25,805 psi. At this stress level, no further hardening occurs. The workhardening curve is shown in Figure 3.20-1.

Transformations and Boundary Conditions

MARC element type 16 has degrees of freedom at each node u, v, $\frac{du}{ds}$, $\frac{dv}{ds}$, where u and v are the global displacements, $\frac{du}{ds}$ and $\frac{dv}{ds}$ are the derivatives of these displacements along the length of the beam. These degrees of freedom are not suitable for application of bending moments and/or boundary conditions, particularly if the beam is to undergo large rotations. For the end nodes 1 and 11, the SHELL TRAN option type 1 is used. This transforms the degrees of freedom of these nodes into u, v, ϕ, and e.

The SHELL TRAN option is used here in conjunction with the FOLLOW FORCE option. This combination ensures that the transformations are carried out in the deformed configuration of the beam. To incrementally prescribe a finite rotation, one applies a nonzero incremental boundary condition to degree of freedom 3 of node 11. The clamped conditions at the other end of the beam are enforced by specifying degrees of freedom 1 to 3 at node 1 as zero.

Geometric Nonlinearity

Large rotations occur in this problem; therefore, the problem is definitely geometrically nonlinear. The nonlinearity in the axial strain terms is included with the LARGE DISP option. This is a problem in which the bending effects are dominant; therefore, the strain correction algorithm is used to handle the nonlinear terms. With this algorithm, large errors in the axial forces during iteration are avoided. Default tolerance is specified on the CONTROL option. The number of iterations is set to a high value in order to obtain results for the load reversal at the end of the analysis. In order to ensure correct calculation of the curvature change, the updated Lagrange formulation must be invoked with the UPDATE option. In that case, reasonably accurate results are obtained for incremental rotations of up to approximately 0.1 radians, which is greater than the incremental rotation in this problem. In this analysis, the strains will only be moderately large, namely about 8%, which follows from simple kinematic considerations. Large strain effects will not be considered in this problem.

Printing, Plotting, and Postprocessing

For nonlinear analysis, the default printout for beam elements yields a large amount of output. In particular, the stress and plastic strains in each layer in which plasticity occurs are printed. The PRINT CHOICE option is used to select printout at only one integration point in one element. Additional output is obtained graphically; in particular, the displaced mesh is shown at the end of the analysis. Finally, a formatted post file is written with a number of element variables included.

Loading

The initially prescribed rotation is 0.025 radians. With this rotation value, the stresses in the extreme fibers remain below yield. Subsequently, 62 equal increments of 0.25 radians are applied, which brings the total rotation to 1.57 radians, a little more than the desired rotation of 90 degrees. In increment 66, the boundary condition at node 11 is removed with the boundary change option, and two zero load increments obtain the unloaded deformed shape of the beam.

Results

The stress printout for increment 0 shows the stress equal to 15,870 psi, or 79.3% of yield. Subsequently, the beam gradually becomes plastic – two layers 1, 2, 6, and 7 in increment 1; all layers, except the central layer 6, in all other increments. In increment 46, maximum stress is reached in the extreme layers. The stress in the subsequent layers almost reaches yield in increment 48. The maximum tip rotation of 1.57 radians is reached in the same increment. The tip displacements at this point are -3.732 inches in the beam direction, and 6.42 inches in the direction perpendicular to the beam. This only slightly differs from the theoretical values of -3.634 inches and 6.366 inches expected for a rotation of exactly 90°. The bending moment at the clamped end at this stage in the analysis is 6054 lb-inch, which is 6.1% less than the moment needed to form a plastic hinge: $\sigma_{max}\, h^2/4 = 61{,}451$ lb-inch.

Up to this point, the secant modulus method does not need any recycling. This is because the first estimate of the stress-strain law is based on the extrapolation of the strain change in the last increment. In increment 66, the tip condition is released. This causes a considerable imbalance. During the first estimate, the constitutive routine assumes continued plastic loading. As a result of the initial imbalance and the assumed plastic loading, the elastic spring back is grossly overestimated.Three iterations are needed to correct this initial error, resulting in an elastic springback of 0.1447 radians. The strain correction method can still yield inaccurate results at this stage; therefore, one more zero increment is applied. This correction is minor, as demonstrated by the results. From the calculated bending moment of 5991.7 lb-inch, the theory predicts an elastic spring back of 0.1438 radians. The numerical results differ only marginally from the theoretically expected results. The displaced mesh representing the permanently deformed beam is shown in Figure 3.20-2.

Parameters, Options, and Subroutines Summary

Example e3x20.dat:

Parameters	Model Definition Options	History Definition Options
ELEMENTS	CONN GENER	AUTO LOAD
END	CONNECTIVITY	CONTINUE
FINITE	CONTROL	DISP CHANGE
FOLLOW FORCE	COORDINATES	PRINT CHOICE
LARGE DISP	END OPTION	PROPORTIONAL INCREMENT
SHELL SECT	FIXED DISP	
SIZING	GEOMETRY	
TITLE	ISOTROPIC	
UPDATE	NODE FILL	
	POST	
	PRINT CHOICE	
	RESTART	
	SHELL TRANFORMATIONS	
	WORK HARD	

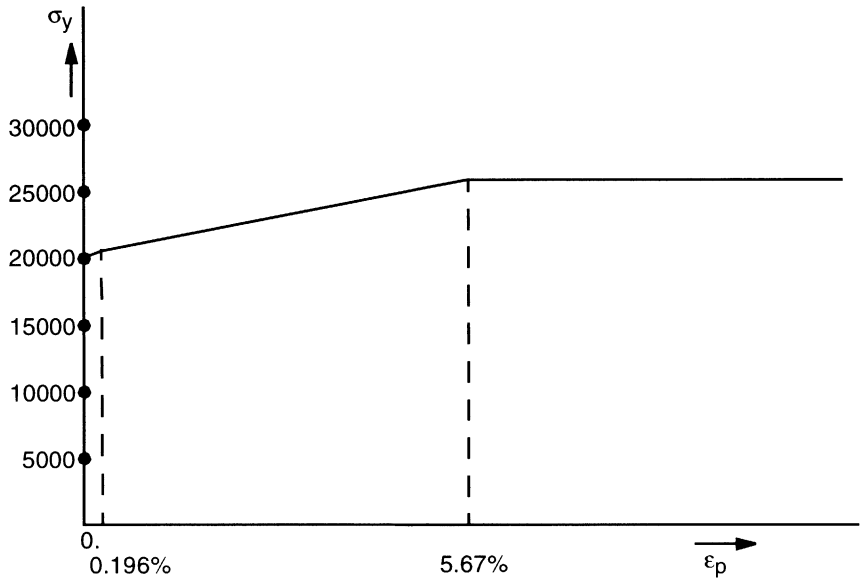

Figure 3.20-1 Workhardening Curve

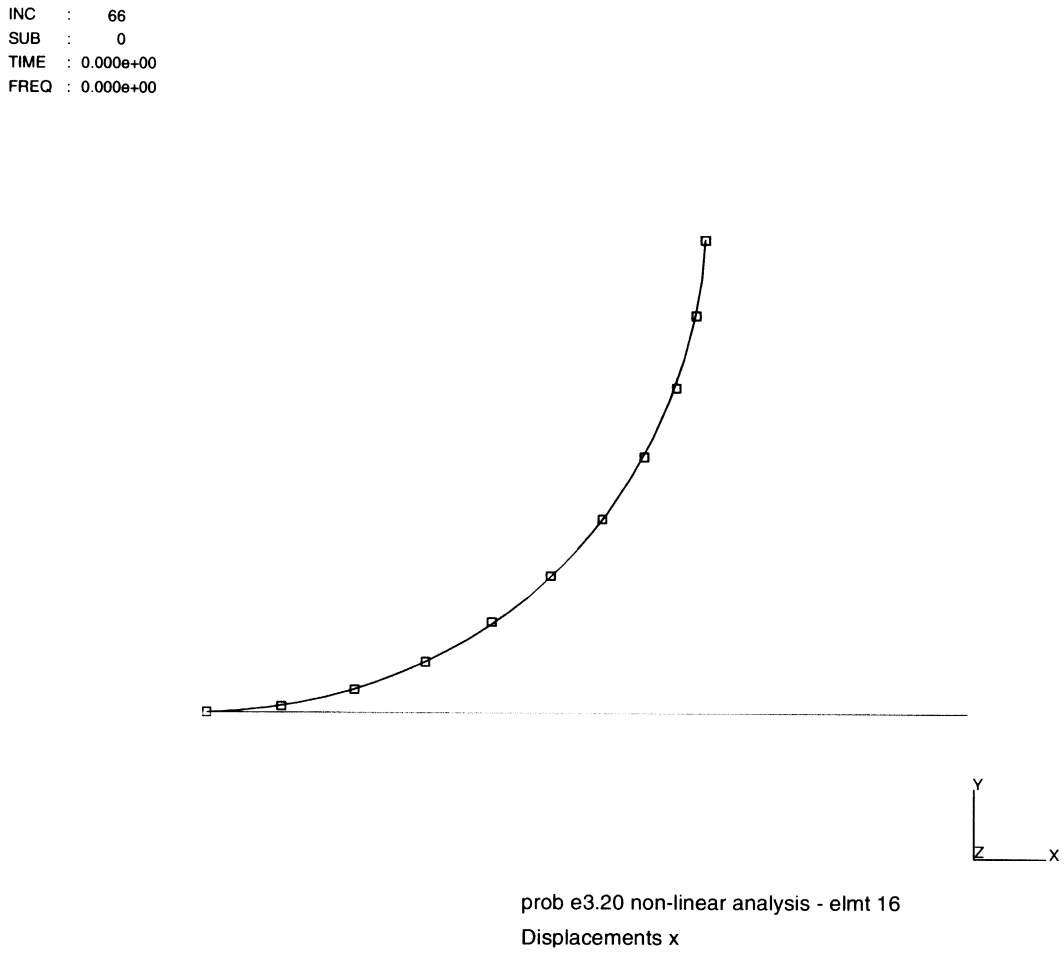

Figure 3.20-2 Deformed Beam after Release of End

3.21 Necking of a Cylindrical Bar

A cylindrical bar of 20 inches long and 6 inches in diameter is loaded in tension. The ends of the bar are clamped and radial motion is prevented. Away from the ends, the deformation is initially homogeneous. At a certain elongation, the deformation starts to localize. The onset of such localization occurs when the load in the bar reaches a maximum.[1]

This problem is modeled using the five techniques summarized below.

Data Set	Element Type(s)	Number of Elements	Number of Nodes	Differentiating Features
e3x21	10	60	80	Fully integrated element
e3x21c	116	60	80	Reduced integration hourglass element
e3x21d	10	60	80	ADAPTIVE meshing
e3x21e	10	60	80	Multiplicative Decomposition (F^eF^p)
e3x21f	10	60	80	CONSTANT DILATATION

Elements

The solution is obtained using first-order isoparametric quadrilateral elements for axisymmetric analysis with element types 10 and 116, respectively. Type 116 is similar to type 10; however, it uses reduced integration with hourglass control.

Model

Because of symmetry, only one-half of the length of the bar is modeled where the axial coordinate x ranges from 0 to 10 inches and the radial coordinate y ranges from 0 to 3 inches. More elements are placed near the middle of the bar at x = 0 and fewer are placed at the end of the bar at x=10 inches. The mesh with numbered elements is shown in Figure 3.21-1 and Figure 3.21-2 shows the numbered nodes. In problem e3x21d, the adaptive meshing procedure is used.

Geometry

To obtain the constant volumetric strain formulation, (EGEOM2) is set to unity. This is applied to all elements of type 10 in models e2x21 and e3x21d. In model e3x21f, the CONSTANT DILATATION parameter is used. This has the same effect. For element type 116, it has no effect because the element does not lock. The incompressibility is automatically in the F^eF^p procedure.

Material Properties

The material for all elements is treated as an elastic perfectly-plastic material, with a Young's modulus of 10.0E+06 psi, Poisson's ratio of 0.3, and a yield strength of 20,000 psi. The LARGE DISP, UPDATE, and FINITE options are used in this analysis. The constant workhardening rate of 30,000 psi applies to the true stress versus logarithmic strain curve.

Boundary Conditions

The symmetry conditions require that all nodes along the x = 0 axis have their x-displacements constrained to zero; all nodes along the y = 0 axis have their y-displacements constrained to zero. All nodes along the x = 10 axis have their y-displacements constrained to zero and an initial x-displacement of .01 inches.

Load History

All nodes along the x = 10 axis will continue to have their x-displacements increased by .01 inches/increment for 9 increments; then increased by 0.1 inches for 59 increments for the bar to reach a total length of 32 inches.

Analysis Control

The CONTROL option is used to specify a maximum of 80 increments and a maximum of 10 iterations. This number of iterations is specified in order to deal with sudden changes in the deformation field. The convergence checking is done on residuals with a control tolerance of 0.01. Several element variables are written onto the post file and subroutine IMPD sums the load for the load-deflection curve.

Adaptive Meshing

The adaptive meshing procedure is used based upon the Zienkiewicz-Zhu error criteria. A maximum of three levels is allowed.

Results

The value of the maximum load is readily calculated. The force, F, in the bar can be expressed in terms of the true stress σ and current cross-sectional area, A, by:

$$F = A\sigma$$

Assuming incompressibility, the current area can be related to the initial area, A_o, and the elongation, λ, by:

$$F = A_o\sigma/\lambda$$

The load reaches a maximum if the force does not change for increasing elongation. This furnishes a condition for the onset of necking, whereby:

$$dF/d\lambda = A_0 (d\sigma/d\lambda - \sigma/\lambda)/\lambda = 0$$

With the introduction of the logarithmic strain $e = \ln \lambda$, this condition can also be expressed as:

$$h = d\sigma/de = \sigma$$

The onset of necking occurs if the true stress is equal to hardening modulus in the true stress-logarithmic strain curve. For a material with constant hardening modulus, h, this relation can be worked out in greater detail. For such a material, the true stress can be expressed in terms of the elongation by:

$$\sigma = \sigma_y + he,$$

where σ_y is the initial yield stress. Substituting yields the logarithmic strain:

$$e = 1 - \sigma_y/h.$$

In the current problem, the initial yield stress, σ_y = 20,000 psi and the hardening modulus, h = 30,000 psi, yielding a logarithmic strain of 33.33%. The onset of necking occurs at an engineering strain (the length change divided by the original length) of 39.56% or an end point displacement of 3.956 inches.

The results from the model shown in Figure 3.21-3 predict the onset of necking occurring earlier at about 3.0 inches. However, the load displacement curve is very flat due to the low value of the hardening modulus and an accurate value is hard to achieve. Also, the load displacement curve shows the model with element type 10, necking more than the element type 116 after the maximum load is reached. The amount of necking is also shown in the deformed plots of Figure 3.21-4 through Figure 3.21-10. This is because element type 116 only has one integration point (element type 10 has four) used for stress recovery and requires more elements.

Figures 3.21-5, 3.21-7, and 3.21-10 show the equivalent plastic strains for the different case. It can be seen that the results obtained with element 10 using the two formulations, additive and multiplicative decompostion, within 2%. Similarly, the reaction forces for the two formulations are also within 2% as indicated by Figure 3.21-4 and Figure 3.21-9. The differences are due to the way incompressibility is imposed in the two formulations. The F^eF^p formulation uses a more accurate tangent with an exact treatment for large strain kinematics and elasticity. However, the reduced integration elements depict a much softer response and does not yield an accurate solution even with the finer mesh.

Parameters, Options, and Subroutines Summary

Example e3x21a.dat:

Parameters	Model Definition Options	History Definition Options
ELEMENTS	CONNECTIVITY	AUTO LOAD
END	CONTROL	CONTINUE
FINITE	COORDINATES	PROPORTIONAL INCREMENT
LARGE DISP	END OPTION	
SIZING	FIXED DISP	
TITLE	GEOMETRY	
UPDATE	ISOTROPIC	
	POST	
	PRINT CHOICE	
	UDUMP	
	WORK HARD	

Example e3x21b.dat:

Parameters
COMBINED
ELEMENTS
END
PRINT
TITLE
USER

Example e3x21c.dat:

Parameters	Model Definition Options	History Definition Options
ALIAS	CONNECTIVITY	AUTO LOAD
ELEMENTS	CONTROL	CONTINUE
END	COORDINATE	PROPORTIONAL INCREMENT
FINITE	END OPTION	
LARGE DISP	FIXED DISP	
SIZING	GEOMETRY	
TITLE	ISOTROPIC	
UPDATE	POST	
	PRINT CHOICE	
	RESTART	
	WORK HARD	

Example e3x21d.dat:

Parameters	Model Definition Options	History Definition Options
ADAPTIVE	ADAPTIVE	AUTO LOAD
ELEMENTS	CONNECTIVITY	CONTINUE
END	CONTROL	PROPORTIONAL INCREMENT
FINITE	COORDINATES	
LARGE DISP	END OPTION	
SIZING	FIXED DISP	
TITLE	GEOMETRY	
UPDATE	ISOTROPIC	
	POST	
	PRINT CHOICE	
	UDUMP	
	WORK HARD	

Example e3x21e.dat:

Parameters	Model Definition Options	History Definition Options
ELEMENTS	CONNECTIVITY	AUTO LOAD
END	CONTROL	CONTINUE
TITLE	COORDINATES	PROPORTIONAL INCREMENT
LARGE DISP	END OPTION	
SIZING	FIXED DISP	
PLASTICITY	WORK HARD	
	ISOTROPIC	
	POST	
	PRINT CHOICE	
	UDUMP	

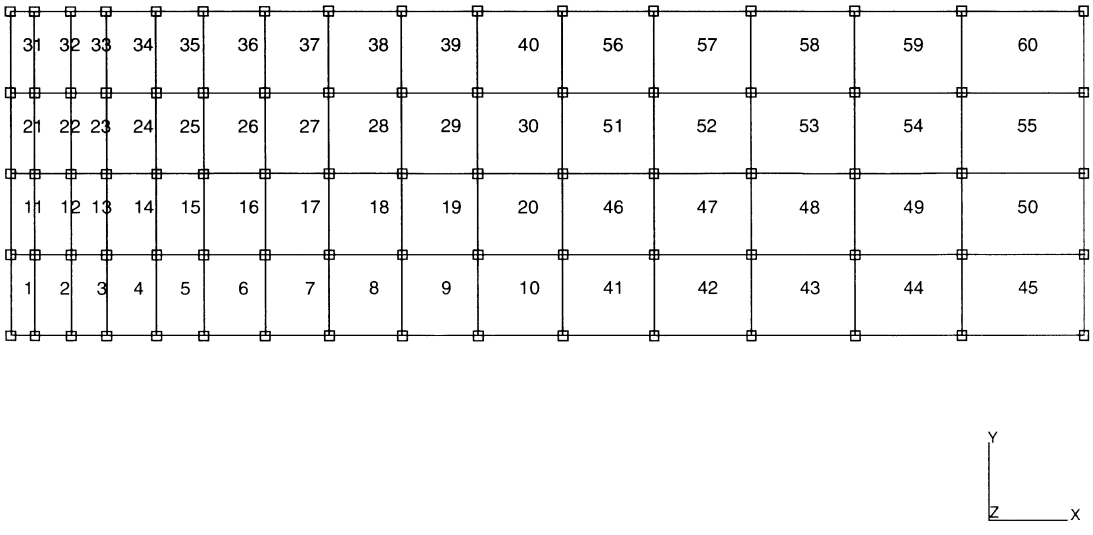

Figure 3.21-1 Model with Elements Numbered

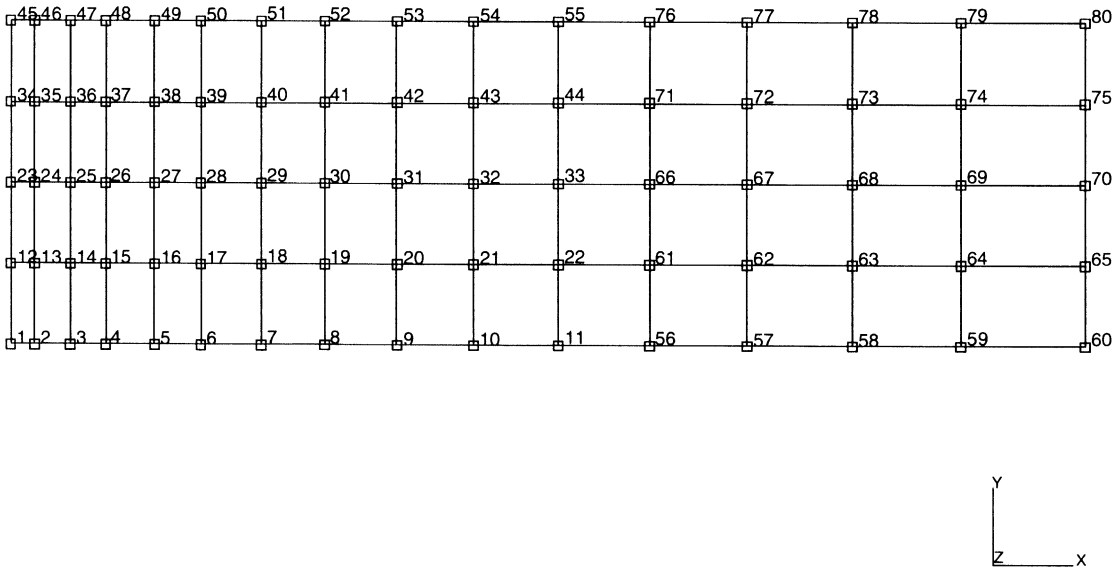

Figure 3.21-2 Model with Nodes Labeled

Displacement	Load (x10**5 lbf)		
	Type 10	Type 116	Type 116 fine
0.0	0.0	0.0	0.0
1.00000E-02	2.86645E+00	2.87316E+00	2.86198E+00
2.00000E-02	5.64279E+00	5.65044E+00	5.65154E+00
3.00000E-02	5.65075E+00	5.65181E+00	5.65312E+oo
2.70000E+00	6.08106E+00	6.08466E+00	6.08170E+oo
2.80000E+00	6.08219E+00	6.08442E+00	6.08266E+00
2.90000E+00	6.08235E+00	6.08293E+00	6.08259E+00
3.00000E+00	6.08144E+00	6.07998E+00	6.08137E+00
3.10000E+00	6.07933E+00	6.07538E+00	6.07879E+00
3.20000E+00	6.07580E+00	6.06831E+00	6.07457E+00
3.30000E+00	6.07060E+00	6.05820E+00	6.06833E+00
3.40000E+00	6.06339E+00	6.04646E+00	6.05973E+00
4.70000E+00	5.56913E+00	5.24714E+00	5.46007E+00
4.80000E+00	5.47695E+00	5.06798E+00	5.34126E+00
4.90000E+00	5.37292E+00	4.84365E+00	5.20284E+00
5.00000E+00	5.25596E+00	4.59166E+00	5.04048E+00

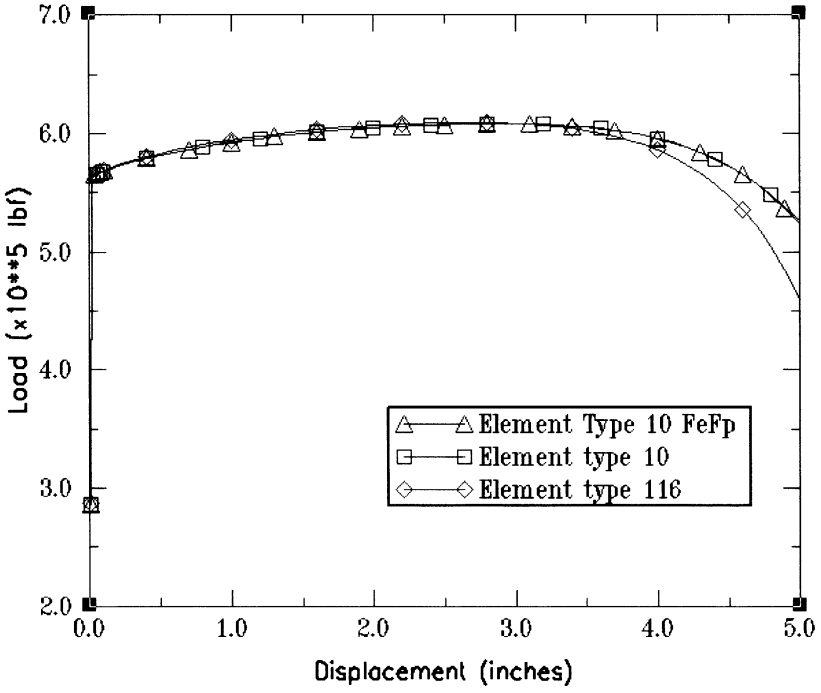

Figure 3.21-3 Load -Displacement Curve

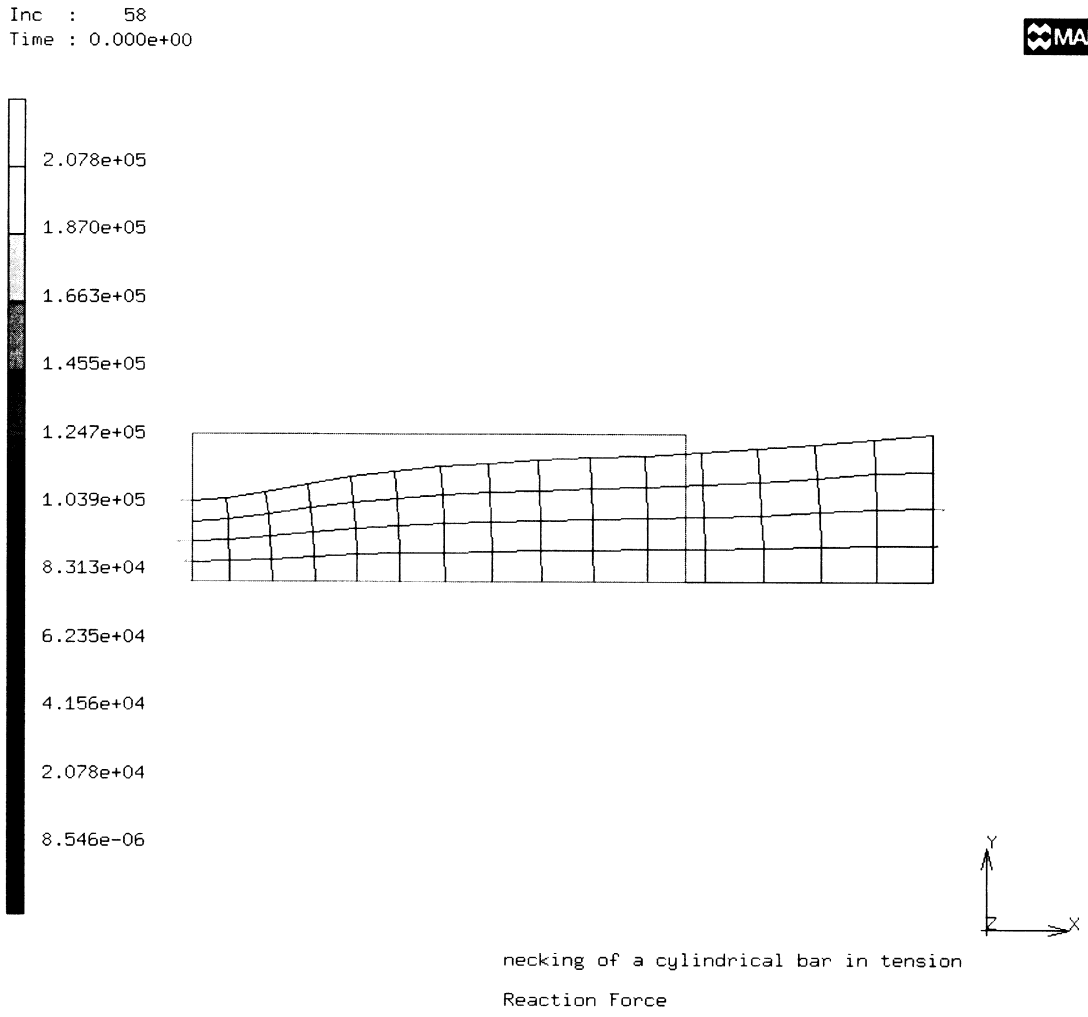

Figure 3.21-4 Vector Plot of Reactions for Type 10

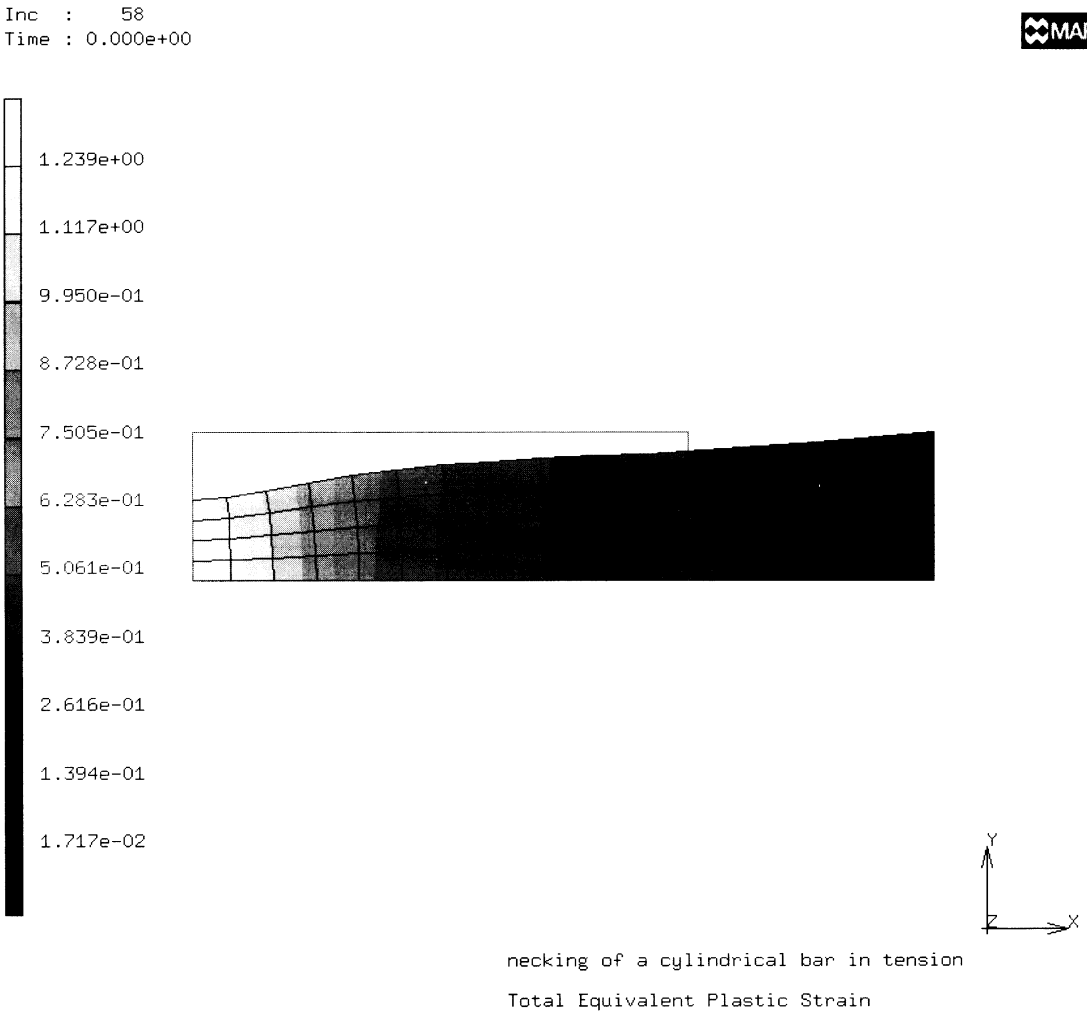

Figure 3.21-5 Contour Plot of Equivalent Strain for Type 10

Figure 3.21-6 Vector Plot of Reactions for Type 116 (Coarse Mesh)

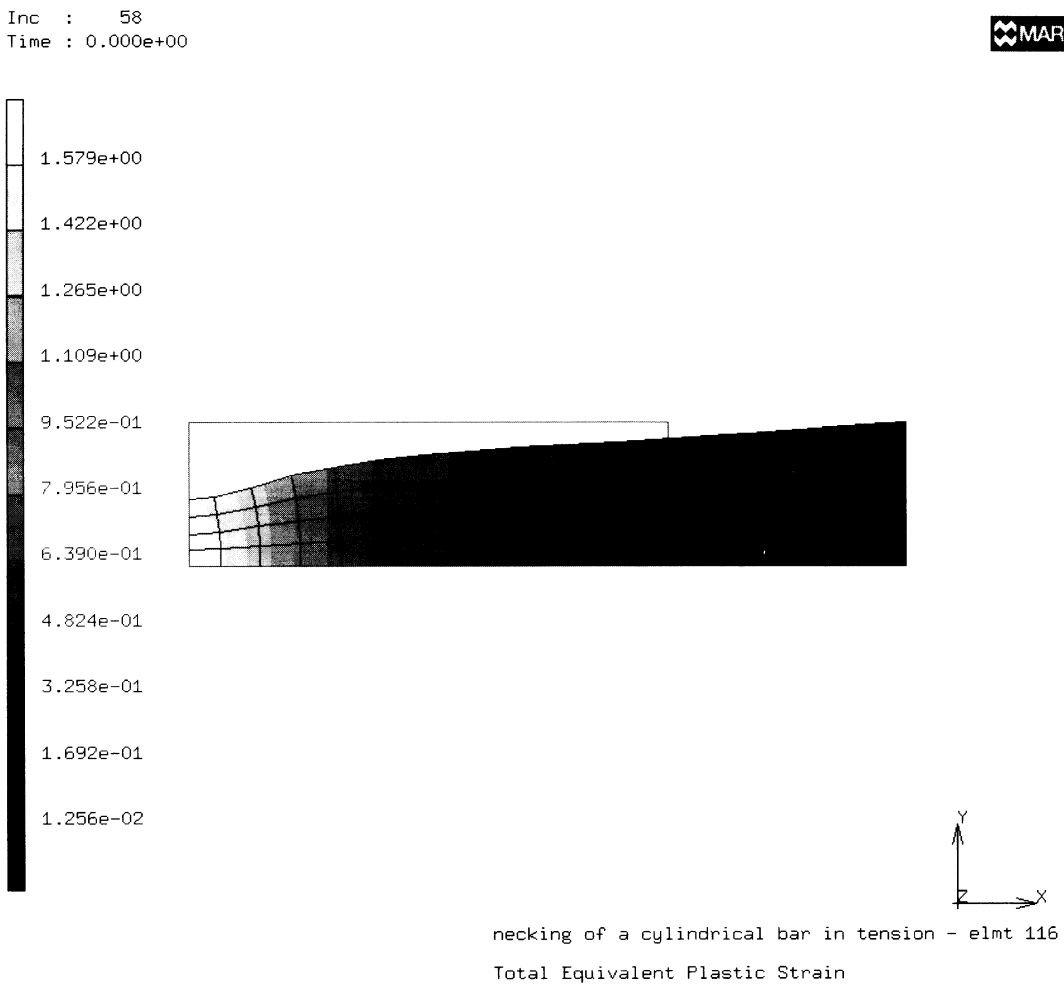

Figure 3.21-7 Contour Plot of Equivalent Plastic Strain for Type 116 (Coarse Mesh)

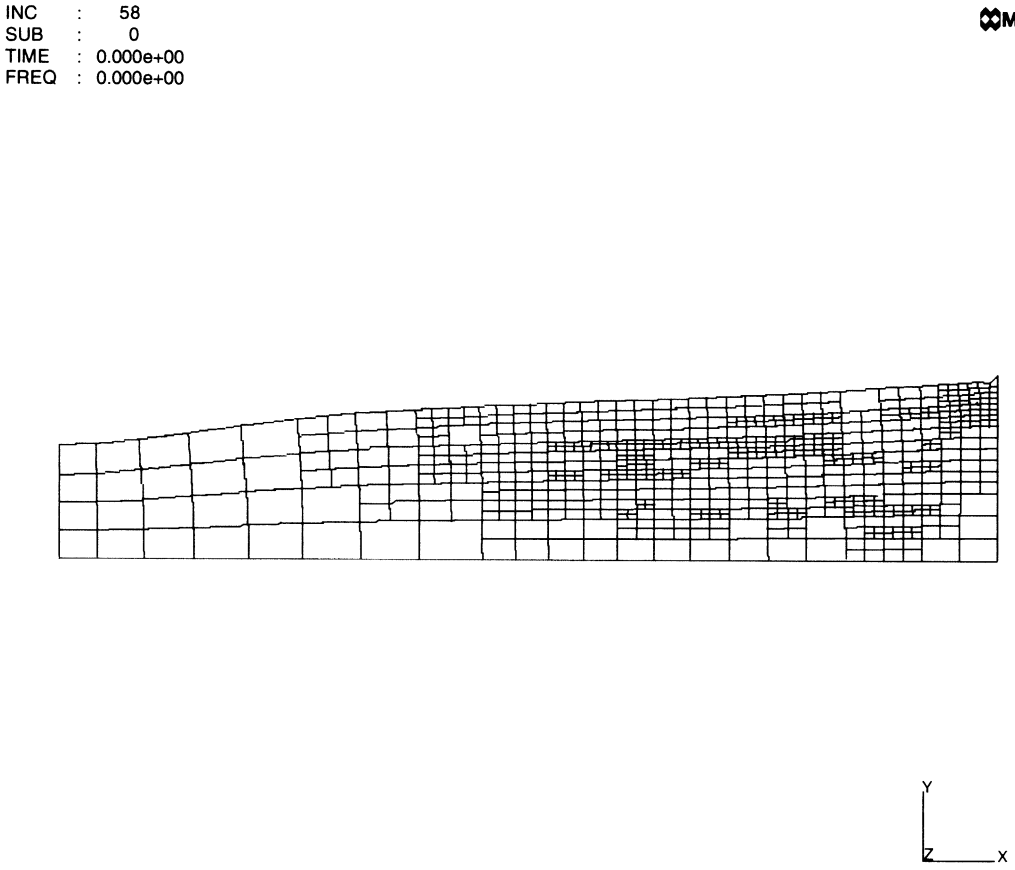

Figure 3.21-8 Final Mesh After Adaptive Meshing

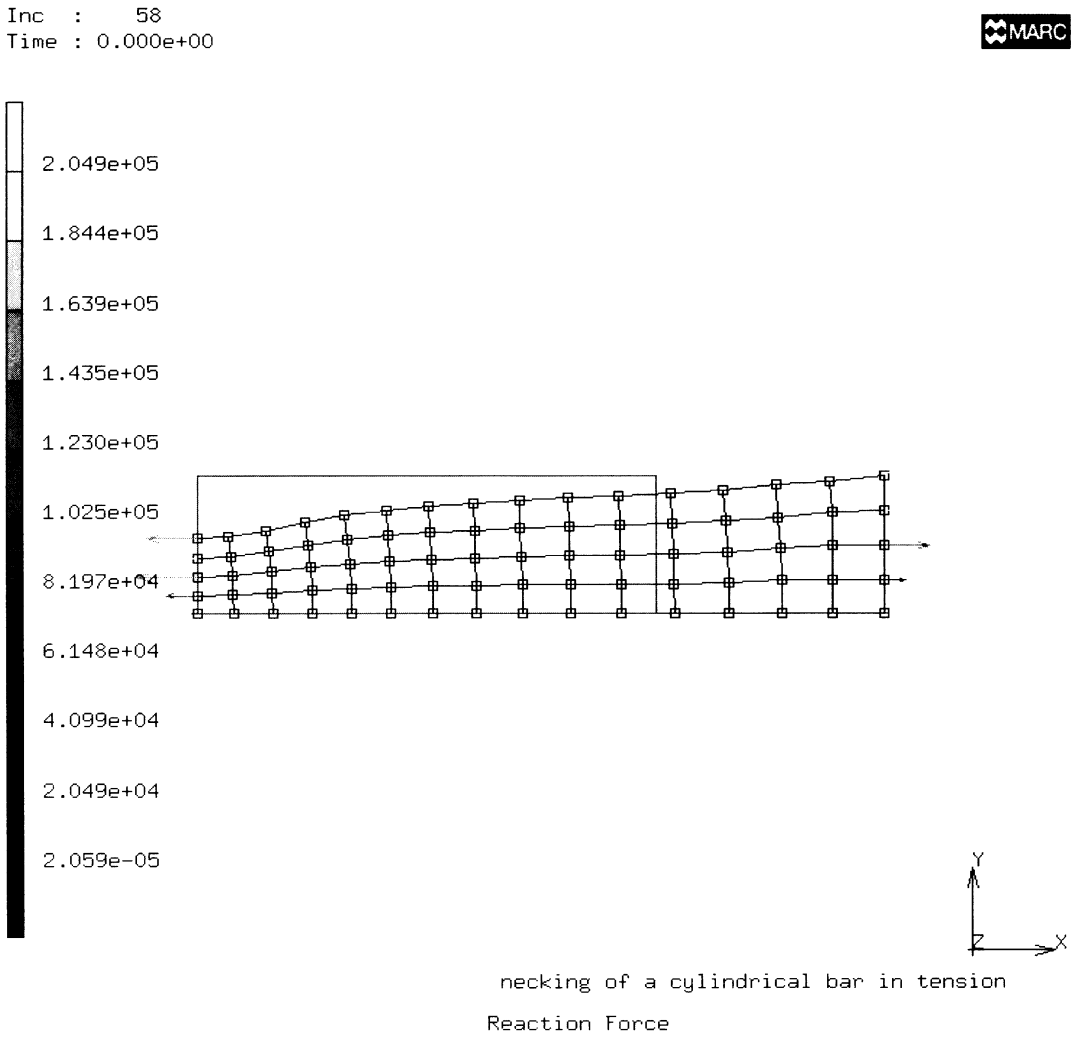

Figure 3.21-9 Vector Plot of Reactions for Type 10 (F^eF^p)

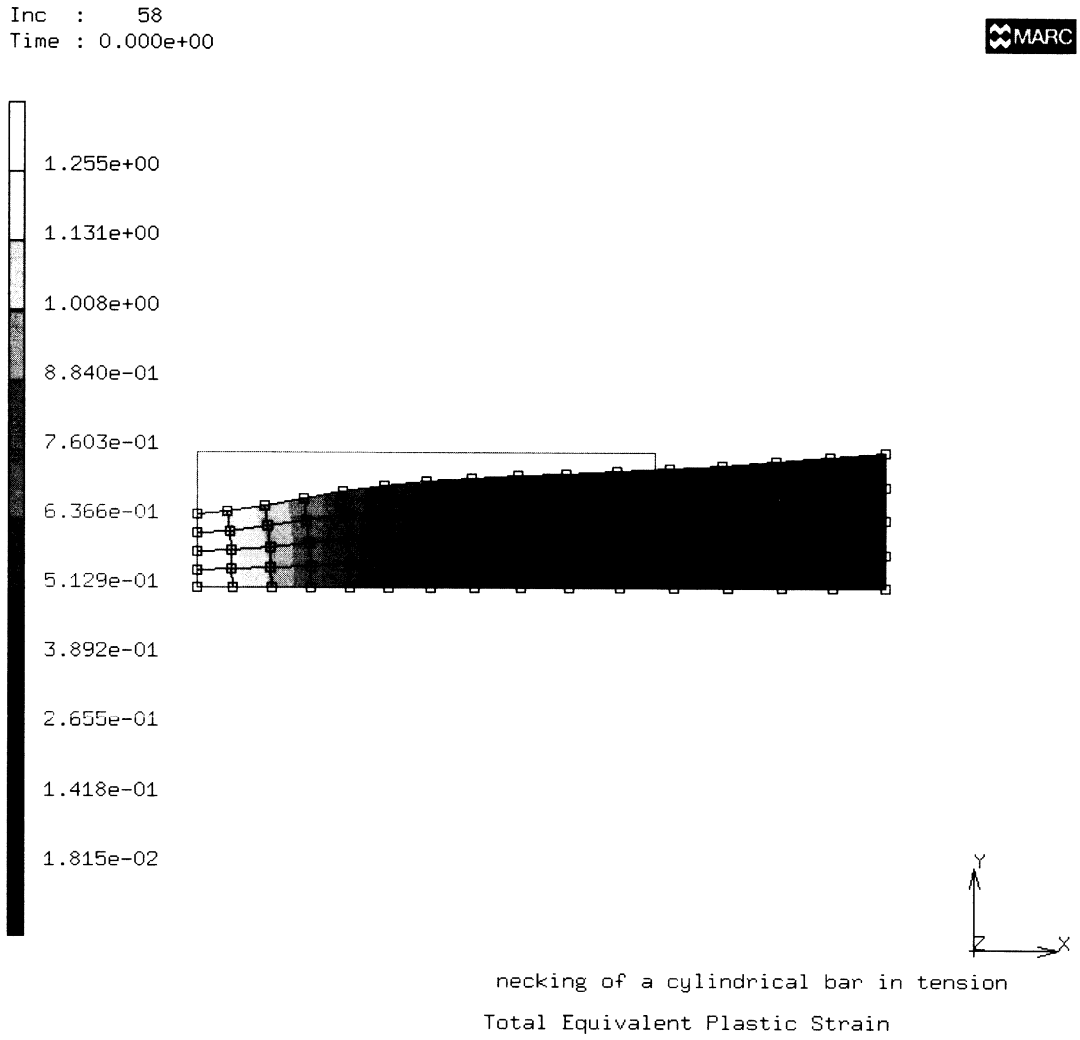

Figure 3.21-10 Contour Plot of Equivalent Strain for Type 10 (F^eF^p)

3.22 Combined Thermal, Elastic-plastic, and Creep Analysis

A realistic design problem, such as thermal ratcheting analysis, involves a working knowledge of a significant number of program features. This example illustrates how these features can be used to analyze a simplified form of a pressure vessel component which is subjected to a uniform pressure and thermal downshock. This type of problem typifies reactor component analysis. The general temperature-time history is shown in Figure 3.22-1 and the pressure history is shown in Figure 3.22-2.

An analysis of this type requires the use of heat transfer analysis to determine the transient temperature distribution in the wall of a cylindrical pressure vessel under cool-down conditions. This temperature distribution must be saved and presented to MARC through the CHANGE STATE option. The AUTO THERM option then creates its own incremental changes in temperature for use in the stress analysis. MARC then proceeds to find the elastic plastic state of stress in the cylinder due to the combined effects of internal pressure and thermal loading and the long time residual effects of creep.

Elements

The 8-node axisymmetric, quadrilateral element is used in this example. The heat transfer element type 42, is used in the determination of the transient temperature distribution while the 8-node distorted quadrilateral element type 28 is used in the stress analysis.

Model

The geometry and mesh for this example are shown in Figure 3.22-3. A cylindrical wall segment is evenly divided in six axisymmetric quadrilateral elements with a total of 33 nodes. The ALIAS parameter block allows you to generate your connectivity data with the stress analysis element and then to replace this element with the corresponding heat transfer element type.

Heat Transfer Properties

It is assumed here that the material properties do not depend on temperature; therefore, no slope-breakpoint data are input. The uniform properties used here are: specific heat (c) of 0.116 Btu/lb-°F, thermal conductivity (k) is 4.85×10^{-4} Btu/in-sec°F, and density (ρ) is 0.283 lb^3/inch.

Heat Transfer Boundary Conditions

The initial temperature across the wall and ambient temperature are 1100°F as specified in the initial conditions block. The outer ambient temperature is held constant at 1100°F. The inner ambient temperature decreases from 1100°F to 800°F in 10 secs and remains constant thereafter.

The FILMS option is used to input the film coefficients and associated sink temperatures for the inner and outer surface. A uniform film coefficient for the outside surface is specified for element 65 as 1.93×10^{-6} Btu/sq.in-sec.-°F providing a nearly insulated wall condition. The

inner surface has a film coefficient of 38.56 x 10^{-5} Btu/sq.in-sec-°F to simulate forced convection. The temperature down-ramp of 300°F for this inner wall is specified here as a nonuniform sink temperature and is applied using user subroutine FILM.

Subroutine FILM linearly interpolates the 300°F decrease in ambient temperature over 10 seconds and then holds the inner wall temperature constant at 800°F. It is called at each time step for each integration point on each element surface given in the FILMS option. This subroutine does nothing if it is called for element 65 to keep the outer surface at 1100°F. It applies the necessary ratio to reduce the inner wall temperature.

The TRANSIENT option controls the heat transfer analysis. MARC automatically calculates the time steps to be used based on the maximum nodal temperature change allowed as input in the CONTROL option. The solution begins with the suggested initial time step input and ends according to the time period specified. It will not exceed the maximum number of steps input in this option.

Finally, note in the heat transfer run the use of the POST option. This allows the creation of a postprocessor file containing element temperatures at each integration point and nodal point temperatures. The file is used later as input to the stress analysis run through the use of the CHANGE STATE and AUTO THERM options.

Heat Transfer Results

The transient thermal analysis is linear; the material properties do not depend on temperature, and the boundary conditions depend on the surface temperature linearly. The analysis is completed using the auto time step feature in the TRANSIENT option.

The TRANSIENT AUTO run reached completion in 33 increments with a specified starting time step of 0.5 seconds. A 15°F temperature change tolerance was input in the CONTROL option and controlled the auto time stepping scheme. The reduction to approximately 800°F throughout the wall was reached in increment 33 at a total time of 250 seconds.

The temperature-time histories of inner wall element (1) and outer wall element (6) for auto time stepping is shown in Figure 3.22-4. The data for plotting was saved using the POST option on a file.

The temperature distribution across the wall at various solution times is shown in Figure 3.22-5. These distributions correspond to incremental solution points in the stress analysis. Convergence to steady state is apparent here. The thermal gradient is characteristic of the downshock.

Stress Analysis

The stress analysis of the cylinder wall was accomplished in three separate runs. The first run proceeds from the elastic, increment 0, pressure load only, through the transient thermal analysis. The second run restarts at increment 27, sets all the elements to a uniform temperature of 800°F, and then proceeds to ramp the temperatures back up to 1100°F in six uniform temperature steps. The third run restarts at this original, stress-free temperature and allows the structure to creep for one hour.

Material Properties

All elements are isotropic. Young's modulus (E) is 21.8 x 10^6 psi; Poisson's ratio (ν) is 0.32; coefficient of thermal expansion (α) is 12.4 x 10^{-6} in/°F; initial stress-free temperature (T) is 1100°F; and yield stress (σ_y) is 20,000 psi. These values are assumed to be independent of temperature.

Loading

A uniform pressure of 900 psi is applied to the inner surface (1-2 face of element 1) of the cylinder and the appropriate end load of 210,344.5 pounds is applied axially to the cylinder through node 3 in increment 0. The mechanical load is held constant throughout the analysis. This is implemented using the PROPORTIONAL INC option.

Boundary Conditions

All nodal points in the left face (Z = 0) plane are restrained against motion in the axial direction. The TYING option is then used to ensure a generalized plane strain condition (all nodes in the Z = 0.1 plane are constrained to move identically to node 3 in the axial direction).

Restart

The analysis shown here was made in three runs using the RESTART option. The option allows you to control the analysis through several smaller runs with fewer increments at a time. Parameters, such as loading rates and tolerances, can be altered and increments then repeated if it is necessary.

The first stress analysis run shown provides the thermal elastic-plastic solution in increments 1 through 27. Restart data is written at every increment. This allows restarting at any point in the solution. The restart data is written to unit 8 and is saved as a file.

The second and third runs allow for reading and writing of restart data. The second run restarts at increment 27 and brings the wall temperature to 1100°F again at increment 34. The third run initiates the creep analysis by restarting at increment 37 and finishes at increment 55. Each of these runs writes the data to unit 8 at every increment to ensure continuation. This may be necessary if an extended creep solution is desired.

Control

The limit on the total number of increments must be properly set from one run to the next. Tolerances can be specified here for any restarted run.

State Variables Options

The INITIAL STATE and the CHANGE STATE options each provides three ways of initializing or changing the state variables specified. A range of elements, integration points and layers and a corresponding state variable values can be read in. Secondly, values can be read in through the corresponding user subroutine INITSV (for initialization) or NEWSV (for a change). Third, the state variable values can be read from a named step of the post file output from a previous heat transfer analysis with MARC. The number of state variable per point can be defined in the STATE VARS parameter block. In this analysis, the default of 1 is used for the temperature as the first state variable at a point.

In the first run, the INITIAL STATE option is used to define the initial stress-free temperature for all six elements and nine integration points at 1100°F. The CHANGE STATE option here uses the values from the post file created in the heat transfer analysis in conjunction with the AUTO THERM option. It is used in the second run to ramp the uniform wall temperature from 800°F to 1100°F in six equal increments.

Auto Therm

This option allows automatic, static, elastic-plastic, thermally loaded stress analysis based on a set of temperatures defined throughout the mesh as a function of time. The CHANGE STATE option must be used with the AUTO THERM option to present the temperatures in MARC. MARC then calculates its own temperature increment based on the temperature change tolerance provided.

A tolerance of 17° was used for the AUTO THERM analysis of the first run. It was calculated as 20% to 50% of the strain to cause yield, equal to $\frac{\bar{\sigma}}{E\alpha}$, where σ is the yield stress, E is the Young's modulus, and α is the coefficient of thermal expansion. This strain size gives an accurate elastic-plastic analysis. The temperature set is provided in the CHANGE STATE option from the heat transfer post file attached as unit 20. These temperatures are from steps 1 through 32 of that heat transfer analysis. A maximum of 35 increments was specified for this AUTO THERM. This provides a limit to avoid excessive computation in case of a data error.

Creep

The CREEP parameter block and CREEP model definition block are required to flag creep analysis and set the type of creep law and creep tolerances. Here the creep law is provided using user subroutine CRPLAW. The creep law used is:

$$\dot{\varepsilon}^{\circ C} = 1.075(10^{-26})\sigma^{5.5}$$

An initial time step size of 0.02 hours and an end time of 1.0 hour is specified in the AUTO CREEP option of the third stress run. The time step is automatically adjusted based on the stress and strain-change tolerance specified. Due to this adjustment, final time of 1.0 hour is obtained in 12 increments rather than the 50 increments that the initial time step would require. The initial time step can be determined using the methods outlined in *MARC Volume A: User Information*.

Print Choice

Because the temperatures and stresses across a layer of an element do not change, the PRINT CHOICE option can be used to reduce the output. Here, the solutions are output in each run for only three integration points per element; one in each layer, points, 2, 5, and 8.

Results

Figure 3.22-6 shows the equivalent stress distribution through the cylinder wall during the elastic-plastic solution. No yielding occurs due to mechanical loading. As the thermal loads are superimposed, yielding advances across the cylinder wall from the inside. The thermal gradients decrease and the inside wall element begins to unload. Here the region of yielding is in the midwall. The outside elements reverse their unloading trend at this time and show yielding stress levels. Finally, at the end of the elastic-plastic solution, the midwall has yielded. The outside elements are very close to yield and the inside wall element has unloaded. The creep solution, shown in Figure 3.22-7, finds the equivalent stress distribution relaxed back to very nearly the isothermal elastic state.

Parameters, Options, and Subroutines Summary

Example e3x22a.dat:

Parameters	Model Definition Options	History Definition Options
ALIAS	CONNECTIVITY	CONTINUE
ELEMENTS	CONTROL	TRANSIENT
END	COORDINATES	
HEAT	END OPTION	
SIZING	FILMS	
TITLE	INITIAL TEMPERATURE	
	ISOTROPIC	
	POST	

User subroutine in u3x22a.f:

FILM

Example e3x22b.dat:

Parameters

ELEMENTS
END
TITLE

Example e3x22c.dat:

Parameters	Model Definition Options	History Definition Options
CREEP	CONNECTIVITY	AUTO CREEP
ELEMENTS	CONTROL	AUTO THERM
END	COORDINATES	CHANGE STATE
SIZING	CREEP	CONTINUE
THERMAL	DIST LOADS	PROPORTIONAL INCREMENT
TITLE	END OPTION	
	FIXED DISP	
	INITIAL STATE	
	ISOTROPIC	
	POINT LOAD	
	PRINT CHOICE	
	RESTART	
	TYING	

User subroutine in u3x22c.f:

CRPLAW

Example e3x22d.dat:

Parameters	Model Definition Options	History Definition Options
ALL POINTS	CONNECTIVITY	AUTO CREEP
CREEP	CONTROL	CHANGE STATE
ELEMENTS	COORDINATES	CONTINUE
END	CREEP	
SIZING	DIST LOADS	
THERMAL	END OPTION	
TITLE	FIXED DISP	
	INITIAL STATE	
	ISOTROPIC	
	POINT LOAD	
	PRINT CHOICE	
	RESTART	
	TYING	

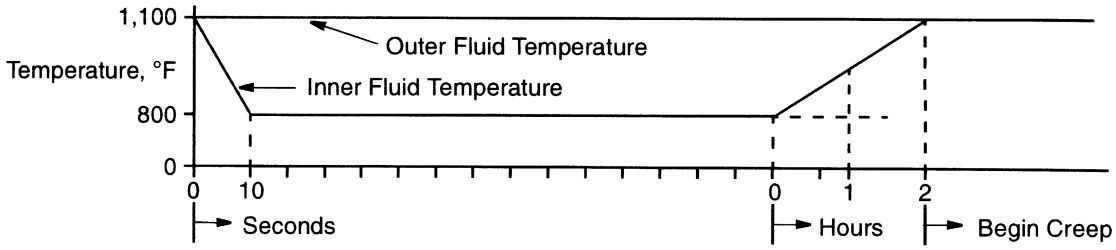

Figure 3.22-1 Temperature-Time History

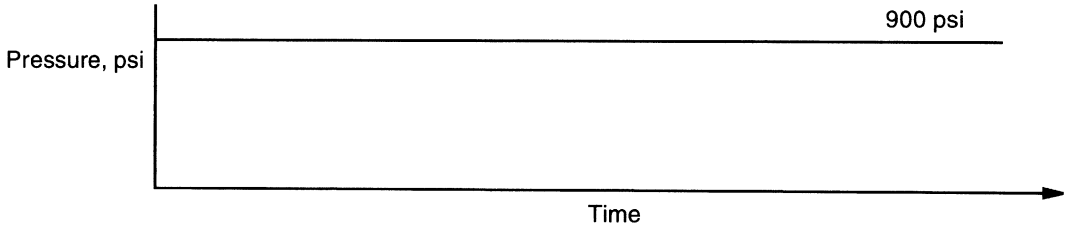

Figure 3.22-2 Pressure-Time History

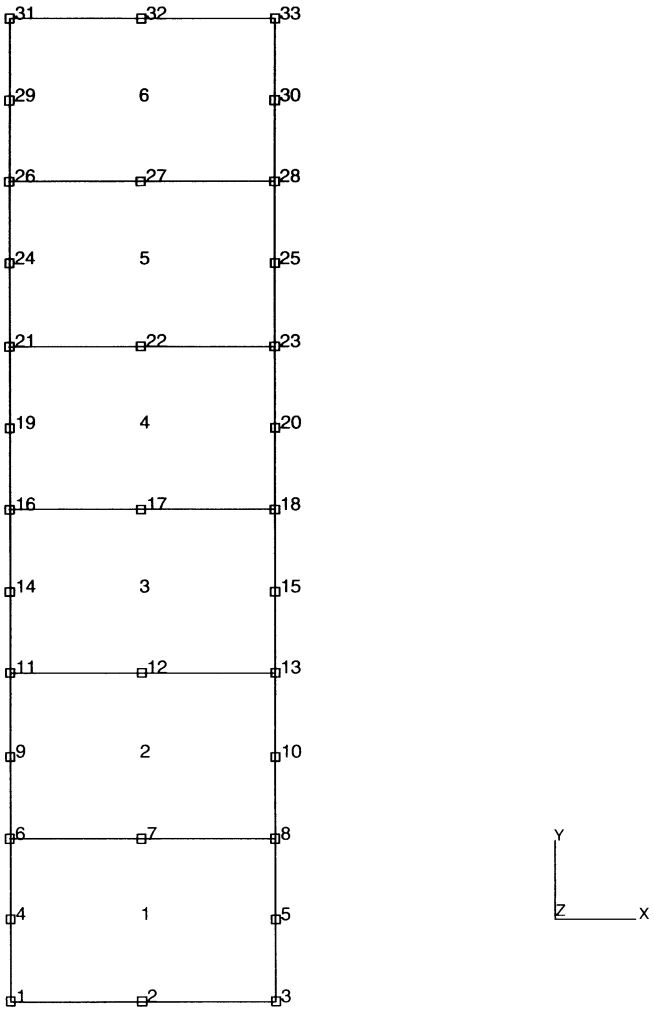

Figure 3.22-3 Geometry and Mesh for Combined Thermal, Elastic-Plastic, and Creep Problem

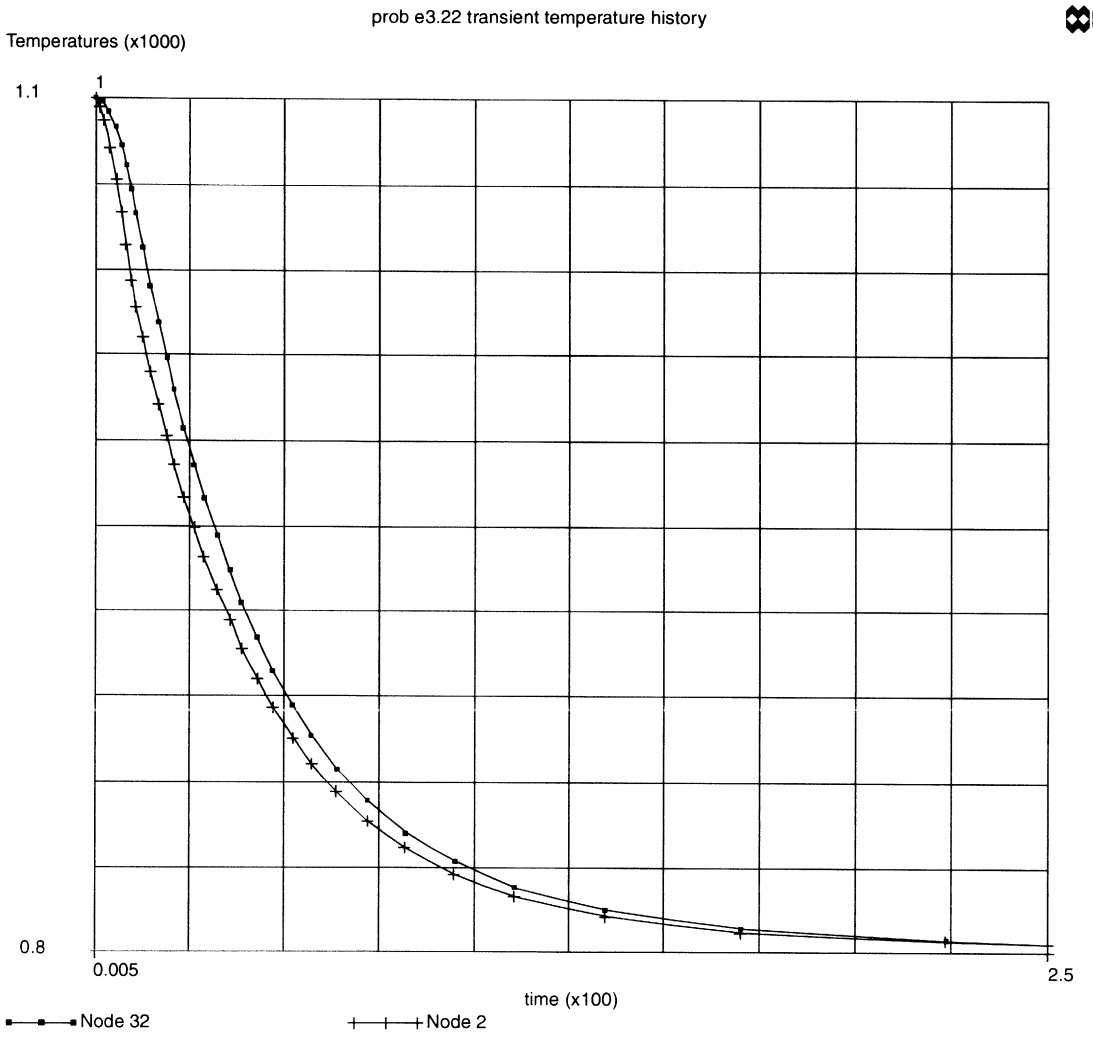

Figure 3.22-4 Transient Temperature Time History (Auto Time Step)

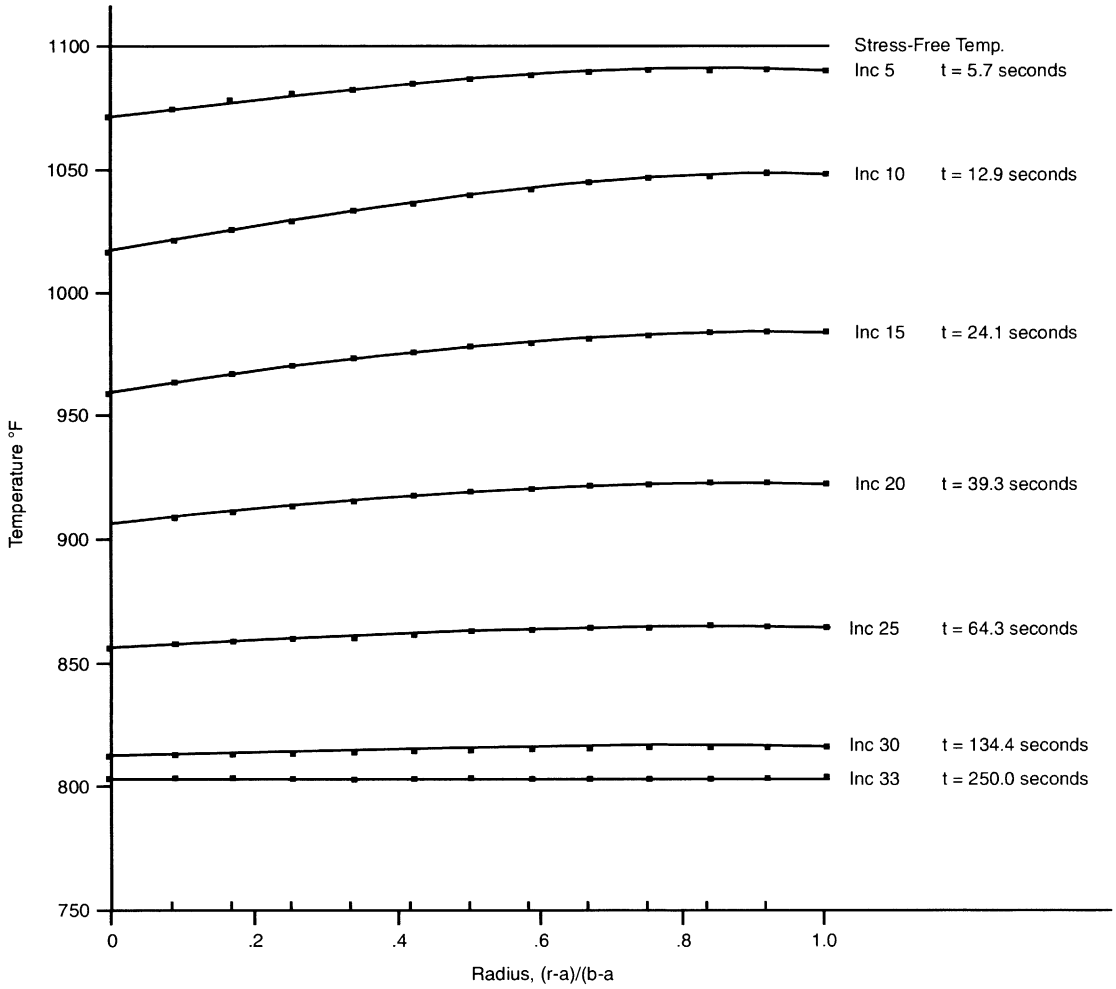

Figure 3.22-5 Temperature Distribution in Cylinder Wall

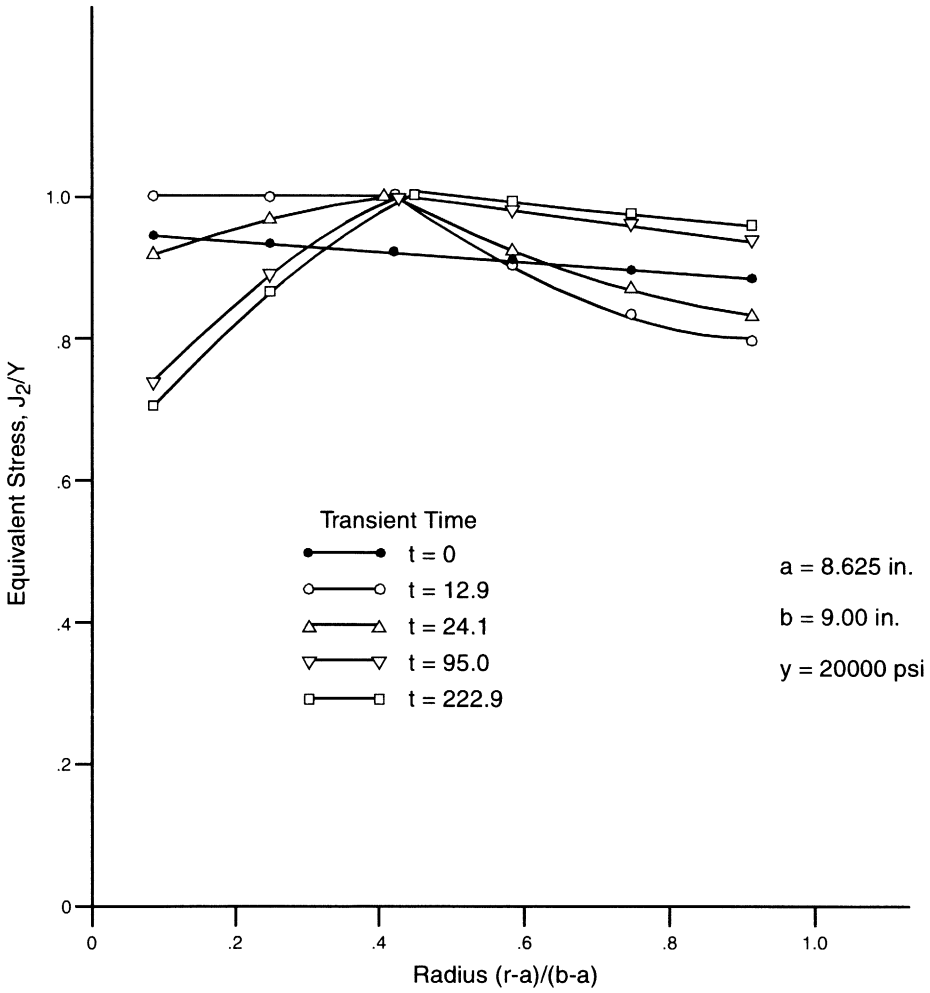

Figure 3.22-6 Thermal Elastic Plastic Results

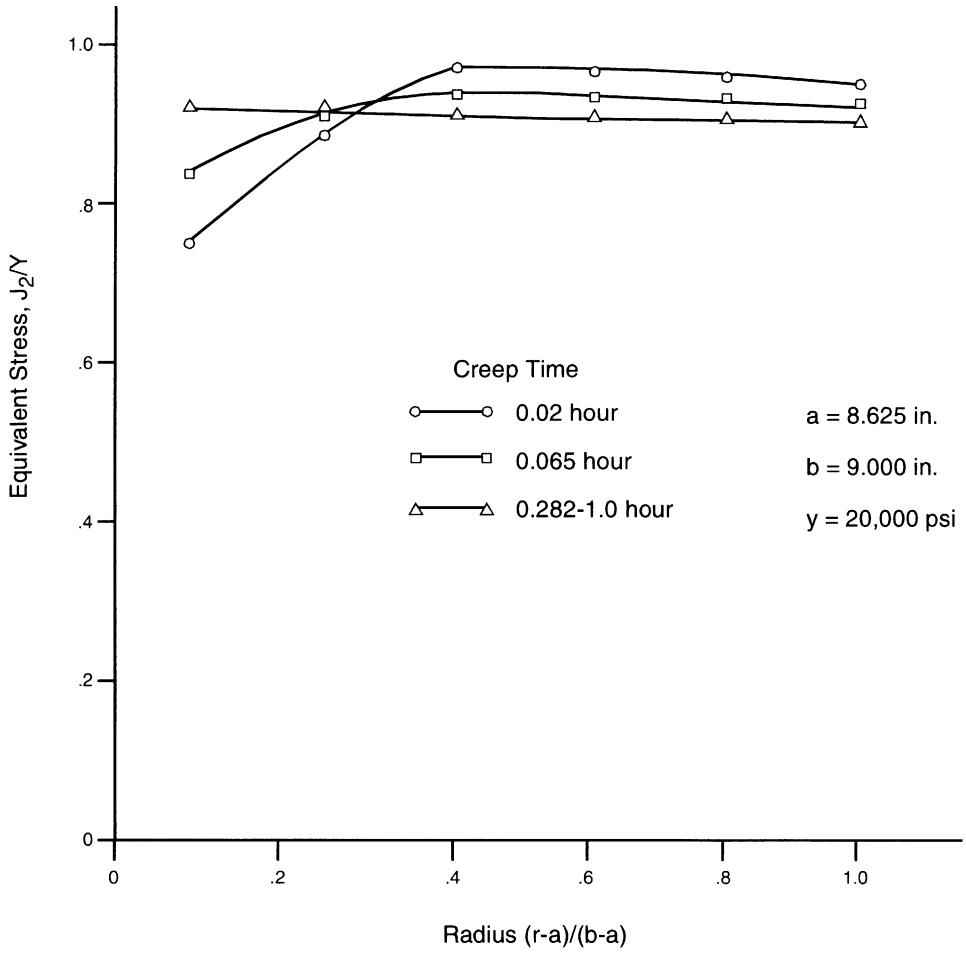

Figure 3.22-7 Creep Results

3.23 Nonlinear Analysis of a Shell Roof, using Automatic Incrementation

A shell roof is supported by a rigid diaphram at the curved edges. A snow load is uniformly applied to the roof. The shell material is modeled as elastic-perfectly plastic, and geometric nonlinearities are considered. An initial load of 3.5 x 10^{-4} N/mm^2 is applied; the load is automatically incremented until the structure is completely plastic. This problem is similar to problem 3.17. However, this problem uses element type 75 and adaptive load incrementation.

This problem is modeled using the two techniques summarized below.

Data Set	Element Type(s)	Number of Elements	Number of Nodes	Differentiating Features
e3x23	75	36	49	AUTO LOAD
e3x23b	75	36	49	AUTO INCREMENT

Elements

Element type 75 is a 4-node, thick-shell element with six global degrees of freedom per node.

Model

One-quarter of the roof is modeled with 36 type 75 elements, with a total of 49 nodes (Figure 3.23-1). The UFXORD option transforms these cylindrical coordinates into global Cartesian coordinates.

Geometry

A thickness of 76 mm is specified in the EGEOM1 field of the GEOMETRY option.

Material Properties

The material is modeled as elastic-perfectly plastic; no workhardening data is given. The elastic properties are specified by a Young's modulus of 2.1 x 10^4 N/mm^2. Plasticity occurs after a von Mises yield stress of 4.2 N/mm^2.

Loading

A gravity-type load models the weight of the snow on the roof. The initial load of 3.5 x 10^{-4} N/mm^2 is applied in increment 0. The AUTO INCREMENT option gradually increases the load to a specified total of 3.5 x 10^{-2} N/mm^2.

Boundary Conditions

Diaphram support conditions are given on the curved edges and appropriate symmetry conditions are given in the FIXED DISP option.

Data Storage

The number of integration stations through the thickness of the shell is set to five with the SHELL SECT option.

Geometric Nonlinearity

The LARGE DISP option is included to invoke geometric nonlinear behavior. The Newton-Raphson iterative technique (default option in MARC) is used to solve the nonlinear equations.

Analysis Control

With the CONTROL option, the maximum number of load increments (including increment 0) is specified as 40. All other CONTROL parameters have the default value. In addition, the elements are assembled in parallel using the PROCESSOR option.

Postprocessing

A post file is written. The PRINT CHOICE option is used to limit print output to one element (36) at one integration point (1), at two layers (1 and 5), and one node (49). More complete nodal data is stored on the post file, whereas plotted information is obtained concerning the plastic strains.

Auto Incrementation

Nine increments are applied with the use of the AUTO INCREMENT option. A final loading of 3.5×10^{-2} N/mm^2 is specified, although complete plasticity is reached well before this load.

Results

The analysis ends at a distributed snow load of 5.0×10^{-3} N/mm^2. At this load, the structure is plastic throughout. The equivalent plastic strains plotted for layers 1, 3, and 5 are shown in Figure 3.23-2, Figure 3.23-3 and Figure 3.23-4, respectively. The final snow loading is equivalent to a 13,040-mm (42.85-ft) layer of freshly fallen snow resting on the shell roof. The vertical displacement of node 49 is plotted against the reaction at the diaphram support in Figure 3.23-5. The displacements at lower loads correspond well with those calculated in Example 3.17. The performance of using the PROCESSOR option to assemble the elements in parallel showed an overall speed improvement of 22%.

Parameters, Options, and Subroutines Summary

Example e3x23.dat:

Parameters	Model Definition Options	History Definition Options
ELEMENTS	CONNECTIVITY	AUTO INCREMENT
END	CONTROL	CONTINUE
LARGE DISP	COORDINATES	DIST LOADS
PRINT	DIST LOADS	
SHELL SECT	END OPTION	
SIZING	FIXED DISP	
TITLE	GEOMETRY	
	ISOTROPIC	
	POST	
	PRINT CHOICE	
	RESTART	
	UFXORD	

Example e3x23b.dat:

Parameters	Model Definition Options	History Definition Options
ELEMENTS	CONNECTIVITY	AUTO INCREMENT
END	CONTROL	CONTINUE
LARGE DISP	COORDINATES	DIST LOADS
PRINT	DIST LOADS	
PROCESS	END OPTION	
SHELL SECT	FIXED DISP	
SIZING	GEOMETRY	
TITLE	ISOTROPIC	
	POST	
	PRINT CHOICE	
	RESTART	
	UFXORD	

User subroutine in u3x23.f:

UFXORD

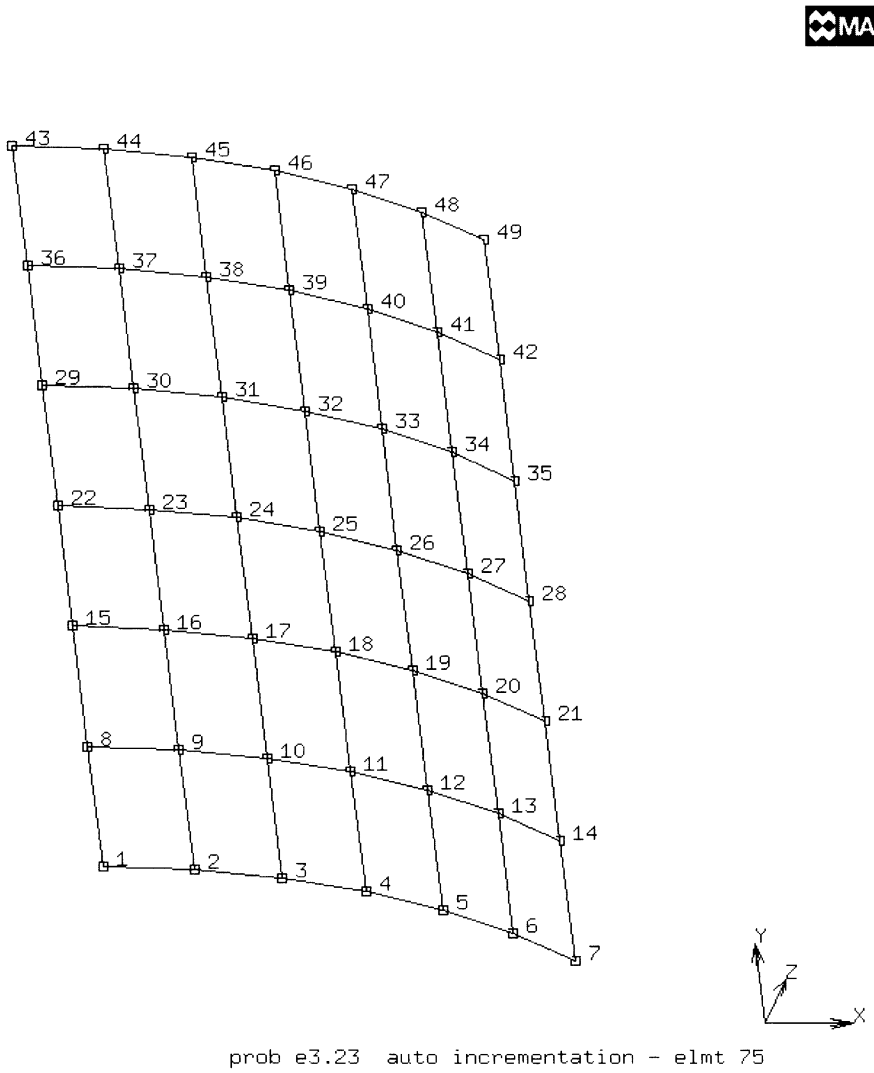

Figure 3.23-1 Model with Elements and Nodes Labeled

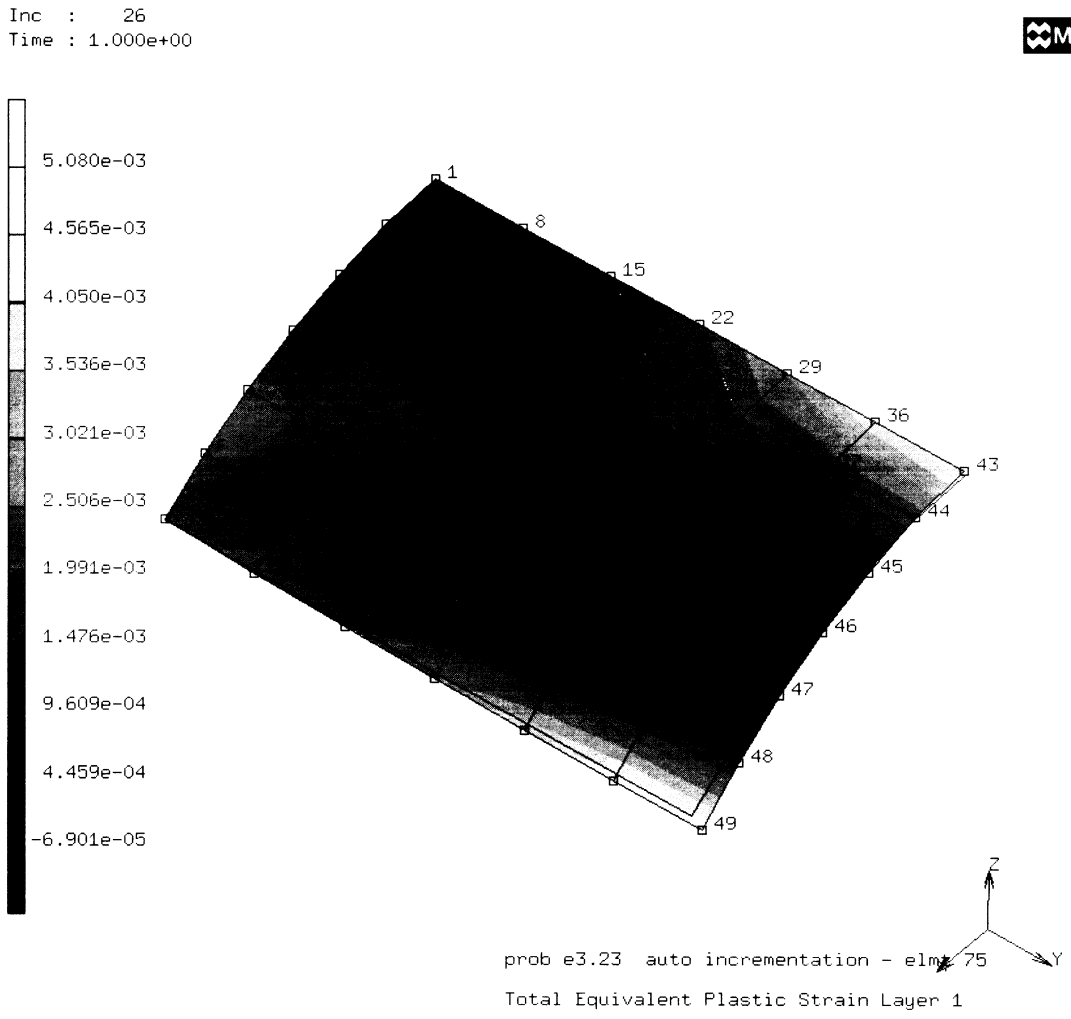

Figure 3.23-2 Equivalent Plastic Strain, Layer 1

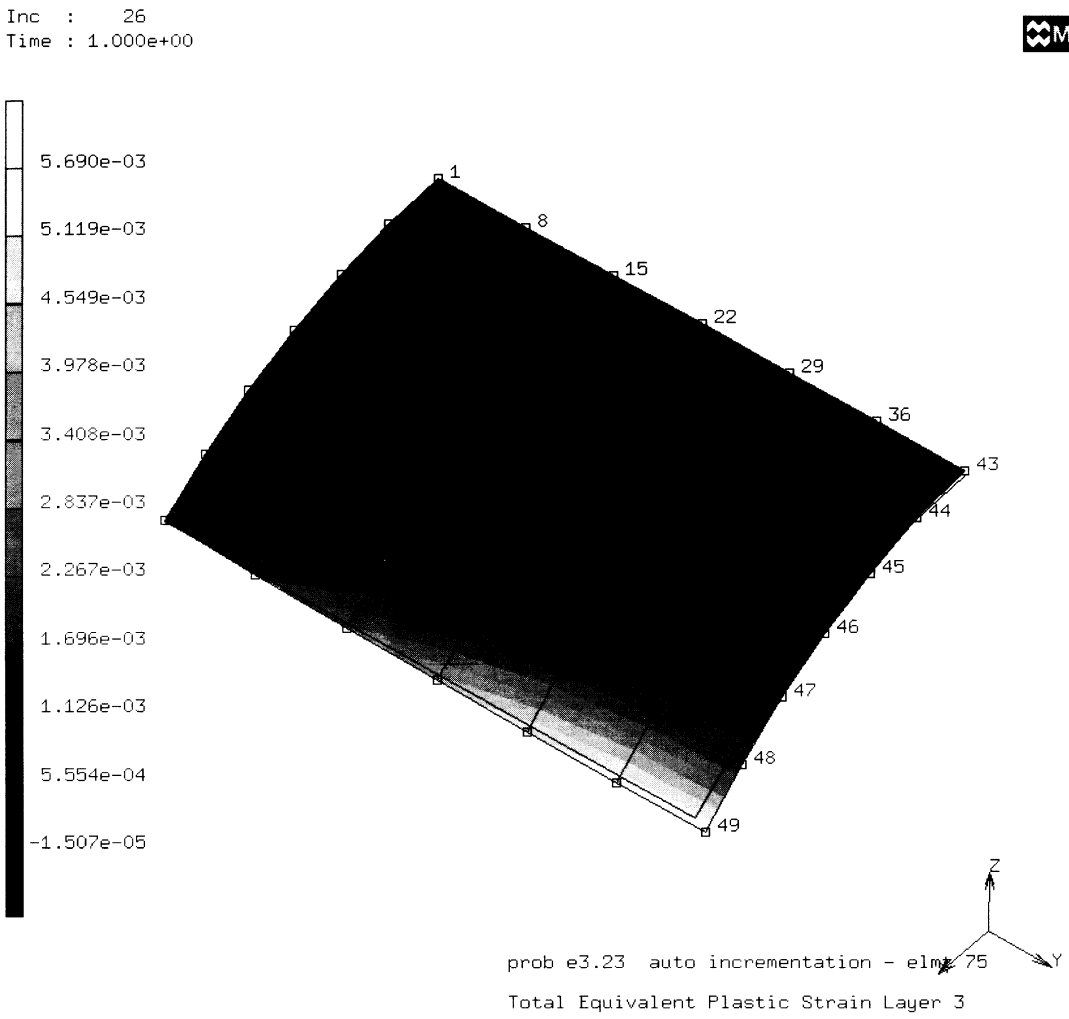

Figure 3.23-3 Equivalent Plastic Strain, Layer 3

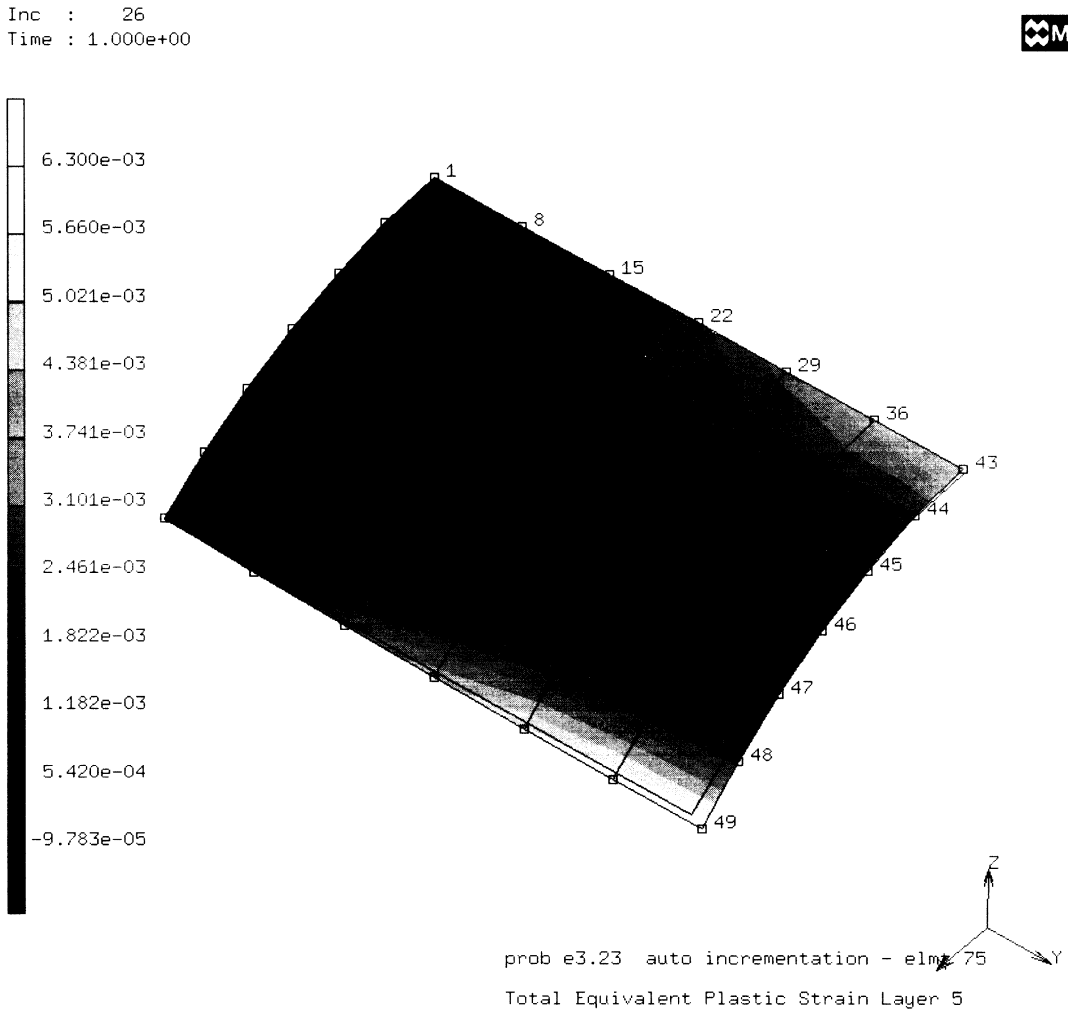

Figure 3.23-4 Equivalent Plastic Strain, Layer 5

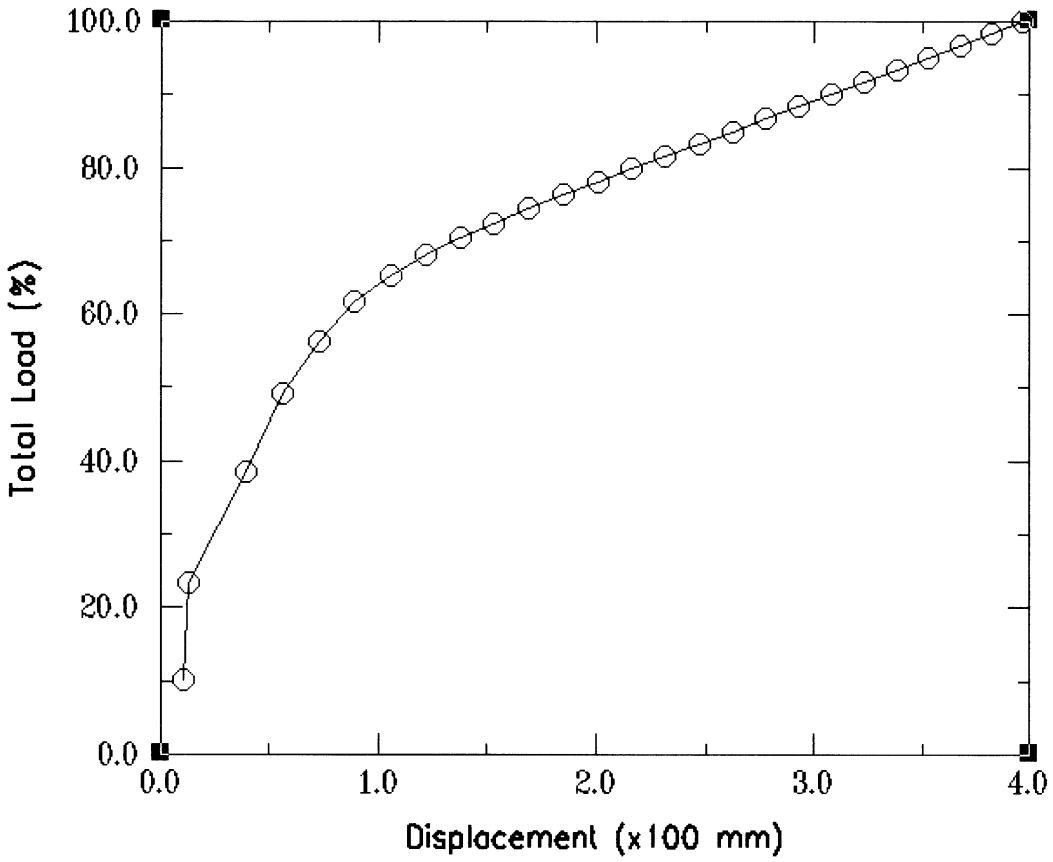

Figure 3.23-5 Load Displacement Curve

3.24 Creep Analysis of a Plate with a Hole using AUTO-THERM-CREEP Option

This problem demonstrates the use of AUTO-THERM-CREEP option for the creep analysis of a plate with a hole, subjected to transient thermal loading. The analysis consists of two parts: a transient heat conduction analysis and a creep analysis.

TRANSIENT HEAT CONDUCTION ANALYSIS

A two-dimensional transient heat conduction problem of a plate with a circular hole is analyzed by using MARC element type 41 (8-node planar elements). Fluid at temperature 1000°F fills the circular hole. The exterior edges of the plate are held at constant temperature (500°F).

Model

Due to symmetry, only a quarter of the plate (see Figure 3.24-1) is modeled for the analysis. See *MARC Volume B: Element Library* for detailed element descriptions.

Material Properties

The conductivity is 0.42117×10^5 Btu/sec-in.-°F. The specific heat is 0.3523×10^3 Btu/lb-°F, and the mass density is 0.7254×10^3 lb/cubic inch.

Geometry

The thickness of the plate is 0.1 inch.

Initial Condition

The initial nodal temperatures are homogeneous at 500°F.

Boundary Conditions

No input data is required at insulated boundary conditions located at lines of symmetry (x = 0 and y = 0). Constant temperatures of 500°F are specified at lines x = 10, and y = 12. Convective boundary conditions are assumed to exist at the inner surface of the circular hole. The fluid temperature is 1000°F, and the film coefficient is 0.46875×10^5 Btu/sec-sq.in.-°F.

Transient

The total transient time in the analysis is assumed to be 5.0 seconds and a constant time step of 0.5 seconds is chosen for the problem. Nonautomatic time stepping option is also invoked; hence, 10 increments will be performed.

Post File

A formatted post file (unit 19) is generated during the transient heat transfer analysis. Element temperatures stored on the post file are to be used for creep analysis. The code number for element temperatures is 9.

CREEP ANALYSIS

Model

The mesh used for creep analysis is the same as that in the heat conduction analysis with the exception that the element type in the mesh is 26 (8-node plane stress element). Due to symmetry, only a quarter of the plate is modeled.

Material Properties

The material is assumed to be linear elastic with a Young's modulus of 30 x 10^6psi; Poisson's ratio of 0.3; and a coefficient of thermal expansion of 1.0 x 10^{-5} in/in/°F.

Geometry

The thickness of the plate is 0.1 inch.

Initial State (Stress-Free Temperature)

The stress-free temperature is assumed to be 500°F for all elements.

Fixed Disp

Zero displacement boundary conditions are prescribed at lines x = 0 and y = 0, for the simulation of symmetry conditions.

d.o.f. 1 = u = 0 at (x = 0)	Nodes 22, 26, 28, 32, 34
d.o.f. 2 = v = 0 at (y = 0)	Nodes 5, 8, 13, 16, 21

Creep

The user subroutine CRPLAW is used for the input of a creep law of the following form:

$$\dot{\varepsilon}_c = 1.075^{-26}\sigma^{5.0}$$

AUTO-THERM-CREEP

The creep analysis is carried out using the AUTO-THERM-CREEP load incrementation option. A detailed discussion of this option can be found in *MARC Volume C: User Input*, "Chapter 5". Input data for this option associated with the current problem is as follows: a temperature change tolerance of 100°F is set for the creation of temperature steps (increments) by the program; the

total transient time in thermal analysis is equal to 5.0; the suggested time increment for creep analysis is 0.1; and the total creep time (time for the termination of this analysis) is 0.6. The total creep time cannot be greater than the total transient time in thermal analysis.

The data in the CHANGE STATE option indicates that the temperatures are stored in a formatted post file and there are four sets of temperatures on the file.

Results

Effective (von Mises) stresses at the centroid (integration point 5) of element 4 are tabulated in Table 3.24-1 and plotted in Figure 3.24-3. The stress increases due to thermal load at each increment, and the stress redistributions due to creep at subincrements, are clearly demonstrated.

Table 3.24-1 von Mises Stresses at Element 4

Inc.	Creep Time (seconds)	EL Temp (°F)	von Mises Stress (σ) (psi)
1	0.0	513.2	9.483×10^3
1.1	0.1	513.2	9.476×10^3
1.2	0.15876	513.2	9.471×10^3
2	0.15876	526.4	1.895×10^4
2.1	0.23536	526.4	1.877×10^4
2.2	0.31752	526.4	1.863×10^4
3	0.31752	539.7	2.811×10^4
3.1	0.33858	539.7	2.784×10^4
3.2	0.36490	539.7	2.759×10^4
3.3	0.39780	539.7	2.735×10^4
3.4	0.43893	539.7	2.711×10^4
3.5	0.47628	539.7	2.692×10^4
4	0.47628	565.2	3.468×10^4
4.1	0.52142	565.2	3.476×10^4
4.2	0.56655	565.2	3.455×10^4
4.3	0.6	565.2	3.433×10^4
5	0.6	565.2	3.433×10^4

Parameters, Options, and Subroutines Summary

Example e3x24a.dat:

Parameters	Model Definition Options	Options
COMMENT	CONNECTIVITY	CONTINUE
ELEMENTS	CONTROL	TRANSIENT
END	COORDINATES	
HEAT	END OPTION	
SIZING	FILMS	
TITLE	FIXED TEMPERATURE	
	GEOMETRY	
	INITIAL TEMPERATURE	
	ISOTROPIC	
	POST	
	PRINT CHOICE	

Example e3x24b.dat:

Parameters	Model Definition Options	History Definition Options
COMMENT	CONNECTIVITY	AUTO THERM
CREEP	CONTROL	CHANGE STATE
ELEMENTS	COORDINATES	CONTINUE
END	CREEP	
SIZING	END OPTION	
TITLE	FIXED DISP	
	GEOMETRY	
	INITIAL STATE	
	ISOTROPIC	
	PRINT CHOICE	

Example e3x24c.dat:

Parameters	Model Definition Options	History Definition Options
COMMENT	CONNECTIVITY	AUTO THERM
CREEP	CONTROL	CHANGE STATE
ELEMENTS	COORDINATES	CONTINUE
END	CREEP	
SIZING	END OPTION	
TITLE	FIXED DISP	
	GEOMETRY	
	INITIAL STATE	
	ISOTROPIC	
	PRINT CHOICE	

User subroutine in u3x24.f:

CRPLAW

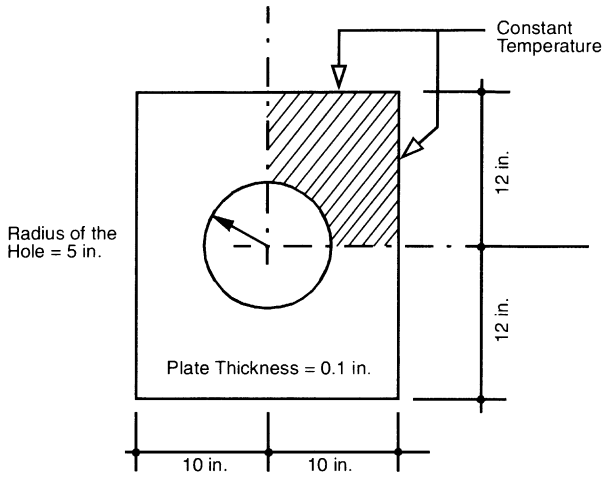

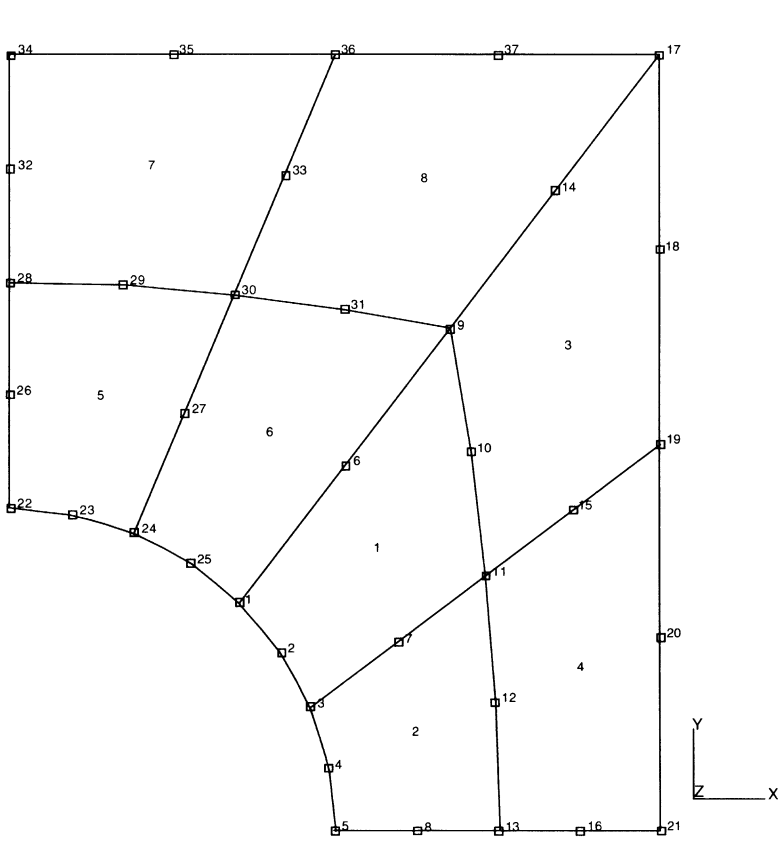

Figure 3.24-1 Plate with a Hole

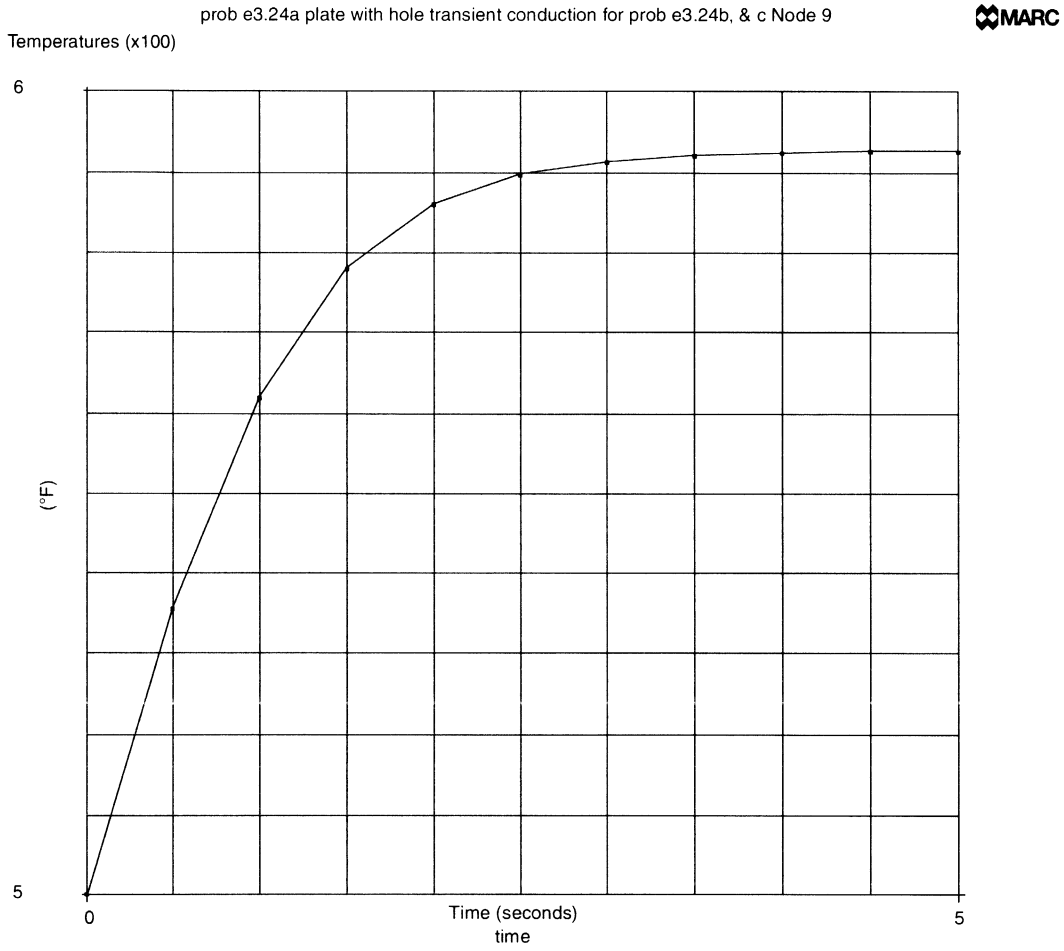

Figure 3.24-2 Nodal Temperature vs. Time (Node 9)

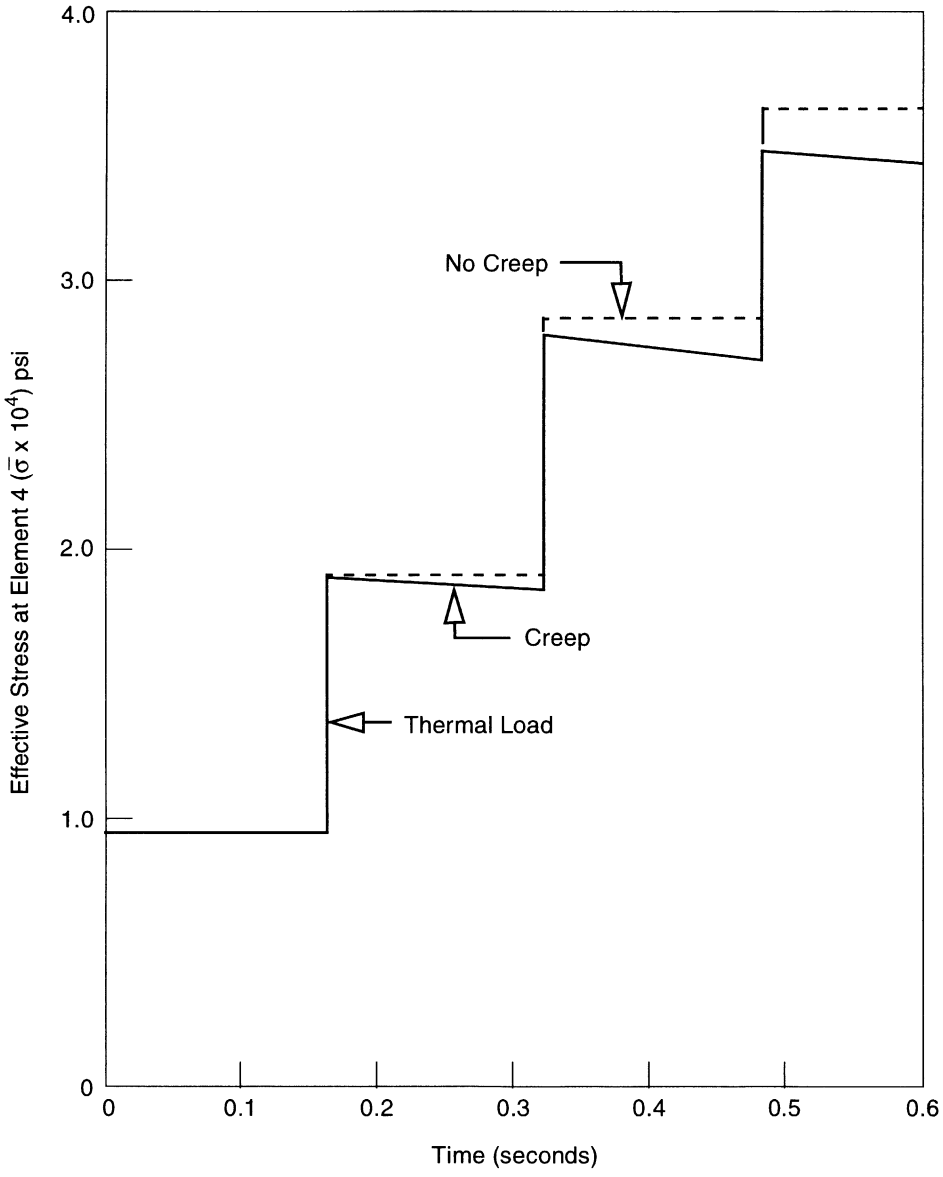

Figure 3.24-3 Effective Stresses at Element 4

3.25 Pressing of a Powder Material

This example illustrates the use of element type 11 and options LARGE DISP, UPDATE, and FOLLOW FORCE for the homogeneous compaction of a rectangular preform. A cyclic pressure is applied to one side of the preform.

Element

Element 11 is a 4-node plane strain element with two degrees of freedom per node used to model the powder. Fifty elements are used in this model. The initial dimensions are 10 by 5 mm as shown in Figure 3.25-1.

Loading

The pressure is first ramped up to 5500 MPa in a period of 2200 seconds. The load is then reduced to 100 MPa in 2160 seconds. The load is then increased to 7600 MPa in 300 seconds and finally reduced back to 100 MPa in 3000 seconds. The load is applied in the x-direction of the elements on the right side.

Material Properties

The powder material is represented by a modified Shima model. The Young's modulus and Poisson ratio are bilinear functions of the relative density and temperature. Because this is an uncoupled analysis, the temperature effects are not included here. See problem 3.26 for an example of a coupled analysis. E_0 and ν_0 are the initial Young's modulus and Poisson ratio equal to 20,000 MPa and 0.3, respectively.

The relative density effects on the elastic properties are given through the RELATIVE DENSITY option. They are entered as multiplicative factors to the values given on the POWDER option or the TEMPERATURE EFFECTS option if applicable. In this problem, the data obtained from an experiment indicates that:

ρ	E (MPa)	ν	E/E_0	ν/ν_0
0.7	20,000	0.3	1.0	1.0
1.0	30,000	0.33	1.5	1.1

The initial yield stress is 6000 MPa and the viscosity is 50,000 seconds. The values of γ and β, which are used to define the yield surface, have initial values of 0.1406174 and 1.375. These material data are functions of the relative density. This is expressed as:

$\gamma = (1. + \bar{\rho})^{5.5}$ and

$\beta = 6.25\ (1 - \bar{\rho})^{-0.5}$

Therefore, b_1, b_2, b_3, b_4 are entered as 1.0, 1.0, 1.0, 5.5 and q_1, q_2, q_3, q_4 are entered as 6.25, -6.25, 1.0, -0.5, respectively. The initial relative density is 0.7.

Boundary Conditions

The left end of the preform is prescribed to have no displacement in the x-direction. Node 23 is fixed in the y-direction to eliminate the rigid body mode.

Control

A control tolerance of 0.01 on residuals is requested. Because this problem involves homogeneous loading, almost no iterations are required.

Results

The results show that the billet is compressed from an initial length of 10 to a final height of 7.523 and a width of 5.731. Figure 3.25-2 shows the externally applied force history on node 33. Note that it is not exactly linear because of the follower force effects. Figure 3.25-3 shows the history of the relative density. We see that the peak density is the value of 0.92 and the final relative density is 0.81. Figure 3.25-4 shows the history of the inelastic strain rate. One observes that there are periods in the load cycle when no inelastic behavior occurs. Finally, Figure 3.25-5 shows the equivalent plastic strain history.

We can check the results for consistency by examining the conservation of mass.

$$\rho_o A_o = \rho A$$
$$0.7 \times 10 \times 5 = .81 \times 7.523 \times 5.731$$
$$35 = 34.92$$

this check is within 0.2%.

Parameters, Options, and Subroutines Summary

Example e3x25.dat:

Parameters	Model Definition Options	History Definition Options
ELEMENTS	CONNECTIVITY	AUTO LOAD
END	CONTROL	CONTINUE
FOLLOW FOR	COORDINATES	DIST LOADS
LARGE DISP	DENSITY EFFECTS	TIME STEP
SIZING	DIST LOADS	
TITLE	END OPTION	
UPDATE	POST	
	POWDER	
	RELATIVE DENSITY	

MARC

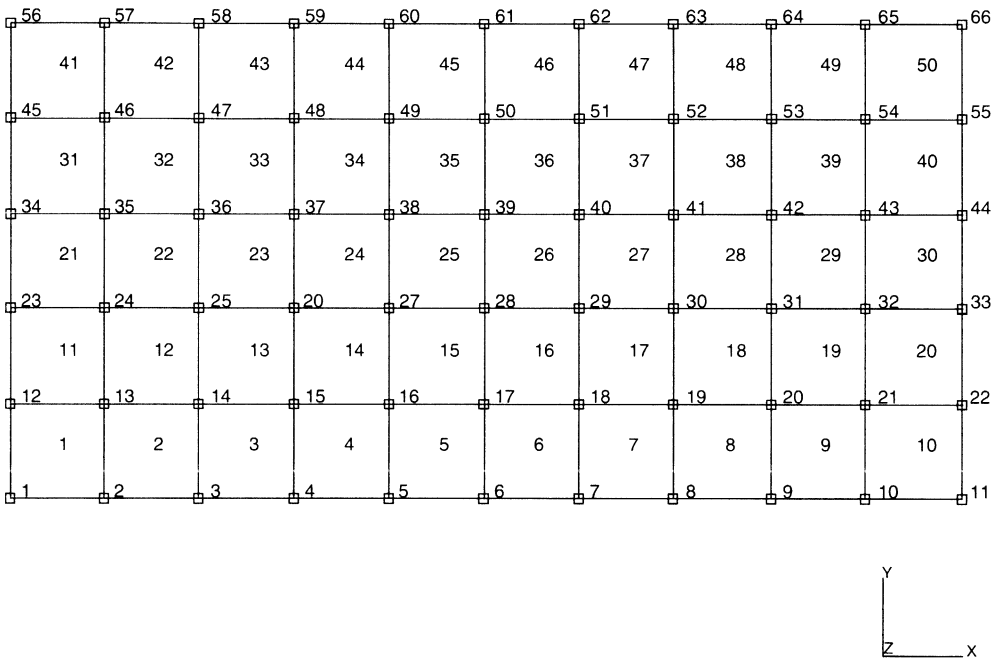

Figure 3.25-1 Finite Element Mesh

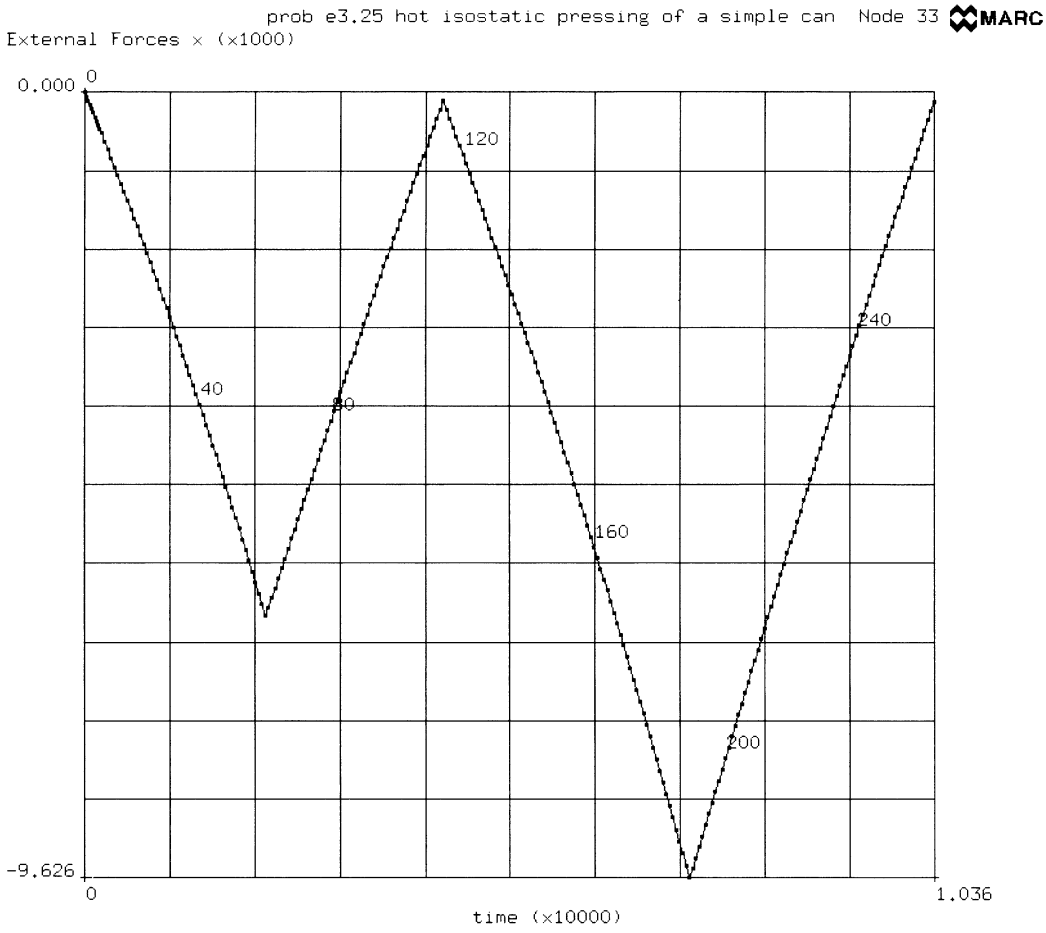

Figure 3.25-2 Time History of Externally Applied Load

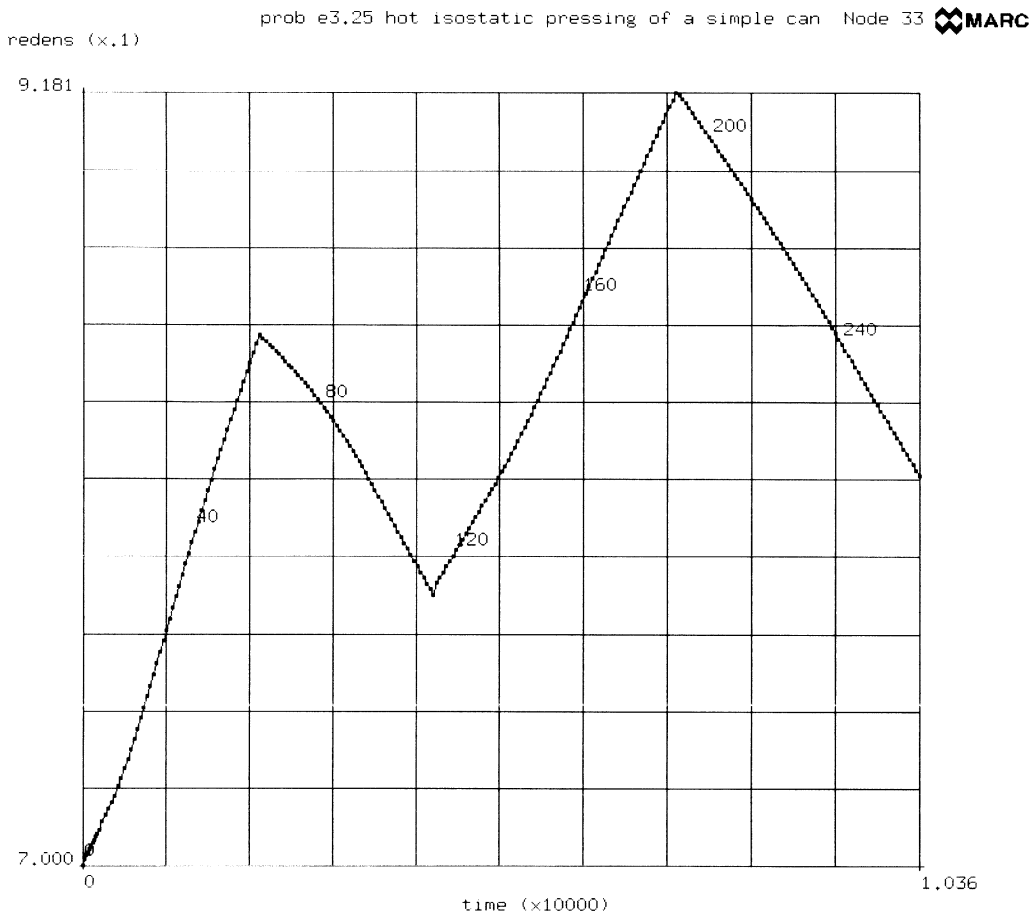

Figure 3.25-3 Time History of Relative Density

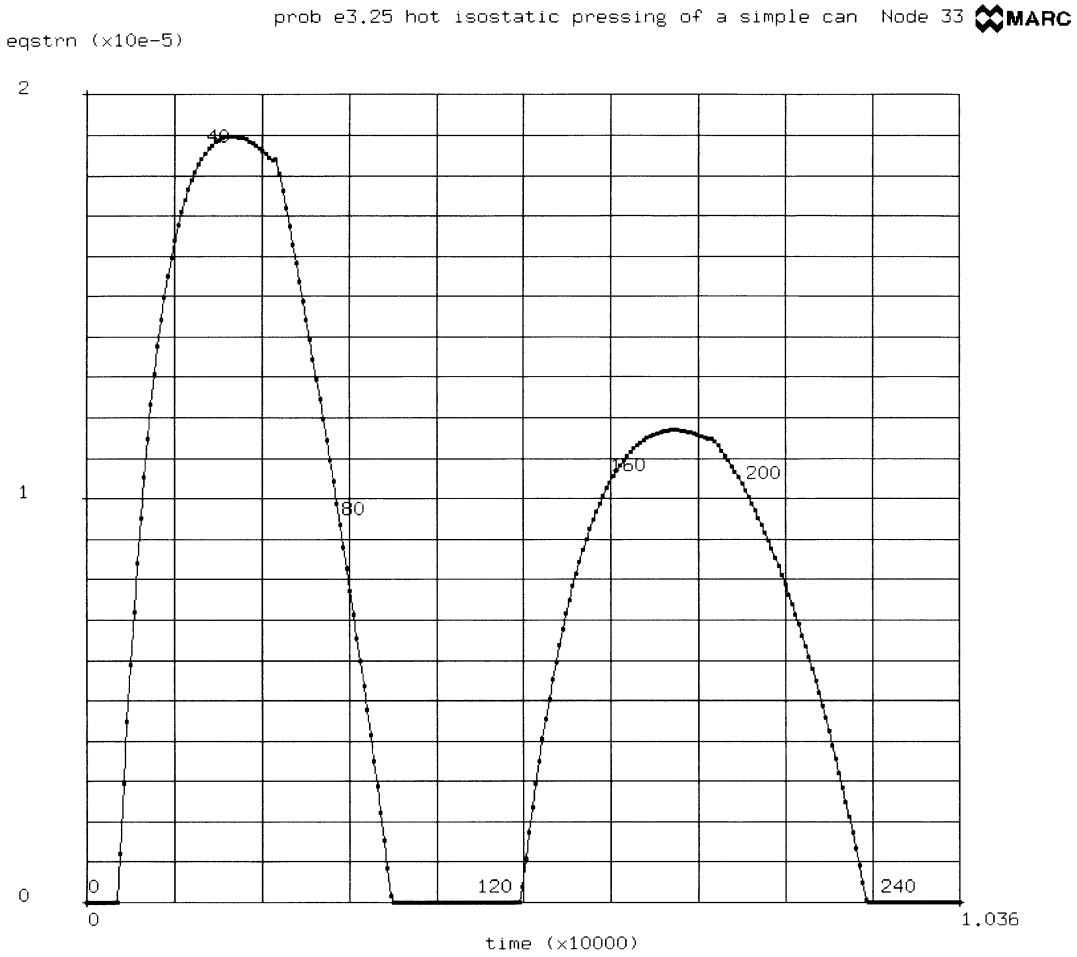

Figure 3.25-4 Time History of Strain Rate

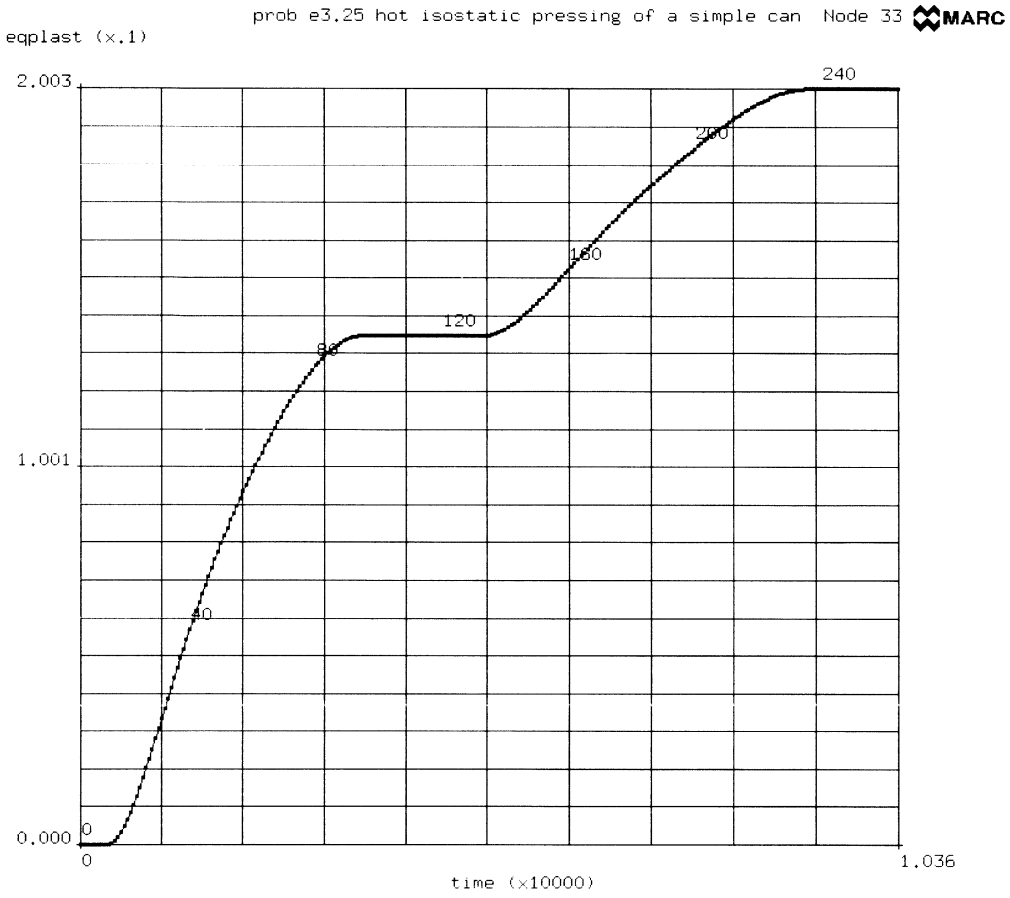

Figure 3.25-5 Time History of Equivalent Plastic Strain

3.26 Hot Isostatic Pressing of a Powder Material

This example illustrates the use of element 28 in a thermal mechanically coupled hot isostatic pressing problem. A powder material is placed into a stiffer cylindrical can which is then subjected to a pressure and thermal cycle.

Element

Element type 28 is an 8-node axisymmetric element used to model the powder and the can. Seventy elements are used to model the powder and 26 to represent the can. In a coupled analysis, element type 42 is the corresponding heat transfer element. The initial dimensions of the powder are 97 mm x 47.0 mm. The can thickness is 3 mm as shown in Figure 3.26-1.

Loading

The loading history is shown in Figure 3.26-3. The external pressure is ramped to 1500 MPa in 9000 seconds; it is then held constant for 10,800 seconds and then reduced to zero in 7200 seconds. The exterior temperature on the can is raised from 0° to 1440°C in the first 9000 seconds and also reduced to zero in 7200 seconds. The FORCDT option is used to prescribe the nodal temperatures. The DIST LOADS option is used to define the external pressure. Note that the FOLLOW FORCE option is used to prescribe the load on the deformed configuration.

Material Properties

As this is a coupled analysis, both mechanical and thermal properties must be prescribed. Furthermore, the material behavior is both temperature and relative density dependent. The powder is represented using the modified Shima model. The Young' modulus and Poisson's ratio are bilinear functions of the relative density and the temperature. E_0 and ν_0 are the initial values 20,000 MPa and 0.3, respectively. The initial yield stress is 1000 MPa.

The experimental data is:

T°(C)	ρ	E (MPa)	ν	σ	E/E_0	ν/ν_0
0.0	0.7	20,000	0.3	1000.0	1.0	1.0
2000.0	0.7	2,000	0.49	100.0	0.1	1.633
0.0	1.0	30,000	0.33	Shima	1.5	1.1

The temperature-dependent properties are entered via data field in the TEMPERATURE EFFECTS option. The relative density effects for Young's modulus and Poisson's ratio are given as multiplicative factors relative to this data via the REALTIVE DENSITY option.

The values of γ and β, which are used to define the yield surfaces dependence on relative density, have initial values of 0.1406174 and 1.375. These material data are functions of the relative density:

$\gamma = (1. + \bar{\rho})^{5.5}$ and
$\beta = 6.25\ (1 - \bar{\rho})^{-0.5}$

Therefore, q_1, q_2, q_3, q_4 are entered as 1.0, 1.0, 1.0, 5.5 and b_1, b_2, b_3, b_4 are entered as 6.25, -6.25, 1.0, -0.5, respectively. The initial relative density is 0.7.

The viscosity is also a function of the temperature with a value of 50,000 at 0°C and 25,000 at 200°C.

The coefficient of thermal expansion is -1×10^{-7} mm/mm°C. The mass density is 4×10^{-6} kg/mm^3.

The thermal conductivity and the specific heat are also bilinear functions of the temperature and relative density.

The experimental data is:

T°C	ρ	KW/m°C	KJ/Kg°C	K/K_o	C/Co
0	0.7	0.03	30.0	1.0	1.0
2000	0.7	0.04	50.0	1.333	1.666
0	1.0	0.042	45.0	1.4	0.9

The temperature dependent properties are entered via the data fields in the TEMPERATURE EFFECTS option. The relative density effects for the conductivity and specific head are defined as multiplicative factors relative to this data via the RELATIVE DENSITY option.

The can is represented as an elastic-plastic material. The properties are a function of temperature only:

T°C	E (MPa)	ν	$\sigma_{y\ (MPa)}$	K	C
0	200,000	0.3	1000	0.03	30
2000	100,000	0.4	500	0.04	50

The coefficient of thermal expansion is 1.0×10^{-6} m/m°C and the mass density is 8.0×10^{-6}. This data is defined in the ISOTROPIC and TEMPERATURE EFFECTS option. The initial relative density of 0.7 is entered through the RELATIVE DENSITY option.

Control

In this problem, the convergence requirement is 10% on relative displacements with a maximum number of 20 iterations. Typically, increments required one to three iterations. The TRANSIENT NON AUTO option was used to provide fixed time steps per increment. As the exterior temperature is completely prescribed, it is not likely that large changes in temperature will occur. The third line on the CONTROL option specifies a maximum allowable temperature difference of 1000 (not used anyway because of fixed time procedure) and an error in temperature of 0.1. This will result in an accurate temperature analysis.

The RESTART option controls the restart to be written every 10 increments. The POST option insures that all the strains, stresses, equivalent plastic strain, strain rate and the relative density may be postprocessed. The post file is written every 10 increments.

Results

The relative density at the end of the analysis is shown in Figure 3.26-3 on the deformed mesh. One can observe that the material has densified to a value of 0.98 in most of the region. The area near the corners shows a reduced level of densification. The time history of relative density, inelastic strain rate, and equivalent plastic strain are shown in Figure 3.26-4, Figure 3.26-5, and Figure 3.26-6, respectively.

Parameters, Options, and Subroutines Summary

Example e3x26.dat:

Parameters	Model Definition Options	History Definition Options
COUPLE	CONNECTIVITY	CONTINUE
ELEMENTS	CONTROL	DIST LOADS
END	COORDINATES	TRANSIENT
LARGE DISP	DEFINE	
SIZING	DENSITY EFFECTS	
TITLE	DIST LOADS	
UPDATE	END OPTION	
	FIXED DISP	
	FIXED TEMPERATURE	
	FORCDT	
	ISOTROPIC	
	POST	
	POWDER	
	RELATIVE DENSITY	
	RESTART	
	TEMPERATURE EFFECTS	
	WORK HARD	

User subroutine in u3x26.f:

FORCDT

MARC

97	7	8	9	10	11	12	13	14	15	16	17	18	98
24	85	86	87	88	89	90	91	92	93	94	95	96	6
23	73	74	75	76	77	78	79	80	81	82	83	84	5
22	61	62	63	64	65	66	67	68	69	70	71	72	4
21	49	50	51	52	53	54	55	56	57	58	59	60	3
20	37	38	39	40	41	42	43	44	45	46	47	48	2
19	25	26	27	28	29	30	31	32	33	34	35	36	1

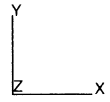

Figure 3.26-1 Mesh

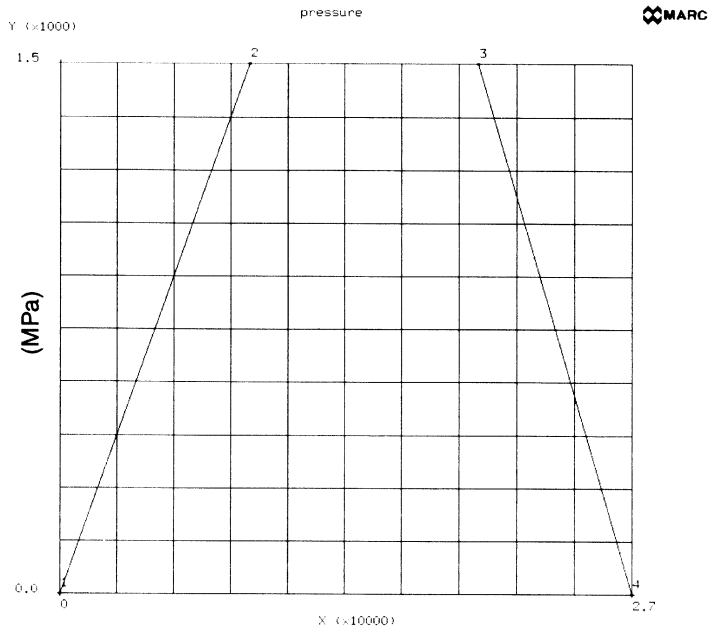

Externally Applied Pressure

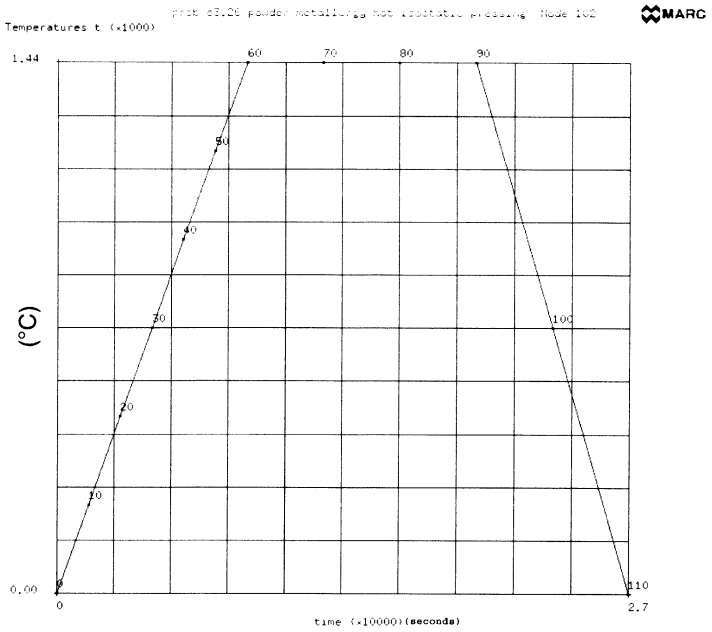

Externally Applied Temperature

Figure 3.26-2 Time History

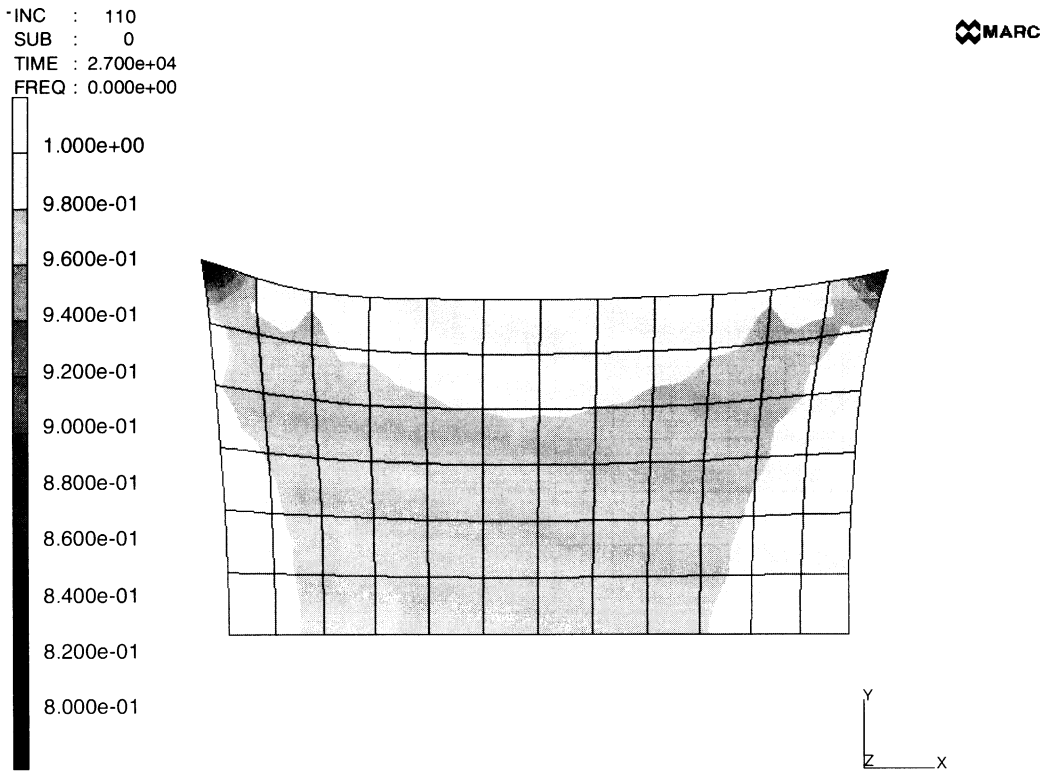

Figure 3.26-3 Final Relative Density

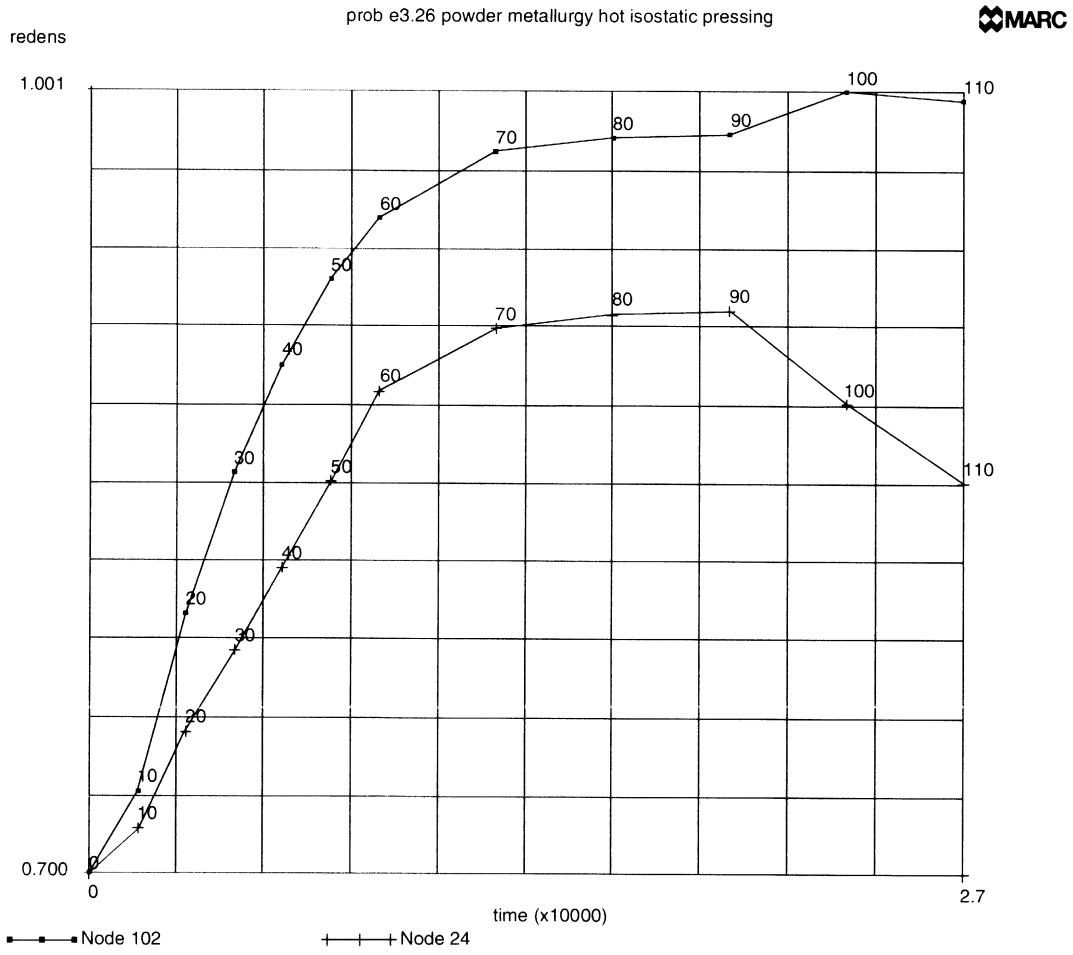

Figure 3.26-4 Time History of Relative Density

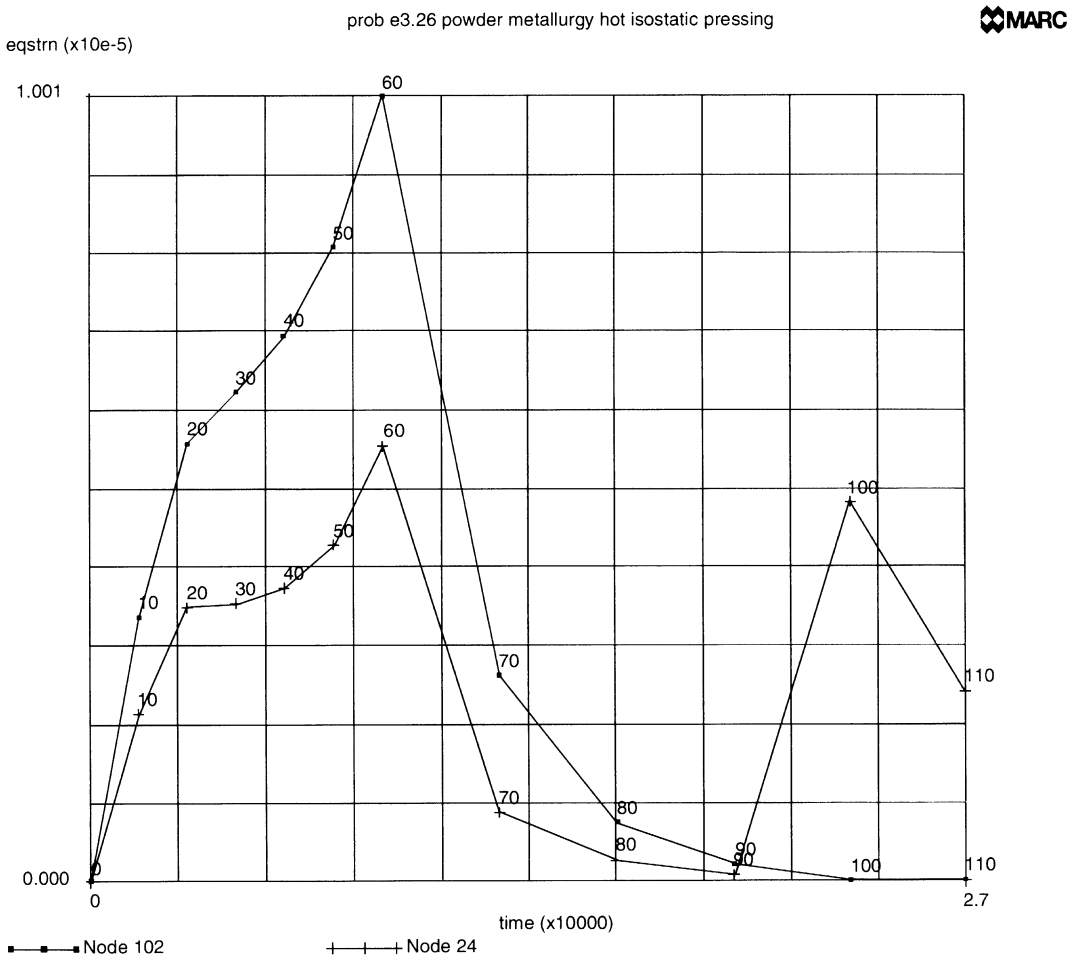

Figure 3.26-5 Time History of Equivalent Strain Rate

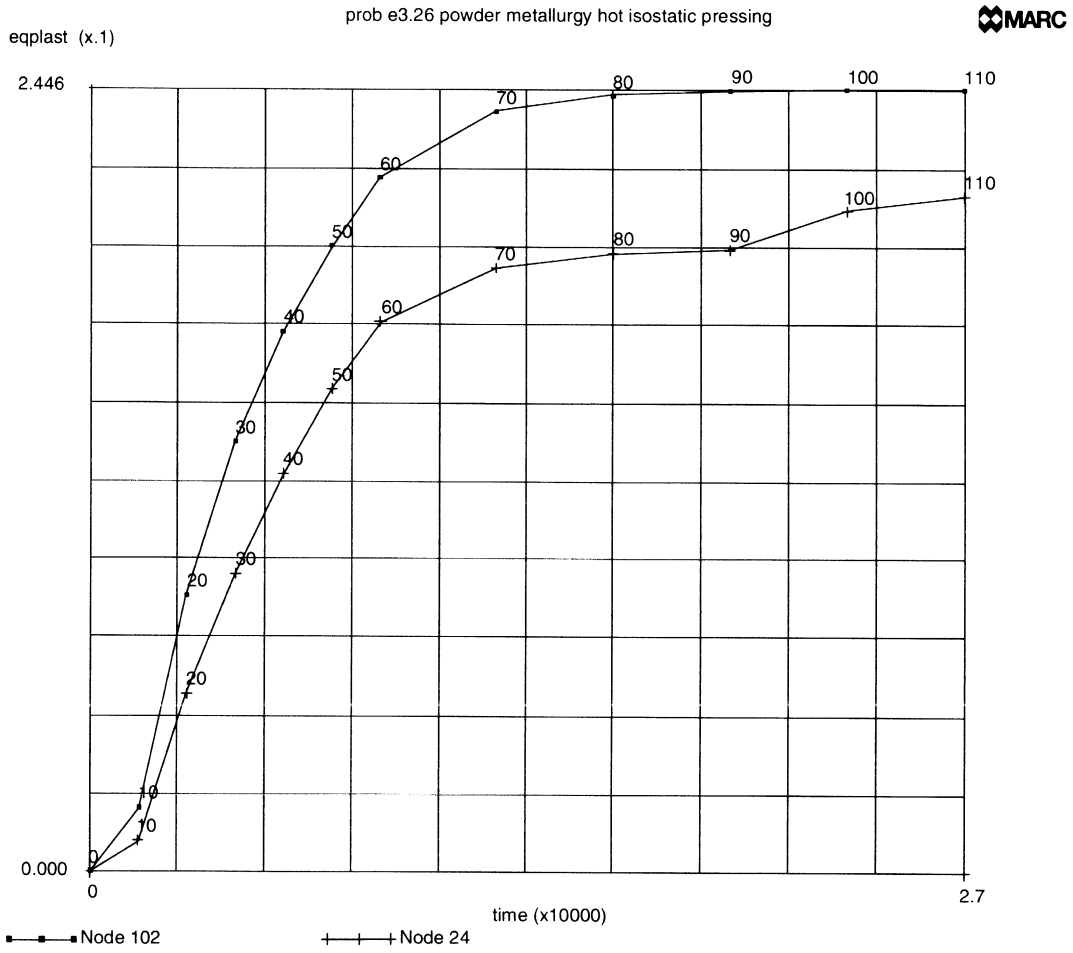

Figure 3.26-6 Time History of Equivalent Plastic Strain

3.27 Shear Band Development

This example illustrates the formation of shear bands in a strip being pulled. The Gurson damage model is used to predict void growth in the material.

Element

Element type 54, a plane strain reduced integration element, is used to model the strip. The strip, as shown in Figure 3.27-1, has dimensions of L = 10 and h = 68 with a slight imperfection at the free end y = h. $\Delta y = 0.0025\cos\left(\frac{\pi x}{L}\right)$. User subroutine UFXORD is used to define this imperfection.

The mesh consists of 8 x 32 eight noded elements.

Boundary Conditions

The boundary conditions are x = 0, v = 0, x = L, v is prescribed, y = 0, v = 0, and y = h is free. The maximum displacement is at increment 280 = 5.6 or log strain of .4447.

Material Properties

The material is an elastic plastic workhardening material with Young's modulus = 30,000 MPa, Poisson's ratio = 0.3 and initial yield of 100 MPa. The workhardening slope is shown in Figure 3.27-2. The Gurson damage model is used to invoke the plastic-strain controlled nucleation model. The parameters used are:

First yield surface multiplier, q_1	=	1.5
Second yield surface multiplier, q_2	=	1.0
Initial void fraction	=	0.0
Critical void fraction, f_c	=	0.15
Failure void fraction, f_f	=	0.25
Mean strain for nucleation	=	0.3
Standard deviation	=	0.1
Volume fraction of void nucleating particles	=	0.04

Control

The convergence ratio required is 2.5%. Because this is a highly nonlinear problem, the maximum number of iterations permitted is 20. The post file is written every 10 increments. The restart file is written every 40 increments.

Results

The deformed meshes at increments 120, 160, and 200 are shown in Figure 3.27-3 through Figure 3.27-5. One can clearly see the formation of the shear bands. The void volume fraction is then shown for the same increments. Again, the largest number of voids occurs where the shear bands form. Figure 3.27-10 shows the time history of the formation of voids for 3 points. One can see that for node 507, which is not in the shear band, the void volume matches that of nodes 607 and 745 until the shear band forms. At this point, "all" of the strain is localized and no additional void volume occurs. While for nodes 607 and 745, which are within the band, one sees an increase in the void volume with node 745 reaching close to the maximum-minus half the standard deviation. At this point, the equivalent plastic strain is 116%. The time history of the plastic strain is shown in Figure 3.27-11.

Parameters, Options, and Subroutines Summary

Example e3x27.dat:

Parameters	Model Definition Options	History Definition Options
ELEMENTS	CONNECTIVITY	AUTO LOAD
END	CONTROL	CONTINUE
FINITE	COORDINATES	DIST CHANGE
LARGE DISP	DAMAGE	
SIZING	DEFINE	
TITLE	END OPTION	
UPDATE	FIXED DISP	
	GEOMETRY	
	ISOTROPIC	
	NO PRINT	
	POST	
	RESTART	
	UFXORD	
	WORK HARD	

User subroutine in u3x27.f:

UFXORD

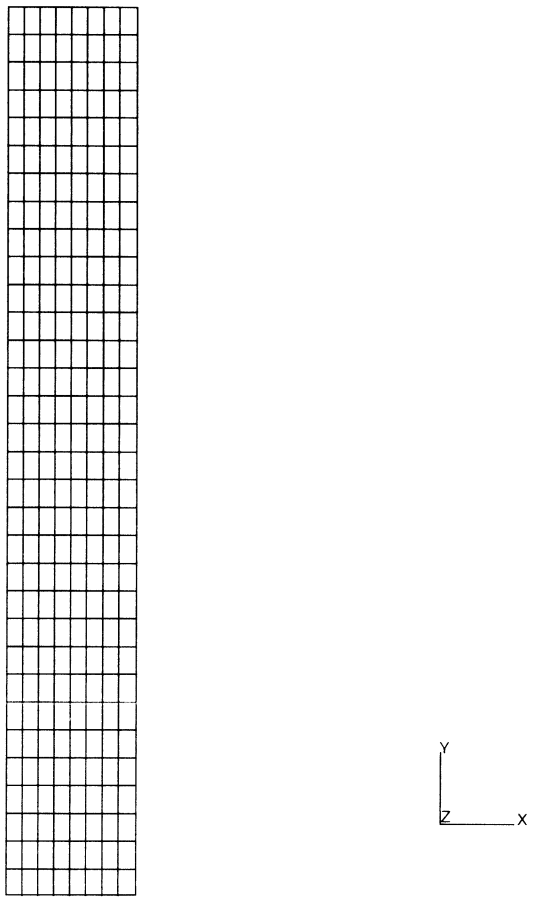

Figure 3.27-1 Finite Element Mesh

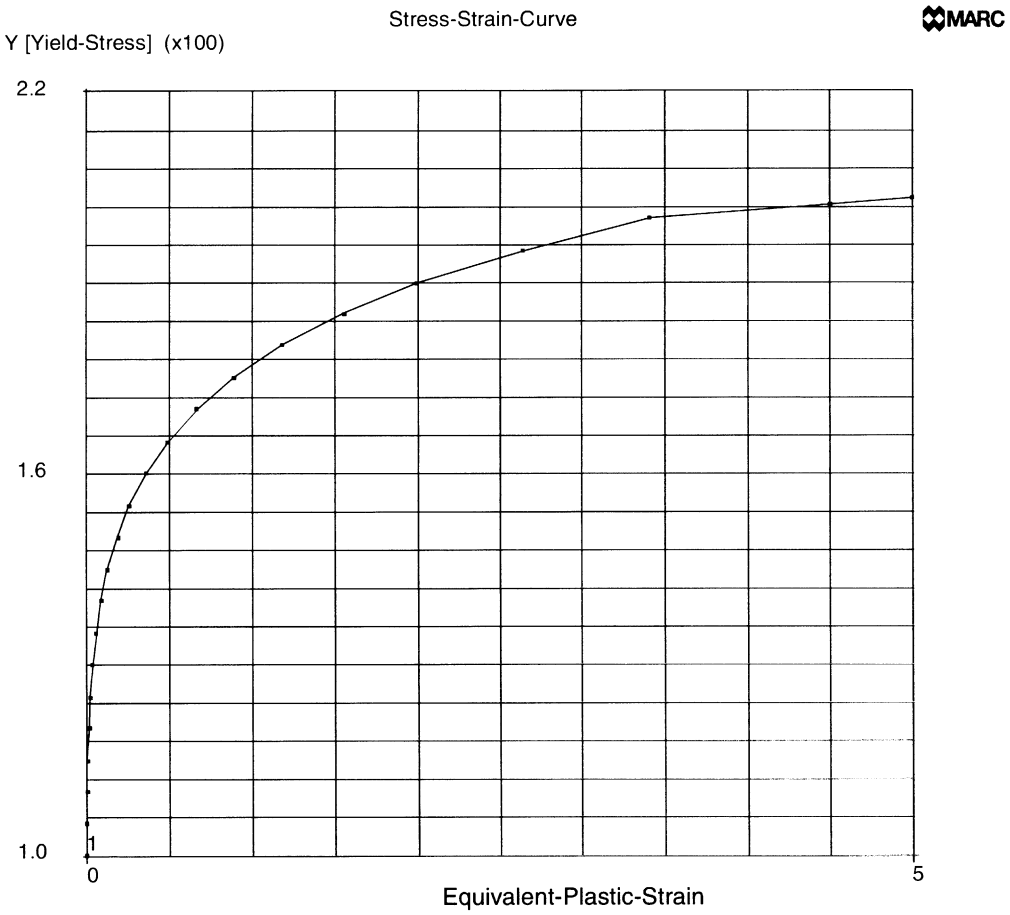

Figure 3.27-2 Stress-Strain Law

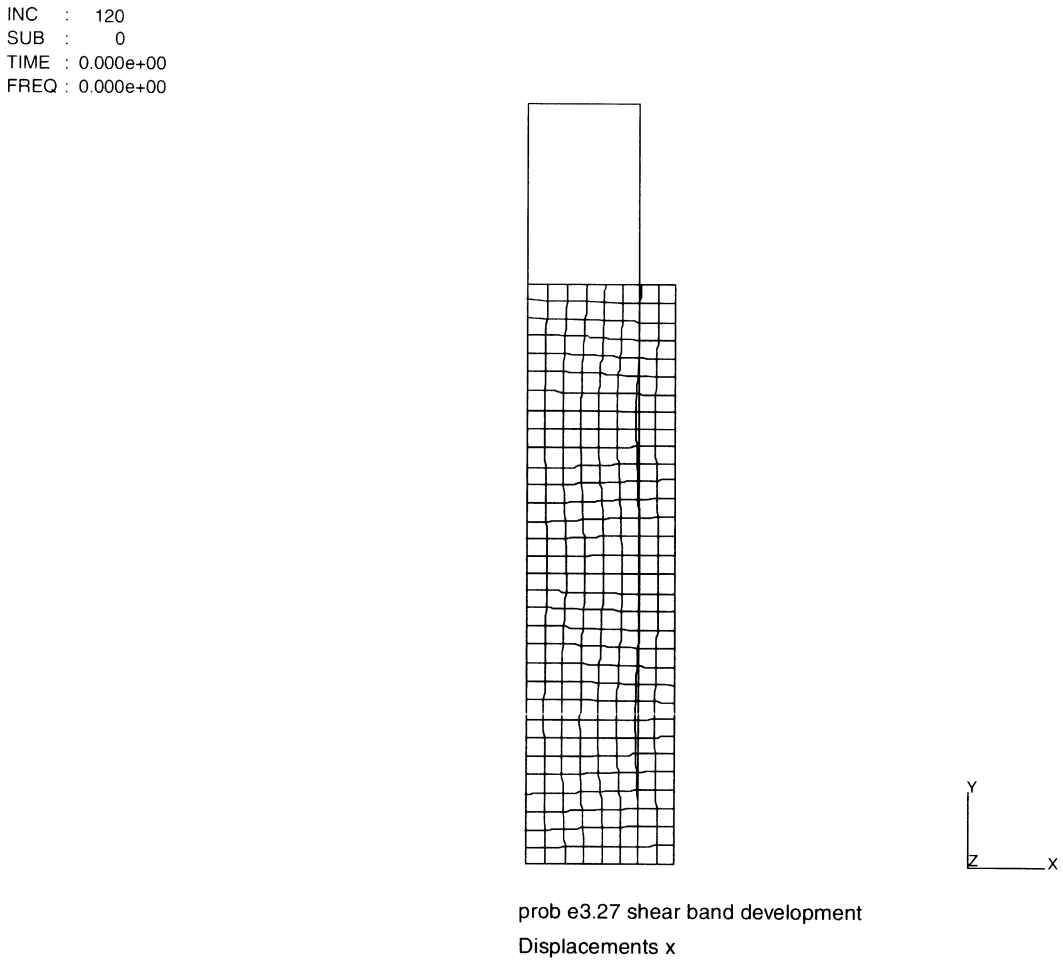

Figure 3.27-3 Deformed Mesh at Increment 120

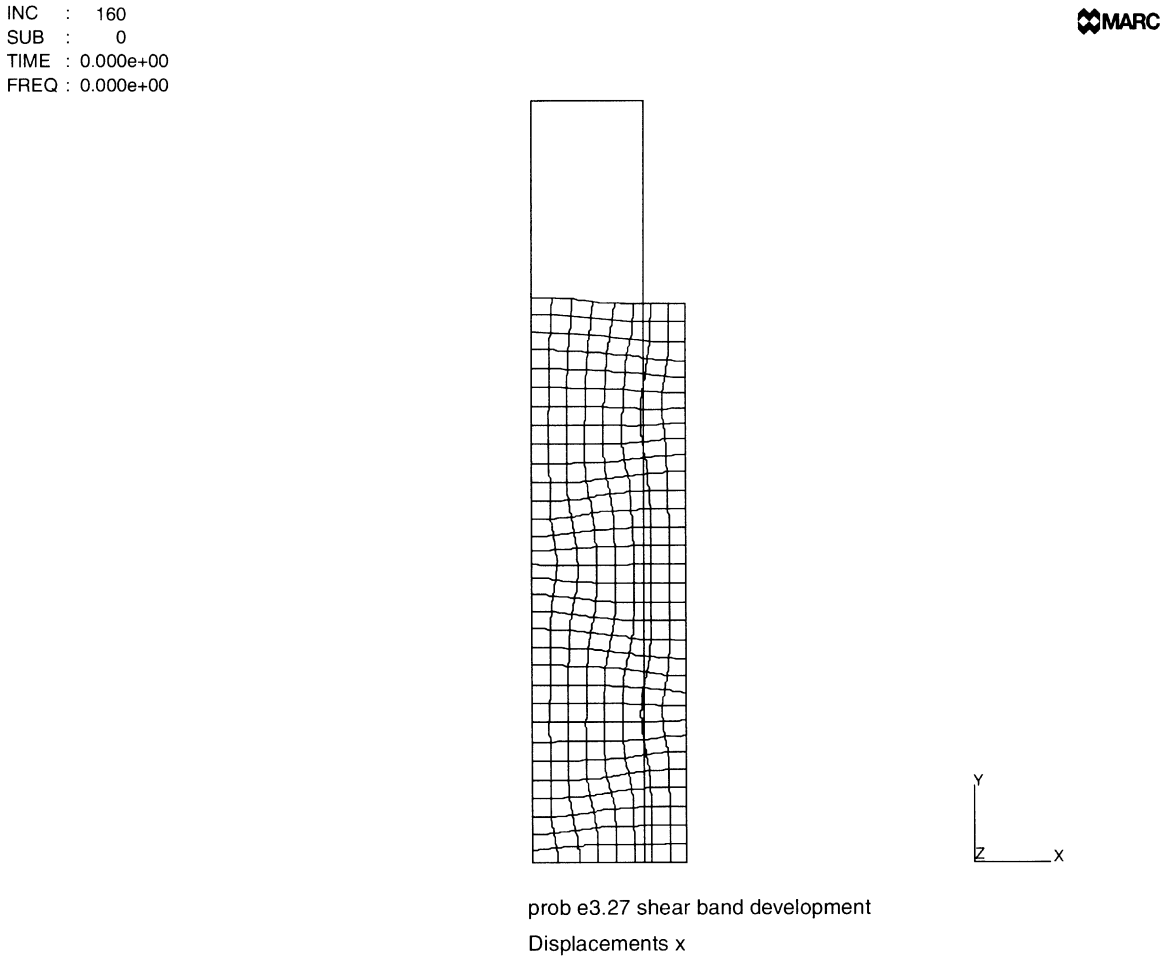

Figure 3.27-4 Deformed Mesh at Increment 160

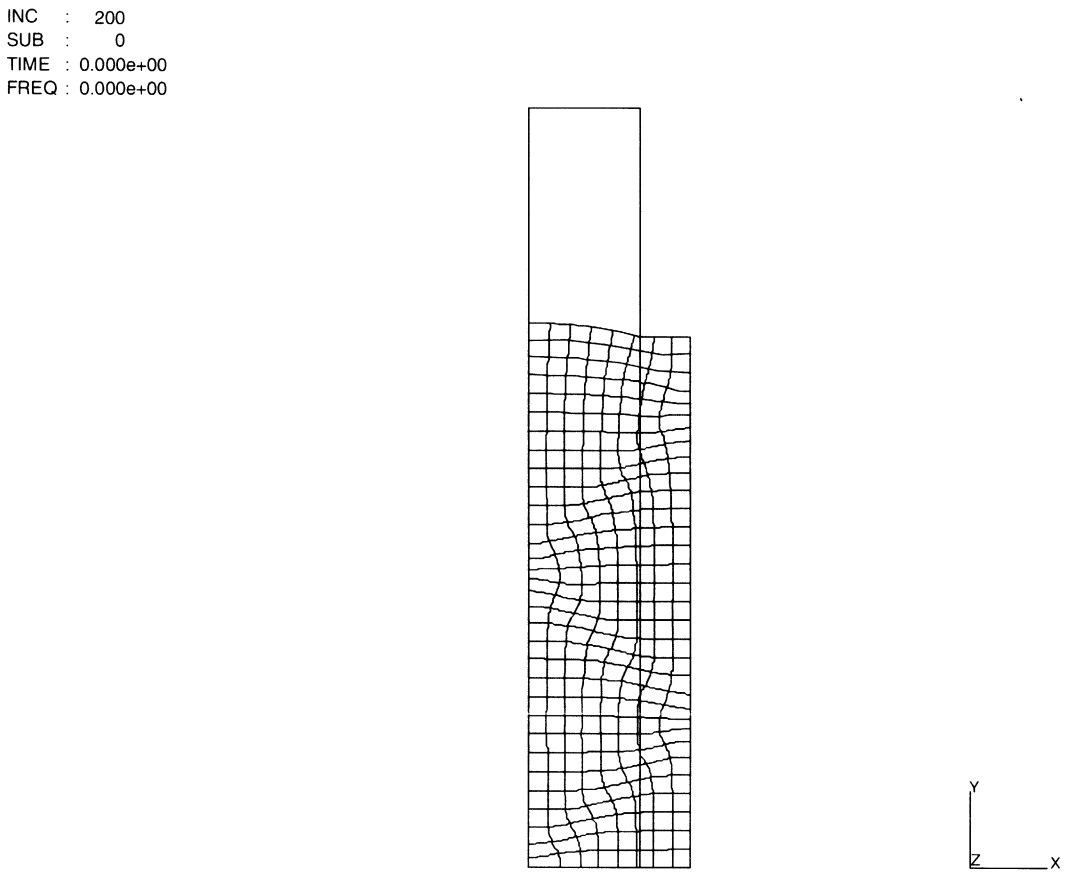

Figure 3.27-5 Deformed Mesh at Increment 200

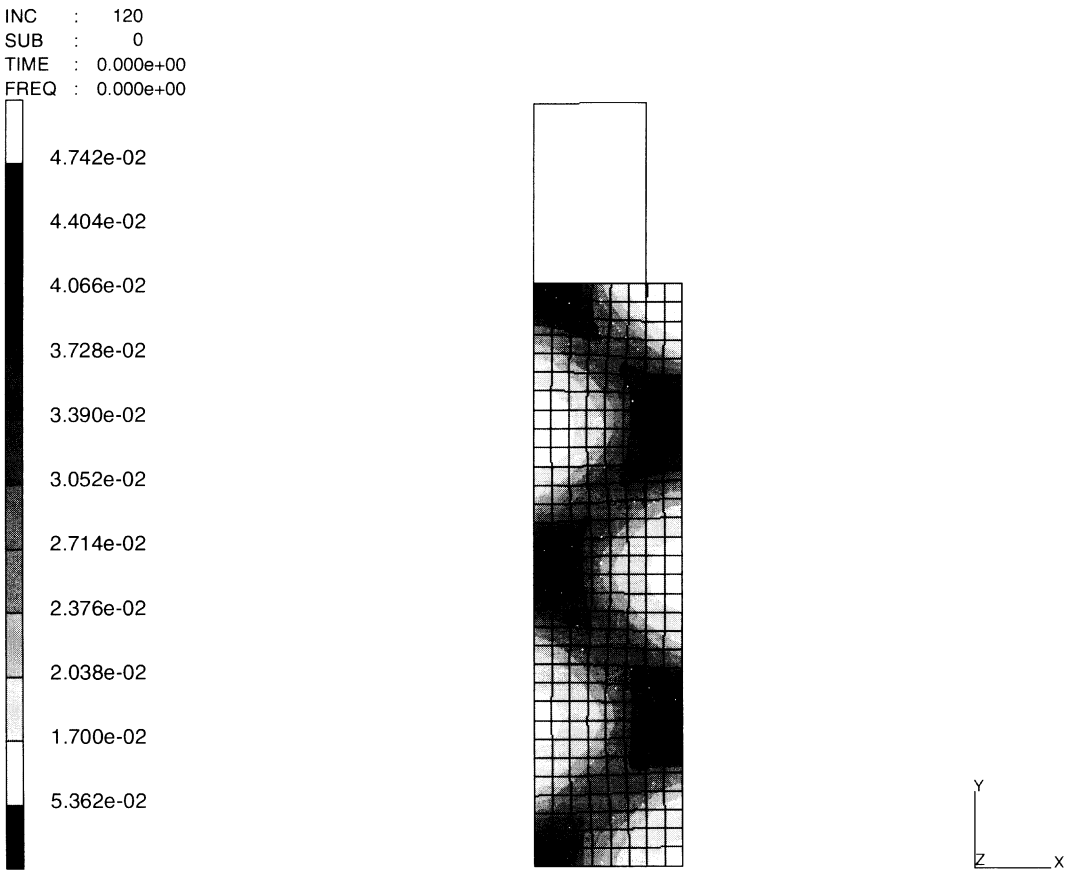

Figure 3.27-6 Void Volume Fraction at Increment 120

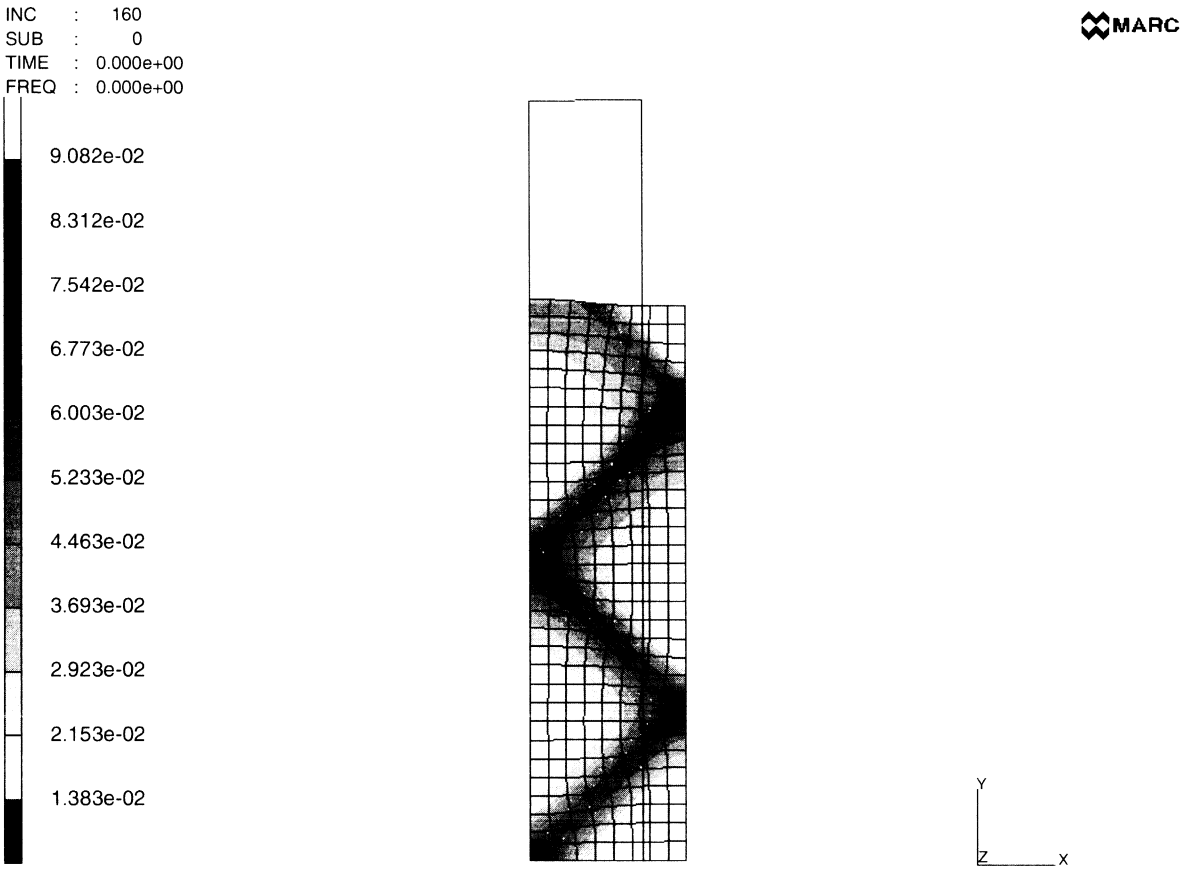

Figure 3.27-7 Void Volume Fraction at Increment 160

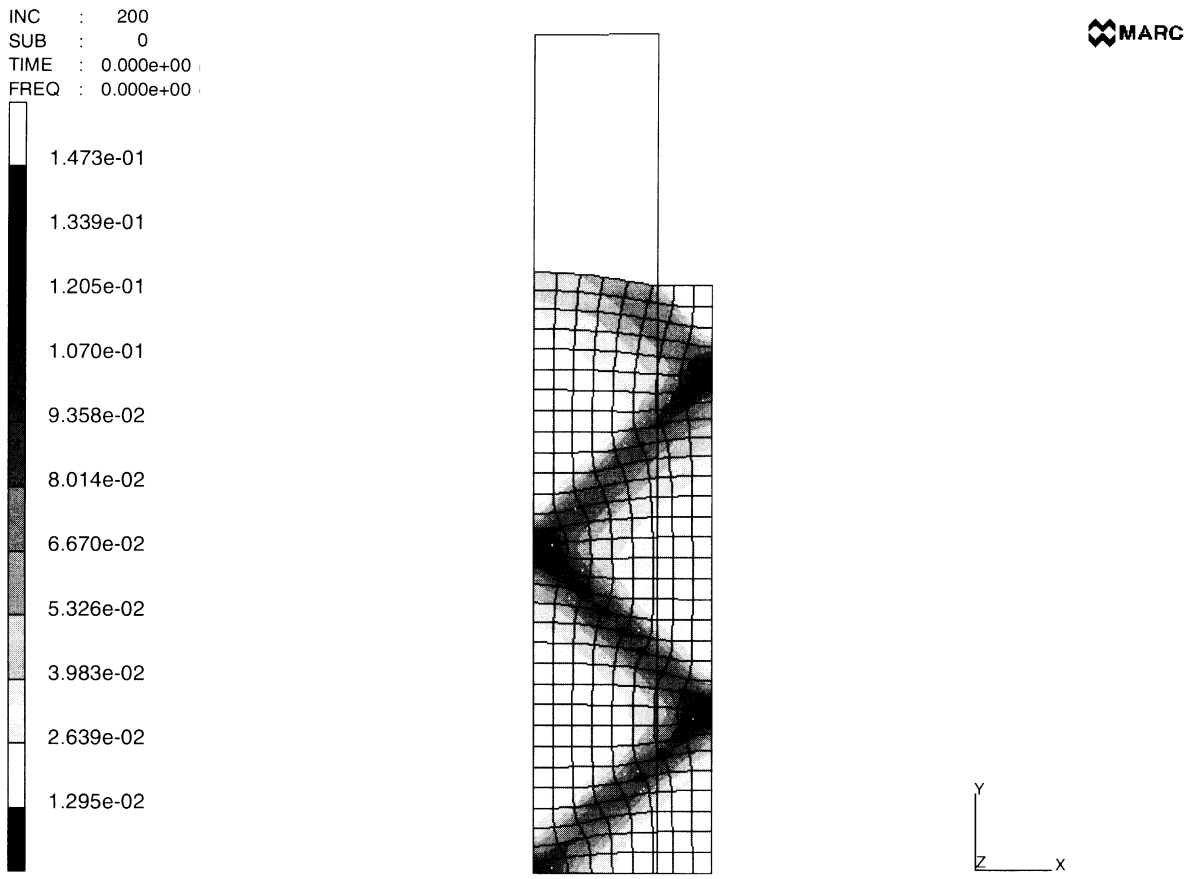

Figure 3.27-8 Void Volume Fraction at Increment 200

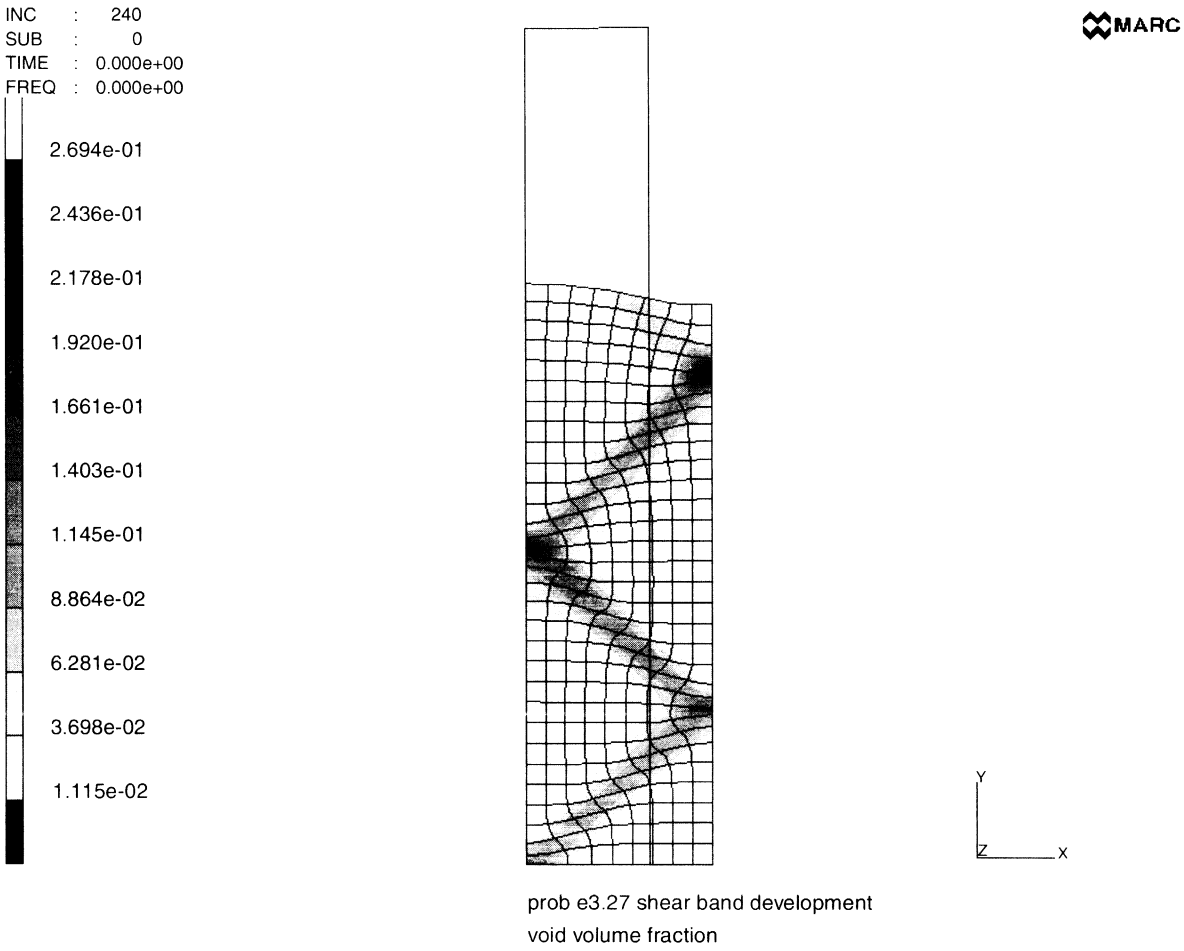

Figure 3.27-9 Void Volume Fraction at Increment 240

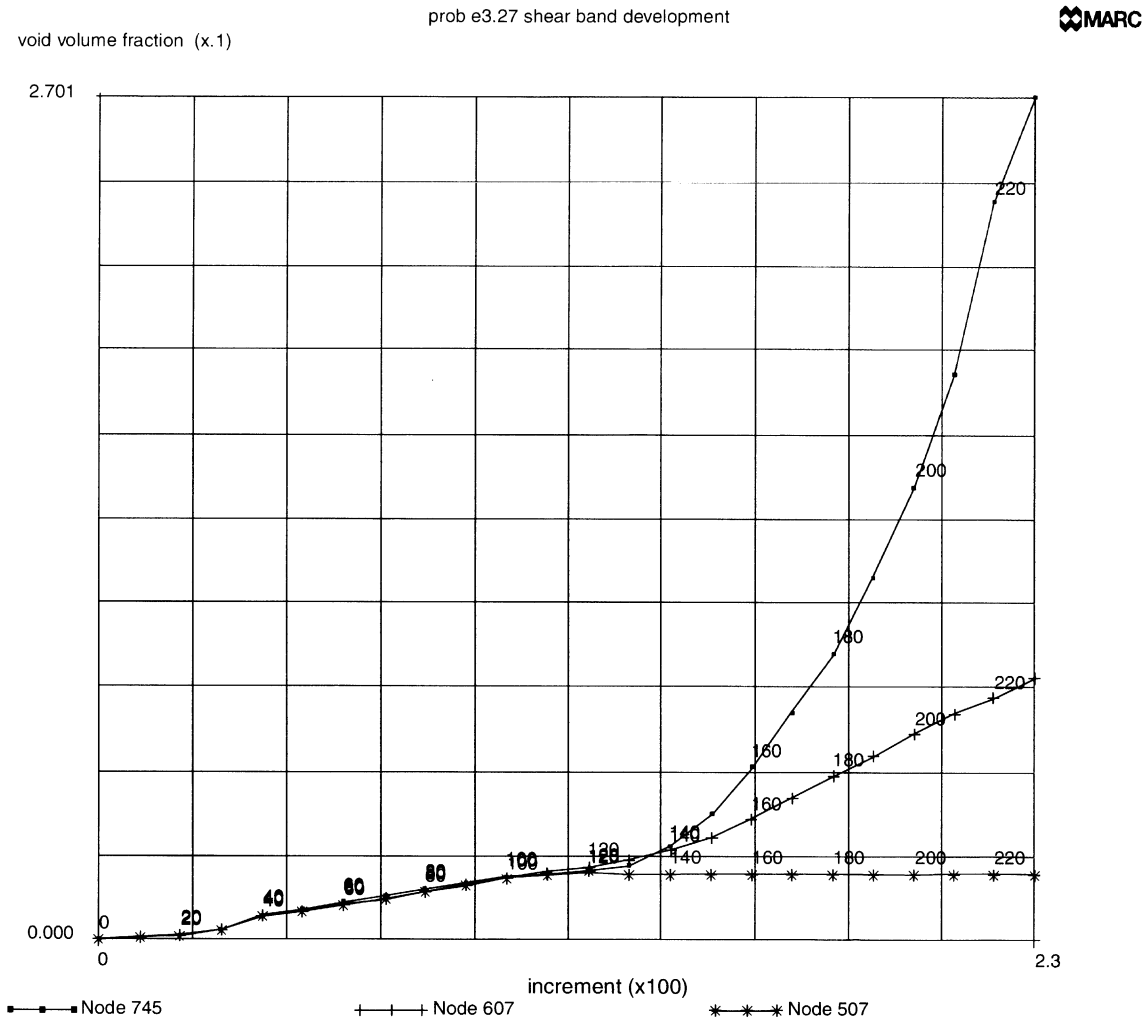

Figure 3.27-10 Time History of Void Volume Fraction

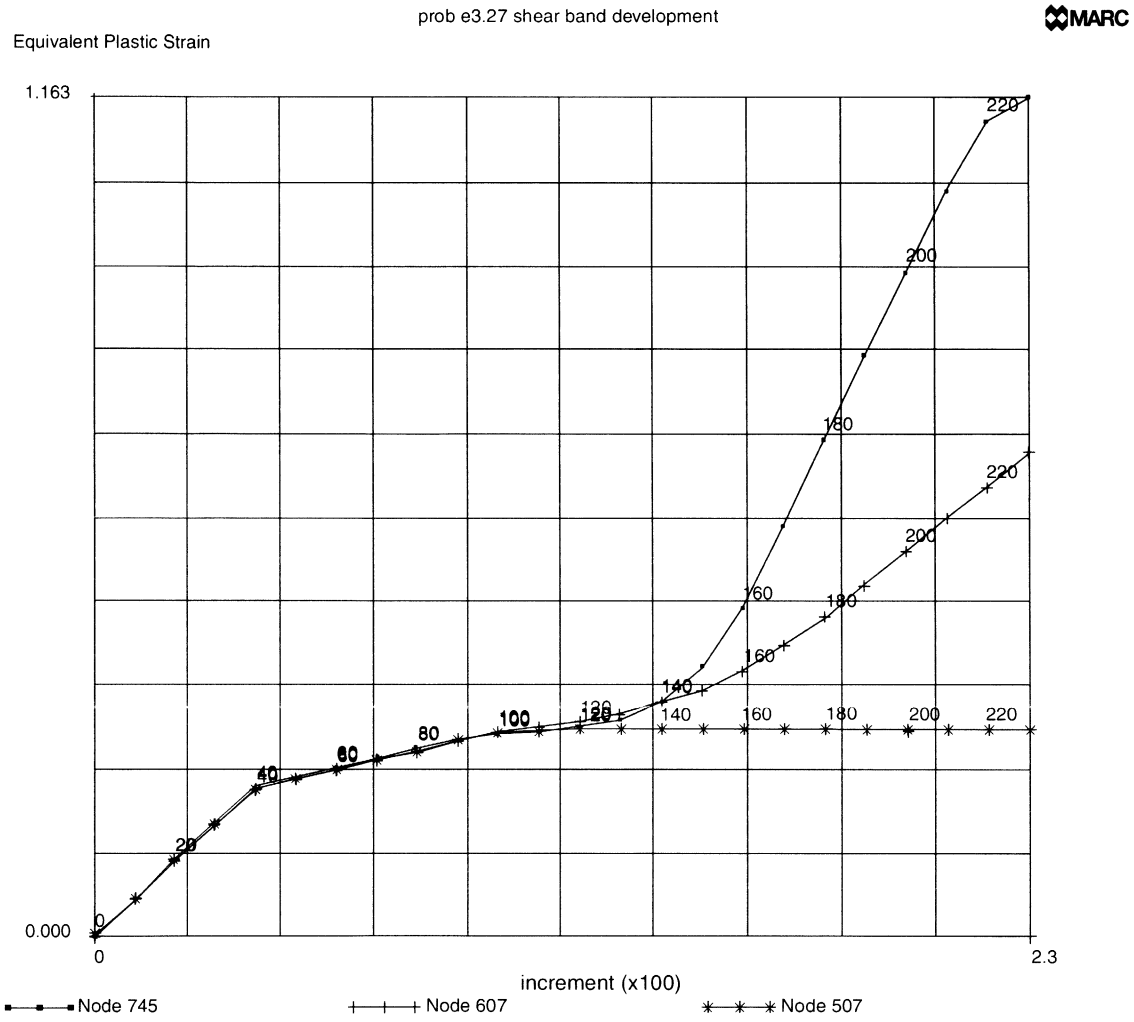

Figure 3.27-11 Time History of Plastic Strain

3.28 Void Growth in a Notched Specimen

This example illustrates the prediction of void growth in a notched specimen. This problem was first analyzed using a damage model by Sun.

Element

Element type 55 is an 8-node reduced integration axisymmetric element used in this analysis. The bar is 25 mm long with a radius of 7mm, and an elliptical notch (minor axis of 3, major of 3.873) is shown in Figure 3.28-1. The model consists of 500 elements and 1601 nodes and is shown in Figure 3.28-2.

Loading

Symmetry conditions are applied on the center line and the left side. The bar has an applied displacement of 1.775 applied in 230 increments using the DISP CHANGE and AUTO LOAD options.

Material Properties

The material is represented using a workhardening model. The Young's modulus is 21,000.0 N/mm^2. The workhardening data is shown in Figure 3.28-3.

The Gurson damage model is invoked using the strain-controlled nucleation model. The parameters used are:

First yield surface multiplier, q_1	=	1.5
Second yield surface multiplier, q_2	=	1.0
Initial void volume fraction, f_i	=	0.00057
Critical void volume fraction, f_c	=	0.3
Failure void volume fraction, f_f	=	0.15
Mean strain for nucleation	=	0.3
Standard deviation	=	0.1
Volume fraction of void nucleating particles	=	0.00408

Control

The required convergence tolerance is 5% on residuals. A maximum of 15 iterations per increment is allowed. The restart file is generated every 20 increments. The post file is generated every 10 increments. The bandwidth is minimized using the Cuthill-McKee optimizer. The AUTO LOAD option is invoked twice; the first time 80 increments of 0.1 mm are taken and then 150 more increments of 0.0025 mm are taken.

Results

The deformed geometry is shown in Figure 3.28-4. The distribution of the void is represented in Figure 3.28-5. Linear elastic analysis would reveal that the highest stress is at the outside radius. Due to the redistribution of the stresses and because of elastic plastic behavior, the highest triaxial stress occurs at the center and the crack initiation due to void coalescence begins here. The equivalent plastic strain is shown in Figure 3.28-6. On subsequent loading, the cracks grow radially along the symmetry line. Figure 3.28-7 shows the history of the void ratio at three nodes along this line.

Parameters, Options, and Subroutines Summary

Example e3x28.dat:

Parameters	Model Definition Options	History Definition Options
ALIAS	CONNECTIVITY	AUTO LOAD
ELEMENTS	CONTROL	CONTINUE
END	COORDINATES	DIST CHANGE
FINITE	DAMAGE	
LARGE DISP	DEFINE	
PRINT	END OPTION	
SIZING	FIXED DISP	
TITLE	ISOTROPIC	
UPDATE	NO PRINT	
	OPTIMIZE	
	POST	
	RESTART	
	WORK HARD	

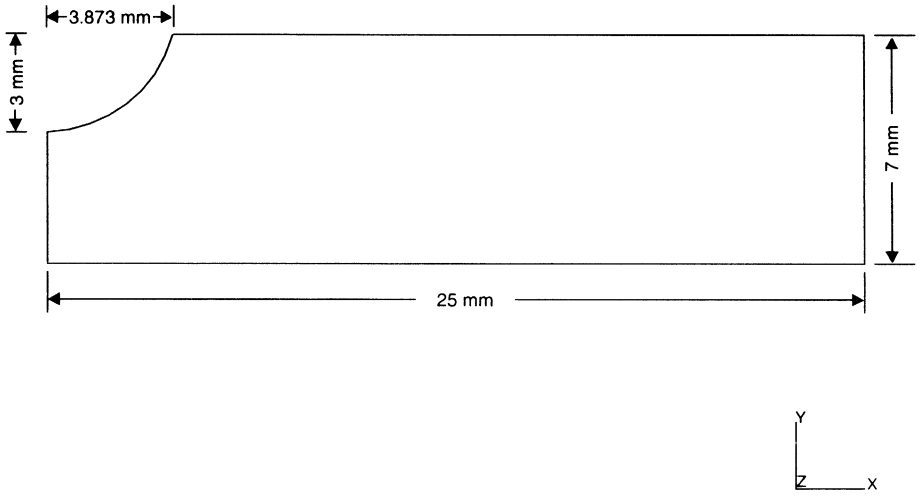

Figure 3.28-1 Notched Specimen

MARC

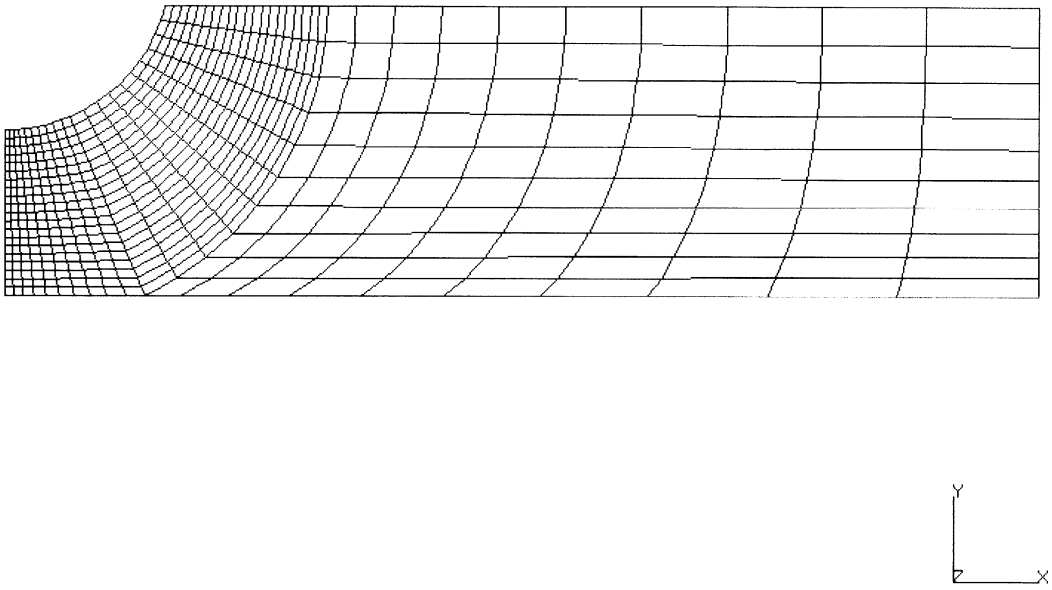

Figure 3.28-2 Mesh

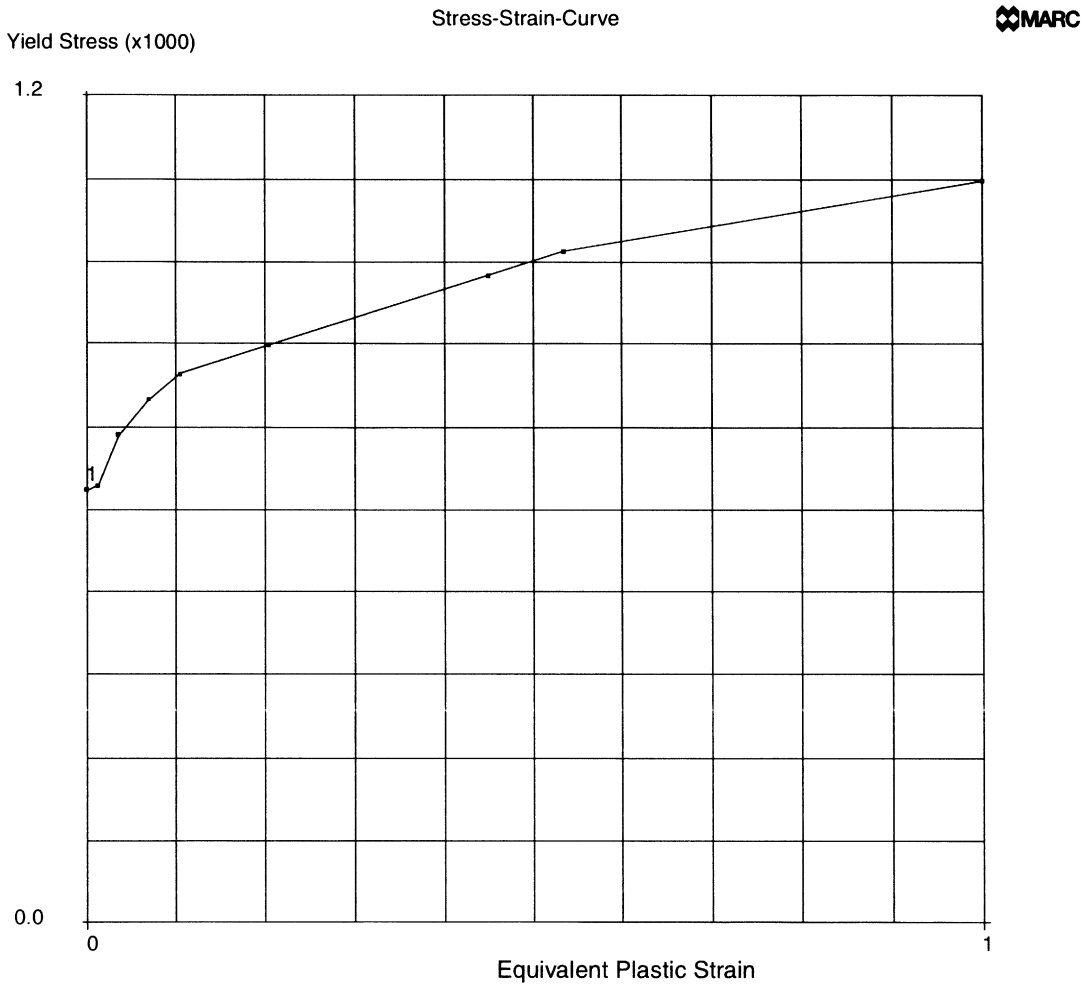

Figure 3.28-3 Stress-Strain Curve

INC : 230
SUB : 0
TIME : 0.000e+00
FREQ : 0.000e+00

MARC

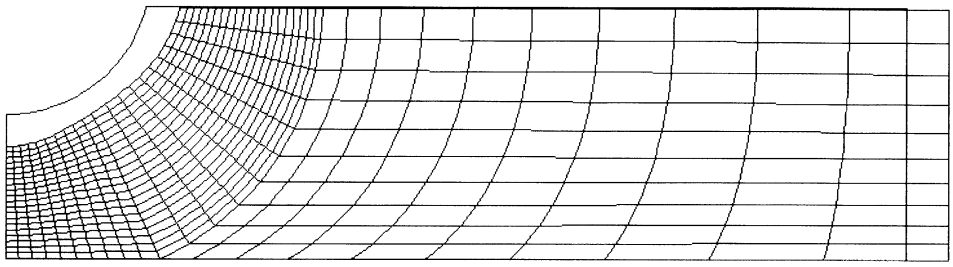

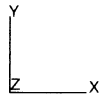

prob e3.28 gurson model, sun specimen
Displacements x

Figure 3.28-4 Deformed Mesh

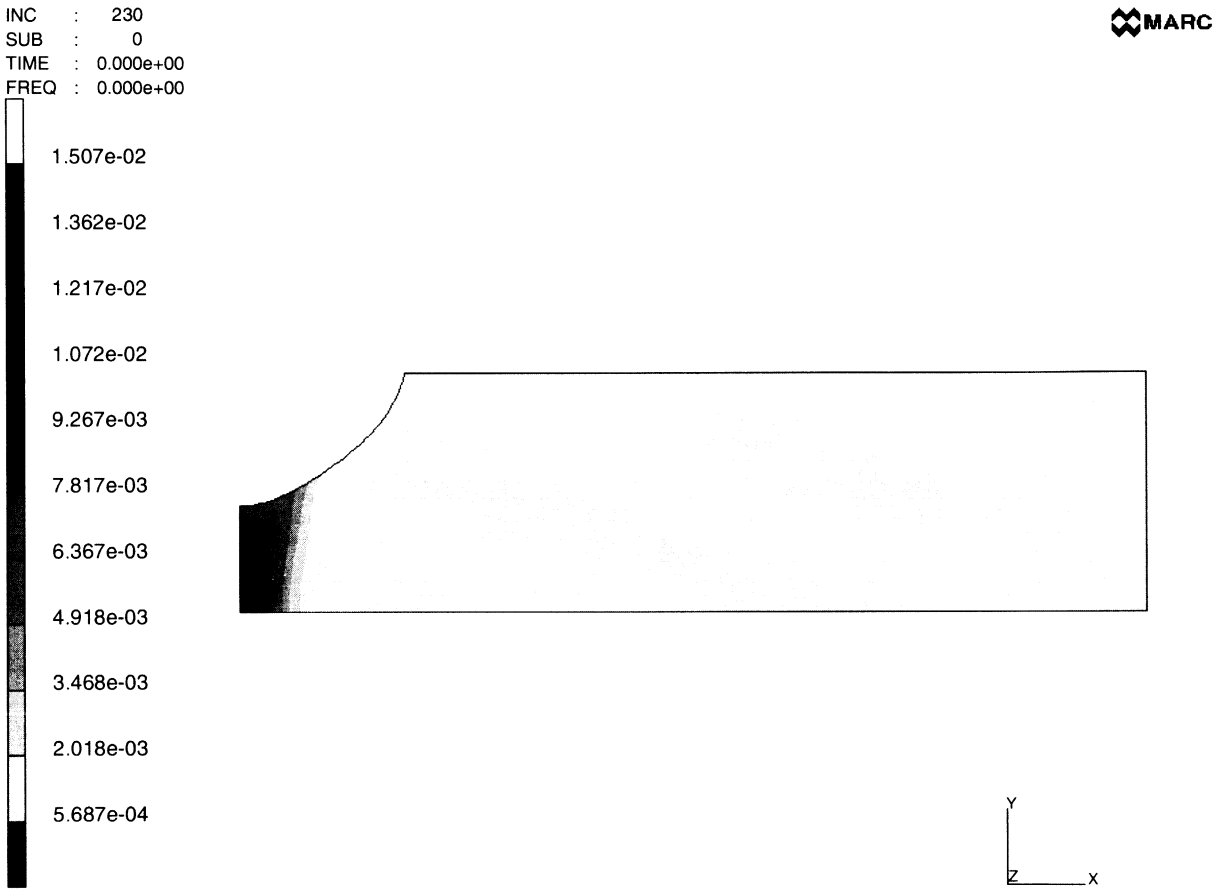

Figure 3.28-5 Void Volume Fraction

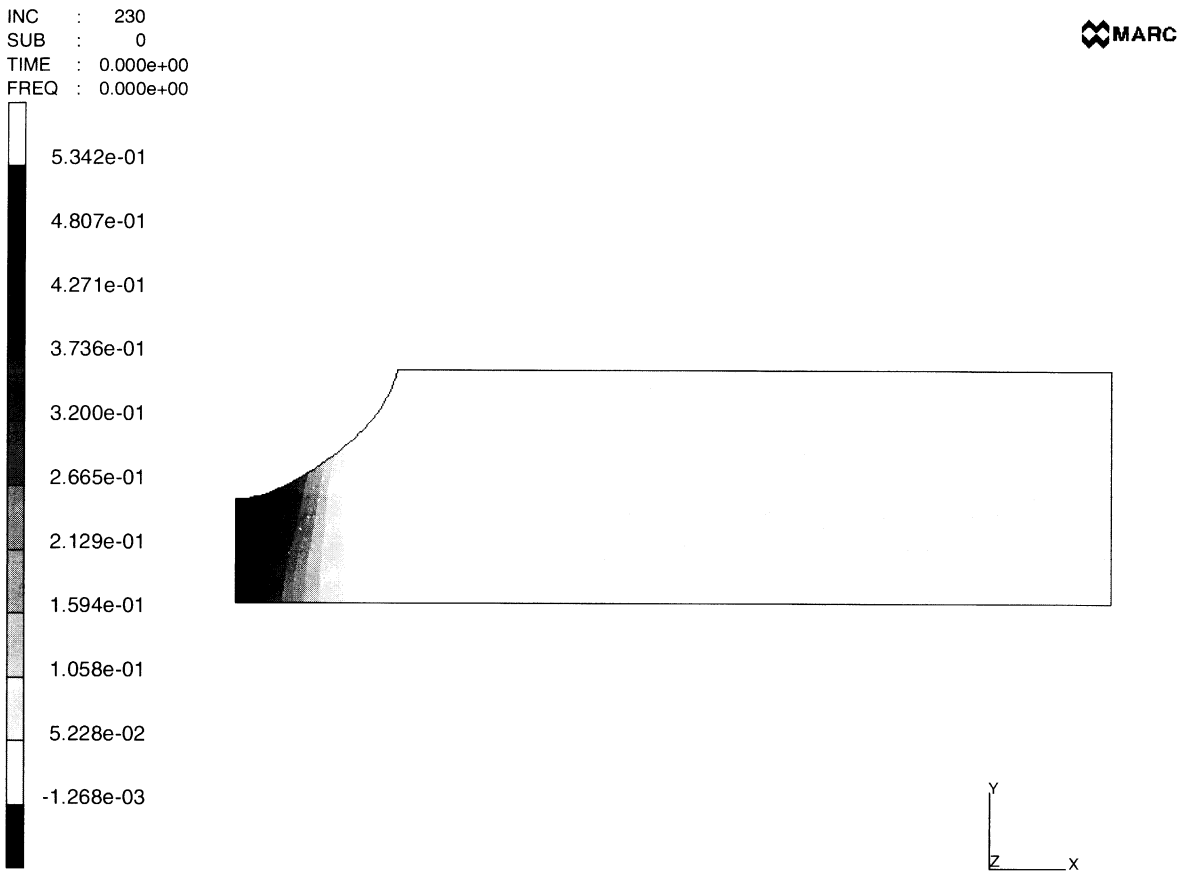

Figure 3.28-6 Equivalent Plastic Strain

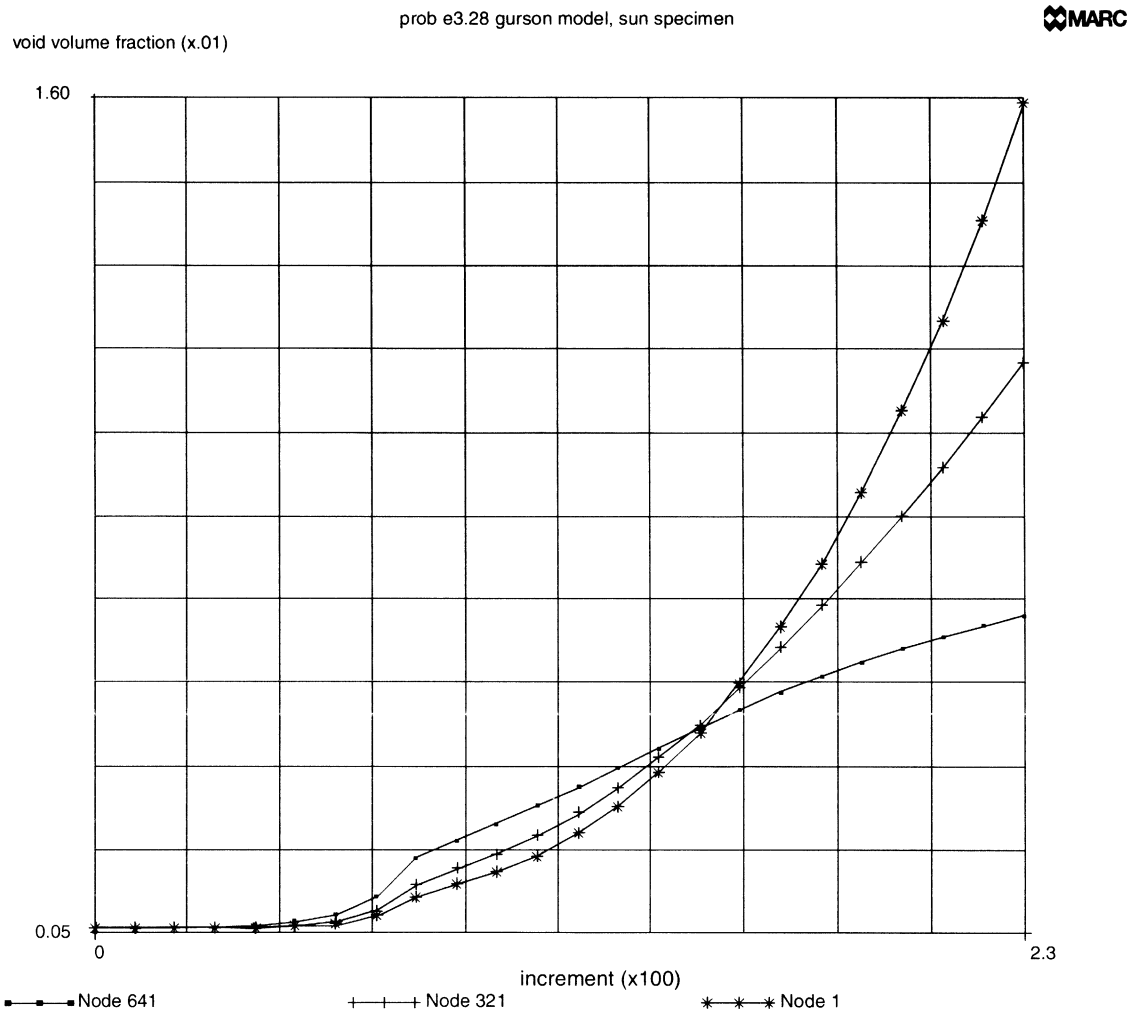

Figure 3.28-7 Time History of Void Volume Fraction

3.29 Creep of a Thick Walled Cylinder - Implicit Procedure

This example illustrates the implicit formulation for performing power-law creep analysis. A thick-walled cylinder is pressurized and then allowed to creep.

Element

Element type 10, the 4-node axisymmetric element is used. The constant dilatation option was used. Twenty elements are used through the cylinder which has an inner radius of one inch and an outer radius of two inches. The mesh is shown in Figure 3.29-1.

Loading

The cylinder is constrained axially along the left edge; the right edge is free to allow expansion. The internal pressure of 14,000 psi is applied in increment one and then held constant during the creep process.

Material Properties

The material is steel with a Young's modulus of 30 x 10^6 psi and a Poisson's ratio of 0.3. The creep strain rate is of the Norton type defined as:

$$\dot{\varepsilon}^{c} = 1 \times 10^{-19} \text{ in/in/hr} \bullet \bar{\sigma}^{3.5}$$

The constants are given in the CREEP model definition block.

Control

The CREEP parameter is used to indicate that this is a creep analysis. The default is that an explicit procedure is used. The third flag indicates that the implicit method will be used. When the implicit method is used, you have three choices on how the stiffness matrix is to be formed (elastic tangent, secant, or radial return). In this analysis, the secant method was chosen by setting the eighth field of the CONTROL option to one. The convergence required was 1% on residuals. The AUTO CREEP option was used to indicate that a total time period of 100 hours was to be covered and the first time step should be one hour.

Results

Using the implicit procedure, the analysis was completed in 28 increments while the explicit procedure required 39 increments. The time history of the resultant analyses are shown in Figure 3.29-2 and Figure 3.29-3, respectively. One should note that the implicit analysis does not exhibit the oscillations that occur when using the explicit method.

Parameters, Options, and Subroutines Summary

Example e3x29.dat:

Parameters	Model Definition Options	History Definition Options
CREEP	CONNECTIVITY	AUTO CREEP
ELEMENTS	CONTROL	CONTINUE
END	COORDINATES	CONTROL
SIZING	CREEP	DIST LOADS
TITLE	DISP LOADS	
	END OPTION	
	FIXED DISP	
	GEOMETRY	
	ISOTROPIC	
	POST	

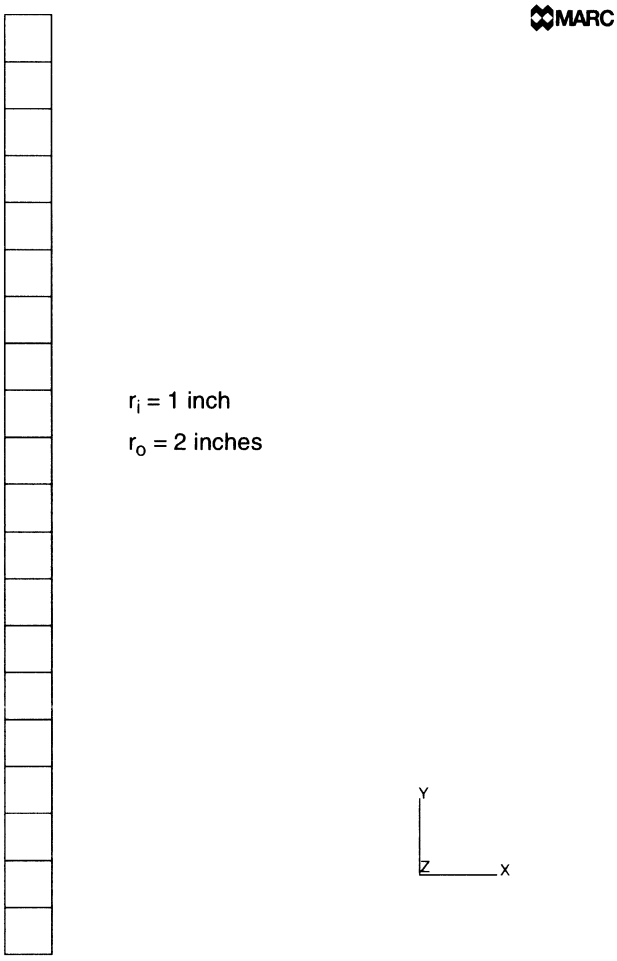

Figure 3.29-1 Finite Element Mesh

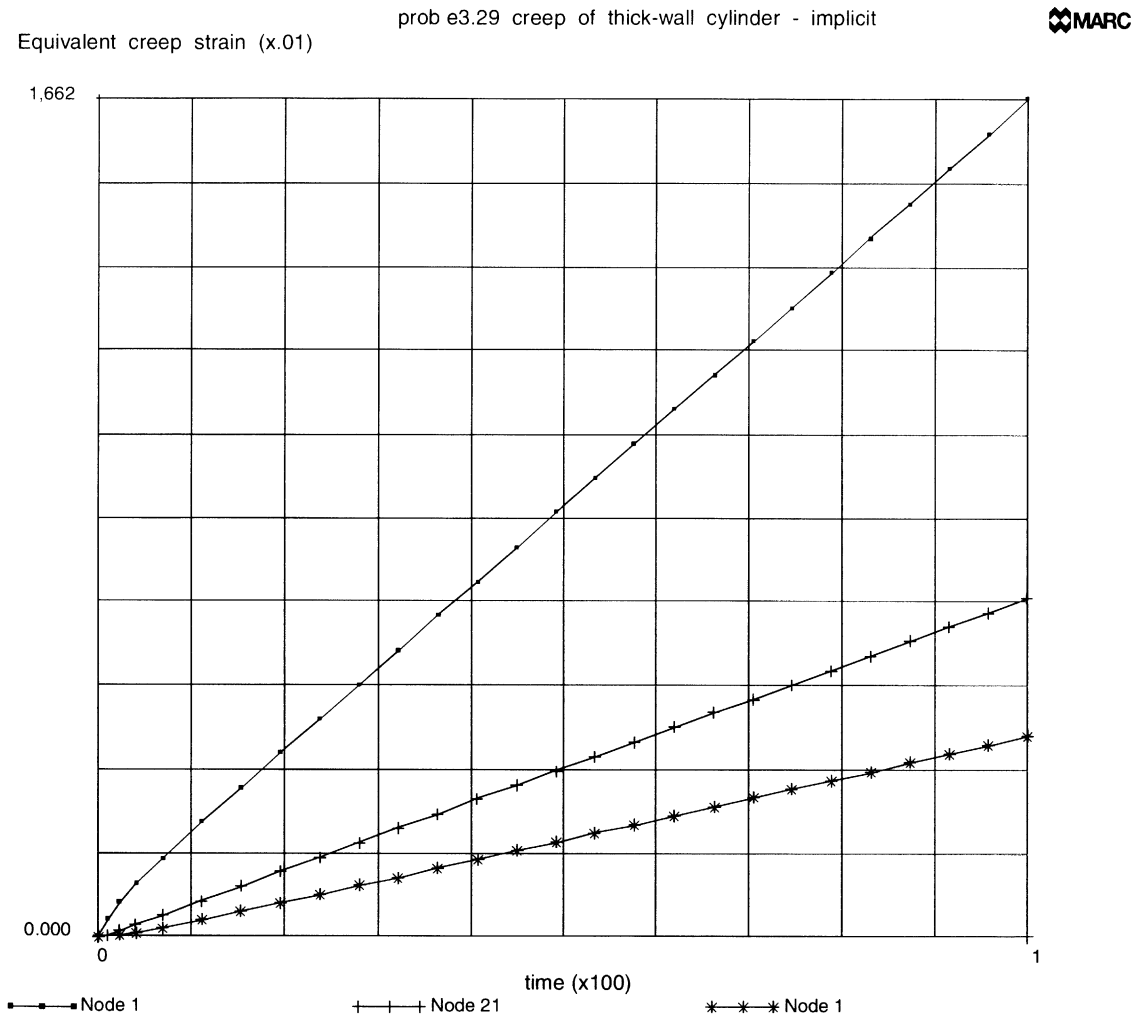

Figure 3.29-2 Time History of Equivalent Creep Strain – Implicit Procedure

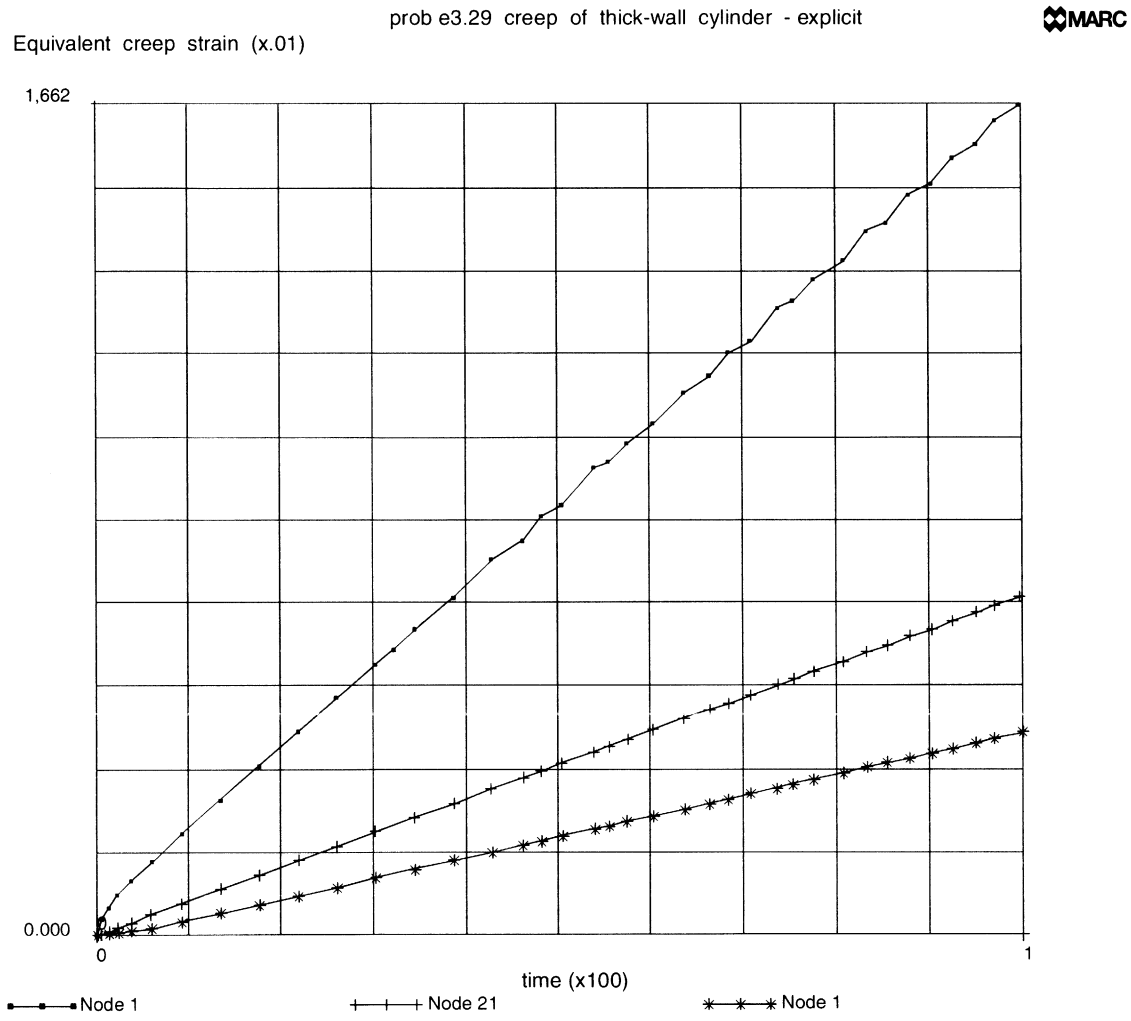

Figure 3.29-3 Time History of Equivalent Creep Strain – Explicit Procedure

3.30 3D Forming of a Circular Blank using Rigid-Plastic Formulation

This problem demonstrates the program's ability to perform stretchforming by a spherical punch using the CONTACT option and the rigid-plastic formulation. First, the problem will be analyzed using membrane elements, and then be analyzed with shell elements.

This problem is modeled using the two techniques summarized below.

Data Set	Element Type(s)	Number of Elements	Number of Nodes
e3x30a	18	112	127
e3x30b	75	112	127

Parameters

The R-P FLOW parameter is included to indicate that this is a rigid-plastic flow problem. The PRINT,8 option requests the output of incremental displacements in the local system. Element type 18 is a 4-node membrane element used in the first analysis. Element type 75 is a 4-node thick shell element used in the second analysis. Eleven layers are used through the thickness of the shell. The ISTRESS parameter is used to indicate that an initial stress is going to be imposed which stabilizes the membrane element solution. In the membrane analysis, the ALIAS option is used to change the element type.

Geometry

A shell thickness of 1 cm is specified through the GEOMETRY option in the first field (EGEOM1).

Boundary Conditions

The first boundary condition is used to model the binding in the stretch forming process. The second and third boundary conditions are used to represent the symmetry conditions.

Post

The following variables are written to a formatted post file:

7 } Equivalent plastic strain 17 } Equivalent von Mises stress

20 } Element thickness

Furthermore, the above three variables are also requested for all shell elements at layer number 4, which is the midsurface.

Control

A full Newton-Raphson iterative procedure is requested. Displacement control is used, with a relative error of 5%. Fifty load steps are prescribed, with a maximum of 30 recycles (iterations) per load step.

Material Properties

The material for all elements is treated as an rigid-plastic material an initial yield stress of 80.6 lbf/cm^2. The yield stress is given in the form of a power law and is defined through the WKSLP user subroutine.

Contact

This option declares that there are three bodies in contact with Coulomb friction between them. A coefficient of friction of 0.3 is associated with each rigid die. The first body represents the work piece. The second body is the lower die, defined as three surfaces of revolution. The first and third surfaces of revolution use a straight line as the generator, the second uses a circle as the generator. The third body (the punch) is defined as two surface of revolution. These surfaces are extended from -0.5 to 101.21 degrees.The rigid surfaces are shown in Figure 3.30-1. The relative slip velocity is specified as 0.01 cm/sec. The contact tolerance distance is 0.05 cm. When using the rigid-plastic option, nodal based friction should be used. This is because the solution of the stresses cannot be accurate.

Load Control

This problem is displacement controlled with a velocity of 1 cm/second applied in the negative Z direction with the AUTO LOAD option. The load increment is applied 40 times. The MOTION CHANGE option is illustrated to control the velocity of the rigid surfaces.

Results

Figure 3.30-2 shows the deformed body at the end of 40 increments with the deformation at the same scale as the coordinates. Due to the high level of friction, significant transverse deformation is shown along the contact surfaces.

Figure 3.30-3 shows the equivalent plastic strain contours on the deformed structure at increment 40, with the largest strain level at 60% using membrane elements.

Figure 3.30-4 shows the equivalent von Mises stress contours on the deformed structure at increment 40 with peak values at 527 lbf/cm^2 using membrane elements.

Figure 3.30-5 shows the equivalent plastic strain contours on the deformed structure at increment 40, with the largest strain level at 52% using shell elements.

Figure 3.30-6 shows the equivalent von Mises stress contours on the deformed structure at increment 40 with peak values at 512 lbf/cm^2 using shell elements.

You can observe very good correlation between the two element formulations. Comparing problem e3x30 with e8x18, there is also very good agreement. As long as springback is not required, the rigid-plastic formulation is viable for performing sheet forming simulations. The benefit of using the rigid-plastic formulation is that the computational times are less than those for a full elastic-plastic analysis.

Parameters, Options, and Subroutines Summary

Example e3x30a.dat:

Parameters	Model Definition Options	History Definition Options
ALIAS	CONNECTIVITY	AUTO LOAD
ELEMENTS	CONTACT	CONTINUE
END	CONTROL	MOTION CHANGE
ISTRESS	COORDINATES	TIME STEP
PRINT	END OPTION	
R-P FLOW	FIXED DISP	
SIZING	GEOMETRY	
TITLE	ISOTROPIC	
	OPTIMIZE	
	POST	
	PRINT CHOICE	
	WORK HARD	

User subroutines in example u3x30a.f:

WKSLP
UINSTR

Example e3x30b.dat:

Parameters	Model Definition Options	History Definition Options
ELEMENTS	CONNECTIVITY	AUTO LOAD
END	CONTACT	CONTINUE
PRINT	CONTROL	MOTION CHANGE
R-P FLOW	COORDINATES	TIME STEP
SIZING	END OPTION	
TITLE	FIXED DISP	
	GEOMETRY	
	ISOTROPIC	
	OPTIMIZE	
	POST	
	PRINT CHOICE	
	WORK HARD	

User subroutine in example u3x30b.f:

WKSLP

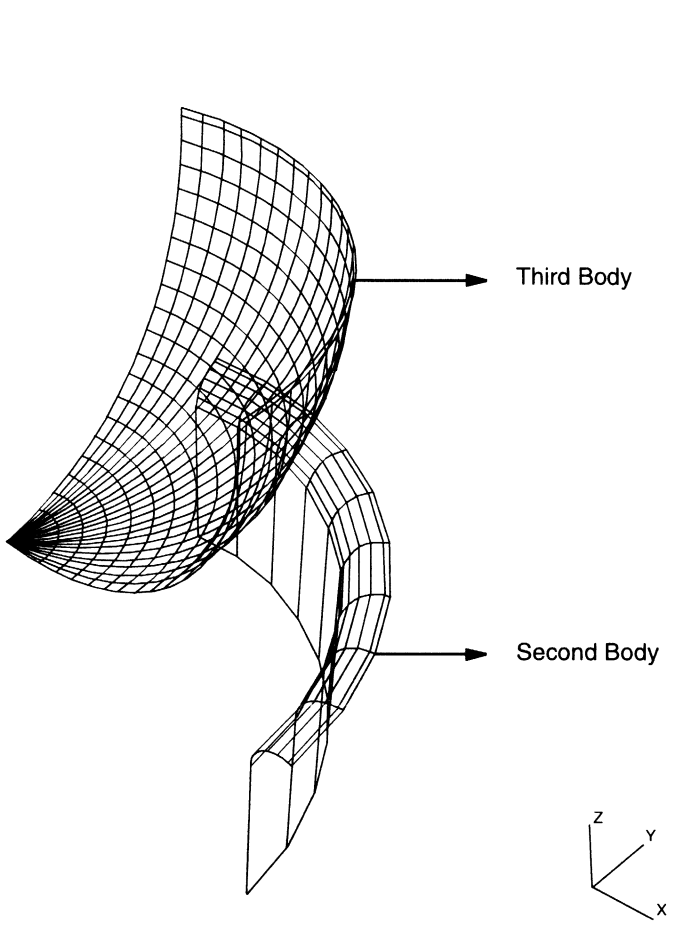

Figure 3.30-1 Circular Blank Holder and Punch

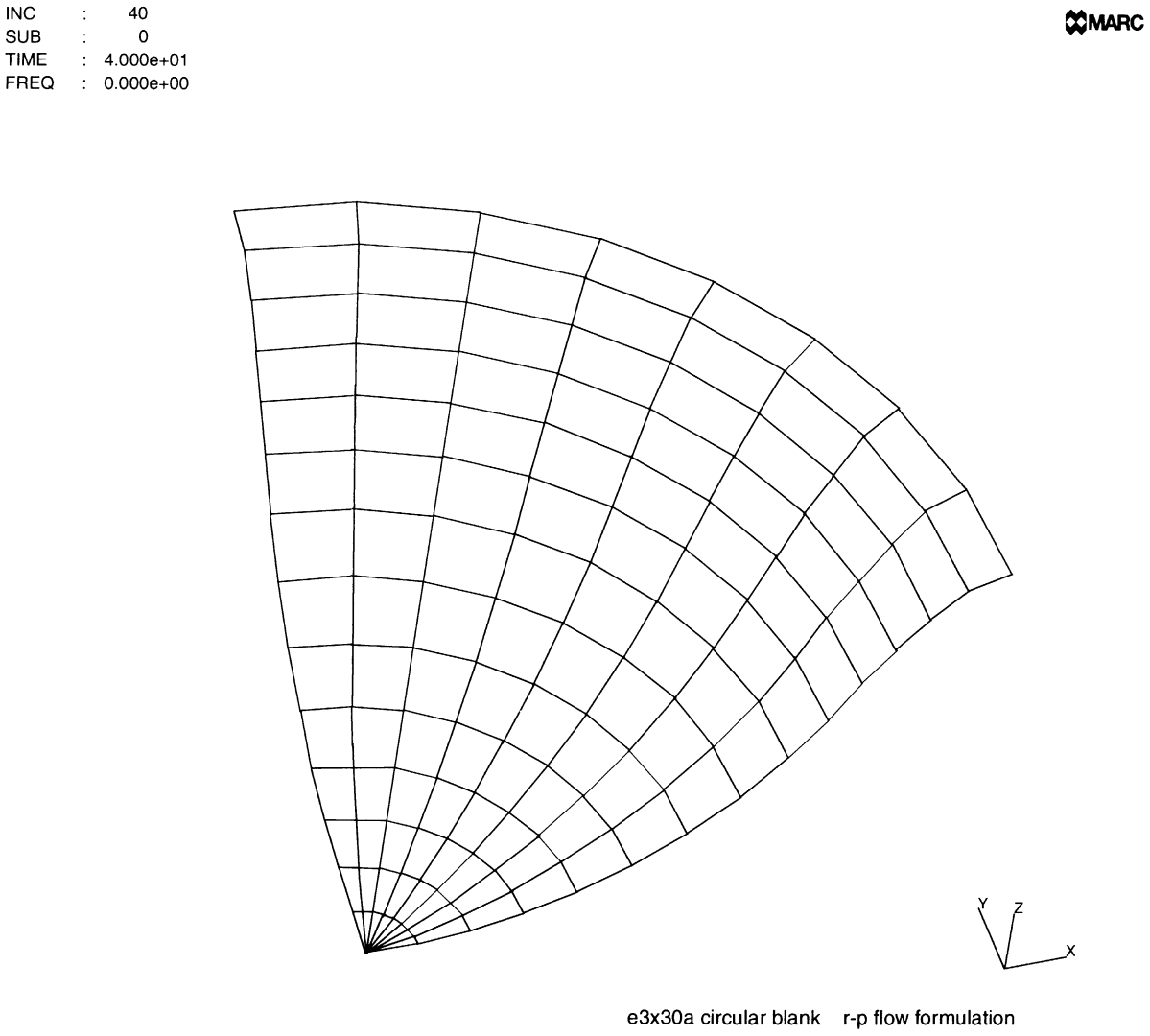

Figure 3.30-2 Deformed Sheet at Increment 40

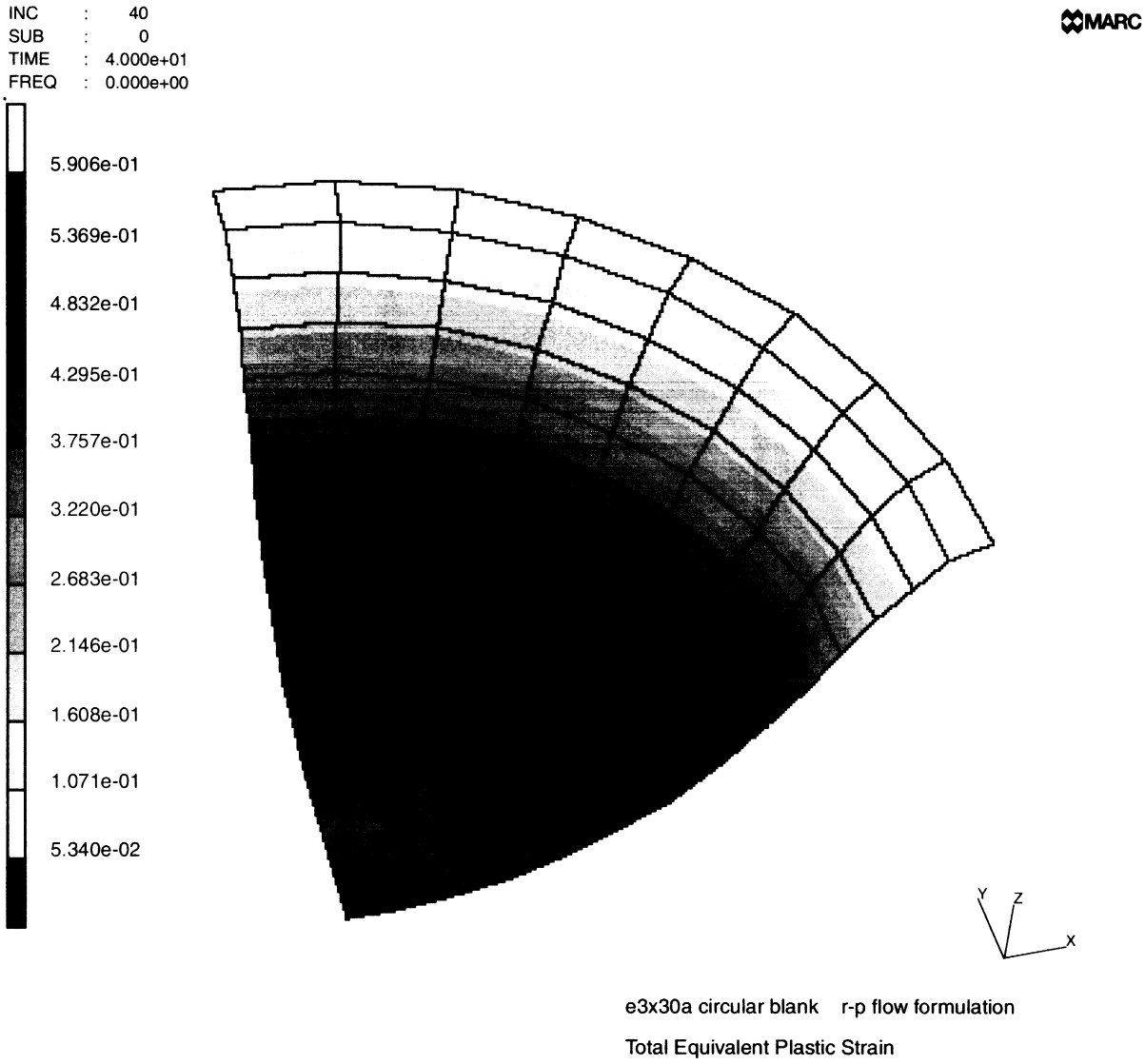

Figure 3.30-3 Equivalent Plastic Strains in Membrane

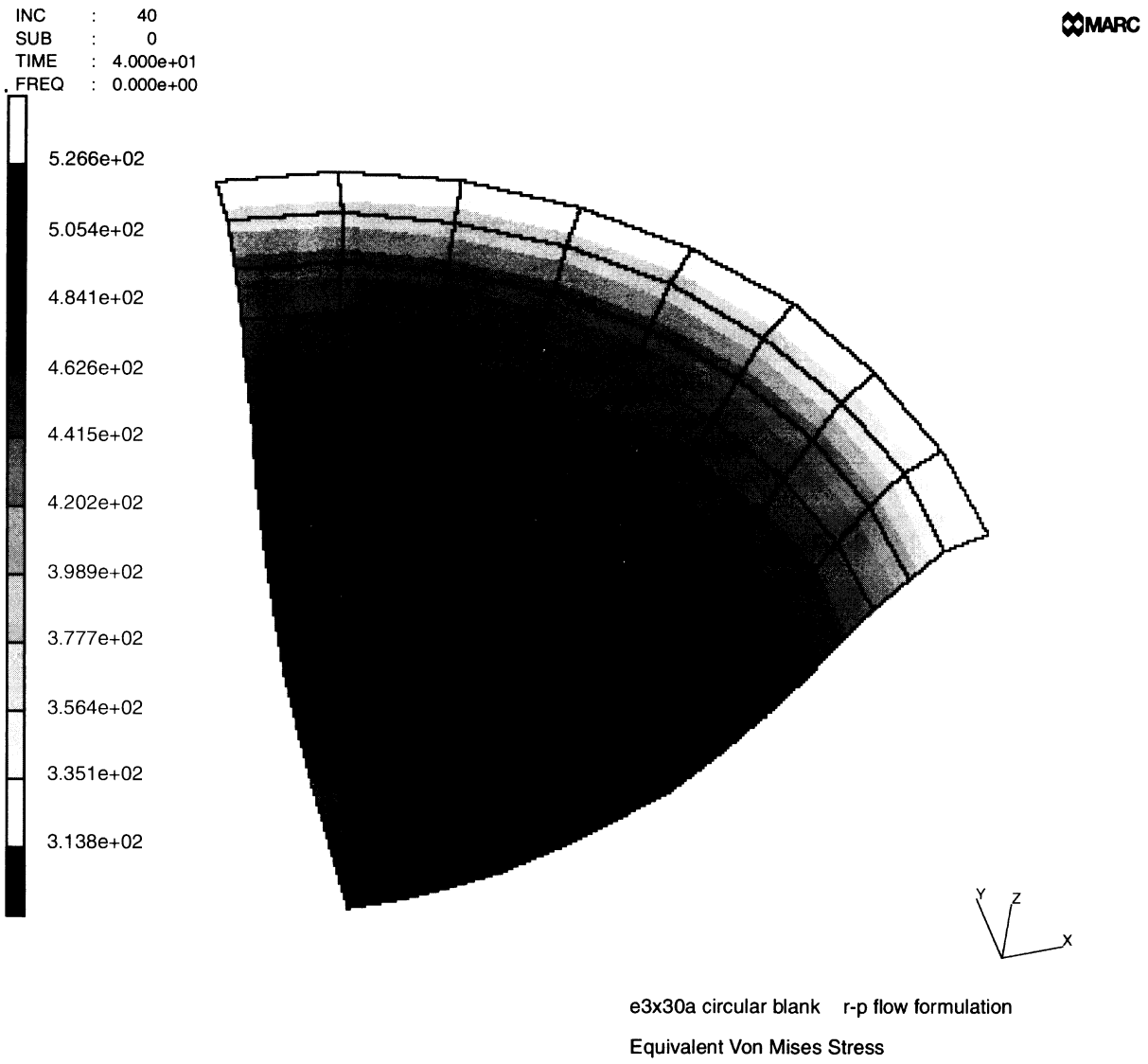

Figure 3.30-4 Equivalent Stresses in Membrane

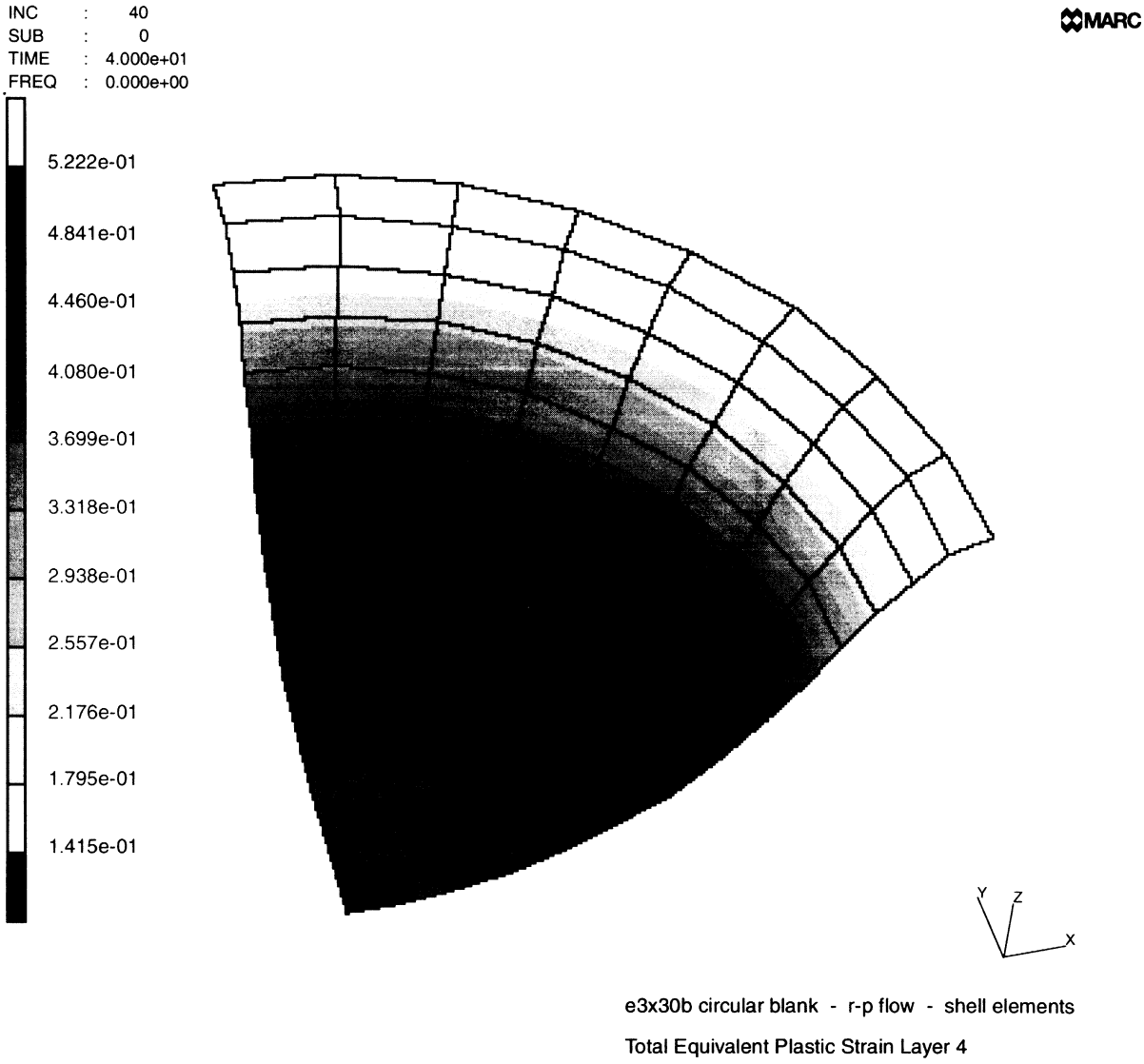

Figure 3.30-5 Equivalent Plastic Strains at Midlayer of Shell

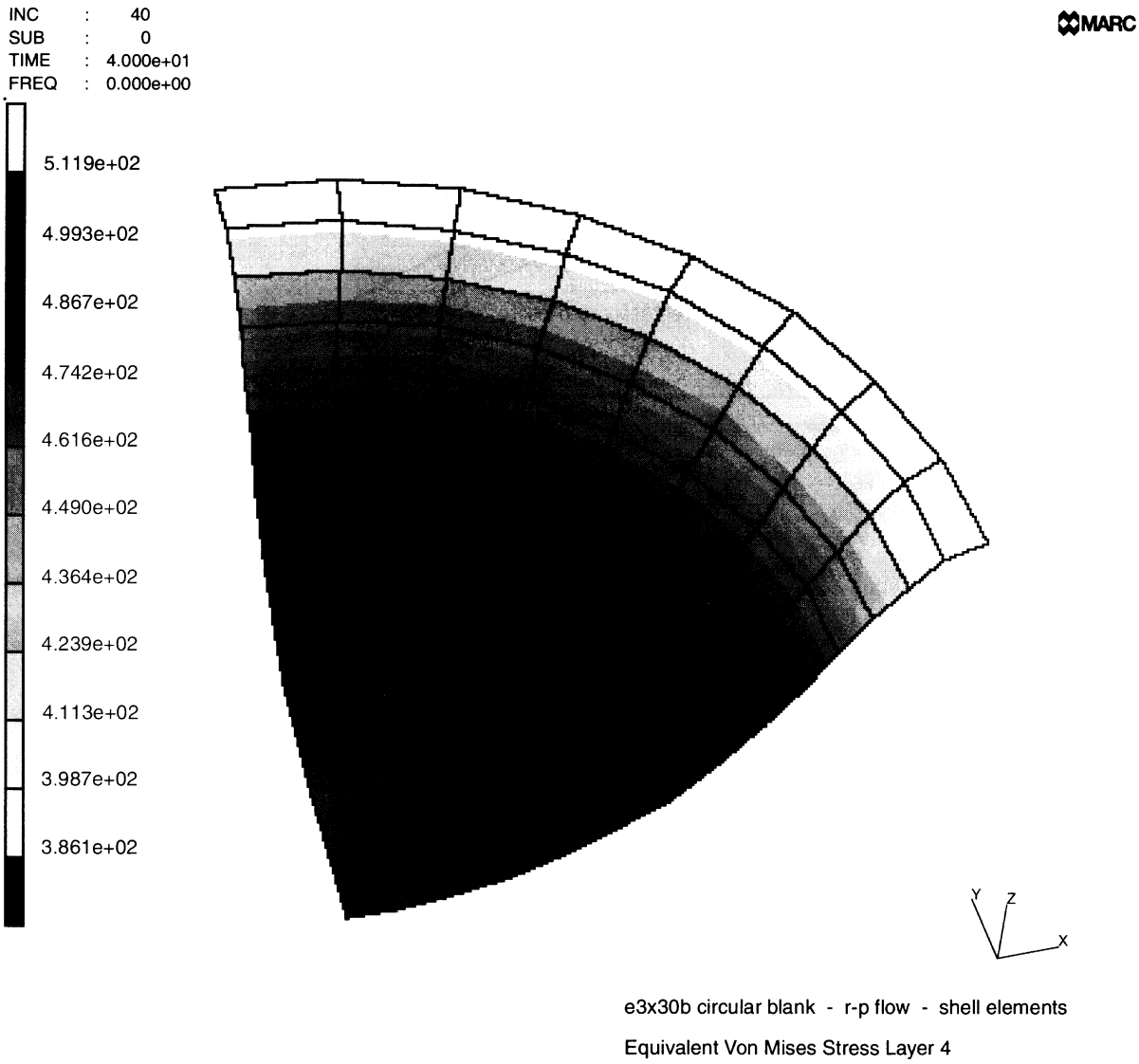

Figure 3.30-6 Equivalent Stresses at Midlayer of Shell

3.31 Formation of Geological Series

This problem demonstrates the capability of MARC to analyze the sliding of geological strata along fault planes until reaching a partial overlap.

In this case, there are two strata separated by an inclined fault. The upper stratum is pushed in the horizontal direction to move against the fault. It will slide along the fault overlapping the lower stratum. The stratum is 6 Km deep and 100 Km long. The computational model is plane strain. The cross section of the strata is represented. Units [N, m].

Element

Library element type 11 is a plane-strain 4-node isoparametric quadrilateral element.

Model

The geometry of the strata and their mesh is shown in Figure 3.31-1. The model consists of 696 plane-strain, type 11, element for a total of 856 nodes. Figure 3.31-3 shows the details of the mesh at the fault plane.

Geometry

This option is not required for a plane-strain element as a unit thickness is assumed.

Boundary Conditions

Symmetry conditions are applied at the edges 1, 2, and 3 (see Figure 3.31-1). Automated contact is applied at the interface of the fault. No friction is assumed between the two deformable strata.

Material Properties

The material of the strata is assumed to be isotropic (no variation along the thickness) with the properties:

Young modulus	$E = 34.15\ E8\ N/m^2$
Poisson ratio	$\nu = 0.23$
Mass density	$\rho = 2200\ kg/m^3$

The linear Mohr-Coulomb criterion is assumed for the ideal yield surface with values of the two constants (refer to *MARC Volume A: User Information*):

$\sigma = 22.25\ E6\ N/m^2$
$\alpha = .15\ N/m^2$

Loading

The strata are loaded with the gravity load in ten increments. In the subsequent 25 increments, an incremental displacement of 250 m in the horizontal direction is assigned to the upper part of edge 3 (see Figure 3.31-1).

Results

The results produced by MARC are shown in the following figures:

Figure 3.31-3 The deformed shape of the strata after a slide of the upper stratum of 6250 m. Notice the growth of a hill of 1019 m in the neighboring of the fault.

Figure 3.31-4 The distribution across the strata of the σ_{xx} stress components (referred to the global axes) at the final step.

Figure 3.31-5 The distribution across the strata of the σ_{yy} stress components (referred to the global axes) at the final step.

Parameters, Options, and Subroutines Summary

Example e3x31.dat:

Parameters	Model Definition Options	History Definition Options
ELEMENTS	CONNECTIVITY	AUTO LOAD
END	CONTACT	CONTINUE
FINITE	CONTACT TABLE	DISP CHANGE
LARGE DISP	CONTROL	DIST LOADS
PRINT	COORDINATES	NO PRINT
SETNAME	DEFINE	POST INCREMENT
SIZING	DIST LOADS	TIME STEP
TITLE	END OPTION	
UPDATE	FIXED DISP	
	ISOTROPIC	
	NO PRINT	
	POST	
	RESTART LAST	

MARC

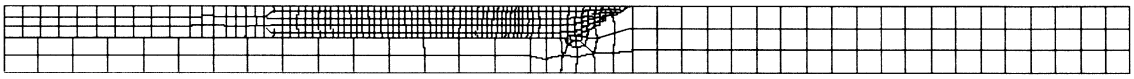

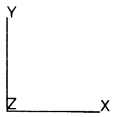

Figure 3.31-1 FEM Model of the Geological Strata

MARC

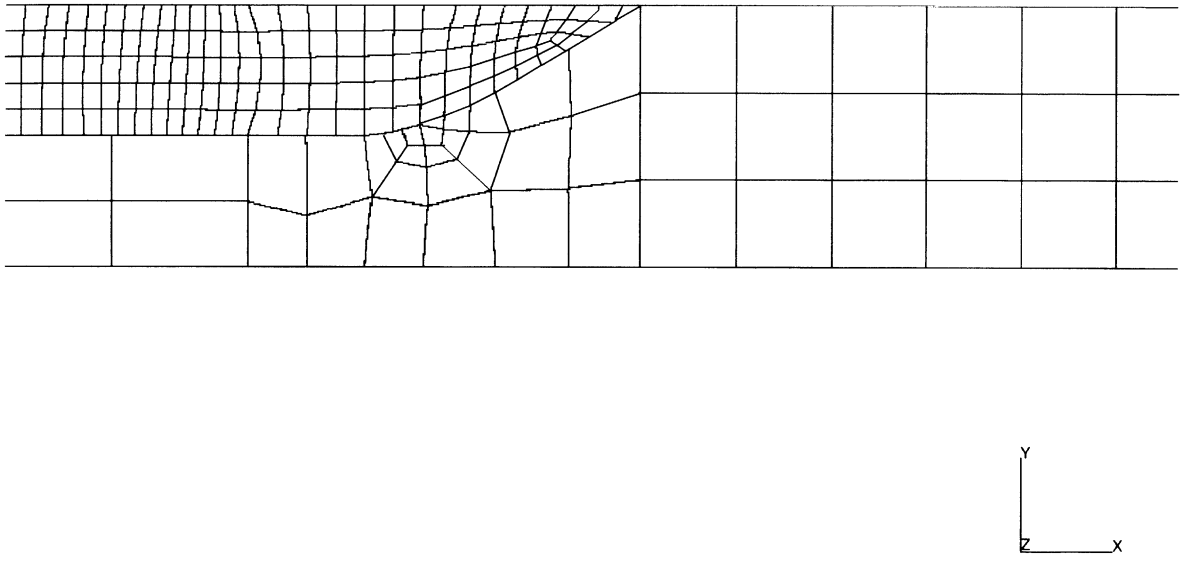

Figure 3.31-2 Detailed Mesh at the Fault Plane

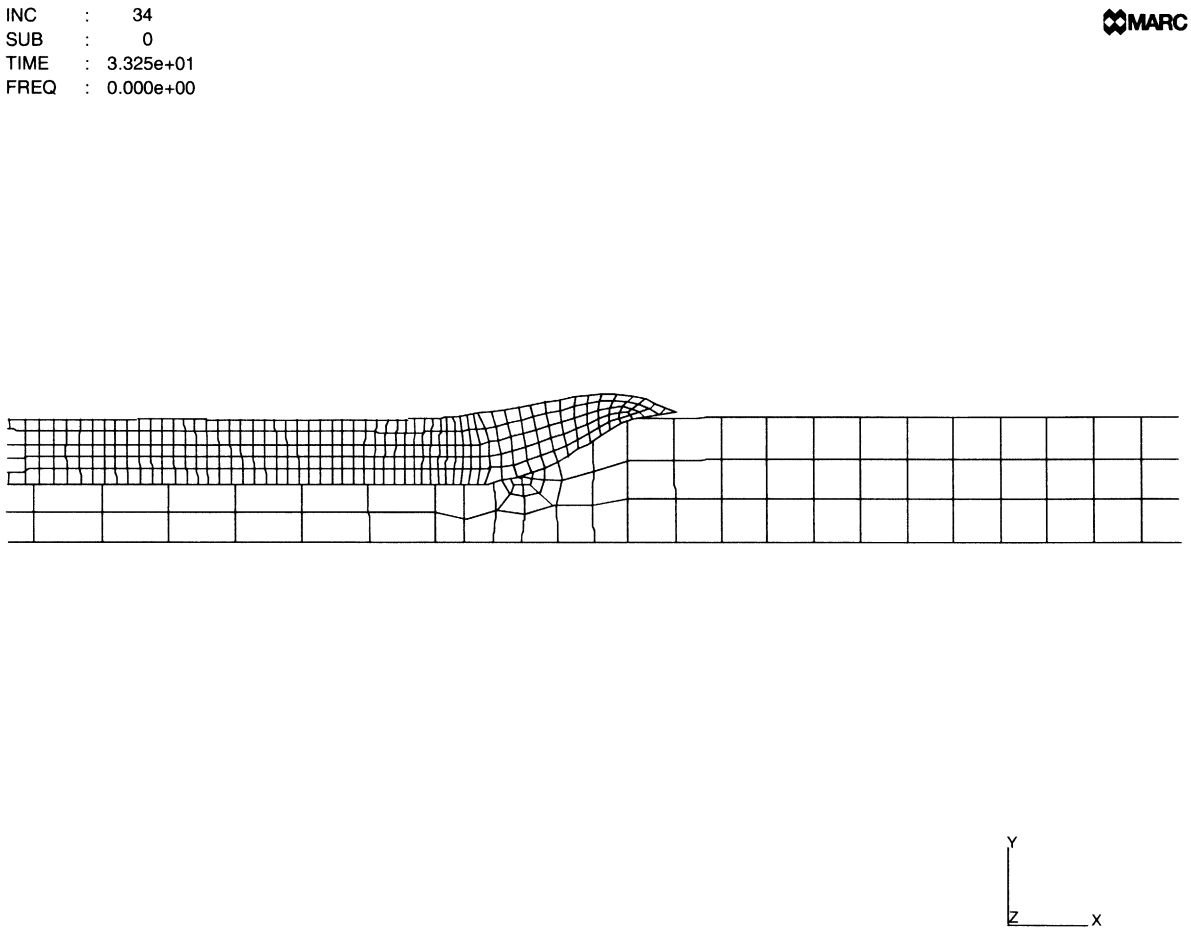

Figure 3.31-3 Overlap of the Geological Strata

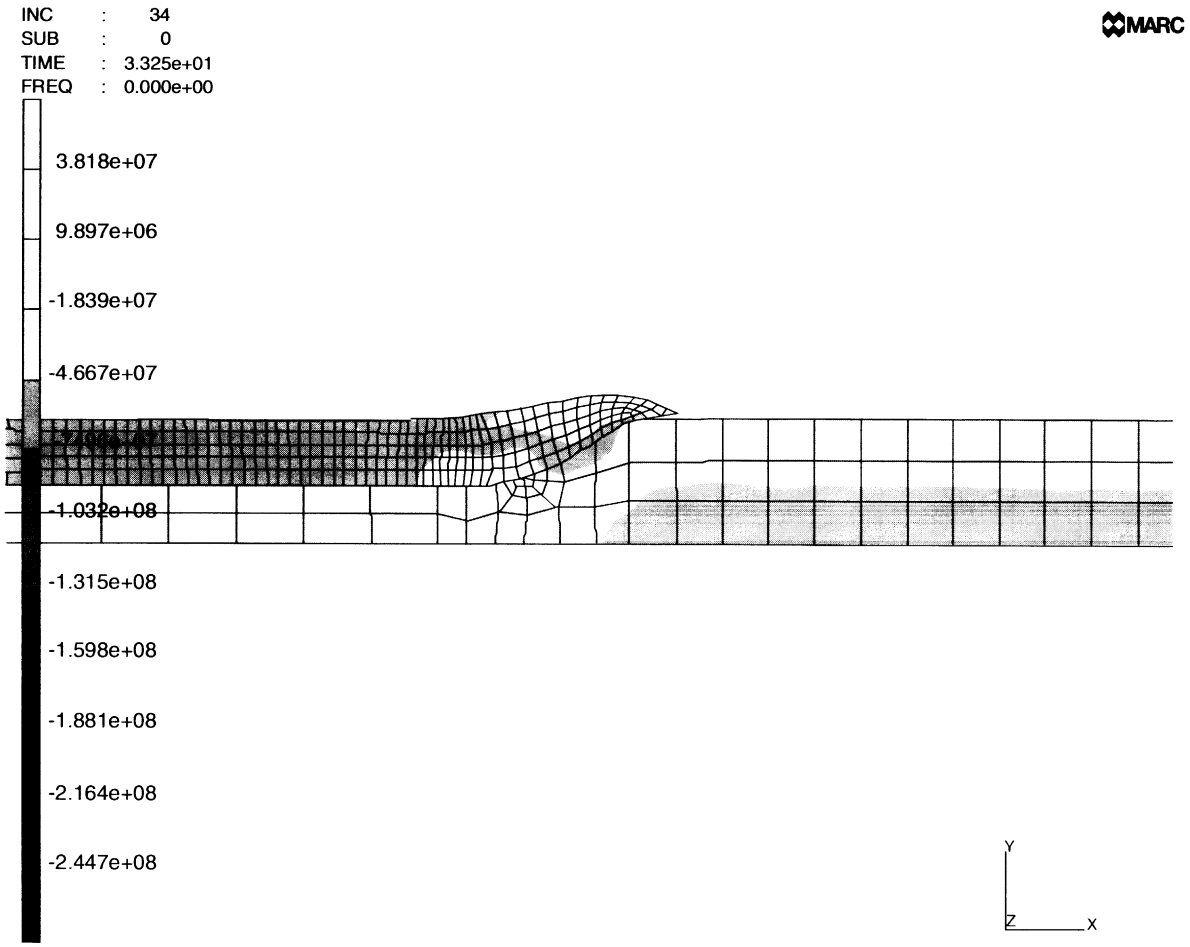

Figure 3.31-4 Distribution of the σ_{xx} Stress Component (Global Axes)

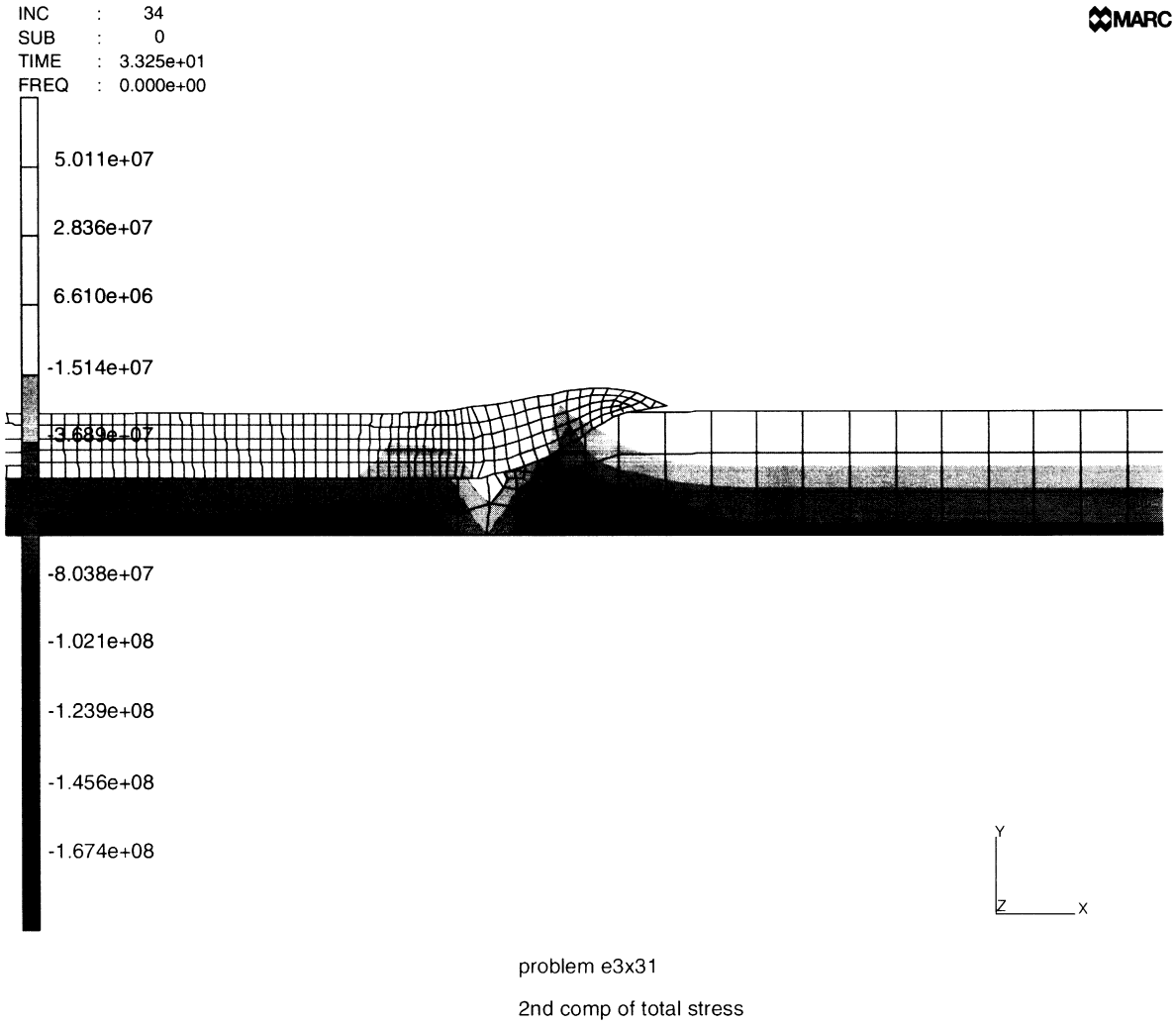

Figure 3.31-5 Distribution of the σ_{yy} Stress Component (Global Axes)

3.32 Superplastic Forming of a Strip

This problem demonstrates how to form a shape with a superplastic material. A two-dimensional flat workpiece is pressurized into a die of the desired final shape. Three different models are constructed using two-dimensional plane strain elements, three-dimensional membrane elements, and three-dimensional shell elements.

This problem is modeled using the three techniques summarized below.

Data Set	Element Type(s)	Number of Elements	Number of Nodes	Differentiating Features
e3x32a	11	340	430	F^eF^p
e3x32b	18	80	162	F^eF^p
e3x32c	75	80	162	Contact

Mesh Generation

These three models consist of 340 4-node isoparametric quadrilateral plane strain elements, 80 membrane elements, and 80 shell elements. The workpiece is 2.3 inches long with an in-plane thickness of 0.078 inches.

Boundary Conditions

The sheet is fixed at both ends in the x-direction and the left end is fixed in the y-direction where the workpiece contacts the die. The membrane and shell models have similar boundary conditions and their out-of-plane displacements are fixed to simulate plane strain. Furthermore, the membrane model will have an initial in-plane tensile stress of 50 psi for the first five increments to avoid any instabilities. This initial state of stress is supplied via user subroutine UINSTR. The workpiece is subjected to a uniform pressure whose magnitude is determined automatically in the user subroutine FORCEM to maintain a target strain rate of 0.0002. The model with these boundary condition is shown in Figure 3.32-1 and Figure 3.32-2 for the plane strain and membrane (shell) models, respectively.

Material Properties

The out-of-plane thickness is 1.0 inch for all models. The constant dilatation from of the plane strain elements is used. Superplastic materials can be viewed as exhibiting time-dependent inelastic behavior with the yield stress a function of time, temperature, strain rate, total stress, and total strain. In this case, the yield stress is only a function of the strain rate and id determined in user subroutine URPFLO. the equation used is $\sigma = \dot{\varepsilon}^b$ where $\dot{\varepsilon}$ = strain rate, σ = yield stress, a = 50,000 psi, b = 0.6

Contact

Each model has one rigid body and one deformable body. In increment 0, the rigid body is moved into first contact with the workpiece and held fixed thereafter.

Loading

The load schedule consists of a single rigid plastic loadcase with a total time period of 2500 seconds and 500 steps with convergence testing on displacements.

Rigid Plastic Analysis Class

Analysis options include the follow force options. The analysis dimension is either plane strain or three-dimensional. The results contain several variables including the pressure supplied through user subroutine PLOTV. In contact control, Coulomb friction with $\mu = 0.5$, a separation force of 1.0e6 lbf, and a sliding velocity of 1.0e-5 inches/seconds are used. For the membrane and shell models, the bias factor is set to .99 to reduce the touching distance because of the large thickness. Because nodal based friction forces must be used with membrane and shell elements, it is used for all models.

Results

Although the total time period is 2500 seconds, the part forms in a little over 2000 seconds (34 minutes). As expected, the bending of the workpiece is insignificant and the results of all models are in close agreement. The membrane elements are superior in conforming to the die shape and are substantially faster (2.5 times faster) than the plane strain or shell models.

Figure 3.32-3 shows the final deformed shape of the plane strain model. The final average thickness is 0.0554 and the sheet has elongated to 3.231 inches, showing virtually no change in volume. The final average thickness can be estimated prior to the finite element analysis since the original and final sheet length are known and the sheet is incompressible.

Figure 3.32-4 shows the pressure schedule for all models with very small differences. These small differences in the pressure schedule are caused when the sheet begins to fill the concave corner. As the sheet begins to fill the concave corner, the pressure must increase rapidly to maintain the target strain rate of 2.03-4/seconds. Note that the sliding velocity is 1/20 of the target strain rate which is a typical value (this is true for length units of inches and would need to be modified for other length units). The maximum pressure is physically limited and has a maximum value of 300 psi set in subroutine FORCEM. Furthermore, Figure 3.32-4 also plots the vertical reaction on the die divided by the sheet area versus time. This die pressure leads the sheet pressure because of friction acting on the vertical portion of the die. Here more

differences exist between the three models. The biggest difference is around 1800 seconds where the friction stops contributing to the die force because of the inability of the plane strain model to completely fill the concave corner.

Figure 3.32-5 shows the thickness profile over the deformed position along the sheet. The largest thinning in all models occurs at the 1.0 inch position or the concave corner. The significant area of difference occurs at the convex radius at the 1.9 inch position. This difference is because of transverse normal stresses caused by bearing on the radius, the plane strain elements thin more since the membrane and shell elements cannot support this deformation state. The membrane elements only thin because they are stretched and must maintain volume. The shell elements thin because they stretch and bend while maintaining volume. The plane strain elements thin because of stretching, bending, and transverse deformations while maintaining volume.

Since friction plays a large roll in the thinning of the sheet and the membrane model runs fastest, a frictionless case is run for the membrane elements. The thickness profiles of the friction and frictionless cases are shown in Figure 3.32-6. Without friction, the thinning is very uniform and the final thickness is almost the average thickness everywhere.

Summary of Parameters, Options, and Subroutines Used

Example e3x32a.dat, e3x32b, e3x32c:

Parameters	Model Definition Options	History Definition Options
ELEMENTS	CONNECTIVITY	AUTO LOAD
END	CONTROL	CONTINUE
FOLLOW FOR	COORDINATES	DIST LOADS
PRINT	DIST LOADS	MOTION CHANGE
R-P FLOW	FIXED DISP	TIME STEP
SIZING	GEOMETRY	
TITLE	ISOTROPIC	
	NO PRINT	
	OPTIMIZE	
	POST	
	SOLVER	

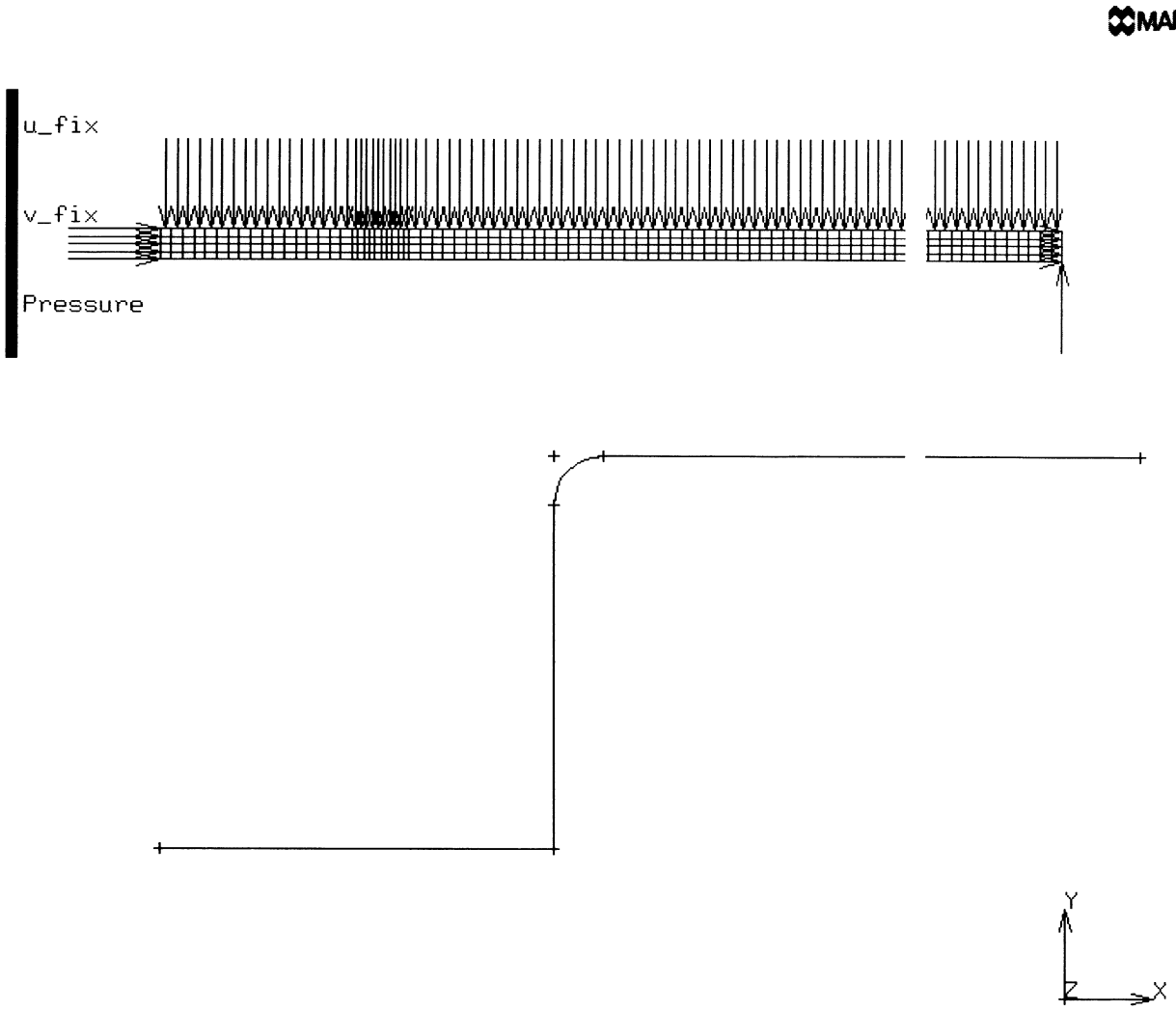

Figure 3.32-1 Plane Strain SPF Model with Boundary Conditions

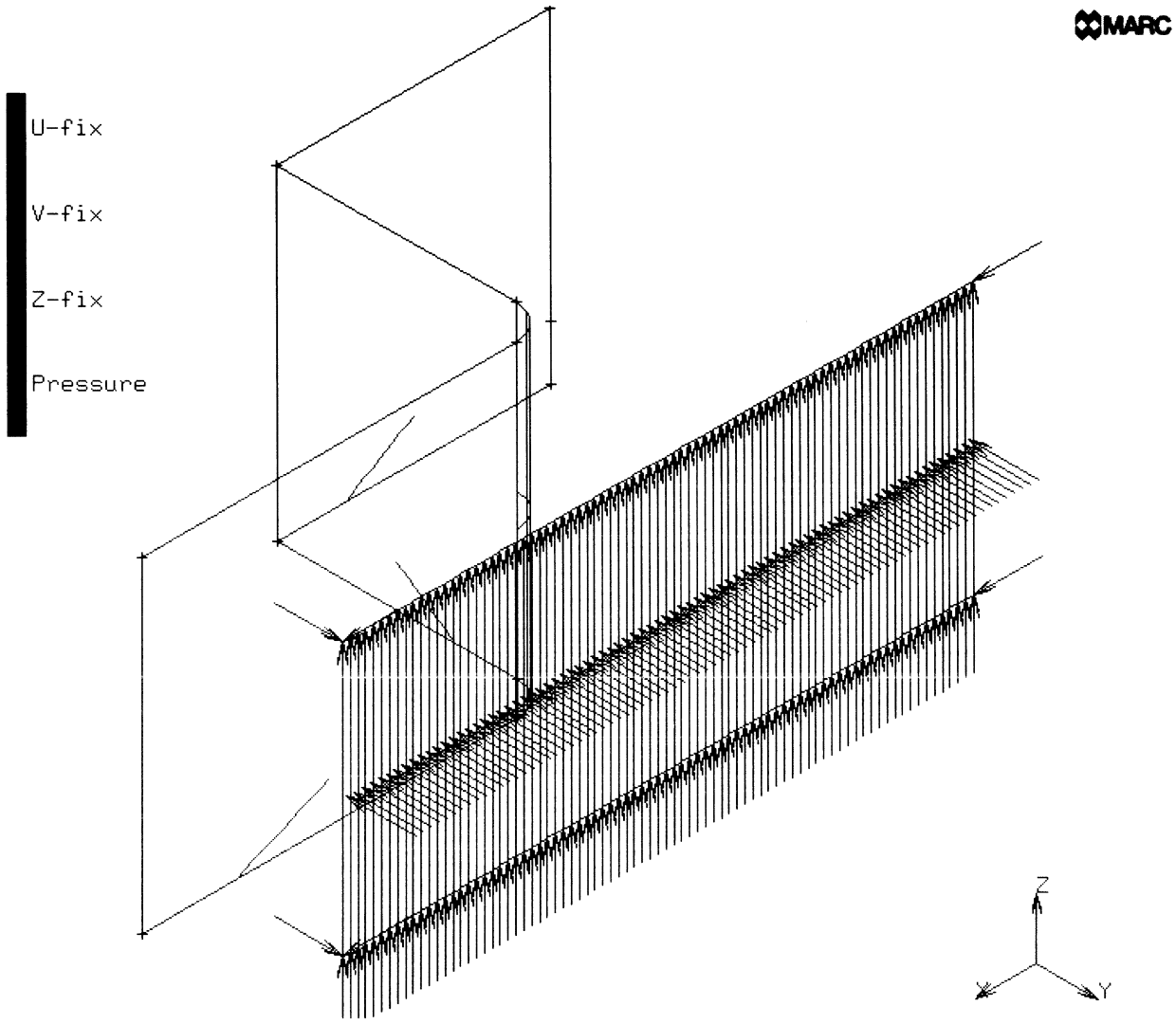

Figure 3.32-2 Membrane and Shell SPF Model with Boundary Conditions

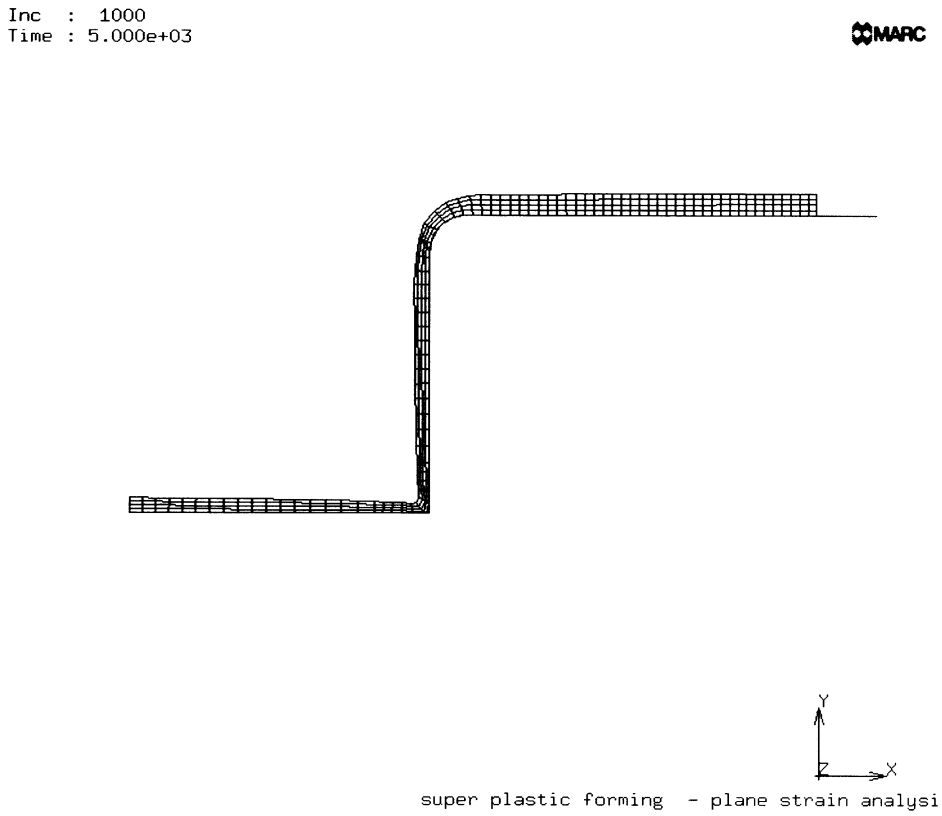

Figure 3.32-3 Plane Strain SPF Model Final Shape

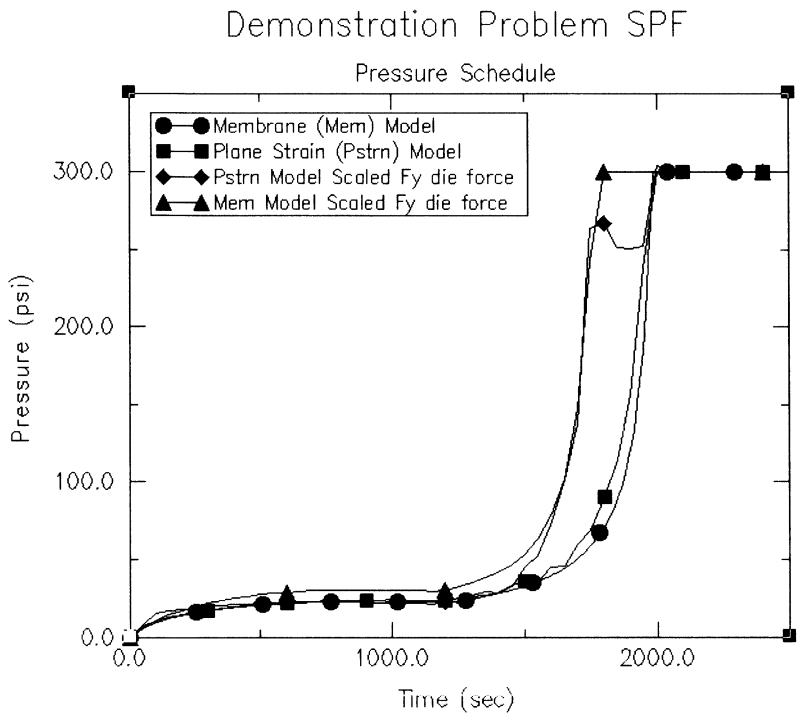

Figure 3.32-4 Pressure Schedule for all Models

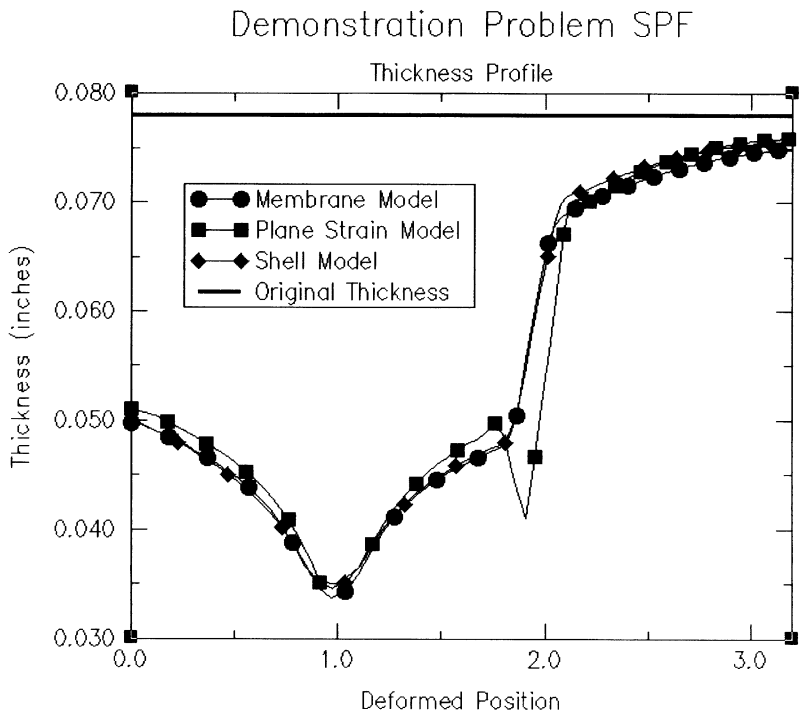

Figure 3.32-5 Thickness Profile for all Models

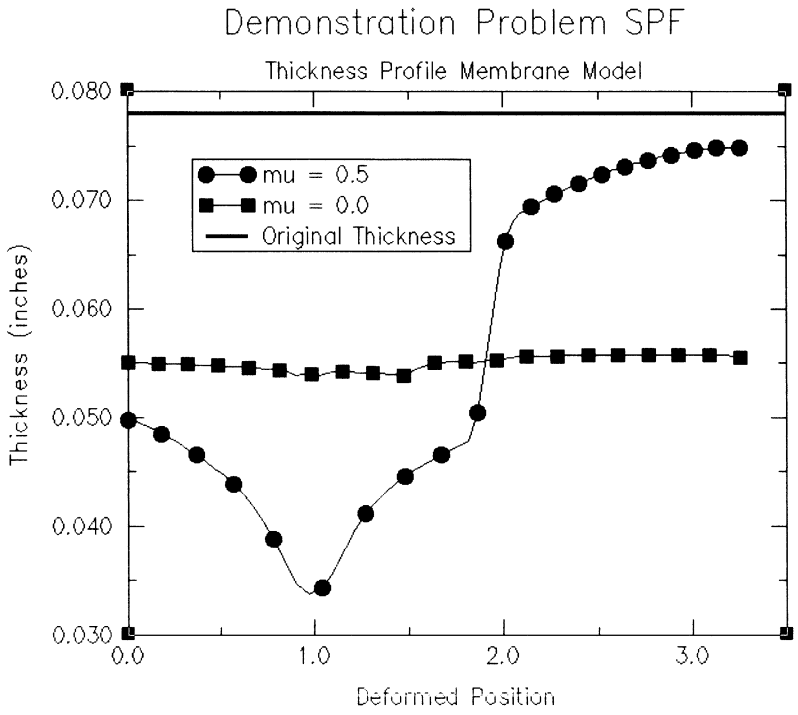

Figure 3.32-6 Thickness Profile Membrane Friction Effects

3.33 Large Strain Tensile Loading of a Plate with a Hole

This problem simulates the tensile loading of a plate with a hole to large strains. The example demonstrates the accuracy of the finite strain plasticity algorithm using F^eF^p formulation to simulate large strains. The multiplicative decomposition procedure is invoked using the PLASTICITY option.

This problem is modeled using two techniques summarized below.

Data Set	Element Type(s)	Number of Elements	Number of Nodes	Differentiating Features
e3x33	26	20	79	Plane Stress
e3x33b	27	20	79	Plane Strain

Element

This problem simulates two-dimensional plane stress and plane strain cases. For the plane stress case, an 8-node plane stress isoparametric element type 26 is used to construct a mesh while for the plane strain case, an 8-node plane stress isoparametric element type 27 is used. There are two degrees of freedom per node with a bi-quadratic interpolation and eight-point Gaussian quadrature for stiffness assembly.

Model

Due to symmetry of the geometry and loading, a quarter of the actual model is simulated. The finite element model is made up of 20 elements and 79 nodes. There is a total of 158 degrees of freedom. The model is shown in Figure 3.33-1.

Geometry

The model is assumed to be a square of side five units from which a quarter of a circle of radius one unit has been cut out. In the plane stress case, the initial thickness is one unit.

Material Properties

The material is assumed to be isotropic elastic plastic. The Young's modulus is 3.0E+07 psi. Poisson's ratio is 0.30. The initial yield stress is 5.0E+04 psi. The hardening behavior is given is Table 3.33-1.

Table 3.33-1 Hardening Behavior

Equivalent Plastic Strain	Workhardening Slope (psi)
0.00	14.30E+06
7.00E-04	3.00E+06
1.60E-03	1.90E+06
2.55E-03	6.70E+05
3.30E-03	3.00E+05
1.00	1.00E+05

Boundary Conditions

The loading is tensile. The lower edge of the model is restrained to have no y displacements, while the left edge the model is constrained to have no x displacements. The top edge is subjected to displacement increments in the y direction.

Results

The contours of effective plastic strain on the deformed model are shown in Figure 3.33-2. Plasticity initiates at the hole due to the stress concentration and accumulates with increasing strain. The maximum value is 186% at the end of the last increment. The history plot of x displacement at node 34 as a function of the increment is shown in Figure 3.33-3. Node 34 is the node on the hole edge and has specified zero y displacement. Figure 3.33-3 shows that the increments of x displacement at node 34 are initially negative, indicating that the hole is shrinking in dimension perpendicular to the loading direction. However, as plasticity accumulates, the x displacement increments become positive, indicating a growth in the hole dimension perpendicular to the loading direction. As the hole surface grows outward, the external surface continues to move inward. This reduces the ligament size available to carry load and necking results. This behavior is also seen for the plane strain case although with different numerical values.

Parameters, Options, and Subroutines Summary

Examples e3x33a.dat and e3x33b.dat :

Parameters	Model Definition Options	History Definition Options
TITLE	CONNECTIVITY	AUTO STEP
SIZING	COORDINATES	DISP CHANGE
ELEMENTS	ISOTROPIC	CONTINUE
LARGE DISP	GEOMETRY	
PLASTICITY	WORK HARD	
	FIXED DISP	

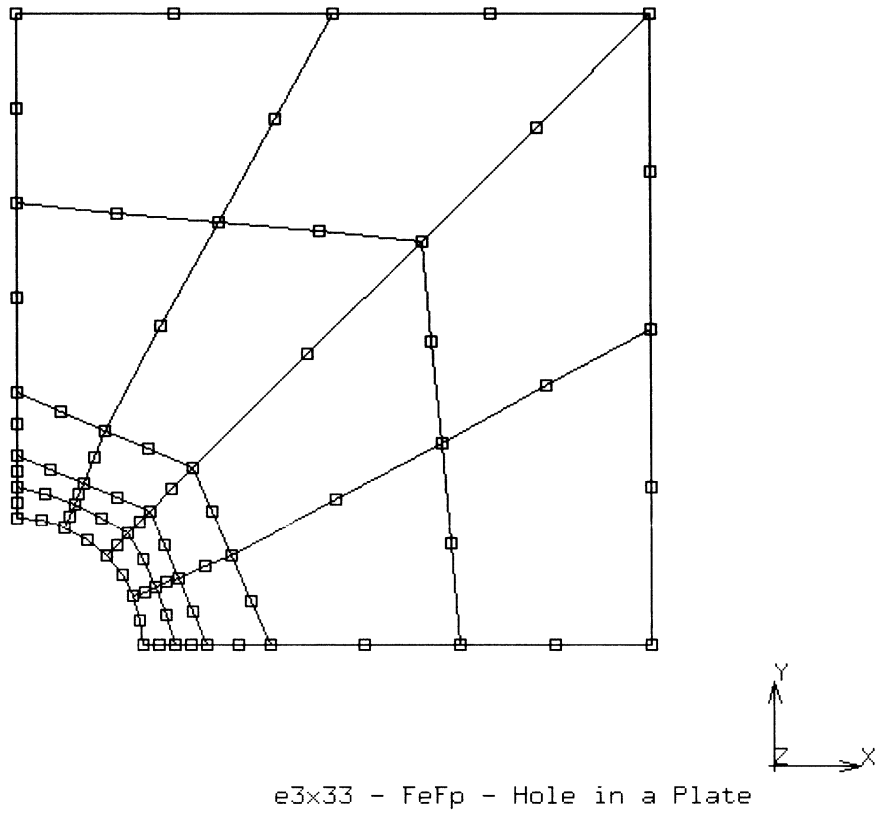

Figure 3.33-1 Initial Model for Hole-in-Plate

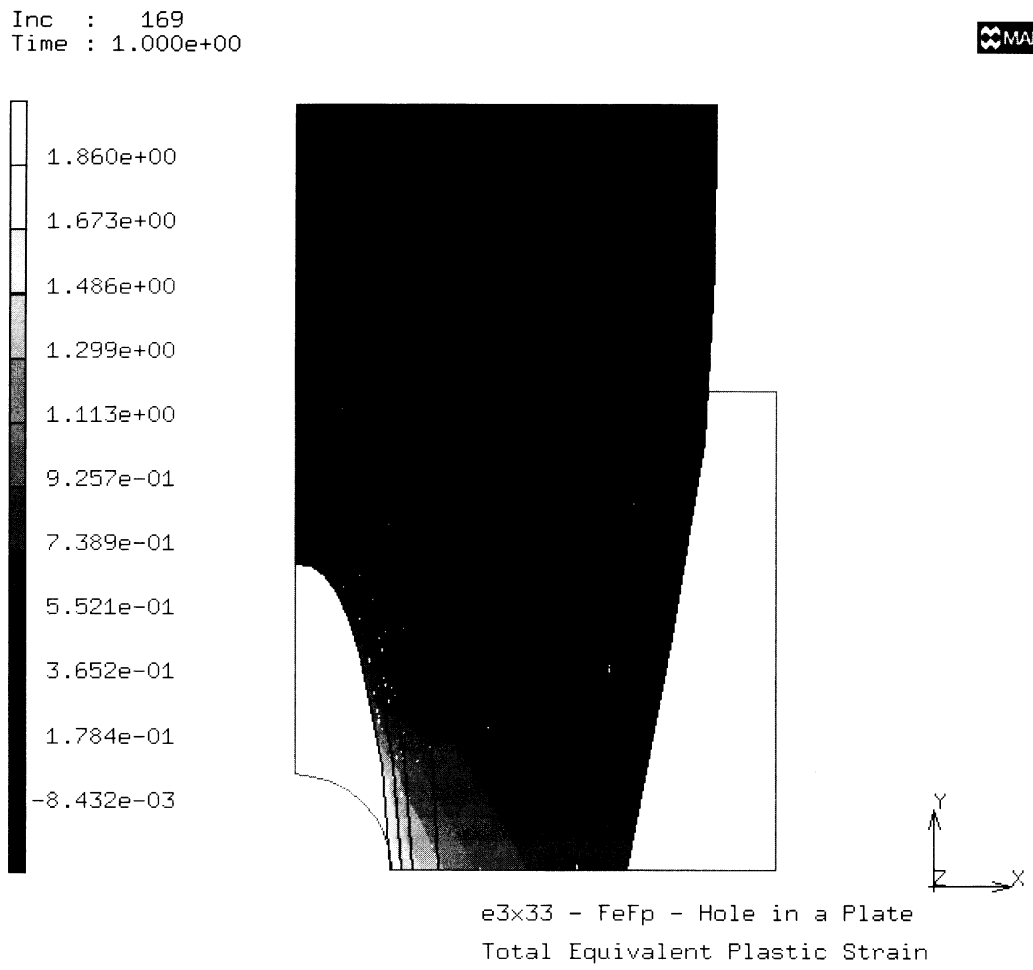

Figure 3.33-2 Equivalent Plastic Strain on the Deformed Model

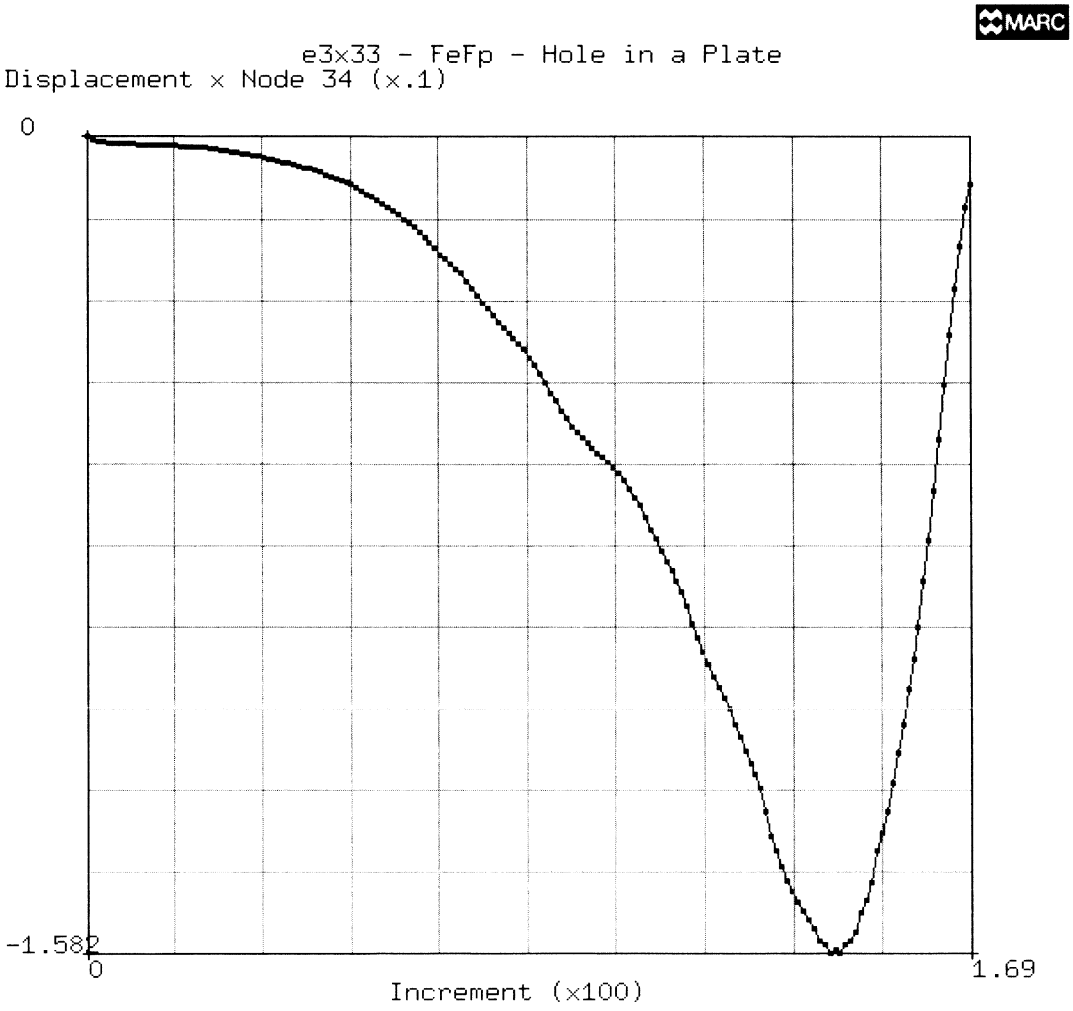

Figure 3.33-3 History Plot of x Displacement versus Increment for Node 34

3.34 Inflation of a Thin Cylinder

This problem simulates the elasto-plastic inflation of a thin cylinder.

Element

The 4-node membrane element type 18 is used. There are three degrees of freedom per node with bilinear interpolation and four-point Gaussian quadrature.

Model

Due to symmetry of the geometry and loading, a quarter of the cylinder is simulated. The finite element model is made up of 100 elements and 126 nodes. There is a total of 378 degrees of freedom. The initial mesh is shown in Figure 3.34-1.

Geometry

The cylinder is of unit radius and a length of 5 units.

Material Properties

The material is assumed to be isotropic elastic plastic. The Young's modulus is 3.0E+07 psi. Poisson's ratio is 0.30. The initial yield stress is 2.5E+04 psi. The slope of the plastic stress strain curve is assumed to be 3.E+05. The multiplicative decomposition radial return procedure is used for this large strain plasticity problem. This is invoked by the PLASTICITY parameter.

Boundary Conditions

The model is restrained to have no Y-displacements on nodes 1, 3, 5, 6, 7, and 8. X-displacements are zero on nodes 2, 4, 123, 124, 125, and 126. The Z-displacements are held to zero on nodes 1, 2, 9, 15, 21, 27, 33, 39, 45, 51, 57, 63, 69, 75, 81, 87, 93, 99, 105, 111, and 117. A distributed load of 200 psi is imposed on all elements to simulate the pressurization of the cylinder. This distributed load is applied consecutively for five increments.

Results

The final deformed mesh is shown in Figure 3.34-2. Due to the nature of the geometry and boundary conditions, the problem is homogeneous. The first increment is purely elastic and plasticity evolves from the second increment. The effective plastic strain is shown as a function of the increments in Table 3.34-1.

Table 3.34-1 Effective Plastic Strain

Increment Number	Total Effective Plastic Strain (%)
1	0.00000
2	5.79726
3	14.89630
4	26.47110
5	43.13700

Parameters, Options, and Subroutines Summary

Example e3x34.dat:

Parameters	Model Definition Options	History Definition Options
APPBC	CONNECTIVITY	AUTO LOAD
ELEMENTS	COORDINATES	CONTINUE
FOLLOW FOR	DIST LOADS	CONTROL
LARGE DISP	FIXED DISP	DIST LOAD
PLASTICITY	GEOMETRY	PROPORTIONAL INC
PRINT	ISOTROPIC	TIME STEP
SIZING	OPTIMIZE	
TITLE	SOLVER	
	WORK HARD	

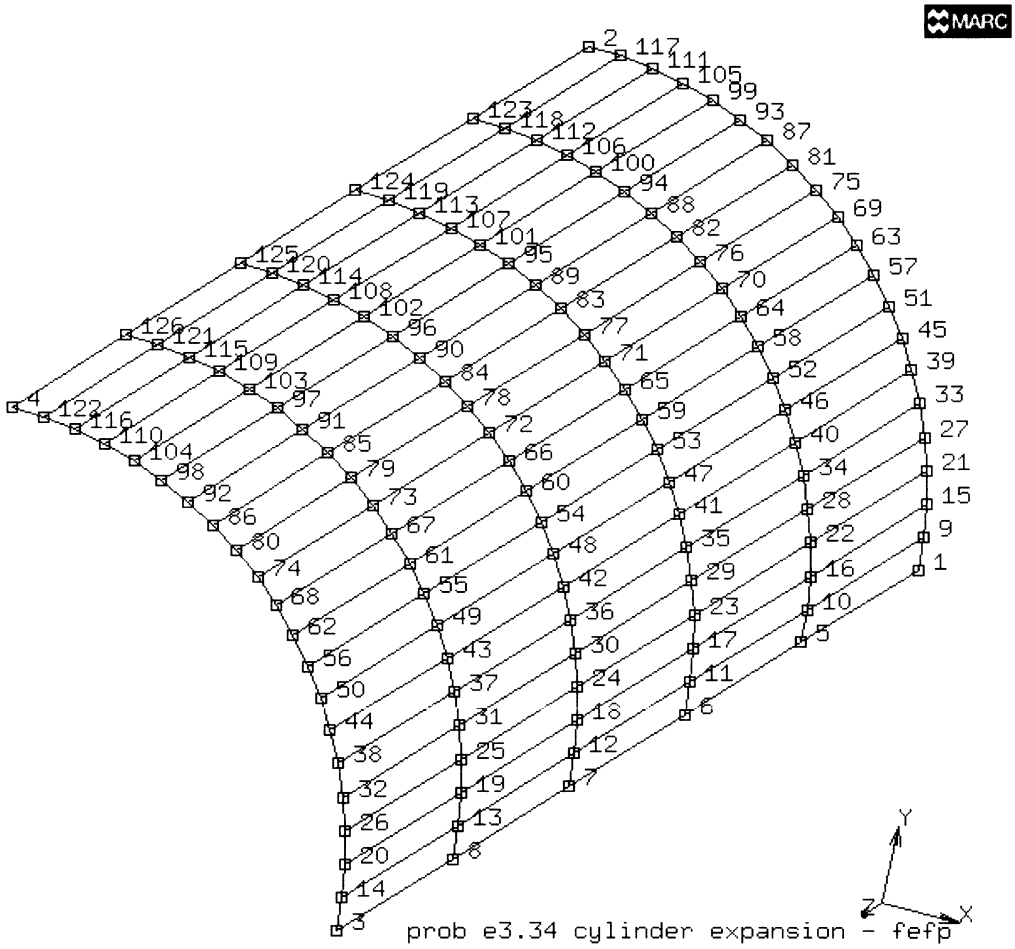

Figure 3.34-1 Initial Mesh for Cylinder Inflation

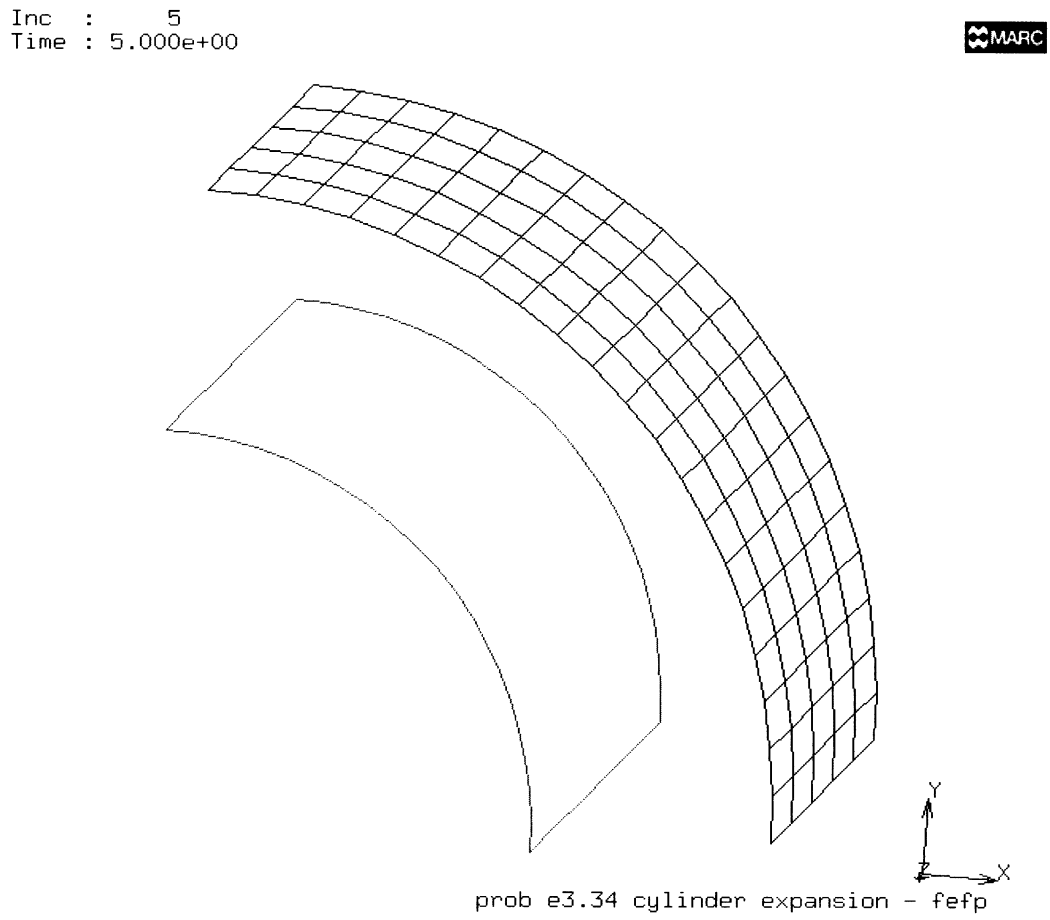

Figure 3.34-2 Initial and Final Configuration for Cylinder Inflation

3.35 Cantilever Beam under Point Load

An large strain elastoplastic analysis is carried out for cantilever beam subjected to point load. This problem demonstrates the use of MARC algorithm for large strain plasticity. The algorithm, activated by option PLASTICITY,5 is based on hyperelasticity and multiplicative decomposition of deformation gradient into a elastic part and a plastic part (F^eF^p). The problem is modeled using element type 11.

Element

Library element 11 is a 4-node bilinear plane strain element with displacements in x and y directions as degrees of freedom.

Model

The total length of the beam is 20 mm. The cross-section of the beam is a quadrilateral with a side length of 1 mm. Figure 3.35-1 illustrates the beam configuration. The beam is modeled using 60 4-node bilinear plane strain elements (see Figure 3.35-2).

Material Properties

All elements have the same properties: Young's modulus is 3.0E7 N/mm^2; Poisson's ratio is 0.3; the initial yield stress is 3.0E4 N/mm^2. A piecewise linear approximation is used to represent the workhardening behavior of the material.

Loading

A point load of -.74E3 N is applied to the tip node at the free end of the beam (see Figure 3.35-1) in 91 increments. It is done by using PROPORTIONAL INC option.

Boundary Conditions

The four nodes at one end of the beam are fixed (see Figure 3.35-1).

Results

The deformed configurations and the distributions of equivalent plastic strains for increments 30 and 90 are shown in Figure 3.35-3 and Figure 3.35-4 respectively.

Parameters, Options, and Subroutines Summary

Example e3x35.dat:

Parameters	Model Definition Options	History Definition Options
ALL POINTS	CONNECTIVITY	AUTO LOAD
ELEMENTS	CONTROL	CONTINUE
END	COORDINATES	POINT LOAD
PLASTICITY	END OPTION	PROPORTIONAL INC
PRINT	FIXED DISP	
SIZING	GEOMETRY	
TITLE	ISOTROPIC	
	NO PRINT	
	OPTIMIZE	
	POST	
	POINT LOAD	
	SOLVER	
	TYING	
	WORK HARD	

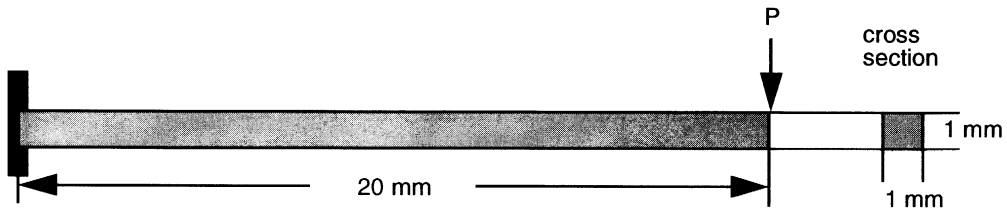

Figure 3.35-1 Cantilever Beam under Point Load

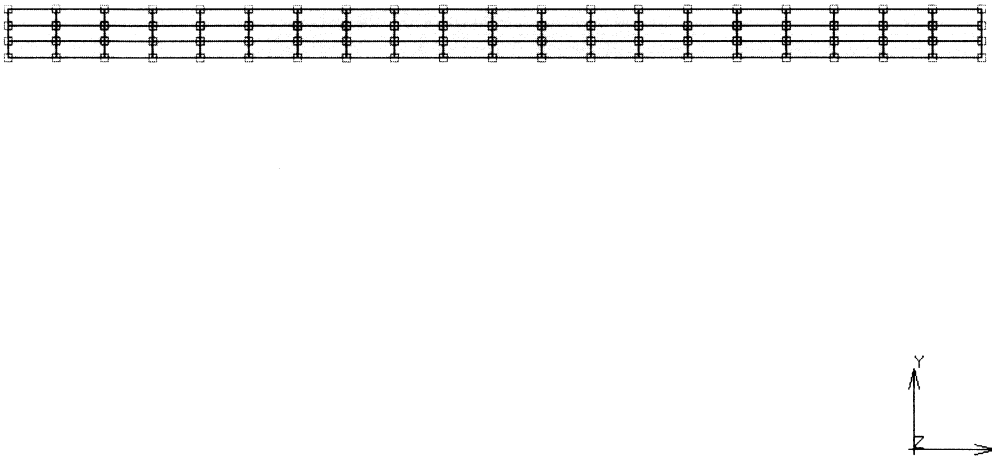

Figure 3.35-2 FE-Mesh

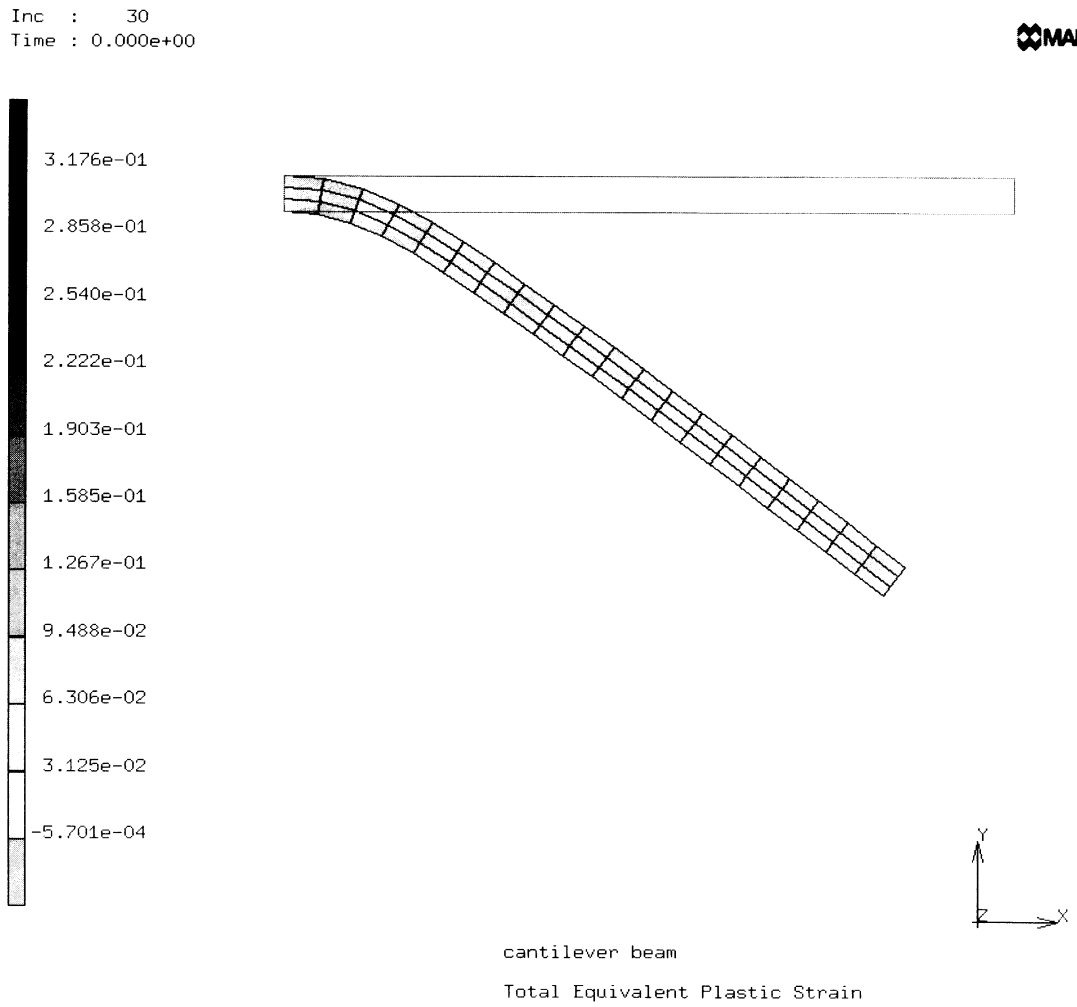

Figure 3.35-3 Deformed Mesh and Distribution of Equivalent Plastic Strain at Increment 30

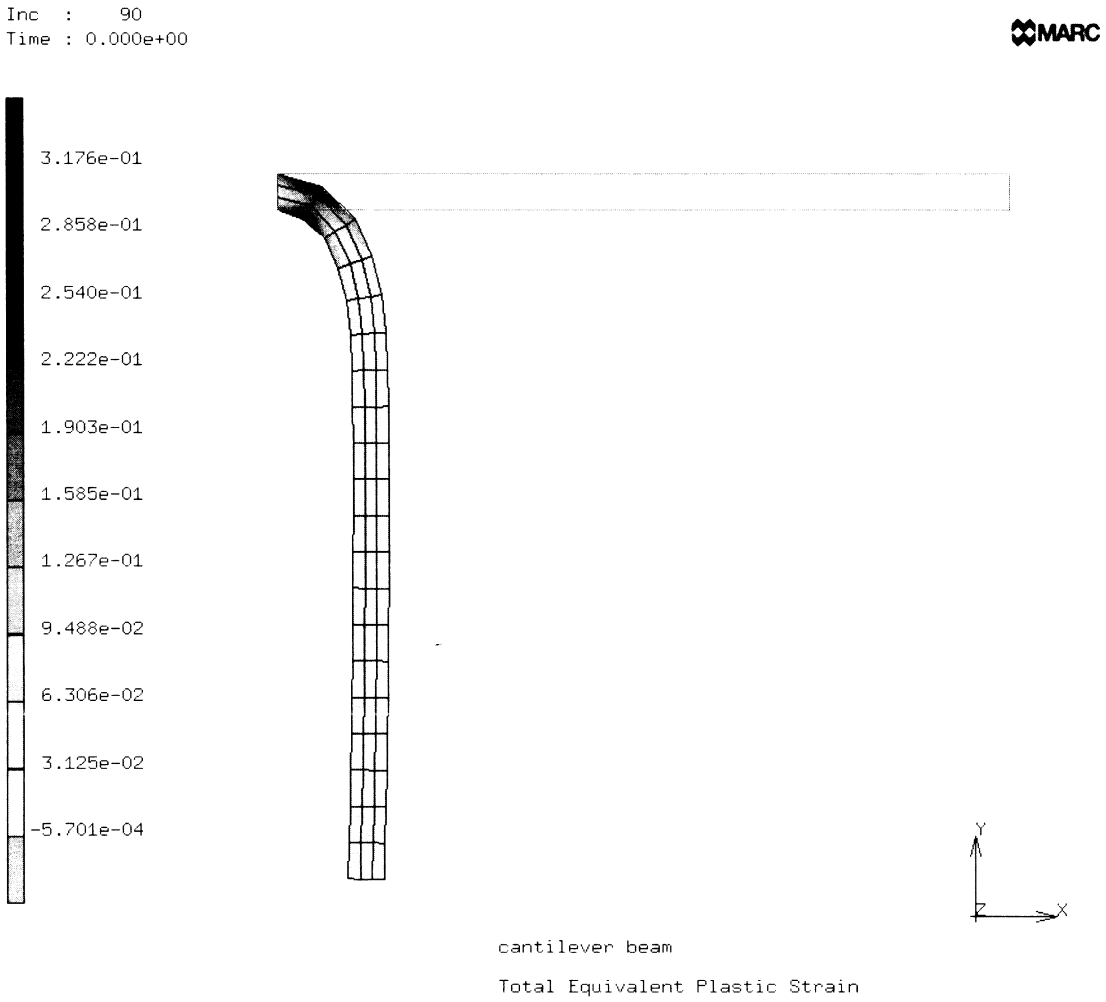

Figure 3.35-4 Deformed Mesh and Distribution of Equivalent Plastic Strain at Increment 90

3.36 Tensile Loading of a Strip with a Cylindrical Hole

This example uses the multiplicative decomposition radial return F^eF^p plasticity to model the tensile behavior of a three-dimensional strip with a through thickness cylindrical hole in the center.

Model

The strip is of square cross section of side 4 mm and a thickness of 0.4 mm. A cylindrical hole of radius 0.6 mm is at the center. Due to symmetry, an eighth of the geometry is modeled. Thus the model is a square of side 2 mm in the x-y plane and a thickness of 0.2 mm in the z-direction, with a cylindrical hole of radius 0.6 mm. The model is comprised of 92 elements and 218 nodes and is shown in Figure 3.36-1.

Element

The 8-node, 3D, brick element type 7 is used in this analysis.

Boundary Conditions

The boundary conditions used reflect the geometrical and loading symmetry in the model. The x- and y-displacements are constrained in the Z = 0.2 plane while the z-displacements are constrained to be zero in the Z = 0 plane.

Material Properties

All elements are treated as isotropic. The Young's modulus is 3×10^7 N/mm^2. The Poisson's ratio is 0.33 and the initial yield stress is 3.5×10^4 N/mm^2. The hardening behavior is specified using the WORK HARD model definition option.

History Definition

The loading of the three-dimensional strip is carried out using displacement increments specified on the top surface along the y-direction as given below:

Number of Increments	Y-displacement Increment (mm)
2	0.001
10	0.002
25	0.020

There are no loads in the x- or z-direction and the strip is free to move in, along these directions. The small thickness in the z-direction compared to the x and y dimensions approximates a case of plane stress along the z-direction. The displacement increments are imposed using the DISP CHANGE and AUTO LOAD history definition options. There are a total of 37 increments.

Results

Increment 1 is elastic. However, plasticity is incipient and increment 2 shows the initiation of plasticity at the stress concentration at the equator of the hole (Figure 3.36-1). At the end of increment 12, a radial swath of plasticity develop with a maximum value of the effective plastic strain is 8.14%. The displacement increments after increment 12 are large and the plastic strain continues to accumulate rapidly from increment 13. The contours of effective plastic strain at increments 20 and 37 are shown in Figure 3.36-2 and Figure 3.36-3 respectively. The shape of the hole develops into a progressively prolate shape. Necking behavior is evident from the deformation. From Figure 3.36-3, it can be seen that the material near the hole thins more rapidly in the z-direction than the material near the edges. Continued loading will lead to failure by loss of load carrying capacity in the X-Z plane.

Parameters, Options, and User Subroutines Summary

Parameters	Model Definition Options	History Definition Options
ALL POINTS	CONNECTIVITY	AUTO LOAD
ELEMENTS	COORDINATES	CONTINUE
END	END OPTION	DISP CHANGE
PLASTICITY	FIXED DISP	
PRINT	GEOMETRY	
SETNAME	ISOTROPIC	
SIZING	WORK HARD	
TITLE		

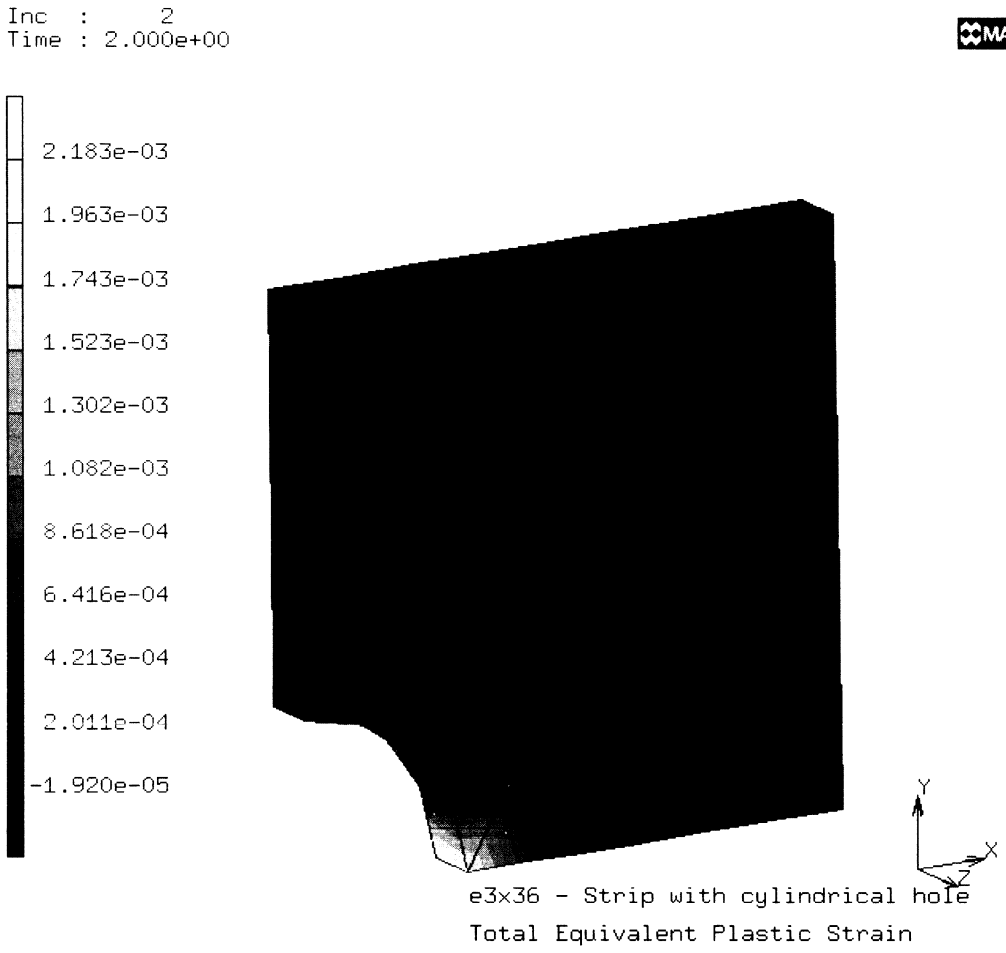

Figure 3.36-1 Plasticity Initiates at the Hole in Increment 2

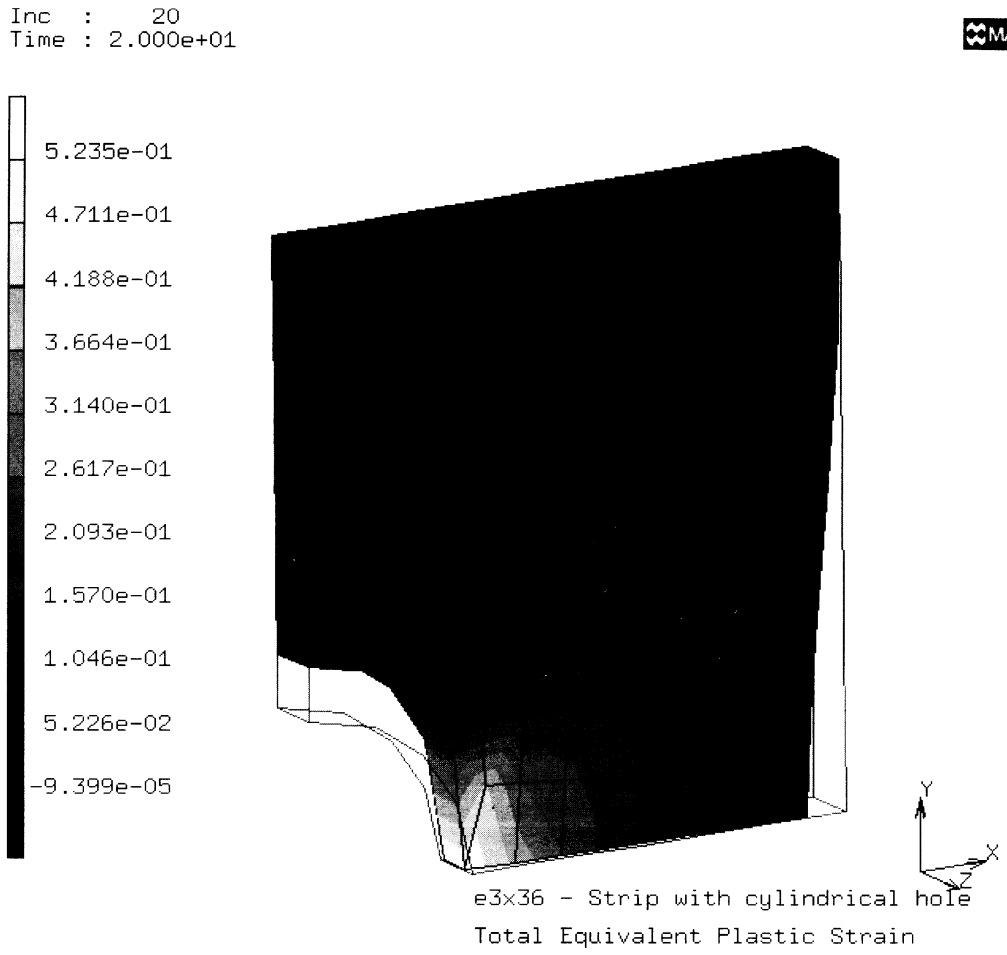

Figure 3.36-2 Contours of Effective Plastic Strain after 20 Increments

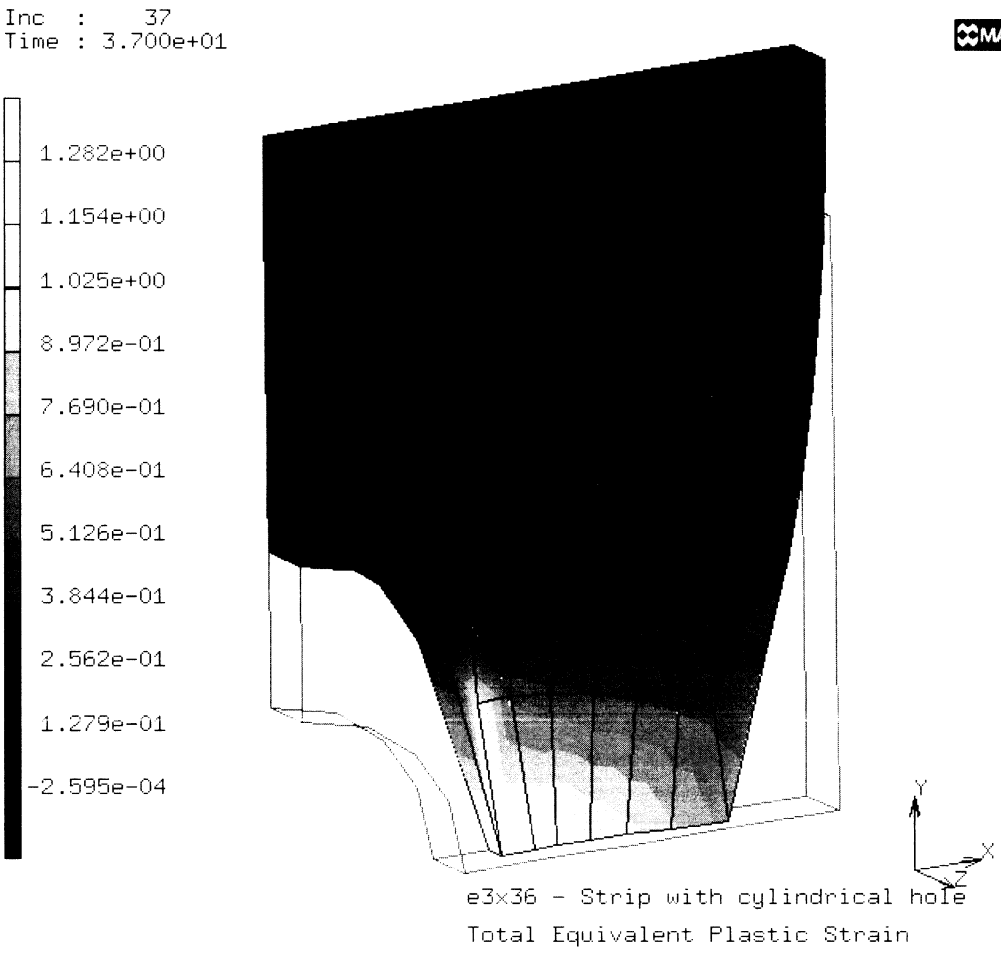

Figure 3.36-3 Contours of Effective Plastic Strain after 37 Increments

3.37 Elastic Deformation in a Closed Loop

This problem shows the fundamental difference between the use of hypoelasticity and hyperelasticity. One plane strain element subjected to a closed loop of large elastic deformation is considered. Element type 11 is employed. To activate hypoelastic constitutive equations, parameter PLASTICITY,3 is used in e3x37a.dat. The problem e3x37b.dat activates hyperelastic constitutive equations via PLASTICITY,5. A very large yield stress is given to guarantee the deformation remains elastic.

Element

Library element 11 is a 4-node bilinear plane strain element with displacements in x and y directions as degrees of freedom.

Model and Boundary Conditions

A quadrilateral element with the side length of 1 mm. The nodes 1 and 2 are fixed.

Material Properties

Material same properties are given as: Young's modulus is 20300.0 N/mm^2; Poisson's ratio is 0.33; Yield stress is 999999999.0 N/mm^2.

Loading

A closed loop of large elastic deformation is applied to the element by using prescribed displacements for the nodes 3 and 4. The sequence of the prescribed displacements for the nodes 3 and 4 are given as: (a) u = 5 mm, (b) v = 5 mm, (c) u = -5 mm, and (d) v = -5 mm. Each is applied with 5 equal increments and is shown in Figure 3.37-1.

Results

Figure 3.37-2 shows the nodal reaction forces obtained from both e3x37a.dat and e3x37b.dat, after the closed loop of large elastic deformation. It can be seen that the use of hypoelasticity in e3x37a.dat results in nonzero reaction forces even if the deformation becomes zero. The job e3x37b.dat which is based on hyperelasticity via PLASTICITY,5 leads to correct results. Figure 3.37-3 is the history plot of the equivalent von Mises stress. Nonzero stress is obtained after the closed loop of elastic deformation for hypoelasticity based solution.

Parameters, Options, and Subroutines Summary

Example e3x37.dat:

Parameters	Model Definition Options	History Definition Options
ELEMENTS	CONNECTIVITY	AUTO LOAD
END	CONTROL	CONTINUE
LARGE DISP	COORDINATES	DISP CHANGE
PLASTICITY	END OPTION	
SIZING	FIXED DISP	
TITLE	GEOMETRY	
	ISOTROPIC	
	POST	

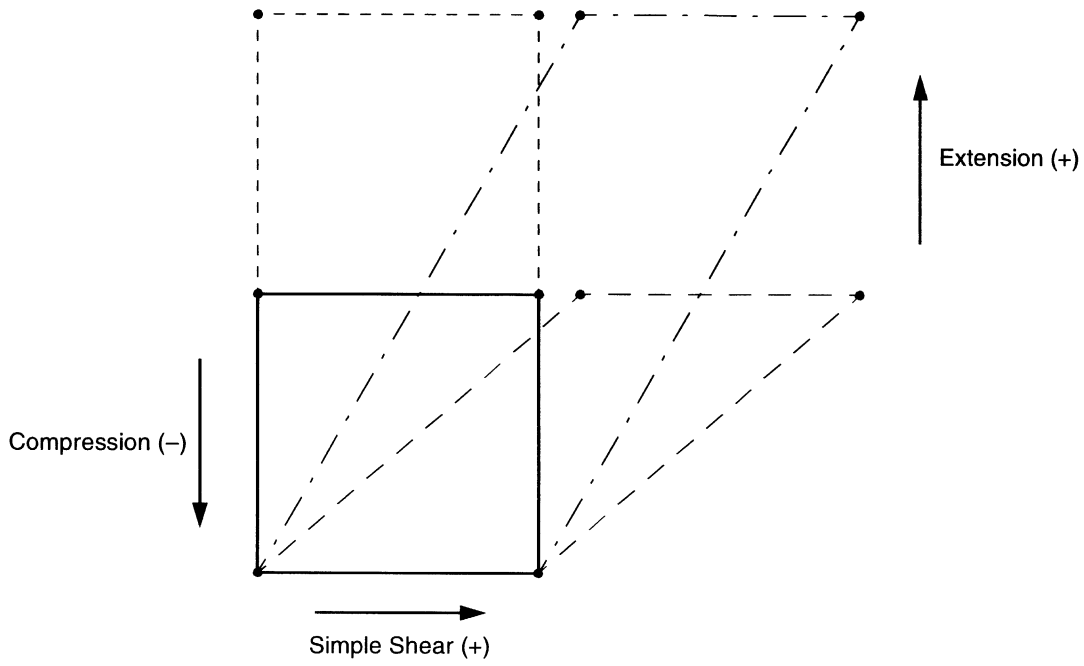

Figure 3.37-1 Elastic Deformation in a Closed Loop

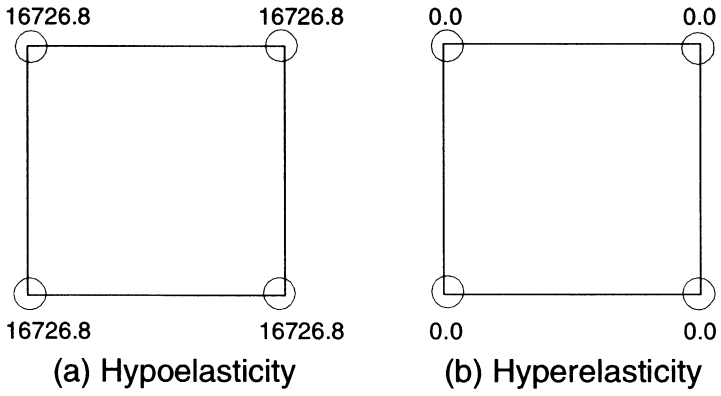

Figure 3.37-2 Nodal Reaction Forces after a Closed Loop of Elastic Deformation

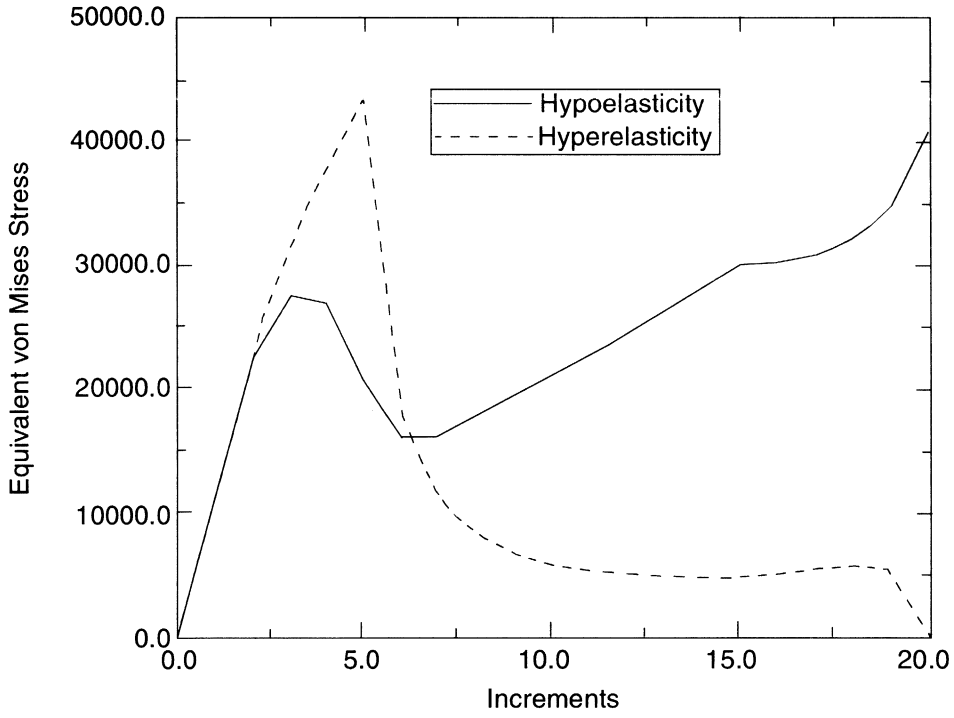

Figure 3.37-3 History Plot of Equivalent von Mises Stress

3.38 Tensile Loading and Rigid Body Rotation

This problem simulates the tensile loading of a sheet to large plastic strains, followed by a large rigid rotation. The solution demonstrates the accuracy of the plasticity model under large strains and rotations.

Element

This problem is simulated as a two-dimensional plane stress case. The 4-node plane stress element 3 is used to construct a mesh. There are two degrees of freedom per node with a bilinear interpolation and full four point Gaussian quadrature.

Model

Due to symmetry of the geometry and loading, a quarter of the actual model is simulated. The finite element model is made up of 9 elements and 16 nodes. There are a total of 32 degrees of freedom. The model is shown in Figure 3.38-1.

Geometry

The model is assumed to be a square of side 9 inches. The initial thickness is one inch.

Material Properties

The material is assumed to be isotropic elastic plastic. The Young's modulus is 1.E+06 psi, Poisson's ratio is 0.30 and the initial yield stress is 1000.0 psi. The hardening behavior is input using a user subroutine and is given by the equation:

$$\bar{\sigma} = \bar{\sigma}_0 + \alpha(2-\alpha)(\bar{\sigma}_\infty - \bar{\sigma}_0); \alpha = \frac{\bar{\varepsilon}^p}{\bar{\varepsilon}^p_\infty}$$

$$\bar{\sigma}_0 = 1000, \bar{\varepsilon}_\infty = 0.6; \bar{\sigma}_\infty = 1200$$

Boundary Conditions

The loading is initially tensile. The lower end of the model (nodes 1, 2, 3, and 10) is restrained to have no vertical motion. The top end (nodes 7, 8, 9, and 16) is subjected to displacement increments in the y direction. The left end (nodes 1, 4, 7, and 12) is held from displacing in the x direction. After 10 increments, the boundary nodes of the model are given specified displacement increments corresponding to a large finite rotation of 90 degrees. This entire rotation is applied in a single increment.

Results

The deformed model is shown after the 10th and 11th increments in Figures 3.38-2 and 3.38-3 respectively. Contours of total effective plastic strain are also superimposed. The deformation is homogeneous as expected. After the 10th increment, the effective plastic strain is 0.4730. The next increment is the rigid rotation of 90 degrees. At the end of this increment, no further plasticity has occurred. The von Mises effective stress at the end of the tenth increment is 1286.46 psi in all the elements. This value remains constant during the rigid body rotation of increment 11. A history plot of the von Mises effective stress as a function of plastic strain is shown in Figures 3.38-4 for nodes 1 and 9. It can be seen that the results are identical for both nodes for all increments. No change in either the von Mises stress or effective plastic strain is observed in increment 11. This shows the accuracy of the plasticity algorithms in MARC for large strains and rotations.

Parameters, Options, and Subroutines Summary

Parameters	Model Definition Options
ELEMENTS	CONNECTIVITY
LARGE DISP	COORDINATES
PLASTICITY	FIXED DISP
PRINT	GEOMETRY
PROCESSOR	ISOTROPIC
SIZING	WORK HARD DATA
TITLE	

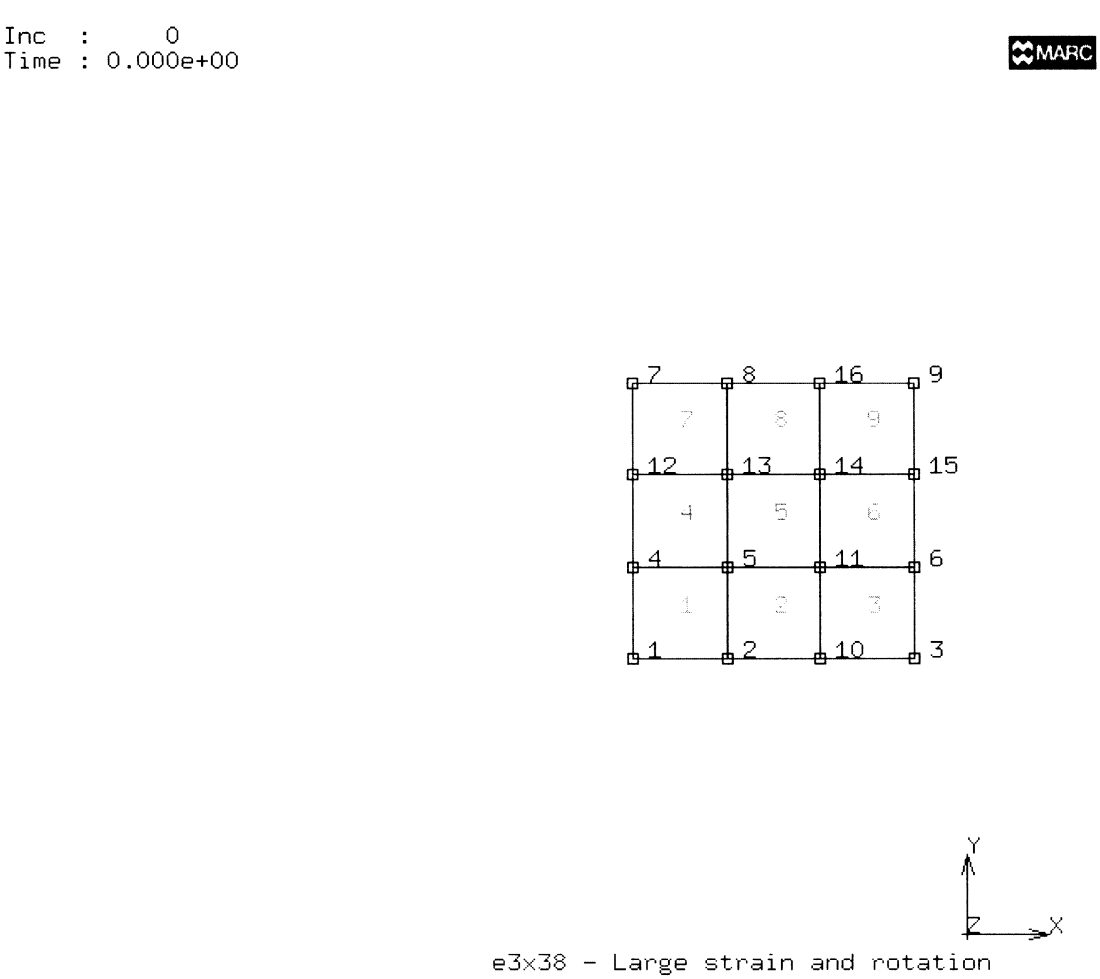

Figure 3.38-1 Initial Model

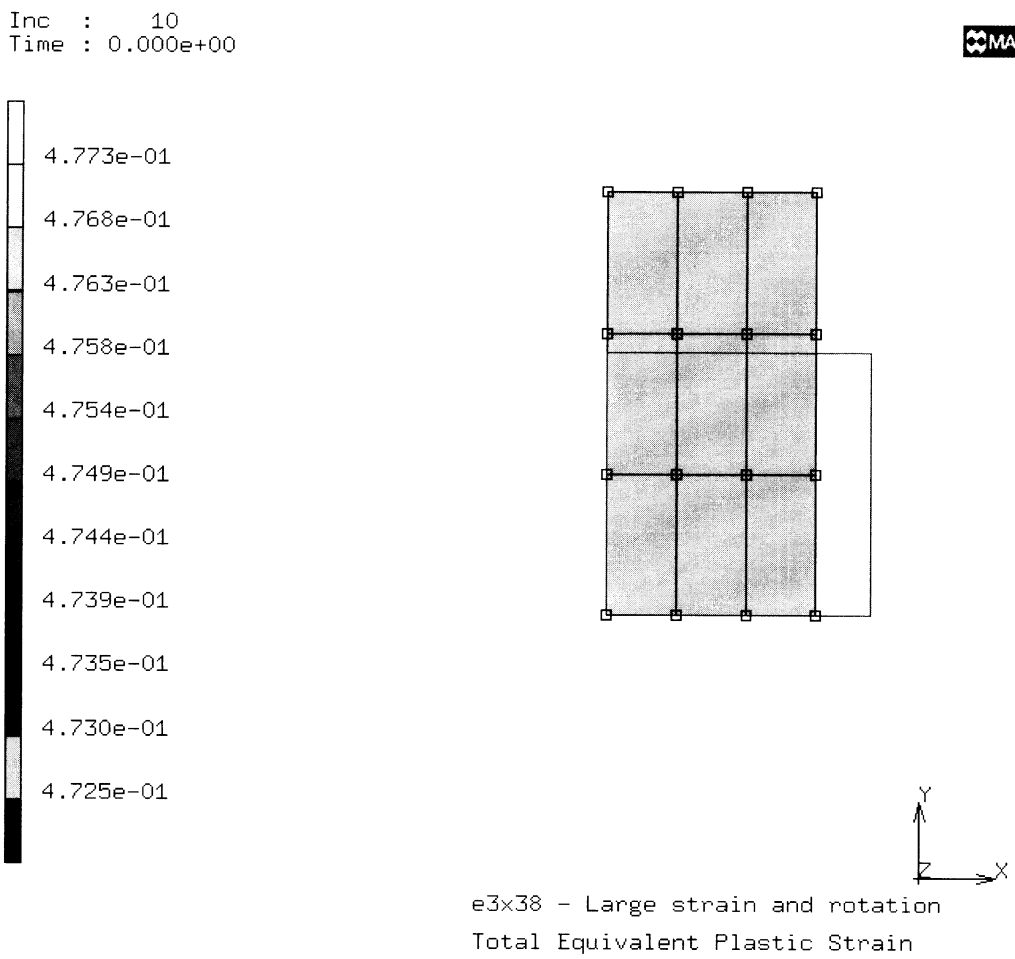

Figure 3.38-2 Deformed Model at the End of Increment 10

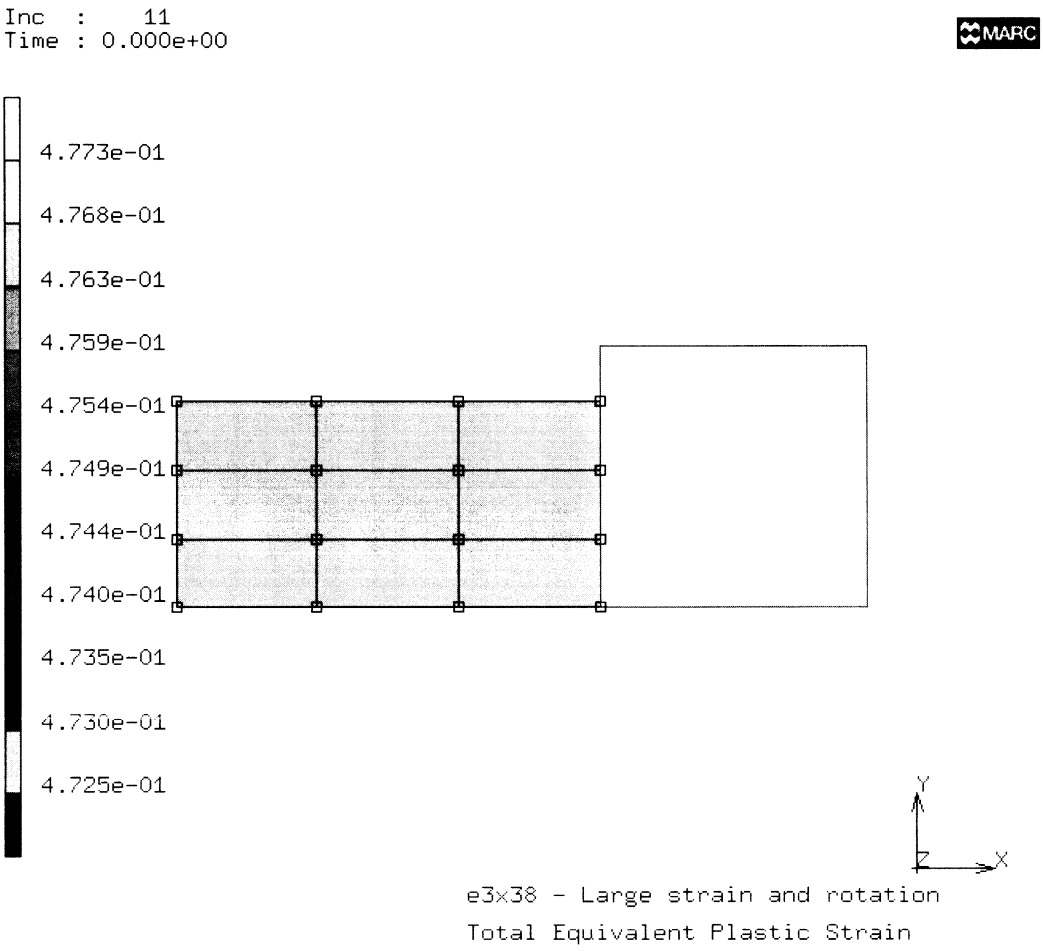

Figure 3.38-3 Deformed Model at the End of Increment 11

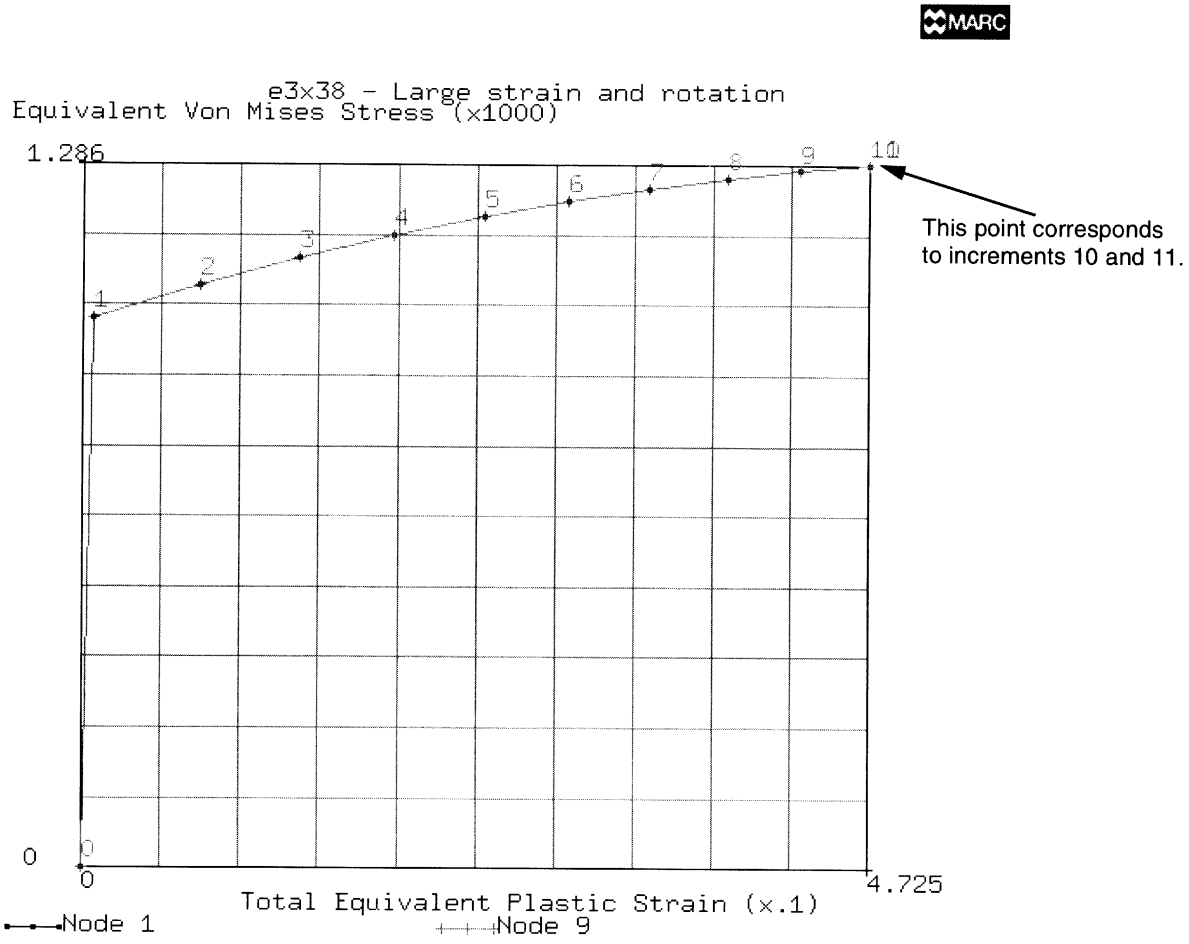

Figure 3.38-4 History Plot of Equivalent Stress versus Effective Plastic Strain for Nodes 1 and 9

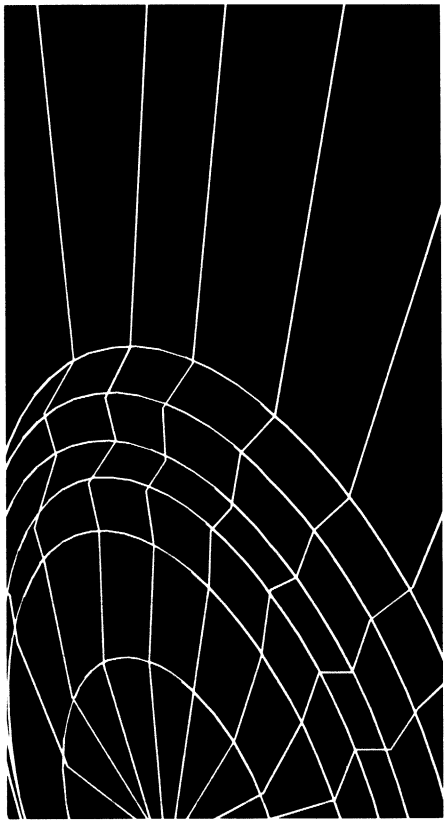

MARC Analysis Research Corporation

MARC

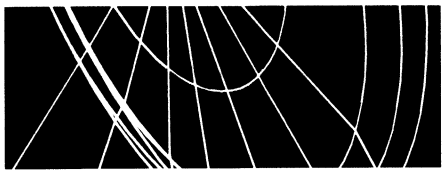

Volume E

Demonstration Problems

Version K7

Chapter 4
Large Displacement

4 Large Displacement Contents

4 Large Displacement List of Figures

Figure **Page**

4 Large Displacement List of Tables

4 Large Displacement

MARC contains an extensive large displacement analysis capability. A discussion of the use of this capability can be found in *MARC Volume A: User Information*. A summary of the features is given below.

Selection of elements

- Available in all stress elements

Choice of operators

- Newton-Raphson
- Strain-Correction
- Modified Newton-Raphson

Estimation of buckling loads

- Elastic-, plastic-, static- and dynamic-buckling

Choice of procedures

- Total Lagrangian
- Updated Lagrangian
- Eulerian

Large strain elastic analysis

Hyperelastic material (Mooney) behavior

Large strain elastic-plastic analysis

Distributed loads calculated based on deformed structure

Compiled in this chapter are a number of solved problems. These problems illustrate the use of the LARGE DISP option for various types of analyses. Table 4-1 shows MARC elements and options used in these demonstration problems.

Table 4-1 Nonlinear Material Demonstration Problems

Problem Number	Element Type(s)	Parameters	Model Definition	History Definition	User Subroutines	Problem Description
4.1	15	LARGE DISP BUCKLE	UFXORD CONTROL TRANSFORMATION	BUCKLE PROPORTIONAL AUTO LOAD AUTO INCREMENT	UFXORD	Elastic, large displacement, buckling analysis of a thin shallow, spherical cap, point load, eigenvalue extraction and load incrementation.
4.2	49 50 22	LARGE DISP ELSTO	CONTROL PRINT CHOICE	AUTO LOAD DIST LOADS	—	Elastic-plastic, large displacement analysis of a square plate, simply supported, distributed load.
4.3	25	LARGE DISP ELSTO UPDATE	CONTROL	AUTO LOAD	—	Elastic, large displacement analysis of a cantilever beam subjected to a tip load.
4.4	15	LARGE DISP BUCKLE	CONN GENER NODE FILL	AUTO LOAD BUCKLE	—	Elastic buckling of a cylinder, axial compression, buckling loads and modal shapes.
4.5	22	LARGE DISP	UFXORD OPTIMIZE POST	AUTO LOAD	UFXORD	Large displacement analysis of a pinched cylinder.
4.6	9	LARGE DISP	SPRINGS CONTROL	AUTO LOAD	—	Large displacement of an elastic truss-spring.
4.7	16	PRINT, 3 UPDATE LARGE DISP SHELL SECT	TRANSFORMATION CONN GENER UDUMP UFXORD	AUTO INCREMENT	UFXORD	Postbuckling of a deep arch.
4.8	51	PRINT, 3 FOLLOW FORCE LARGE DISP	DIST LOADS	AUTO LOAD	—	Analysis of a cable network.
4.9	90	SHELL SECT BUCKLE	—	BUCKLE	—	Buckling of a radially loaded ring.

Table 4-1 Nonlinear Material Demonstration Problems (Continued)

Problem Number	Element Type(s)	Parameters	Model Definition	History Definition	User Subroutines	Problem Description
4.10	90	SHELL SECT BUCKLE	—	DISP CHANGE BUCKLE	—	Nonsymmetric buckling modes of a circular cylinder.
4.11	49	LARGE DISP	FIXED DISP POINT LOAD	AUTO LOAD POINT LOAD	—	Large displacement analysis of a tapered plate.
4.12	3	LARGE DISP BUCKLE	FIXED DISP POINT LOAD BUCKLE INCREMENT	BUCKLE	—	Buckling of a strut using perturbation method.
4.13	67 142 10 144 20 145	LARGE DISP FOLLOW FOR	REBAR	AUTO LOAD DIST LOADS	—	Analysis of a thin cylinder with helical plys.
4.14	18 147 30 148	LARGE DISP FOLLOW FOR	REBAR MOONEY UTRANFORM	AUTO LOAD DIST LOADS	UTRANS	Analysis of a thin cylinder with a helical ply.
4.15	75	BUCKLE	TYING SOLVER	BUCKLE RECOVER	—	Buckling of a cylinder tube

4 *Large Displacement*

4.1 Elastic Large Displacement – Shell Buckling

In this example, we illustrate a typical large displacement analysis, and the effectiveness of the eigenvalue buckling estimate analysis. The objective is to estimate the elastic collapse load of a thin, shallow, spherical cap under an apex point load.

This problem is modeled using the four techniques summarized below.

Data Set	Element Type(s)	Number of Elements	Number of Nodes	Differentiating Features
e4x1a	15	5	6	Modified Newton
e4x1b	15	5	6	Strain correction
e4x1c	15	5	6	Full Newton
e4x1d	15	5	6	Lanczos Method, Modified Newton

Model/Element

The geometry of the shallow spherical cap is shown in Figure 4.1-1. The collapse is assumed to be axisymmetric. If asymmetric buckling were probable, the analysis would be performed using a complete doubly-curved shell formulation, such as element types 22, 49, 72, 75, 138, 139, or 140. The axisymmetric assumption indicates a choice of element type 15. Element 15 is preferred over element 1, since the latter uses shallow shell theory with linear and cubic interpolations along and normal to the secant. Element 15 uses a full cubic interpolation, and hence contains all the rigid-body modes needed for accurate large displacement analysis. Experience shows element 15 to be rapidly convergent. In this problem, the deformation is expected to be global (rather than a local snap-through), so only five elements are used. The UFXORD user subroutine is used to generate the coordinates for this model.

Geometry

The thickness of the shell is 0.01576 inches. This value is entered in EGEOM1.

Material Properties

The Young's modulus is 1.0×10^7 psi. Poisson's ratio is 0.3 for this material.

Loading

In a simple problem such as this, it is possible to proceed with displacement loading and thus control the solution more accurately as the collapse occurs, since the extent of collapse is prescribed in each increment. However, in a distributed load problem (the more common case) displacement control is not possible. Also, eigenvalue buckling estimates would not make sense if the apex has a vertical displacement boundary condition. In this demonstration, we begin with

load control. The difficulty with load control is the certainty of nonpositive-definiteness if the system collapses. If post-collapse behavior must be studied, the AUTO INCREMENT option should be used. In this example, the first data set uses a point load and eigenvalue analysis to anticipate the collapse load. The second data set uses displacement control. In this example, the structure never actually collapses, so that the entire response could be obtained by either loading method. The load begins at 2.0 lb for increment 0. In the third analysis, a point load is applied to the structure – the magnitude of which is controlled by the AUTO INCREMENT option. The fourth analysis is similar to the first analysis, but the Lanczos method is used to extract the eigenmodes.

Boundary Conditions

The boundary conditions in the input deck reflect the symmetry of the problem as well as the built-in edge of the cap.

BUCKLE

The size of the load step is important in order to satisfy the piecewise linear approximation of the tangent modulus technique. As a general rule, the analysis may first be approached by taking 5 to 15 steps to initial collapse estimate obtained from the BUCKLE option. The procedure suggested is:

1. Apply an arbitrary load step and ask for a BUCKLE collapse estimate.
2. The eigenvalue obtained indicates (roughly) the multiplier to collapse for the applied load. Based on this estimate, choose a load step of 1/5 to 1/15 of the collapse load and perform a nonlinear incremental analysis.
3. The estimated collapse load may also give an idea of whether material nonlinearities (for example, plasticity) can occur during the collapse since the eigenvalue can also be used as a multiplier on stress to estimate the stress at collapse.
4. It is very important to plot and study the eigenvector predicted in this way – the mesh must be of sufficient detail to describe the collapse mode accurately (for example, no curvature change reversals in a single element); otherwise, the collapse estimates can have large errors.

The BUCKLE option is based on second-order expansion of the total equilibrium equation (see *MARC Volume F: Background Information*, "Effective Use of the Incremental Stiffness Matrix"). The option allows eigenvalue estimates to be made by second-order expansion from an arbitrary point in the history. This is illustrated in this example.

ALL POINTS

The analysis involves large displacement and, hence, is nonlinear. Clearly, the residual load correction (total equilibrium check) is essential. This depends on integration of stress throughout the mesh, and, since element 15 is basically cubic, the stress must be $0(s^2)$; thus, the ALL POINTS option is necessary for accurate stress integration. This is the general case for nonlinear analysis with higher order elements. This is the default in MARC.

Results

The initial BUCKLE option gives a collapse estimate of 15 lb. Based on this, a load step of 2 pounds per increment is chosen. The collapse mode (eigenvector) appears quite smooth in this case (a global collapse) and seems adequately described by the 5-element mesh.

The incremental load blocks are arranged to apply increments of loads and obtain collapse estimates alternately. This is an extreme demonstration. In a more realistic analysis, the BUCKLE estimate would probably be obtained only during the first part of the history, and the analysis discontinued when the estimates converged. As an alternative, the BUCKLE INCREMENT model definition option could be used effectively. For this purpose, the RESTART option is of great value.

Following this analysis (Figure 4.1-3), a displacement-controlled analysis is also shown with more of the response. This technique is often not useful, since a true collapse often gives rise to a nonpositive definite system even with displacement loading (except in the trivial case of a one degree of freedom system). In this case, a step size of 0.005 inch is used, based on the observed response in the initial load-controlled analysis. Since the structure does not, in fact, buckle but always retains some positive stiffness, it is possible to follow the solution arbitrarily far through the inversion of the cap.

The results are summarized in Table 4.1-1 and in Figure 4.1-2 and Figure 4.1-3. Notice the nonlinear load-displacement behavior. The collapse load estimates converges on 15.0 pounds after four increments, and it is apparent that a definite lack of stiffness is present above this load level.

Based on this preliminary study, the analyst can have enough information for design purposes. He now knows that the structure is extremely weak (about 10% of its initial stiffness) above a 12 pound load. If more detail is required, a restart would be made at about 8 or 9 pound load (assuming that a restart file had been written) and smaller steps would be used. With displacement control instead, we pursue this possibility and find (Figure 4.1-3) that, although the structure becomes extremely weak, it does not "snap through", but retains positive stiffness until it is folded back and continues to support load in an inverted cap mode essentially with membrane action, so that its stiffness then becomes quite high compared to the initial bending stiffness.

Table 4.1-1 Collapse Load Estimates

Inc. No.	Load No.	Previous Load	Eigenvalues λ (LARGE DISP Option)			Collapse Load P^c (LARGE DISP Option)		
			No. 0	No. 1	No. 2	No. 0	No. 1	No. 2
0	2	0	7.81	7.66	7.81	15.62	15.32	15.62
1	2	2	5.92	5.84	5.92	13.84	13.68	13.85
2	2	4	4.47	4.40	4.47	12.94	12.80	12.94
3	2	6	3.23	3.16	3.23	12.46	12.32	12.46
4	2	8	2.19	2.11	2.19	12.38	12.22	12.38
5	2	10	1.37	1.29	1.37	12.74	12.58	12.74
6	2	16	.78	.76	.78	13.56	13.40	13.56
7	2	14	.235	.33	.38	14.47	14.66	14.76
8	2	16	.184	.16	–	16.37	16.32	–

Note: $P^c = P + \lambda\Delta P$

The solution obtained here can be compared with the semianalytic solution presented by Timoshenko and Gere [1]. Using their notation:

$$b = 0.9,\ a = 4.76,\ h = 0.01576,\ E = 10^7$$

$$\lambda = b^4/a^2h^2 = 116.585$$

$$\mu = \sqrt{0.093 \times (\lambda + 115)} - 0.94 = 2.511$$

$$P_c = \mu E h^3/a = 20.6$$

The collapse load obtained by MARC, which includes all geometry nonlinearity effects, is less than the classical buckling load.

Reference

Timoshenko, S. P., and Gere, J. M.,*Theory of Elastic Stability*, (McGraw-Hill, New York, 1961).

Parameters, Options, and Subroutines Summary

Example e4x1a.dat:

Parameters	Model Definition Options	History Definition Options
BUCKLE	CONNECTIVITY	BUCKLE
ELEMENT	CONTROL	CONTINUE
END	END OPTION	PROPORTIONAL INCREMENT
LARGE DISP	FIXED DISP	
SIZING	GEOMETRY	
TITLE	ISOTROPIC	
	POINT LOAD	
	TRANSFORMATIONS	
	UFXORD	

User subroutine in u4x1a.f:

UFXORD

Example e4x1b.dat:

Parameters	Model Definition Options	History Definition Options
ELEMENT	CONNECTIVITY	AUTO LOAD
END	CONTROL	CONTINUE
LARGE DISP	END OPTION	
SIZING	FIXED DISP	
TITLE	GEOMETRY	
	ISOTROPIC	
	PRINT CHOICE	
	TRANSFORMATIONS	
	UFXORD	

User subroutine in u4x1b.f:

UFXORD

Example e4x1c.dat:

Parameters	Model Definition Options	History Definition Options
ELEMENT	CONNECTIVITY	AUTO INCREMENT
END	CONTROL	CONTINUE
LARGE DISP	COORDINATE	POINT LOAD
SHELL SECT	END OPTION	
SIZING	FIXED DISP	
TITLE	GEOMETRY	
	ISOTROPIC	
	POINT LOAD	
	PRINT CHOICE	
	TRANSFORMATIONS	

Example e4x1d.dat:

Parameters	Model Definition Options	History Definition Options
BUCKLE	CONNECTIVITY	BUCKLE
ELEMENT	CONTROL	CONTINUE
END	END OPTION	PROPORTIONAL INCREMENT
LARGE DISP	FIXED DISP	
SIZING	GEOMETRY	
TITLE	ISOTROPIC	
	POINT LOAD	
	TRANSFORMATIONS	
	UFXORD	

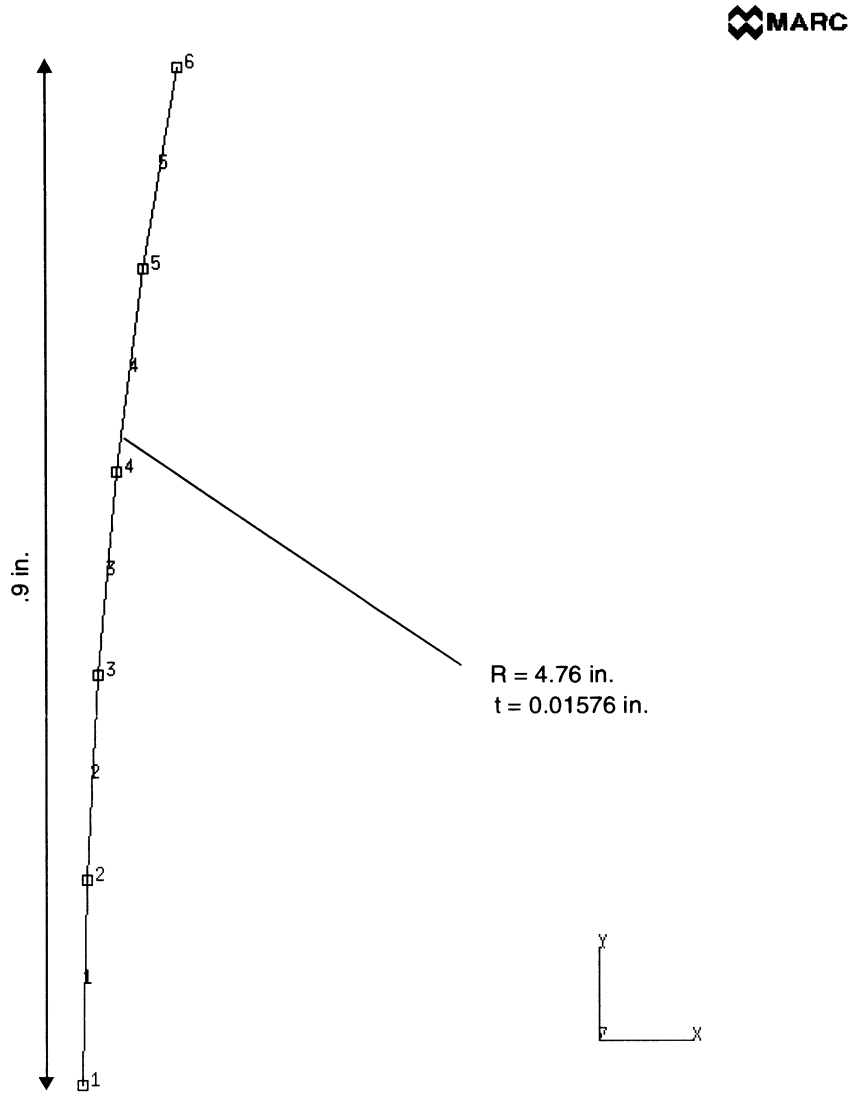

Figure 4.1-1 Geometry for Elastic Large Displacement Example

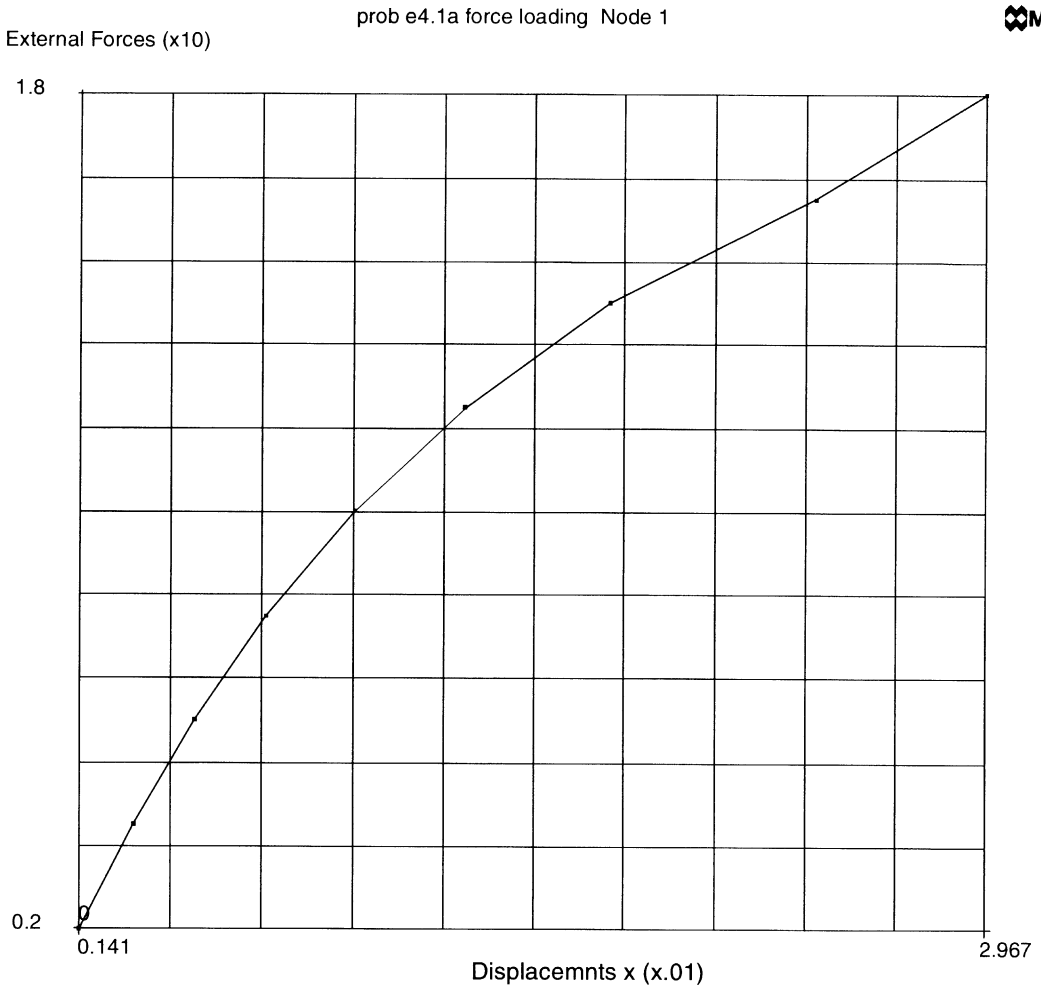

Figure 4.1-2 Point Loaded Shell Cap Force Loading

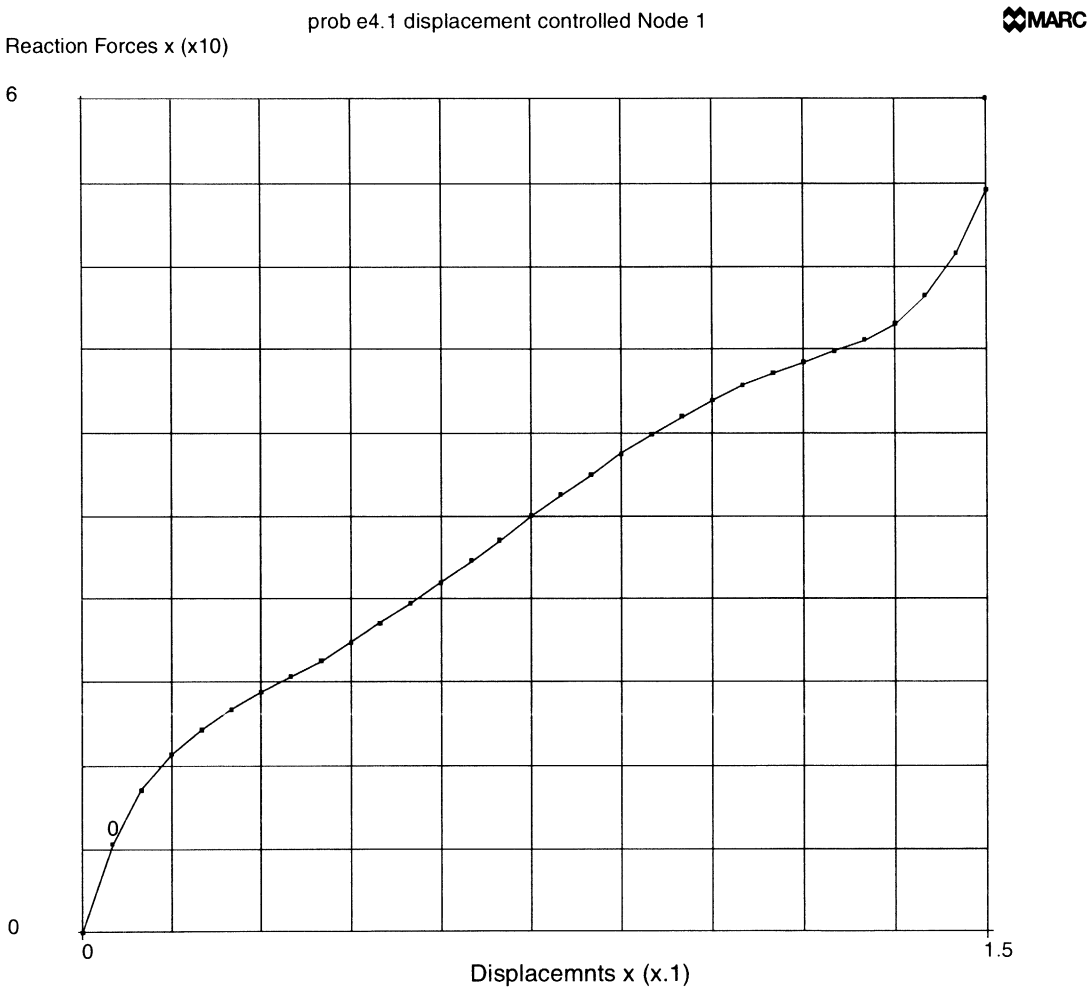

Figure 4.1-3 Point Loaded Shell Cap Displacement Loading

4.2 Square Plate under Distributed Load

A simply-supported square plate subjected to uniformly distributed pressure is analyzed. MARC element types 49, 75, 138, 139, and 140 are utilized. In the analysis, geometrically nonlinear effects are considered. The AUTO LOAD option is used for the load incrementation.

This problem is modeled using the four techniques summarized below.

Data Set	Element Type(s)	Number of Elements	Number of Nodes
e4x2	49	32	81
e4x2a	49	8	25
e4x2b	75	4	36
e4x2c	138	50	36
e4x2d	139	25	36
e4x2e	140	25	36

Element

Library element type 49 is a 6-node triangular thin shell element.

Library element type 75 is a 4-node quadrilateral thick shell element.

Library element type 138 is a 3-node triangular thin shell element.

Library element type 139 is a 4-node quadrilateral thin shell element.

Library element type 140 is a 4-node quadrilateral thick shell element.

The length to thickness ratio is 10/0.25 = 40, which suggests that the thin shell theory is appropriate for this problem.

Model

The dimensions of the plate and the finite element mesh are shown in Figure 4.2-1. Based on symmetry considerations, only one quarter of the plate is modeled.

Material Properties

The material is elastic with a Young's modulus of 10×10^6 N/mm^2 and a Poisson's ratio of 0.3.

Geometry

A uniform thickness of 0.25 mm is assumed. In thickness direction, three layers are chosen using the SHELL SECT parameter.

Boundary Conditions

Symmetry conditions are imposed on the edges x = 10 ($u_x = 0$, $\phi = 0$) and y = 10 ($u_y = 0$, $\phi = 0$). Notice that the rotation constraints only apply for the midside nodes. Simply supported conditions are imposed on the edges x = 0 and y = 0 ($u_x = u_y = u_z = 0$).

Loading

A uniform pressure load of 50 N/mm^2 is applied in ten equally sized increments. The default control settings are used. Convergence control is accomplished by a check on relative residuals with a tolerance of 0.1.

Results

The displacement history of node 1 is shown in Figure 4.2-2. For increment 10, stress contours of the von Mises stress in the outer layers are shown in Figure 4.2-3 and Figure 4.2-4. Due to the geometrically nonlinear effects, the stress distribution is clearly not symmetric with respect to the midplane of the plate. The deflections at the center of the plate are given by:

Pressure (N/mm^2)	Normalized Deflection w/h						
	e4x2	e4x2a	e4x2b	e4x2c	e4x2d	e4x2e	Reference
10	0.86	0.77	0.92	0.67	0.90	0.91	0.84
20	1.14	1.08	1.28	1.04	1.19	1.20	1.17
30	1.32	1.29	1.51	1.35	1.39	1.40	1.37
40	1.47	1.46	1.69	1.50	1.54	1.56	1.53
50	1.59	1.59	1.83	1.63	1.67	1.69	1.65

The reference solution can be found in "Bending of Rectangular Plates with Large Deflection" by S. Levy in the NACA Report 737, Washington, DC, 1942.

Parameters, Options, and Subroutines Summary

Example e4x2a.dat and e5x2a.dat:

Parameters	Model Definition Options	History Definition Options
ALL POINTS	CONNECTIVITY	AUTO LOAD
ELEMENTS	COORDINATES	CONTINUE
DIST LOADS	DEFINE	CONTROL
END	DIST LOADS	DIST LOAD
LARGE DISP	END OPTION	TIME STEP
SET NAME	FIXED DISP	
SHELL SECT	GEOMETRY	
SIZING	ISOTROPIC	
	NO PRINT	
	OPTIMIZE	
	PRINT	
	SOLVER	

Example e4x2b.dat:

Parameters	Model Definition Options	History Definition Options
ALL POINTS	CONNECTIVITY	AUTO LOAD
ELEMENTS	COORDINATES	CONTINUE
DIST LOADS	DEFINE	CONTROL
END	DIST LOADS	DIST LOAD
LARGE DISP	END OPTION	TIME STEP
SET NAME	FIXED DISP	
SHELL SECT	GEOMETRY	
SIZING	ISOTROPIC	
	NO PRINT	
	OPTIMIZE	
	PRINT	
	SOLVER	

Example e4x2c.dat:

Parameters	Model Definition Options	History Definition Options
ALL POINTS	CONNECTIVITY	AUTO LOAD
ELEMENTS	COORDINATES	CONTINUE
DIST LOADS	DEFINE	CONTROL
END	DIST LOADS	DIST LOAD
LARGE DISP	END OPTION	TIME STEP
SET NAME	FIXED DISP	
SHELL SECT	GEOMETRY	
SIZING	ISOTROPIC	
	NO PRINT	
	OPTIMIZE	
	PRINT	
	SOLVER	

Example e4x2d.dat:

Parameters	Model Definition Options	History Definition Options
ALL POINTS	CONNECTIVITY	AUTO LOAD
ELEMENTS	COORDINATES	CONTINUE
DIST LOADS	DEFINE	CONTROL
END	DIST LOADS	DIST LOAD
LARGE DISP	END OPTION	TIME STEP
SET NAME	FIXED DISP	
SHELL SECT	GEOMETRY	
SIZING	ISOTROPIC	
	NO PRINT	
	OPTIMIZE	
	PRINT	
	SOLVER	

Example e4x2e.dat:

Parameters	Model Definition Options	History Definition Options
ALL POINTS	CONNECTIVITY	AUTO LOAD
ELEMENTS	COORDINATES	CONTINUE
DIST LOADS	DIST LOADS	CONTROL
END	END OPTION	DIST LOAD
LARGE DISP	FIXED DISP	TIME STEP
SET NAME	GEOMETRY	
SHELL SECT	ISOTROPIC	
SIZING	NO PRINT	
	OPTIMIZE	
	POST	
	SOLVER	

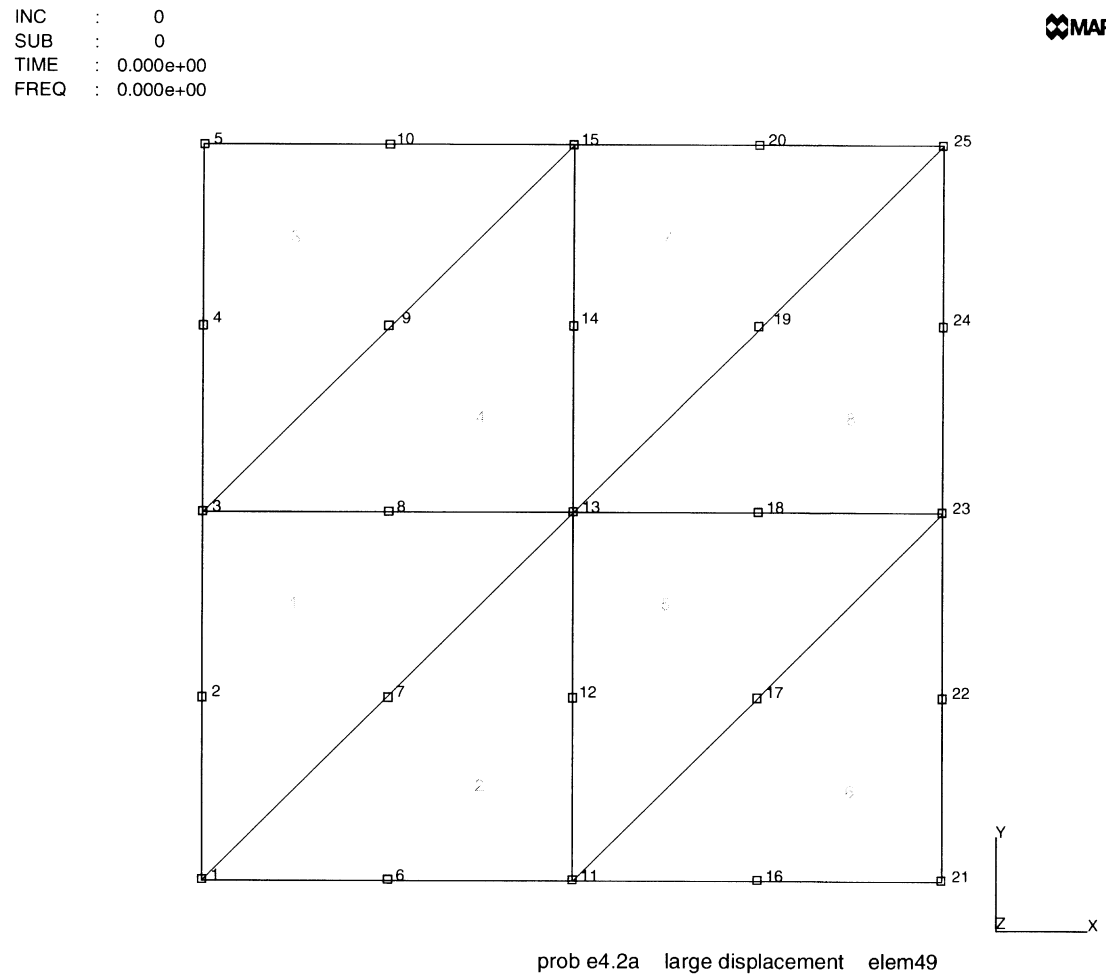

Figure 4.2-1 Square Plate, Finite Element Mesh, and Boundary Conditions

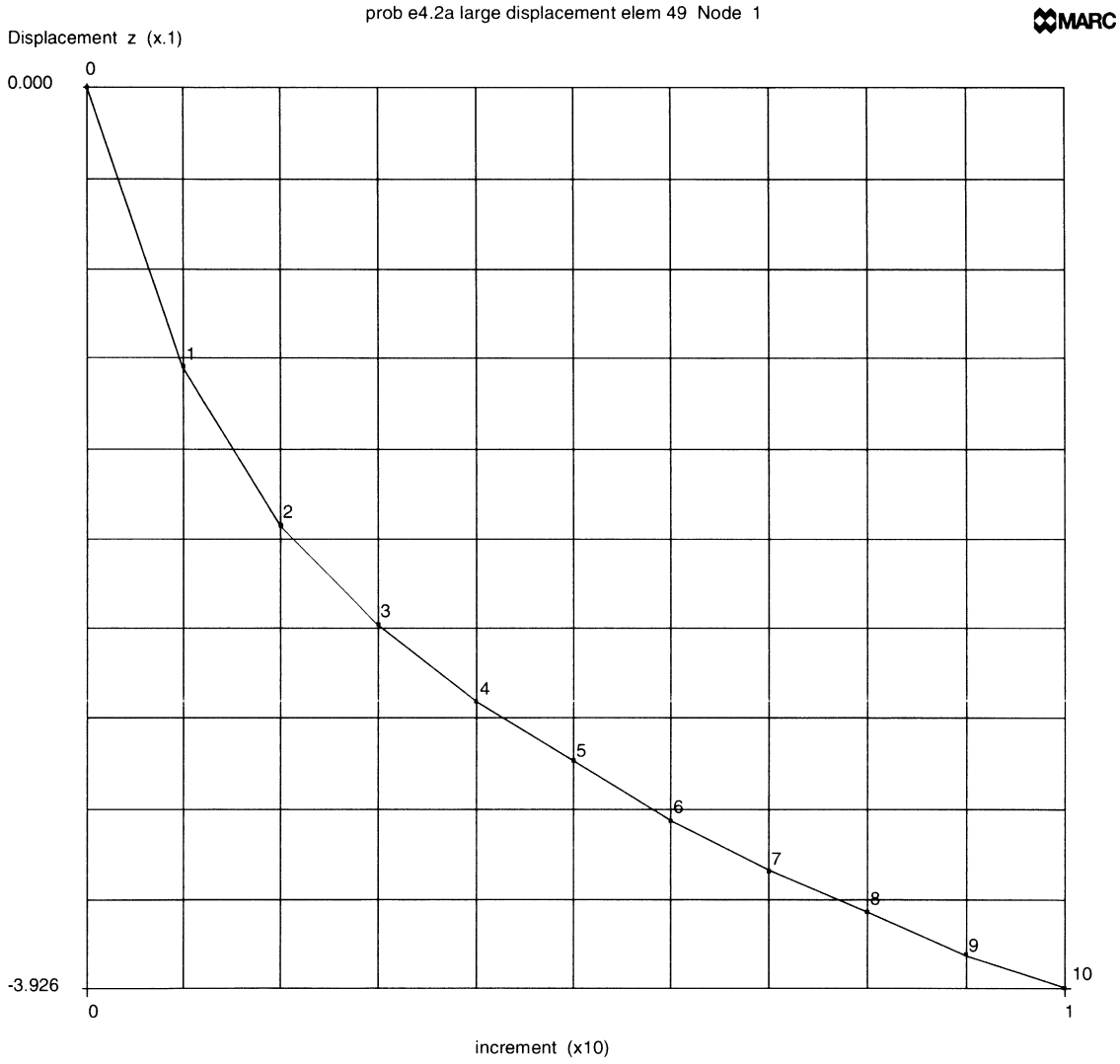

Figure 4.2-2 Node 1 Displacement History

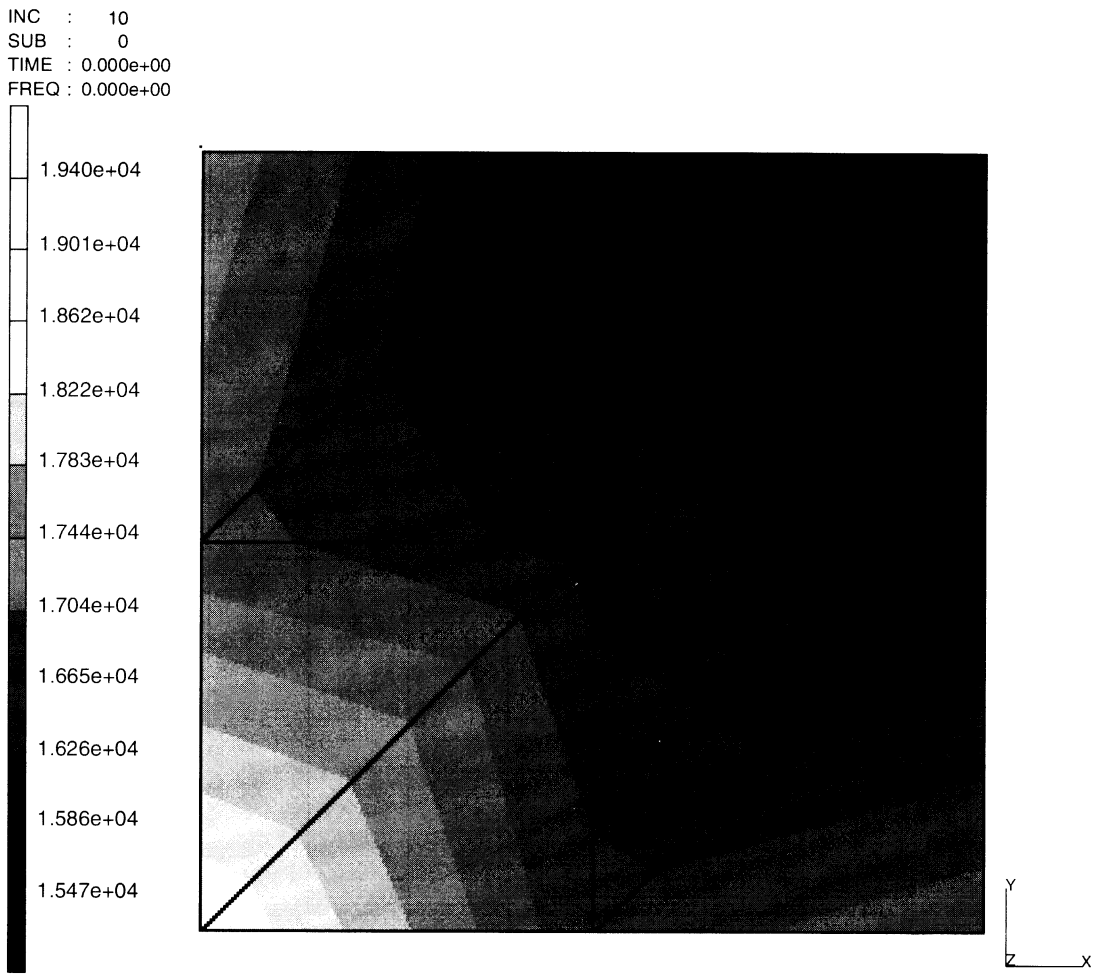

Figure 4.2-3 Stress Contour of von Mises Stress in Layer 1 (Increment 10)

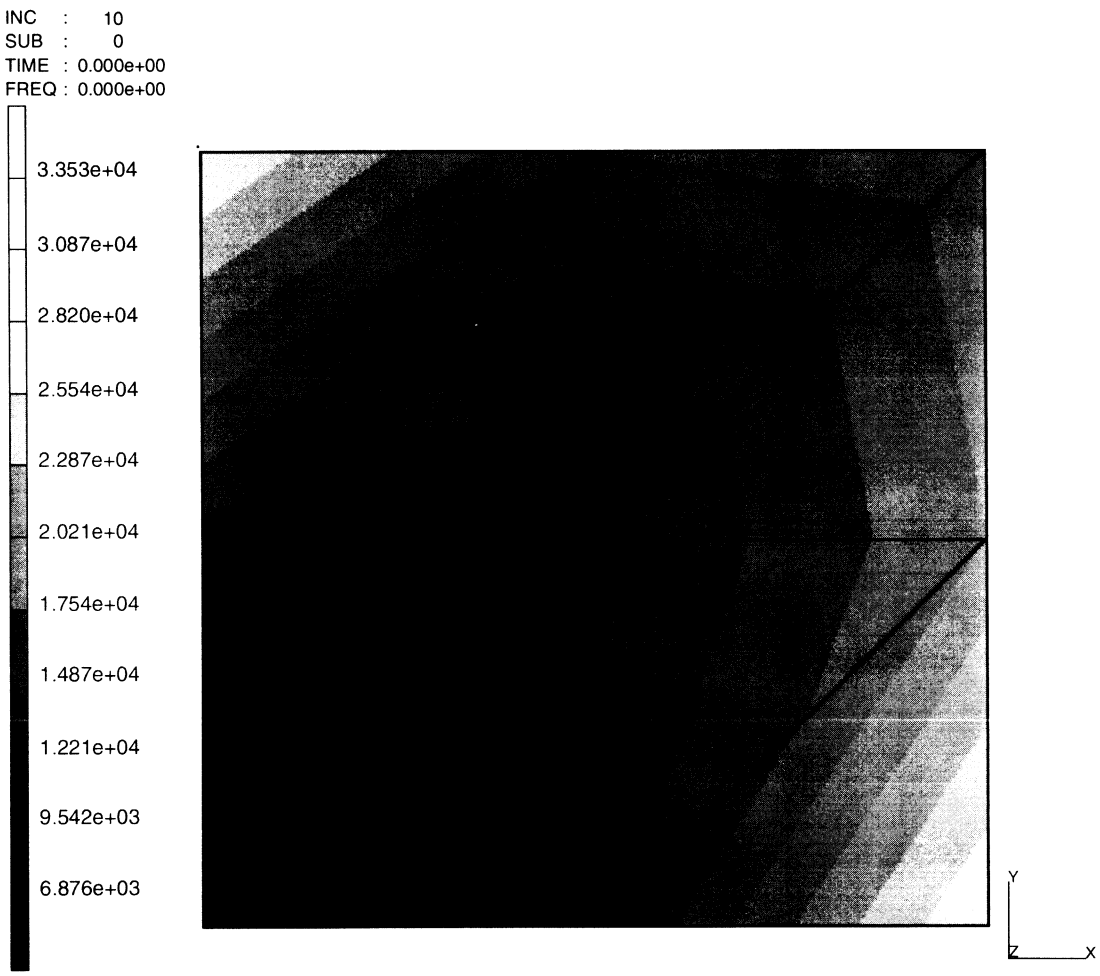

Figure 4.2-4 Stress Contour of von Mises Stress in Layer 3 (Increment 10)

4.3 Cantilever Beam under Point Load

An elastic, large displacement analysis is carried out for a cantilever straight pipe subjected to a tip load. This problem illustrates the use of MARC element type 25 (three-dimensional thin-walled beam) and options LARGE DISP, UPDATE, and ELSTO for large displacement analysis.

Model/Element

The beam, whose total length is 100 inches, is modeled using five elements and six nodal points. A plot of the beam and mesh is shown in Figure 4.3-1. Element 25 is a very accurate element to use for nonlinear beam analysis.

Material Properties

The material of the beam is assumed to be linear elastic with a Young's modulus of 31.63×10^6 psi and a Poisson's ratio of 0.3.

Geometry

The thickness of the circular beam cross section is 0.001 inch and the mean radius of the section is 3.00 inches.

Loading

A total point load of 2.7 pounds is applied at the tip of the beam in the negative y-direction. It is applied in ten equal load increments by using the AUTO LOAD option.

Boundary Conditions

All degrees of freedom at node 1 are constrained for the simulation of a fixed-end condition.

LARGE DISP

This option indicates that the problem is a large displacement analysis. The updated Lagrange technique is used in this analysis. The solution is obtained using the full Newton-Raphson method.

ELSTO

This option allows the use of out-of-core element storage for element data; this reduces the amount of workspace necessary.

Results

A load-deflection curve is shown in Figure 4.3-2. This is in excellent agreement with the solution given in Timoshenko. In increment one, several iterations were necessary, which indicates that the load applied in the zeroth linear increment was too large. Later increments required only one

iteration per increment. As this problem involves primarily rotational behavior, a high tolerance was placed on force residuals and a tight tolerance was placed on moment residuals. The displaced mesh is illustrated in Figure 4.3-3. Examination of the deformed structure indicates that very large rotations occurred. The output of the residual loads indicates that mesh refinement near the built-in end is necessary. Figure 4.3-4 shows the resultant moment diagram; this was obtained by using the LINEAR plot option.

Parameters, Options, and Subroutines Summary

Example e4x3.dat:

Parameters	Model Definition Options	History Definition Options
ELEMENT	CONNECTIVITY	AUTO LOAD
END	CONTROL	CONTINUE
LARGE DISP	COORDINATE	POINT LOAD
SIZING	END OPTION	
TITLE	FIXED DISP	
UPDATE	GEOMETRY	
	ISOTROPIC	
	POINT LOAD	
	RESTART	

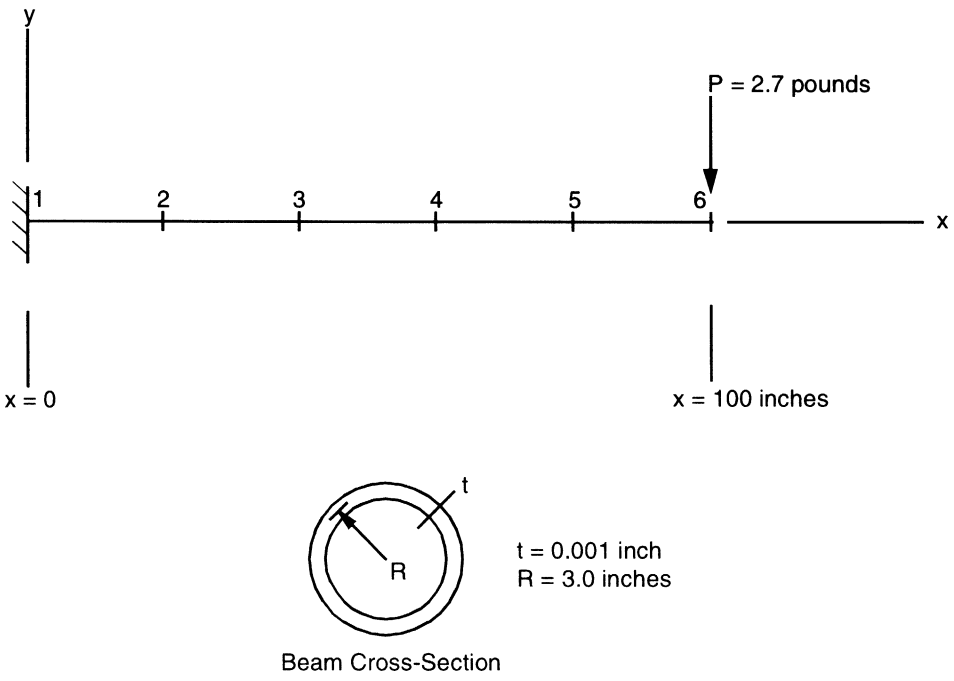

Figure 4.3-1 Cantilever Beam and Mesh

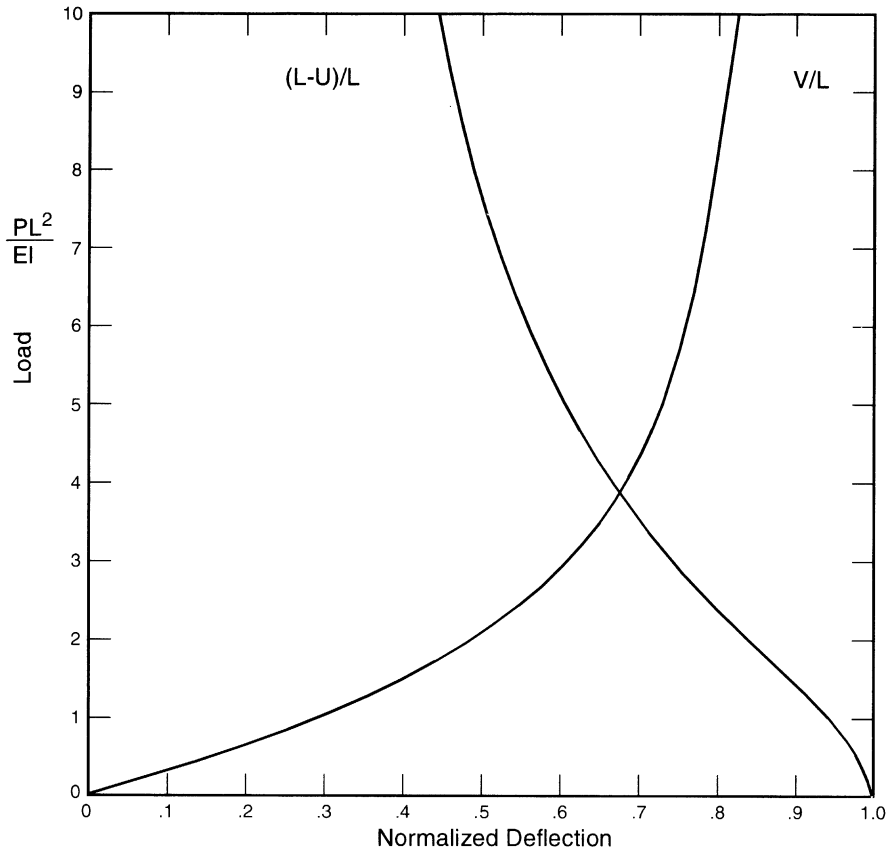

Figure 4.3-2 Load vs. Deflection

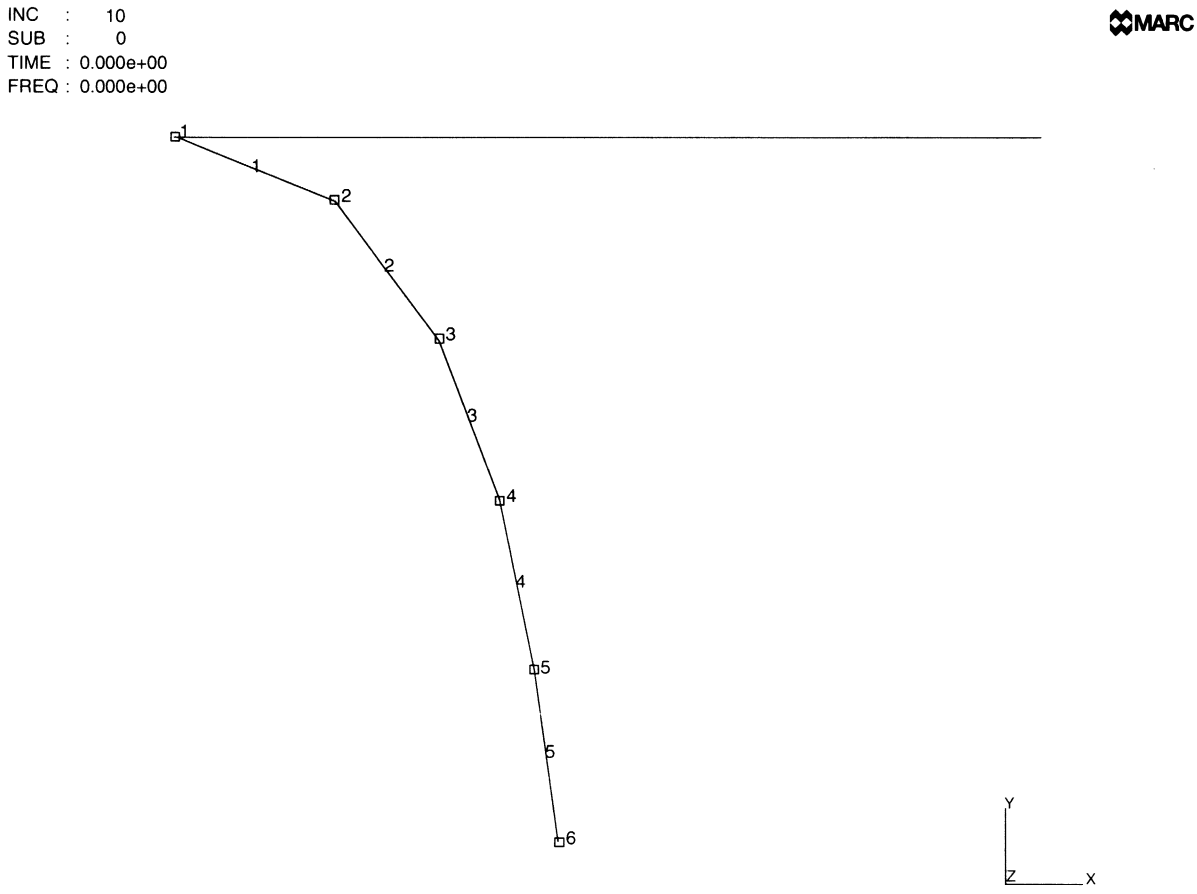

Figure 4.3-3 Displaced Mesh

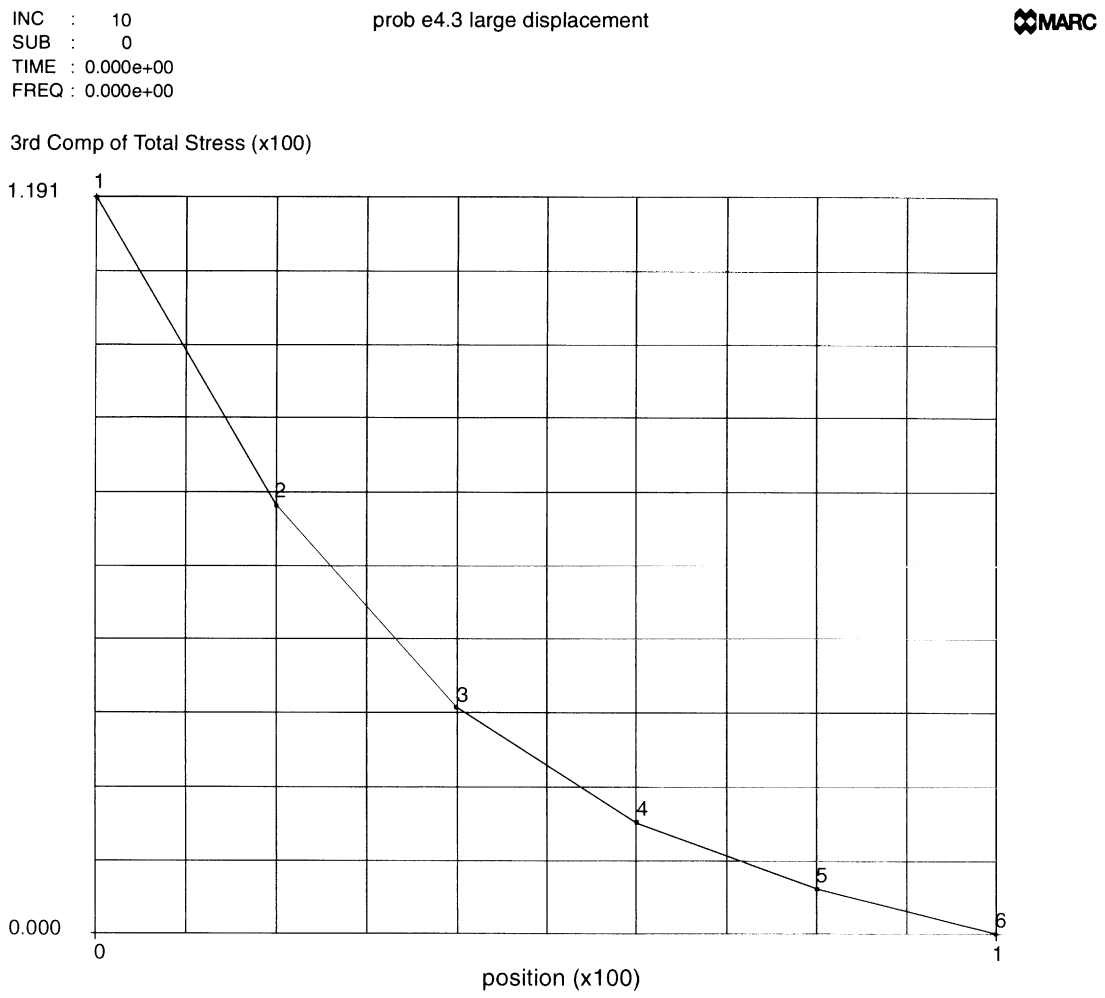

Figure 4.3-4 Moment Diagram

4.4 Axisymmetric Buckling of a Cylinder

An elastic buckling analysis is carried out for a short right cylinder subjected to axial compression. This problem illustrates the use of MARC element type 15 (axisymmetric shell element) and option LARGE DISP and BUCKLE for finding the first four buckling loads and mode shapes.

This problem is modeled using the two techniques summarized below.

Data Set	Element Type(s)	Number of Elements	Number of Nodes	Differentiating Features
e4x4	15	10	11	Inverse Power Sweep
e4x4b	15	10	11	Lanczos

Model/Element

They cylinder has a length of 100 inches and a radius of 80 inches. Because of symmetry, only one half of the cylinder is modeled.

The model consists of ten elements and 11 nodal points. Incremental mesh generation options CONN GENER and NODE FILL are used for the mesh generation. The cylinder and a finite element mesh are shown in Figure 4.4-1.

Material Properties

In this analysis, the Young's modulus and Poisson's ratio are assumed to be 1.0×10^4 psi and 0.3, respectively.

Geometry

The wall thickness of the cylinder is 2.5 inches (EGEOM1).

Loading

Two point loads, equal and opposite, are applied at nodal points 1 and 11. The magnitude of the load increment is 22,800 pounds. This load represents an integrated value along the circumference.

Boundary Conditions

Both ends of the cylinder are simply supported (v = 0, at nodes 1 and 11) and axial movement is constrained at the line of symmetry (u = 0 at node 6).

Buckle

The parameter BUCKLE indicates a buckling analysis is to be performed in this problem. It also asks for a maximum number of four buckling modes to be estimated. It is also used to indicate which method, the inverse power sweep or the Lanczos, is to be used.

In the load incrementation block, the BUCKLE option allows the use to input control values for eigenvalue extractions. The default values of 40 iterations and 0.0001 convergence tolerance are used for this analysis. The AUTO LOAD option allows you to apply additional load increment prior to the eigenvalue extraction.

Results

Eigenvalues and collapse load estimations are identical for e4x4 and e4x4b as expected and are shown in Table 4.4-1 and mode shapes are depicted in Figure 4.4-2. The PRINT CHOICE option was used to restrict the printout to integration point 2 of element 1.

The analytic solution for the critical load is 189 psi, as given in Timoshenko and Gere's *Theory of Elastic Stability.*

Table 4.4-1 Cylinder Buckling (Eigenvalues and Collapse Load Estimations)

Eigenvalues (λ)					
Mode	**Inc 0**	**Inc 1**	**Inc 2**	**Inc 3**	**Inc 4**
1		7.81	6.79	5.71	4.65
2		10.63	9.57	8.40	7.23
3		18.04	16.87	15.48	14.05
4		25.83	24.51	15.49	20.66
Previous Load: (N-Multiple of ΔP)					
Mode	**Inc 0**	**Inc 1**	**Inc 2**	**Inc 3**	**Inc 4**
1	1	2	3	4	5
2	1	2	3	4	5
3	1	2	3	4	5
4	1	2	3	4	5
Collapse Load Estimations: ($N_{i-1} + \lambda_i$, i = 1, 4, multiple of ΔP)					
Mode	**Inc 0**	**Inc 1**	**Inc 2**	**Inc 3**	**Inc 4**
1		9.81	9.79	9.71	9.65
2		12.63	12.57	12.40	12.23
3		20.04	19.87	19.48	19.05
4		27.83	27.51	19.49	25.66

Note: First Mode Collapse Load= 9.65 ΔP = 9.65 x 22,769 = 219,721

Critical Load= 219,721/(2π x 2.5 x 80) = 175 psi

Parameters, Options, and Subroutines Summary

Example e4x4.dat and e4x4b.dat:

Parameters	Model Definition Options	History Definition Options
BUCKLE	CONN GENER	AUTO LOAD
ELEMENT	CONNECTIVITY	BUCKLE
END	CONTROL	CONTINUE
LARGE DISP	COORDINATE	
SIZING	END OPTION	
TITLE	FIXED DISP	
	GEOMETRY	
	ISOTROPIC	
	NODE FILL	
	POINT LOAD	
	PRINT CHOICE	

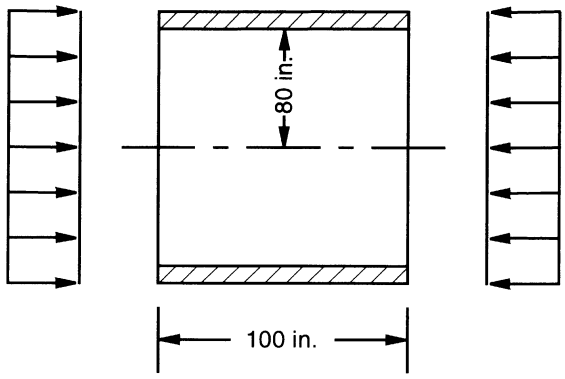

MARC

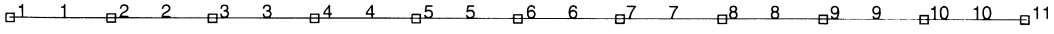

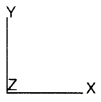

Figure 4.4-1 Cylinder Buckling

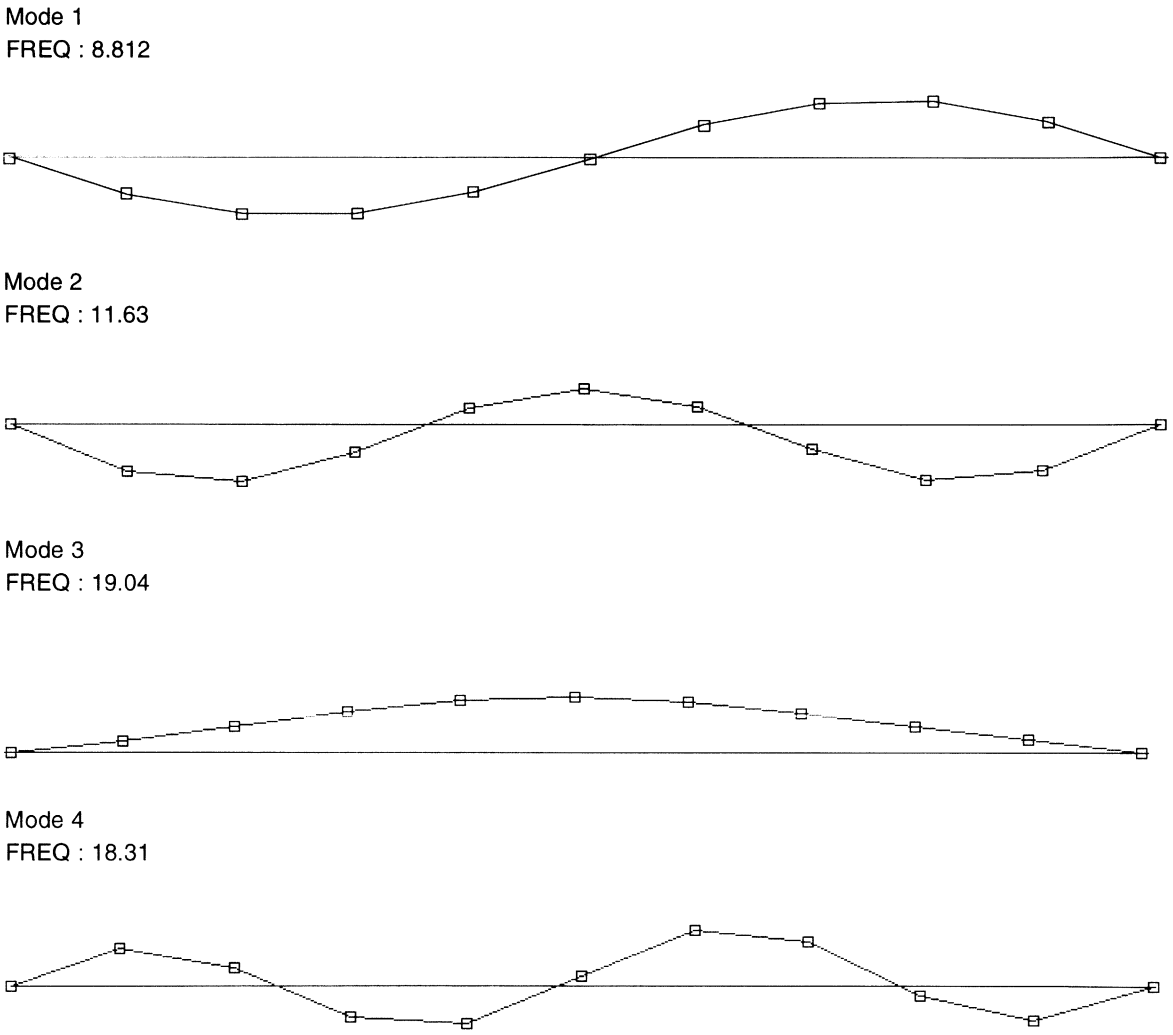

Figure 4.4-2 Mode Shapes

4.5 Large Displacement Analysis of a Pinched Cylinder

An elastic, large displacement analysis is carried out for a pinched cylinder subjected to a line load. This problem illustrates the use of MARC element type 22 (8-node thick shell element) and option LARGE DISP for a large displacement analysis.

Model/Element

The mesh consists of eight elements (type 22) and 37 nodal points. The dimensions of the cylinder and a finite element mesh are shown in Figure 4.5-1 and Figure 4.5-2. The coordinates are first generated in a plane. User subroutine UFXORD is then used for the modification of nodal coordinates. Bandwidth optimization option OPTIMIZE is also chosen for renumbering the mesh.

Material Properties

The Young's modulus and Poisson's ratio are assumed to be 30 x 10^6 psi and 0.3, respectively.

Loading

Total nodal forces of 100, 400, 200, 400, and 100 pounds are applied at nodal points 34, 35, 36, 37, and 17, respectively. The loads are applied in 10 equal increments through the AUTO LOAD option.

Boundary Conditions

Degrees of freedom are constrained at the lines of symmetry.

Results

A displaced mesh is shown in Figure 4.5-3 and stress contours are depicted in Figure 4.5-4. As anticipated, the largest stresses are near the cutout. This problem converges to typically 2% error in equilibrium in one to two iterations.

Parameters, Options, and Subroutines Summary

Example e4x5.dat:

Parameters	Model Definition Options	History Definition Options
ELEMENT	CONNECTIVITY	AUTO LOAD
ELSTO	CONTROL	CONTINUE
END	COORDINATE	
LARGE DISP	END OPTION	
SIZING	FIXED DISP	
TITLE	GEOMETRY	
	ISOTROPIC	
	OPTIMIZE	
	POINT LOAD	
	POST	
	RESTART	
	UFXORD	

User subroutine in u4x5.f:

UFXORD

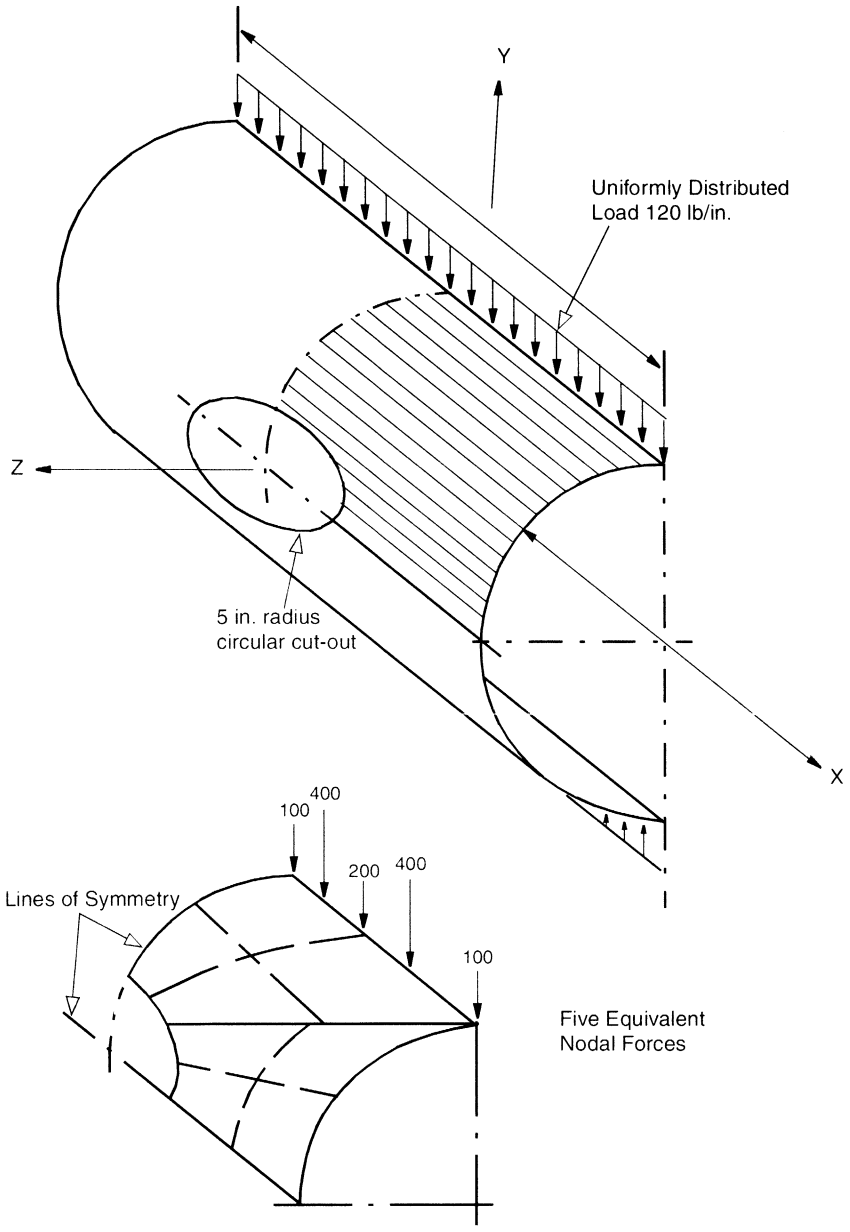

Figure 4.5-1 Pinched Cylinder and Mesh Blocks

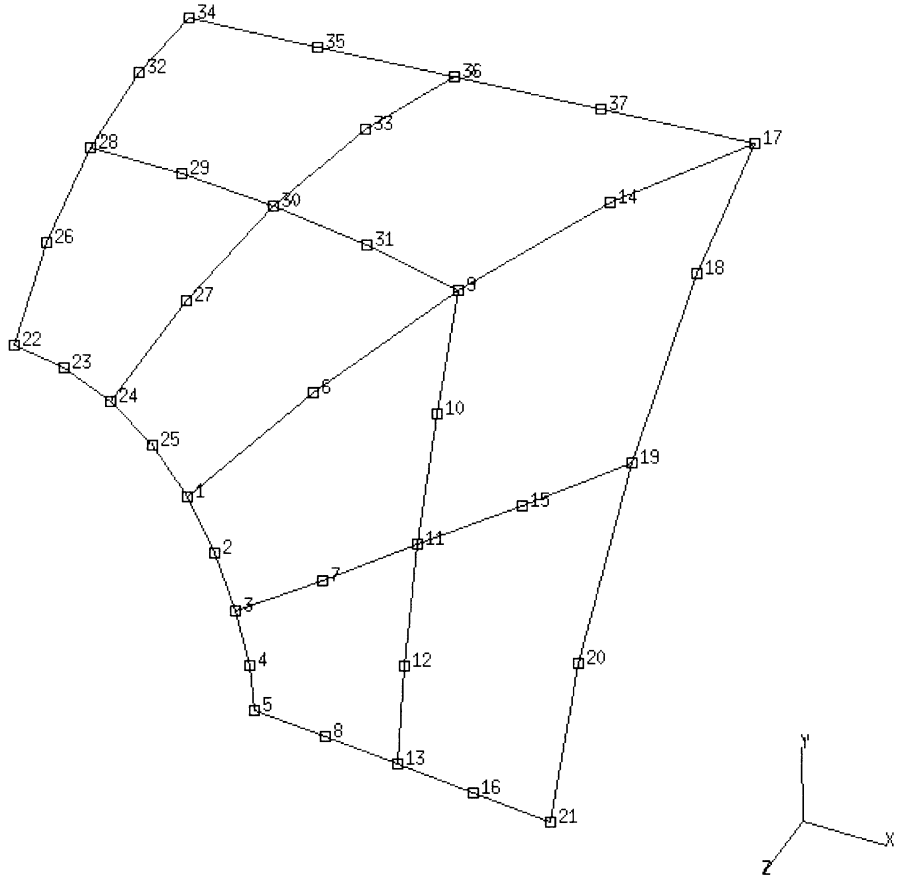

Figure 4.5-2 Finite Element Mesh for a Pinched Cylinder

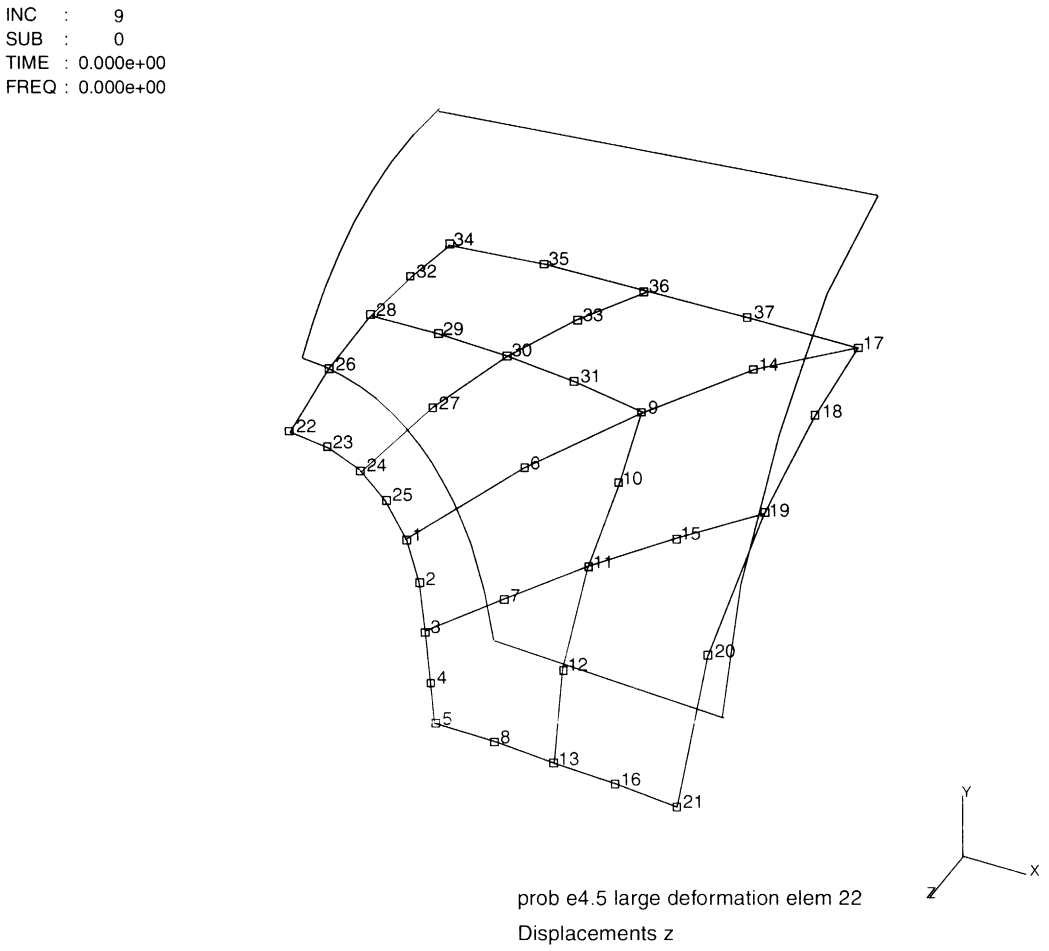

Figure 4.5-3 Displaced Mesh for a Pinched Cylinder

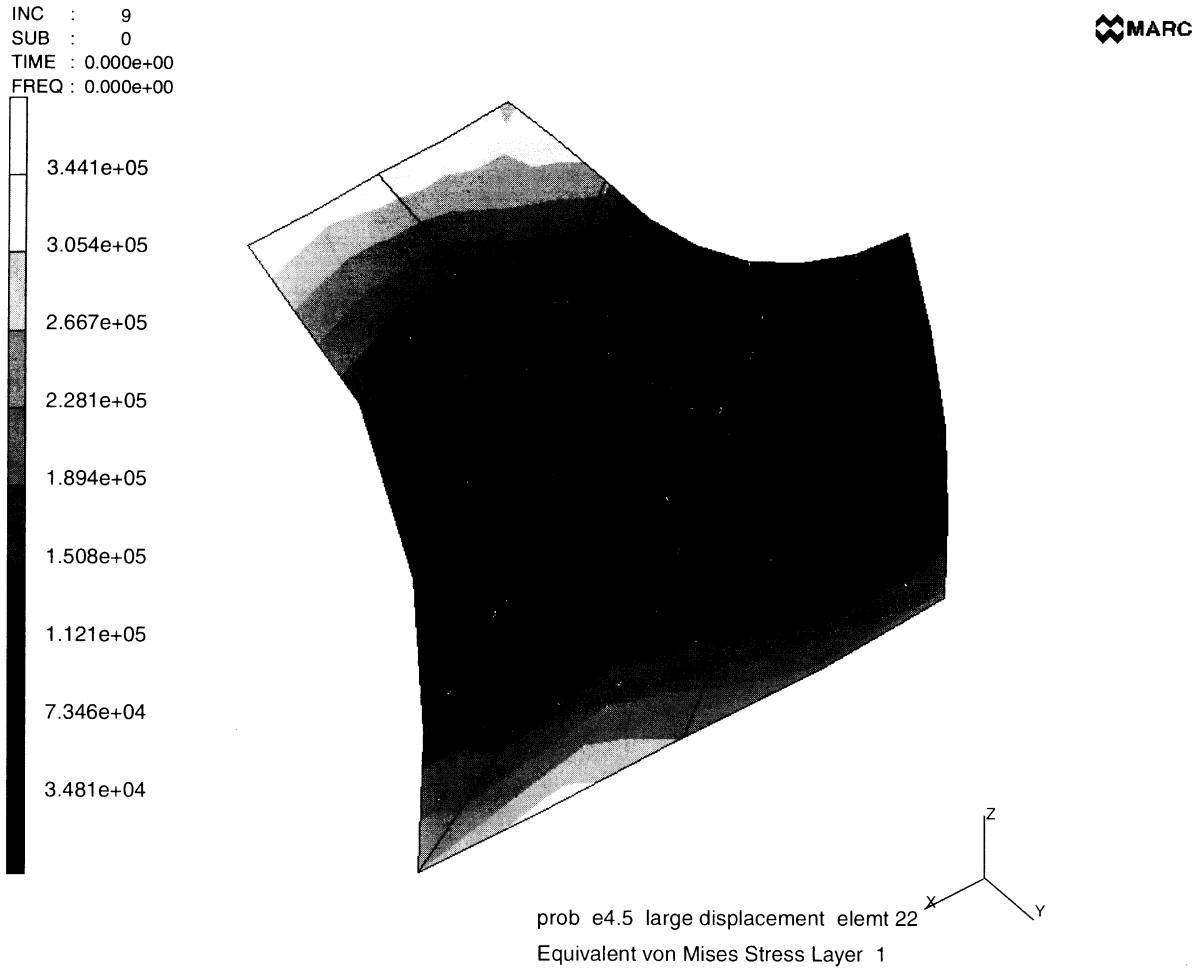

Figure 4.5-4 Stress Contours Equivalent Stress

4.6 One-Dimensional Elastic Truss-Spring System

A linear truss-spring system is analyzed by using the MARC element type 9 and the SPRINGS and LARGE DISP options.

Model

The model consists of one truss element and a linear spring. Dimensions of the model and a finite element mesh are shown in Figure 4.6-1.

Material Properties

The modulus of elasticity and Poisson's ratio of the truss element are assumed to be 1.0×10^7 and 0.3, respectively.

Boundary Conditions

One end of the truss element (node 1) is assumed to be fixed and the other end of the truss element is constrained to move only in the vertical direction.

Geometry

The truss has a unit cross-sectional area.

Loading

A concentrated force of 30 pounds is applied at node 2 in the negative y-direction. Various load increments (0.5, 0.1, and 1.0) were used in the analysis.

Springs

As shown in Figure 4.6-1, the moving end of the truss is supported by a linear spring. The spring constant is assumed to be 6 lb/in.

Auto Load

The total load of 30 pounds has been subdivided into four loading sequences. A different incremental load was used in each sequence. As an alternative, AUTO INCREMENT could have been used to adaptively adjust the load.

Results

The MARC finite element solution is shown in Figure 4.6-2. The exact solution (smooth curve) was obtained by numerical integration using a Runge-Kutta technique.

Parameters, Options, and Subroutines Summary

Example e4x6.dat:

Parameters	Model Definition Options	History Definition Options
ELEMENT	CONNECTIVITY	AUTO LOAD
END	CONTROL	CONTINUE
LARGE DISP	COORDINATE	POINT LOAD
SIZING	END OPTION	
TITLE	FIXED DISP	
	GEOMETRY	
	ISOTROPIC	
	POINT LOAD	
	SPRINGS	

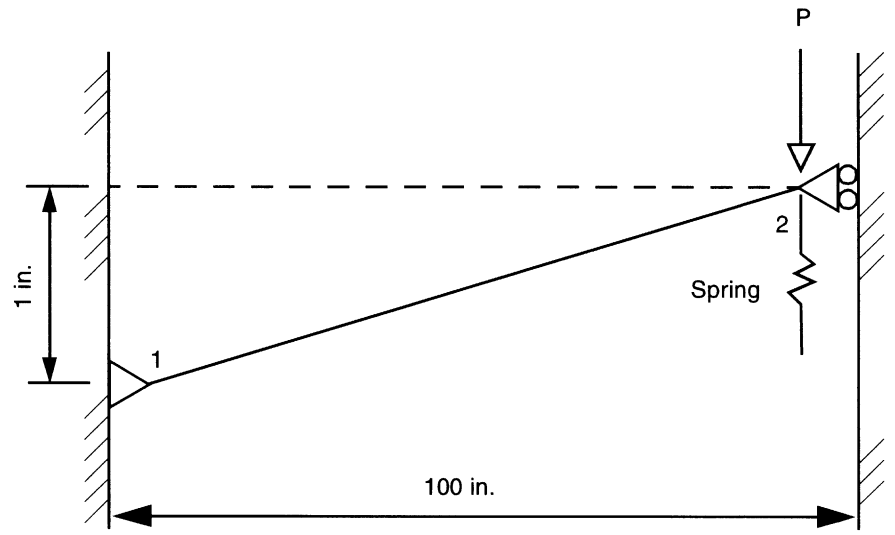

Figure 4.6-1 Truss-Spring System

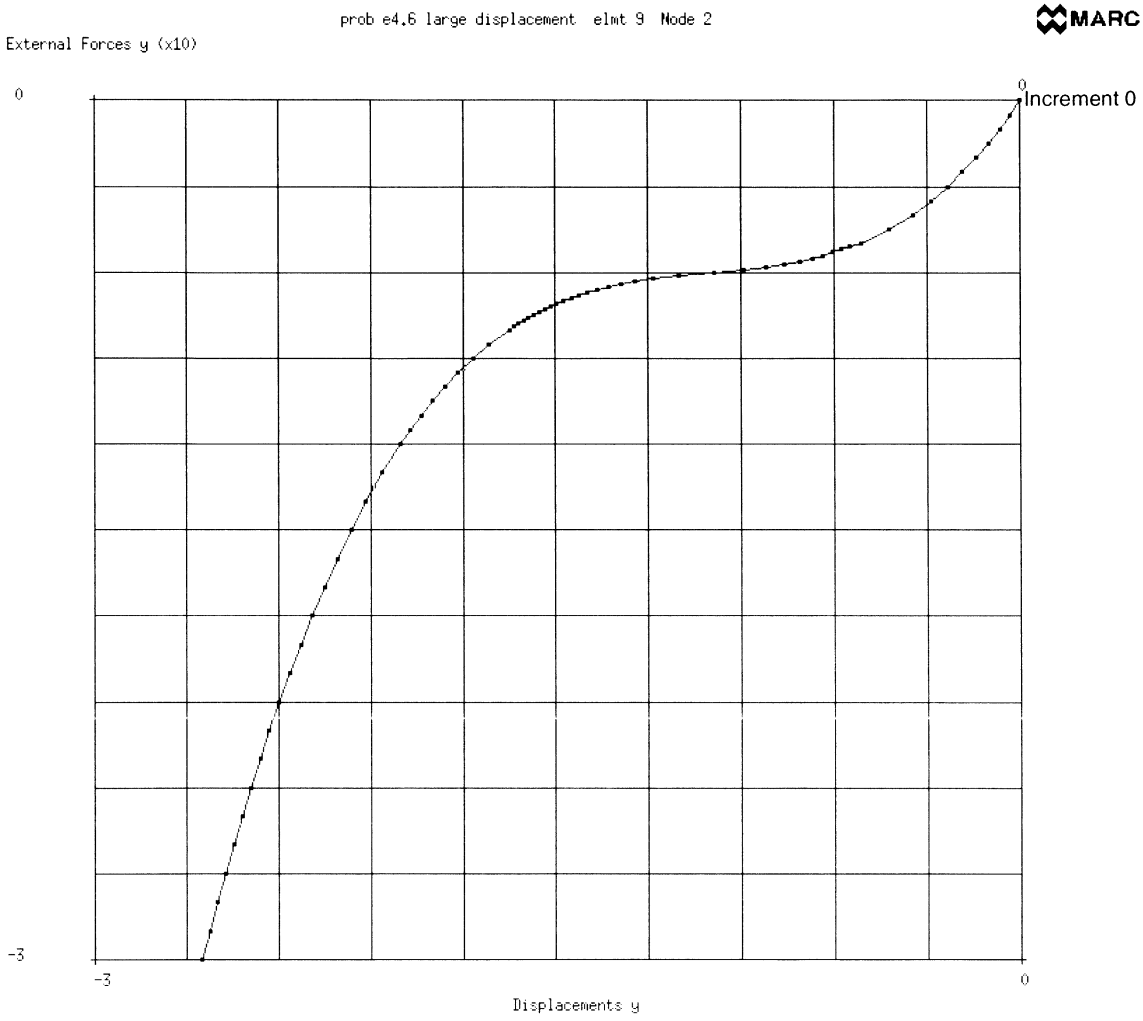

Figure 4.6-2 Load vs. Displacement at Node 2

4.7 Post-Buckling Analysis of a Deep Arch

A point load is applied to the apex of a semicircular arch. The arch gradually collapses as the applied load is incremented. The arch configuration after collapse is calculated and plotted. The load-displacement curve at the apex is plotted. This analysis utilizes the AUTO INCREMENT option to control the magnitude of the incremental solution and, hence, the magnitude of the load increment. The second analysis is the same as the first, but the arch is not allowed to penetrate itself. The analysis is performed elastically for both the pre- and post-buckling configurations.

This problem is modeled using the three techniques summarized below.

Data Set	Element Type(s)	Number of Elements	Number of Nodes	Differentiating Features
e4x7	16	20	21	AUTO INCREMENT
e4x7b	16	20	21	AUTO INCREMENT and CONTACT
e4x7c	16	20	21	AUTO STEP

Element

Element type 16 is a 2-node curved beam, with cubically interpolated global displacement and displacement derivatives. There are four degrees of freedom at each node. Membrane and curvature strains are output as well as axial stresses through the element thickness.

Model

The arch is modeled using 20 beam elements and 21 nodes. Only connectivity of element 1 is specified in the input. The connectivities for elements 2 through 21 are generated by option CONN GENER using element 1 as a model. The node coordinates are generated using user subroutine UFXORD. The coordinates are generated around a semicircle of radius 100 inches subtending an angle of 215 degrees. The finite element mesh is shown in Figure 4.7-1.

Material Properties

A Young's modulus of 12.0 x 10^6 psi and a Poisson's ratio of 0.2 are specified in the ISOTROPIC option.

Geometry

The beam thickness is 1 inch, as specified in EGEOM1. The width of the arch elements are specified as 1 inch in EGEOM2. Omission of the third field indicates a constant beam thickness.

Loading

The total applied load is specified in the POINT LOAD block, following the END OPTION. A total load of 1200 pounds is applied at node 11, over a maximum of 300 increments. The maximum load that can be applied in the first increment is 10% of the total load, or 120 pounds. These maxima are set in the AUTO INCREMENT option.

Boundary Conditions

The arch is pinned at one support and built in at the other. Thus, the degrees of freedom at node 1 (u and v) are constrained. At node 21, a coordinate transformation is carried out such that the boundary conditions here are simply specified. So, in the transformed coordinates at node 21, degrees of freedom u', v', and $\partial u'/\partial s$ are constrained.

Contact

The results of the first analysis indicate that the arch will pass through itself which is physically impossible. To prevent this, the second data set uses the CONTACT option.

This option declares that here is only one flexible body which is made up of 20 elements. In order to avoid unexpected separation, the high separation forces are entered as the arch hits the left support. Contact tolerance distance is 0.02 which is 2% of thickness of shell.

Notes

A 5% residual force relative error is specified in the CONTROL OPTION.

The option SHELL SECT reduces the number of integration points through the element thickness from a default value of 11 to the specified three points.This greatly reduces computation time with no loss of accuracy in an elastic analysis.

The PRINT parameter is set to 3. This option forces MARC to solve nonpositive definite matrices; this parameter is required for all post-buckling analyses.

The UPDATE parameter assembles the stiffness matrix of the current deformed configuration; as well, this parameter writes out the stresses and strains in terms of the current deformed geometry.

The UDUMP model definition option indicates by default that all nodes and all elements are made available for postprocessing by user subroutines IMPD and ELEVAR. In this example, the data is postprocessed to create a load-displacement curve for the arch.

Results Without CONTACT

The analysis ends in increment 75, at a load of 290.4 pounds. The total requested load is not reached due to an excessive number of recycles required for solution in the last increment. Resetting the maximum number of recycles and residual load tolerance allows the analysis to be continued using the RESTART file generated during the analysis. Displaced mesh plots are shown in Figure 4.7-2 (a) through Figure 4.7-3 (d). The displaced plots are obtained using the

second data set. The POSITION option is used to access the restart file at several different increments. The structure actually loops through the pinned support as there is no obstruction to this motion. A load-deflection curve is plotted for node 77 in Figure 4.7-4.

Results With CONTACT

In example e4x7b, as the CONTACT option is used, the left support prevents the arch from passing through and gives the reasonable deformation shape. Figure 4.7-5 through Figure 4.7-7 show a progression of the deformation. From the load deflection curve (Figure 4.7-8), you can observe the strong nonlinearities due to the contact which leads to a stiffening effect in the structure and a different snap-through behavior.

Parameters, Options, and Subroutines Summary

Example e4x7.dat:

Parameters	Model Definition Options	History Definition Options
END	CONN GENER	AUTO INCREMENT
LARGE DISP	CONNECTIVITY	CONTINUE
PRINT	CONTROL	POINT LOAD
SHELL SECT	END OPTION	
SIZING	FIXED DISP	
TITLE	GEOMETRY	
UPDATE	ISOTROPIC	
	PRINT CHOICE	
	RESTART	
	TRANSFORMATIONS	
	UDUMP	
	UFXORD	

User subroutine in u4x7.f:

UFXORD

Example e4x7b.dat:

Parameters	Model Definition Options	History Definition Options
END	CONNECTIVITY	AUTO INCREMENT
LARGE DISP	CONTACT	CONTINUE
PRINT	CONTROL	POINT LOAD
SHELL SECT	COORDINATE	
SIZING	END OPTION	
TITLE	FIXED DISP	
UPDATE	GEOMETRY	
	ISOTROPIC	
	PRINT CHOICE	
	POINT LOAD	
	POST	

Example e4x7c.dat:

Parameters	Model Definition Options	History Definition Options
END	CONN GENER	AUTO STEP
LARGE DISP	CONNECTIVITY	CONTINUE
PRINT	CONTROL	POINT LOAD
SHELL SECT	END OPTION	
SIZING	FIXED DISP	
TITLE	GEOMETRY	
UPDATE	ISOTROPIC	
	PRINT CHOICE	
	POINT LOAD	
	POST	
	TRANSFORMATIONS	
	UFXORD	

User subroutine in u4x7.f:

UFXORD

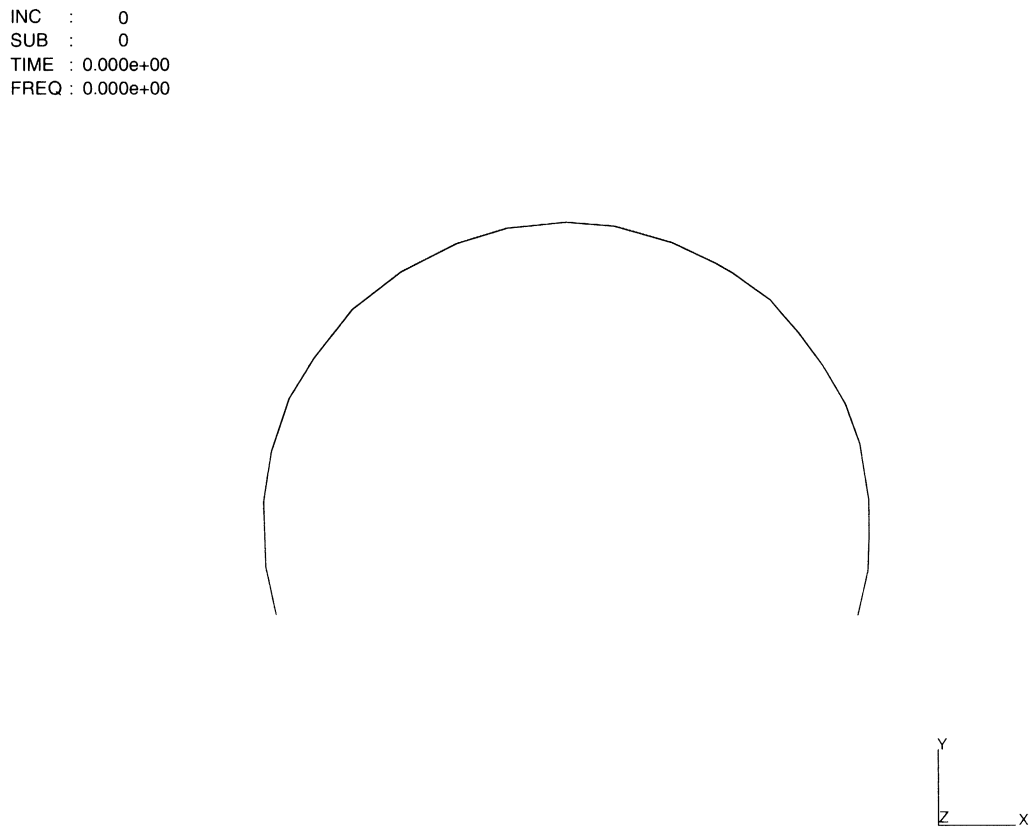

Figure 4.7-1 Deep Arch

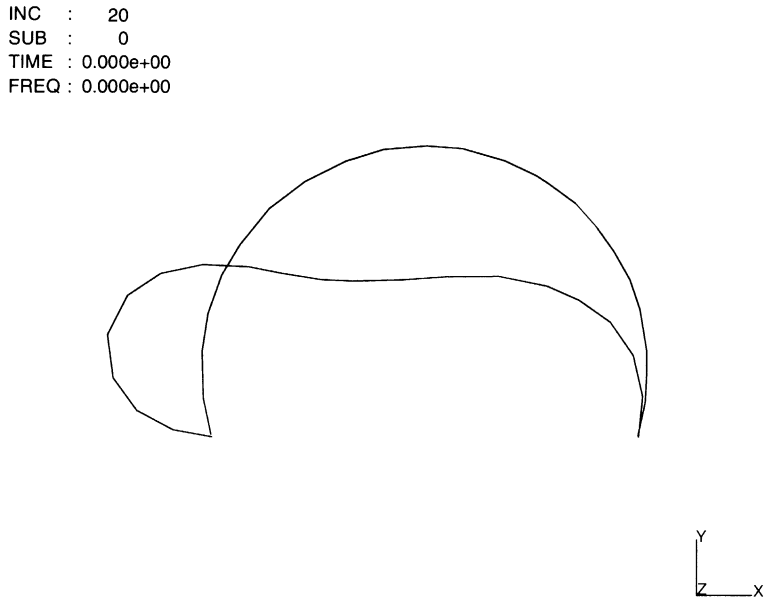

(a)

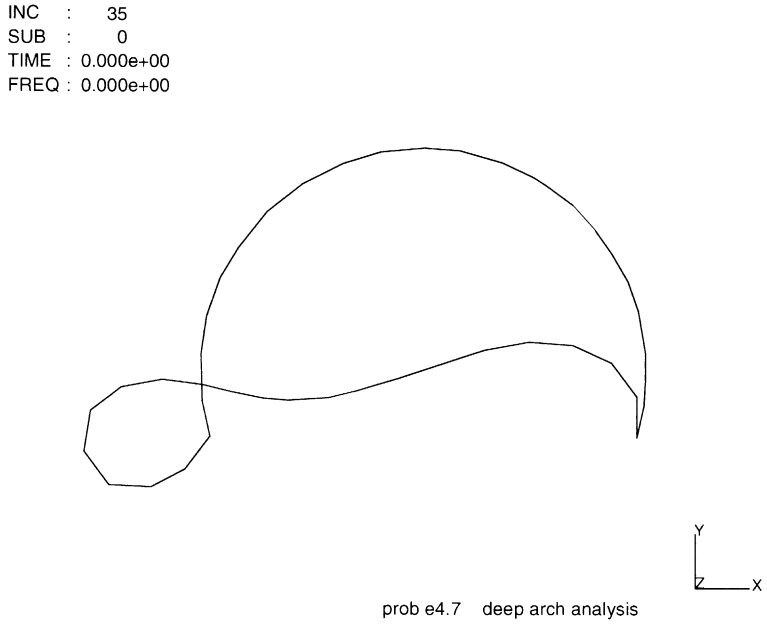

(b)

Figure 4.7-2 Displaced Mesh

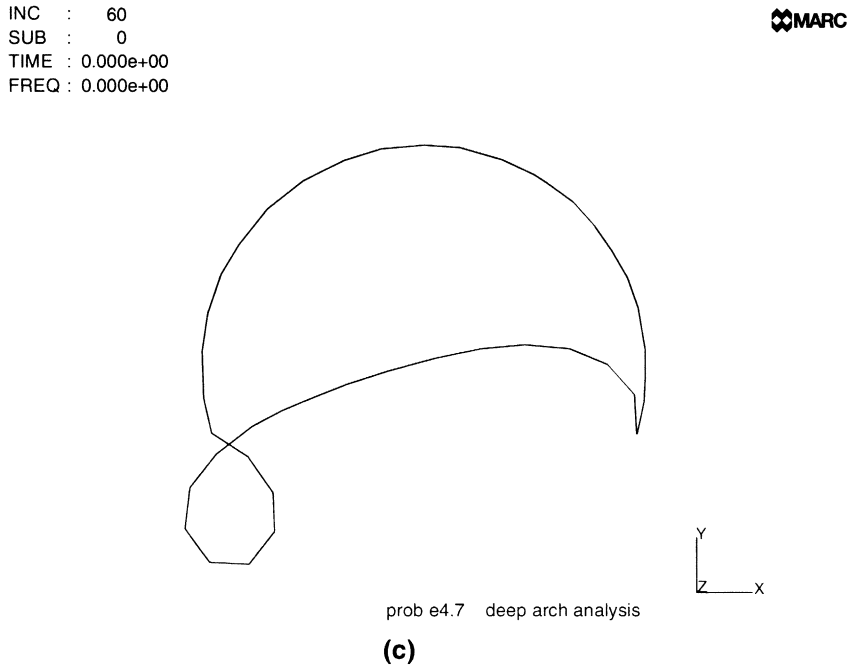

(c)

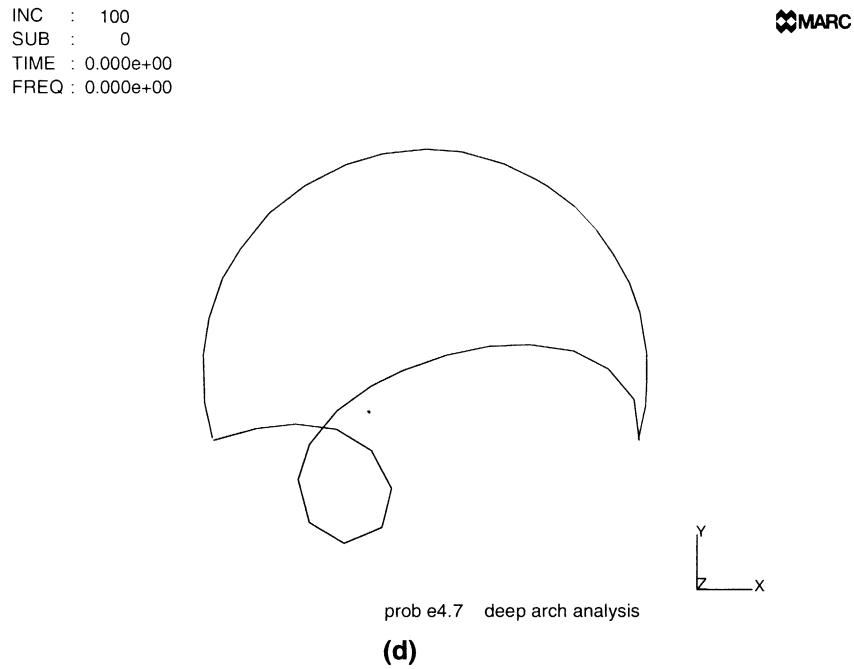

(d)

Figure 4.7-3 Displaced Mesh (Continued)

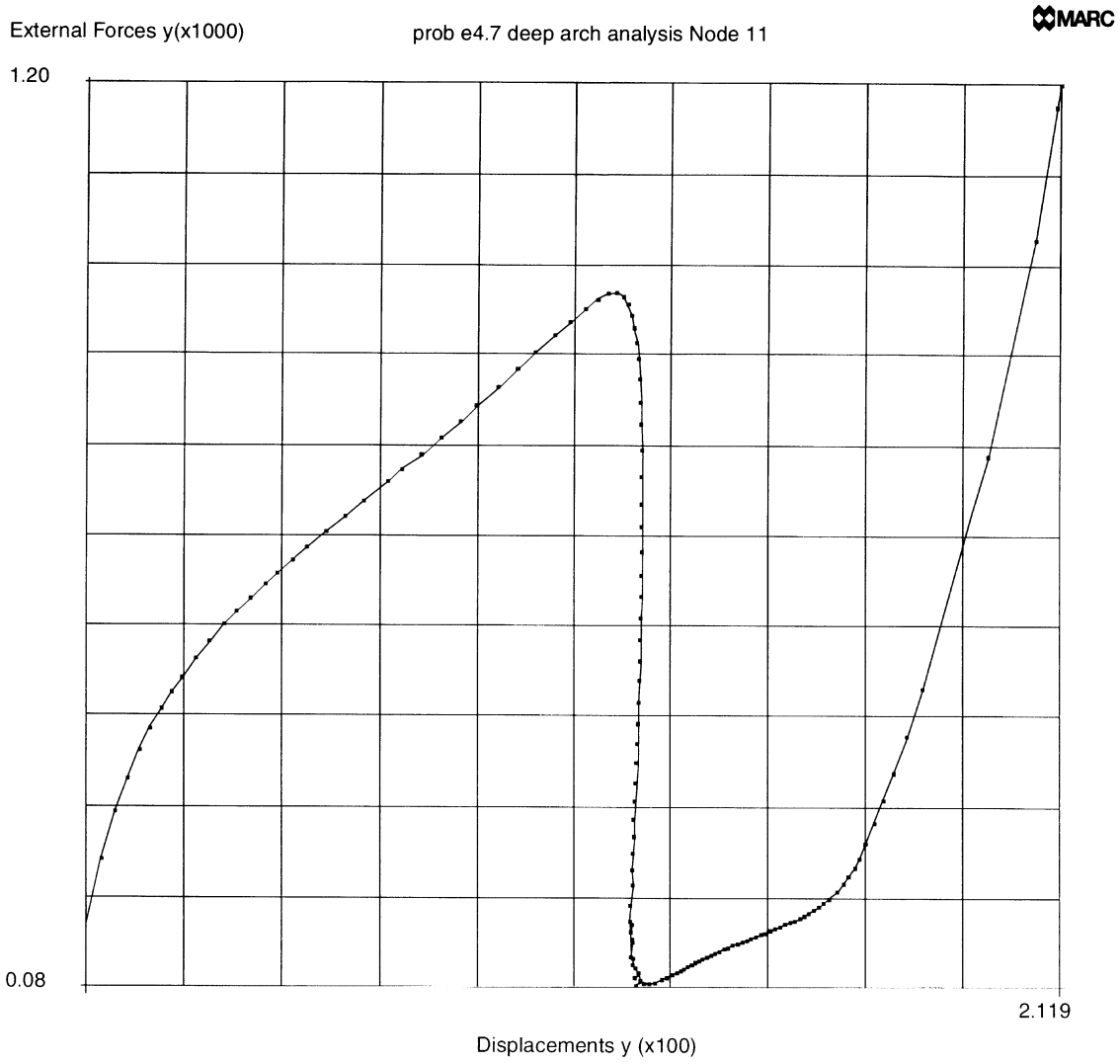

Figure 4.7-4 Load vs. Displacement (Node 77) – No Contact

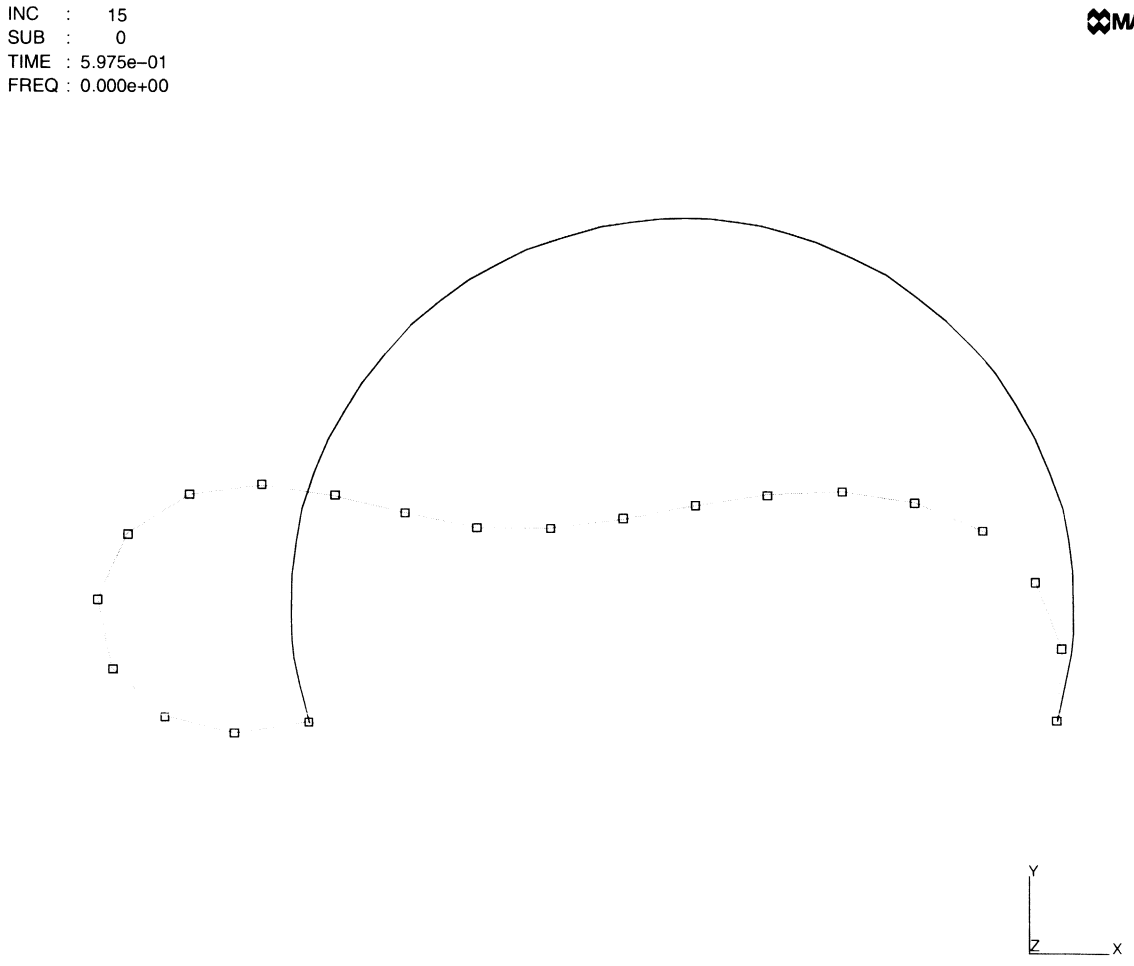

Figure 4.7-5 Displaced Mesh with Contact at Pin

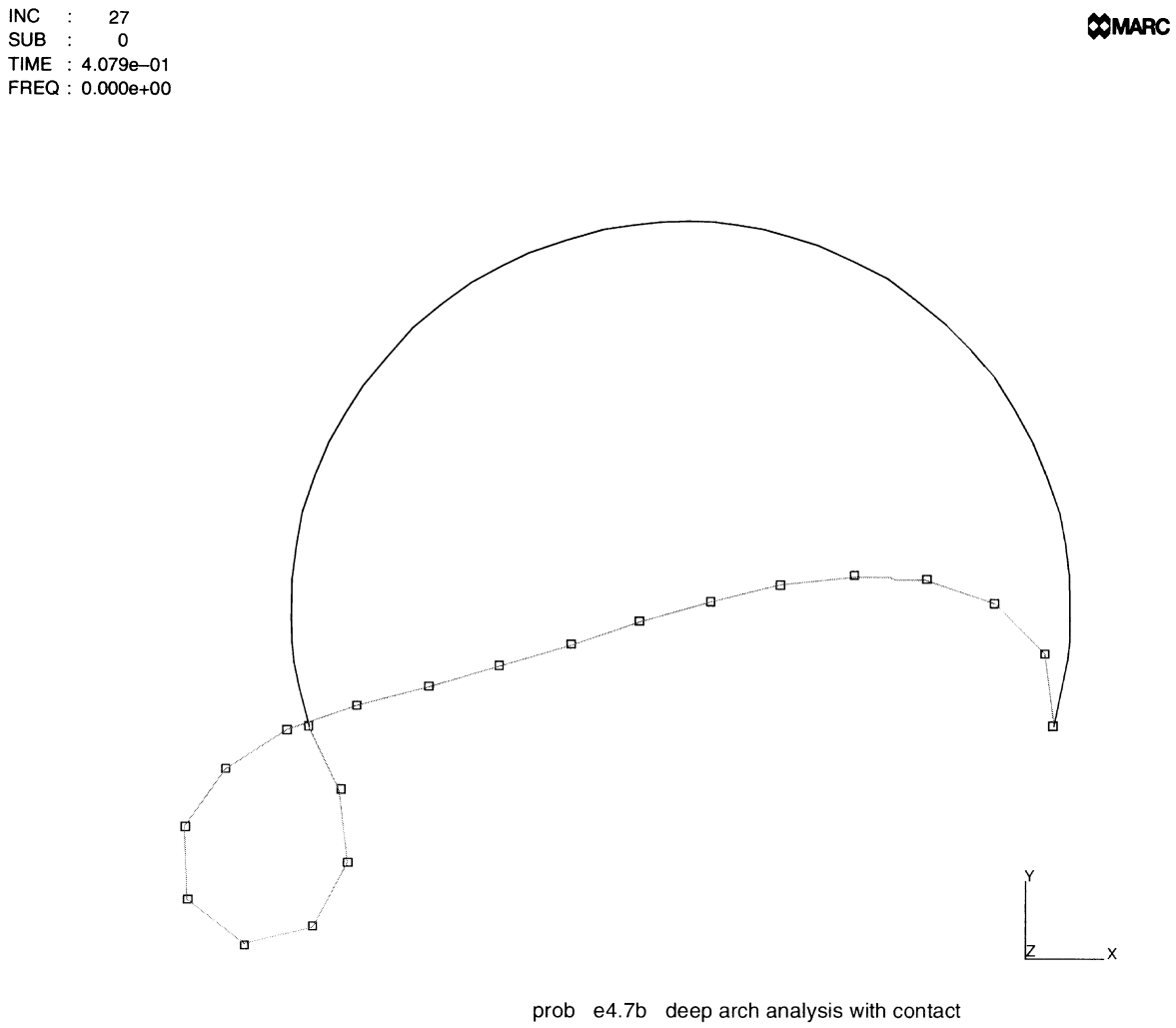

Figure 4.7-6 Displaced Mesh with Contact at Pin

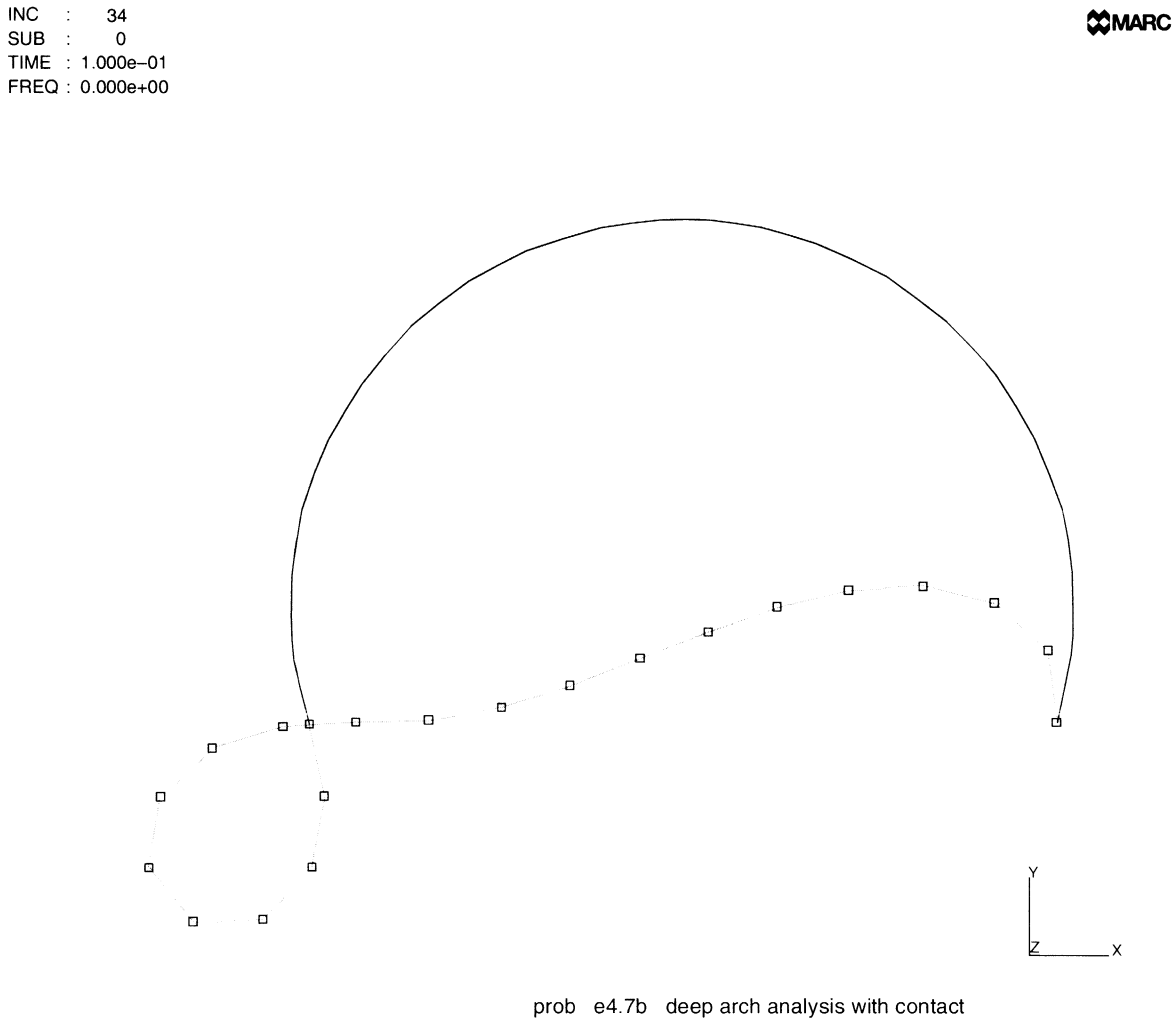

Figure 4.7-7 Displaced Mesh with Contact at Pin

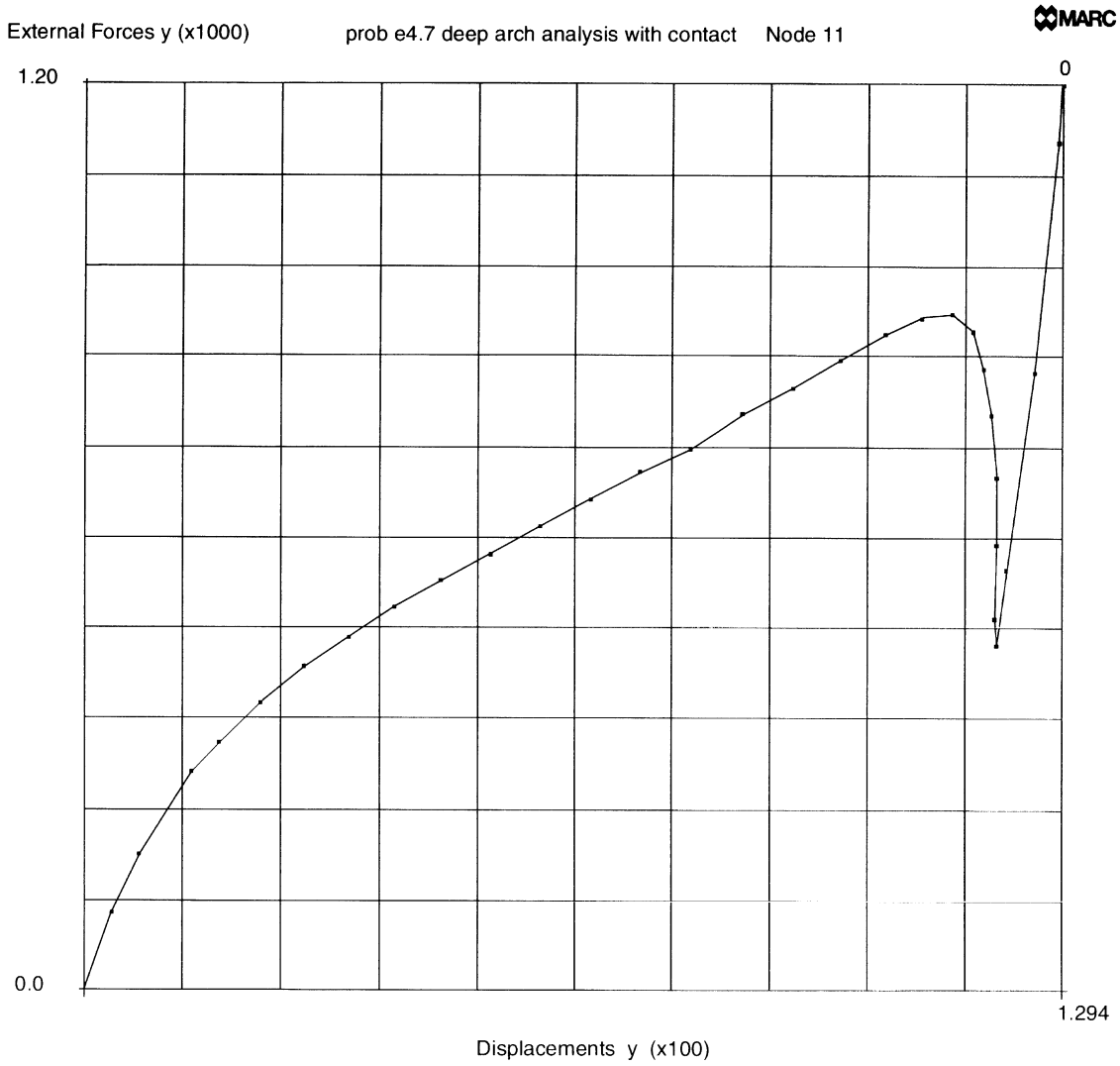

Figure 4.7-8 Load vs. Displacement (Node 77) with Contact at Pin

4.8 Large Displacement Analysis of a Cable Network

A cable network subjected to gravity and wind loads is analyzed using MARC cable element (element type 51). The analysis includes both large displacement and follower force effects.

Element

Element 51 is a 3D, 2-node cable element, defined in space by global coordinates (x,y,z) at two nodal points with three translational DOFs (u,v,w) at each node. The load-displacement relationship of this element is directly, numerically calculated and requires to be acted on by at least one type of distributed load (for example, weight of the cable) for the proper formulation of the stiffness matrix. Detailed discussion on this element can be found in *MARC Volume B: Element Library.*

Model

As shown in Figure 4.8-1, there are 45 cable elements in the mesh. The number of nodes in the mesh is 27 and the total degrees of freedom is 81. The network is assumed to be fully supported at end of the six legs.

Geometry

The first data field, EGEOM1, specifies the cross-sectional area. The second data field, EGEOM2, specifies the cable length. The third data field, EGEOM3, specifies the initial stress. In this example, the second data field is set to zero because the cable length is assumed to be equal to the cable distance. If the EGEOM2 data is entered as 0.0, the program calculates the distance between the two nodes and then automatically takes it as the cable length. Another situation is that we know the initial stress, but not the cable length. In this case, you can use the third data field (EGEOM3) to specify the initial stress and set to zero the second data field (EGEOM2).

Material Properties

The Young's modulus is 1.0×10^2 psi.

Displacement Loads

A gravity load of -1.0 pounds in the y-direction is applied to all elements in the zeroth increment. A zero incremental load is then applied for one increment to reduce the residual load. A wind load of -2.0 pounds in the z-direction is applied for the second, third and fourth increments as incremental load. As a result, a -1.0 pounds gravity load and -6.0 pounds wind load are applied to the cable network as the total distributed loads.

Fixed Displacement

Three degrees of freedom (u = v = w = 0) of six (6) end points (nodes 1, 3, 24, 27, 25, and 4) are fully fixed.

Large Displacement

The LARGE DISP option flags the program control for large displacement analysis. MARC calculates the geometric stiffness matrix and the initial stress stiffness matrix when the LARGE DISP option is flagged.

Follow Force

The FOLLOW FOR option allows MARC to form all distributed loads on the basis of current geometry. This is an important consideration in a large displacement analysis.

PRINT,3,

In the analysis of a cable network, the initial stiffness matrix of the network can possibly be singular for the lack of cable forces in the system. The PRINT,3, option allows for the completion of numerical computations of an initially singular system, and for the continuation of subsequent load increments.

Results

Deformed meshes of the cable network are plotted in Figure 4.8-2 and Figure 4.8-3.

Parameters, Options, and Subroutines Summary

Example e4x8.dat:

Parameters	Model Definition Options	History Definition Options
ELEMENT	CONNECTIVITY	AUTO LOAD
END	CONTROL	CONTINUE
FOLLOW FORCE	COORDINATE	DIST LOADS
LARGE DISP	DIST LOADS	PROPORTIONAL INCREMENT
PRINT	END OPTION	
SIZING	FIXED DISP	
TITLE	GEOMETRY	
	ISOTROPIC	
	POST	

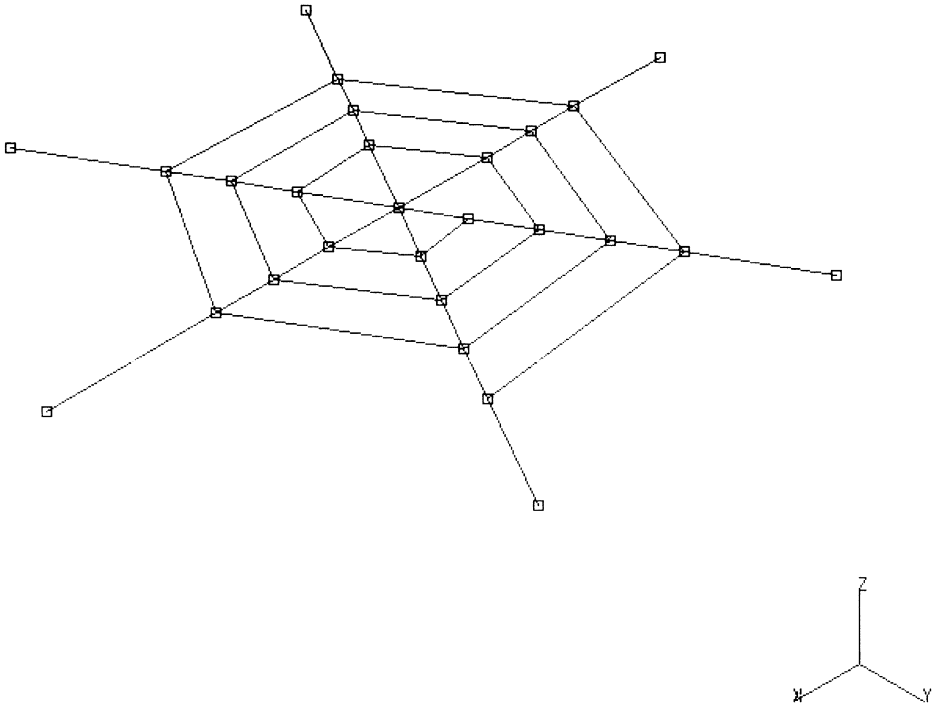

Figure 4.8-1 Cable Network Mesh

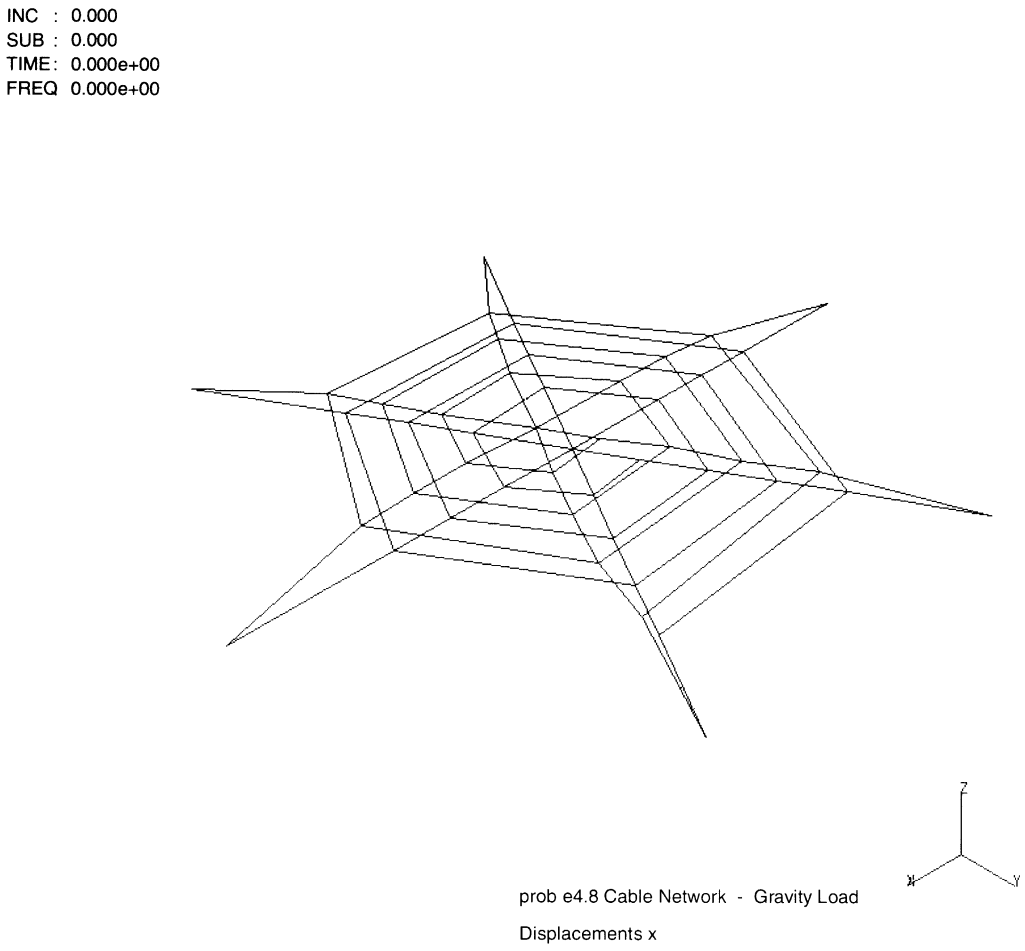

Figure 4.8-2 Cable Network Deformed Mesh (Gravity Load)

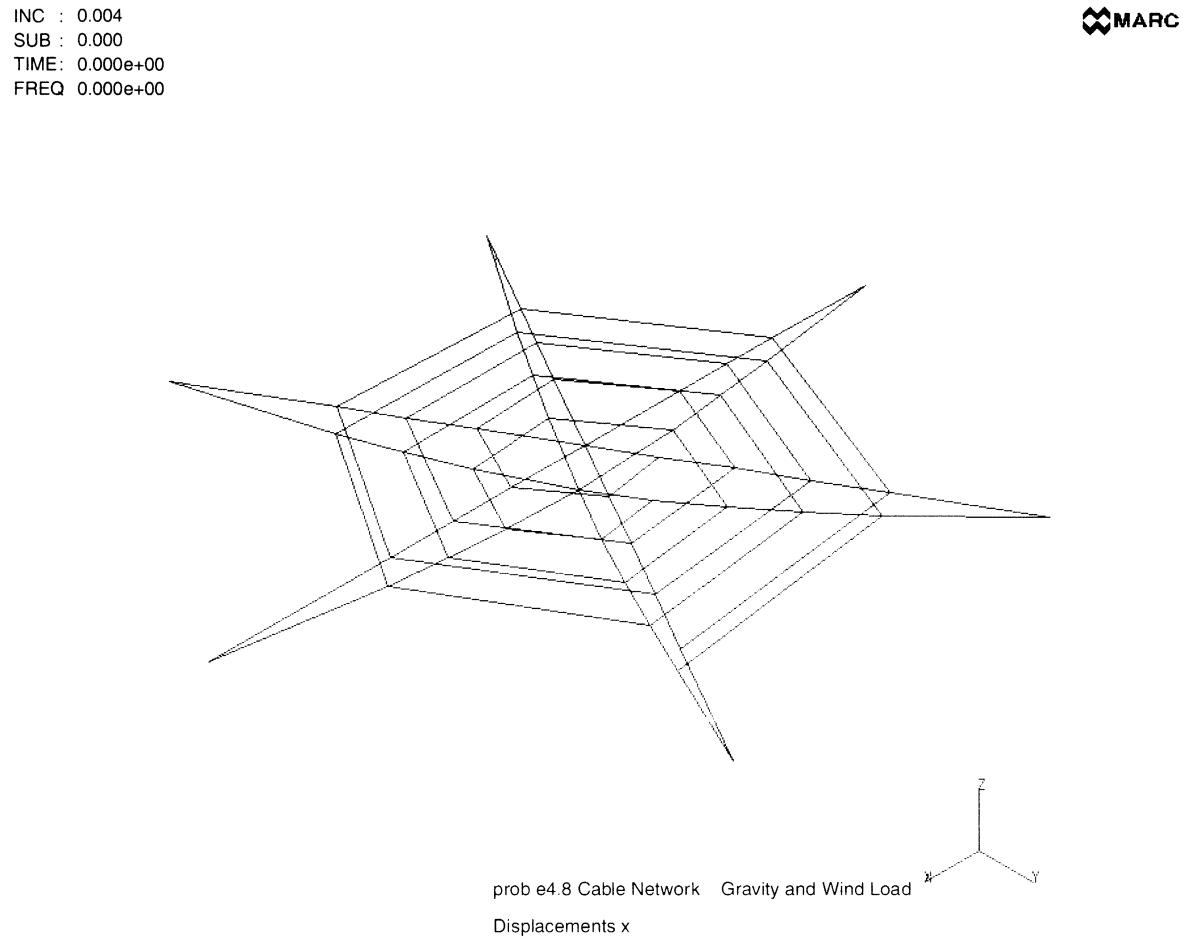

Figure 4.8-3 Cable Network Deformed Mesh (Gravity + Wind Load)

4.9 Nonsymmetric Buckling of a Ring

The buckling load of a radially loaded ring is determined using MARC element 90. It is important to notice that the load is radially directed, not only with respect to the initial geometry, but also with respect to the deformed one. Since MARC uses the stresses following from the linear pre-buckling state, this problem is easily analyzed. On the other hand, if the load would be of fluid-type, the buckling load could be approximated by means of an incremental nonlinear analysis using 3D shell elements, with the parameter blocks FOLLOW FOR and LARGE DISP.

This problem is modeled using the two techniques summarized below.

Data Set	Element Type(s)	Number of Elements	Number of Nodes	Differentiating Features
e4x9	90	1	3	Fourier Buckling Inverse Power Sweep
e4x9b	90	1	3	Fourier Buckling Laczos

Element

Element type 90 is a 3-node thick shell element for the analysis of arbitrary loading of axisymmetric shells. Each node has five degrees of freedom. Although for this problem, the (initial) geometry and the loading are axially symmetric, the buckling mode is not.

Model

The ring with a length of 2.0 inches is modeled using 1 element. This is sufficient since the problem is actually one-dimensional as shown in Figure 4.9-1.

Geometry

The radius and the wall thickness are 10.0 inches and 0.1 inch, respectively.

Material Properties

All elements have the same properties: Young's modulus equals 1.2E7 psi, while Poisson's ratio equals 0.0.

Loading

A uniform pressure (IBODY = 0) of 1.0 is applied to the element.

Boundary Conditions

The boundary conditions for the linear elastic calculation and the buckling analyses are not the same. As for the linear elastic calculation, the axial and circumferential displacement of nodal point 3 are suppressed in order to be sure that no rigid body motions are present. To obtain a homogeneous deformation in axial direction, the rotations in the Z-R plane are also suppressed. As for the buckling analyses, it is essential to release the circumferential displacement of nodal point 3; otherwise, the structure would behave too stiff.

Analysis

After a linear elastic calculation (increment 0), several buckling analyses are performed. The maximum number of iterations, the tolerance and the harmonic number are set equal to 100 and 0.00001, respectively. Since, in general, the harmonic number corresponding to the lowest buckling load is unknown a priori, the harmonic number is chosen to vary from 2 to 7. The meaning of the parameters SHELL SECT,3 and BUCKLE,5,1,0,3 can be explained as follows:

SHELL SECT,3 : 3: use 3 integration points in thickness direction of the elements.

BUCKLE,5,1,0,3,0,0: 5: in a buckling analysis, 5 modes are required;

1: 1 mode must correspond to a positive eigenvalue: once a mode with a positive eigenvalue is found, the program will stop, even if not all 5 previously mentioned modes are found;

0: the eigenvectors are not stored on the post file;

3: a Fourier buckling analysis is performed.

0: Inverse power sweep method

0: In the third analysis, this last parameter is set to 1 to indicate that the Lanczos method is used

The model definition option BUCKLE INCREMENT cannot be used since, in this problem, the buckling analyses are performed using the stress state corresponding to increment 0, but with modified boundary conditions. Using BUCKLE INCREMENT, you can either perform buckling analyses using the stress state corresponding to increment 0 with the boundary conditions of increment 0, or buckling analyses in increment 1 using modified boundary conditions, but also with a modified stress state (since an eigenvalue analysis is always performed using the incremental stresses).

Discussion

The analytical solution for the lowest buckling load is given by (for example, Don O. Bruce and Bo O. Almroth, *Buckling of Bars, Plates and Shells*, McGraw-Hill, 1975):

$$q_{analytical} = \frac{(n^2-1)^2}{(n^2-2)} \cdot \frac{EI}{r^3}, \text{ with } I = \frac{Lh^3}{12}$$

Here n represents the harmonic number. The lowest buckling load corresponds to n = 2. Substituting further E = 1.2e7, L = 2.0, r = 10.0 and h = 0.1.

$$q_{analytical} = 9.000$$

so the critical pressure is:

$$P_{analytical} = \frac{1}{L} q_{analytical} = 4.50$$

The MARC solutions for the buckling load for the various numbers of n are given below (where the corresponding analytical values are also presented):

n	Buckling Load		
	Inverse Power Sweep	Lanczos	Analytical
2	4.498	4.498	4.500
3	9.497	9.497	9.143
4	16.49	16.49	16.07
5	25.49	25.49	25.04
6	36.48	36.48	36.03
7	49.46	49.46	49.02

The MARC solution for the lowest buckling load turns out to be:

$$P_{MARC} = 4.428 \text{ for } n = 2.$$

The difference between this and the analytical solution is about 0.04%.

Parameters, Options, and Subroutines Summary

Example e4x9.dat and e4x9b.dat:

Parameters	Model Definition Options	History Definition Options
BUCKLE	CONNECTIVITY	BUCKLE
ELEMENT	COORDINATES	CONTINUE
END	DIST LOAD	DISP CHANGE
SHELL SECT	FIXED DISP	
SIZING	END OPTION	
TITLE	GEOMETRY	
	ISOTROPIC	
	POST	

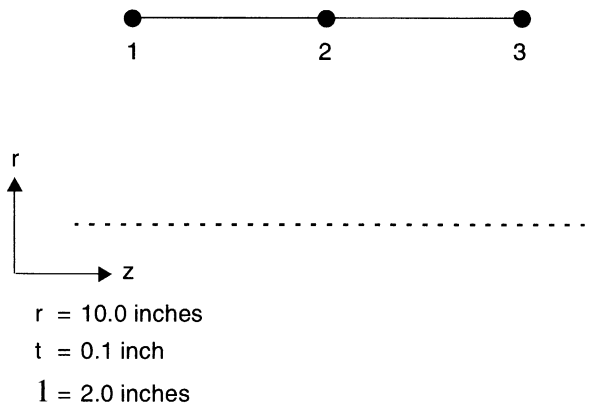

Figure 4.9-1 Mesh

4.10 Nonsymmetric Buckling of a Cylinder

The buckling load of an axially loaded cylinder is determined using MARC element 90.

This problem is modeled using the two techniques summarized below.

Data Set	Element Type(s)	Number of Elements	Number of Nodes	Differentiating Features
e4x10	90	20	41	Inverse power sweep
e4x10b	90	20	41	Lanczos method

Element

Library element 90 is a 3-node thick shell element for the analysis of arbitrary loading of axisymmetric shells. Each node has five degrees of freedom. Although for this problem, the (initial) geometry and the loading are axially symmetric, the buckling mode is not.

Model

The cylinder with a length of 20.0 inches is divided into 20 equally sized elements as shown in Figure 4.10-1.

Geometry

The radius and the wall thickness are 20.0 inches and 0.2 inches, respectively.

Material Properties

All elements have the same properties: Young's modulus equals 10.0E6 psi, while Poisson's ratio equals 0.3.

Loading

A point load of –1.0 pounds is applied to nodal point 41; thus, introducing an axial load.

Boundary Conditions

The boundary conditions for the linear elastic calculation and the buckling analyses will not be the same. This is necessary to make a comparison with the analytical solution possible. As for the linear elastic calculation, the radial displacements at the ends of the cylinder remain free in order to obtain a homogeneous pre-buckling state. The remaining degrees of freedom of node 1 and node 41, with exception of the axial displacement of node 41, are suppressed. In the buckling analyses, the radial displacements at the ends are suppressed as well.

Analysis

After a linear elastic calculation (increment 0), a number buckling analyses are performed. The maximum number of iterations and the tolerance are set equal to 100 and 0.001, respectively. Since, in general, the harmonic number corresponding to the lowest buckling load is unknown a priori, the harmonic number, is chosen to vary from 1 to 15. The meaning of the parameter options SHELL SECT,3 and BUCKLE,5,1,0,3 can be explained as follows:

SHELL SECT,3 : 3: use 3 integration points in thickness direction of the elements.

BUCKLE,5,1,0,3,0,0: 5: in a buckling analysis, 5 modes are required;

1: 1 mode must correspond to a positive eigenvalue: once a mode with a positive eigenvalue is found, the program will stop, even if not all 5 previously mentioned modes are found;

0: the eigenvectors are not stored on the post file;

3: a Fourier buckling analysis is performed.

0: Inverse power sweep method

For data set 4x10b, this last parameter is set to 1 to indicate that the Lanczos method is used

The model definition option BUCKLE INCREMENT cannot be used since, in this problem, the buckling analyses are performed using the stress state corresponding to increment 0, but with modified boundary conditions. Using BUCKLE INCREMENT, one can either perform buckling analyses using the stress state corresponding to increment 0 with the boundary conditions of increment 0, or buckling analyses in increment 1 using modified boundary conditions, but also with a modified stress state (since an eigenvalue analysis is always performed using the incremental stresses).

Discussion

For this problem, no closed form analytical solution for the lowest buckling load is available. The solution has to be deduced from (e.g, Don O Bruce and Bo O. Almroth, *Buckling of Bars, Plates and Shells*, McGraw-Hill, 1975):

$$F(anal)/(2*\pi*r) = \{mb*mb+n*n)*(mb*mb+n*n)/(mb*mb)\}*\{D/(r*r)\}+ \{(mb*mb)/\{(mb*mb+n*n)*mb*mb+n*n)]\}*(1-\nu*\nu)*C,$$

with $C = E*h/(1-\nu*\nu)$ and $D = E*h*h*h/\{12*(1-\nu*\nu)\}$

By means of a simple program, the minimum value of F(anal), depending on mb and n, can easily be determined. With E = 10.0E6, ν = 0.3, L = 20.0, r = 20.0 and h = 0.2, one finds:

F(anal) = 1.521E6, corresponding to n = 9 and m = 3, where m is given by $m = mb*L/(\pi*r)$.

The MARC solution for the lowest buckling load for the various numbers of n are given below:

n	Buckling Load (MARC)
1	1.607E6
2	1.605E6
3	1.602E6
4	1.595E6
5	1.586E6
6	1.573E6
7	1.573E6
8	1.522E6
9	1.532E6
10	1.547E6
11	1.666E6
12	1.806E6
13	1.968E6
14	2.176E6
15	2.396E6

The MARC solution for the lowest buckling load turns out to be:

F(MARC) = 1.522E6, for n = 8.

The difference between this and the analytical solution is about 0.07%. The corresponding harmonic numbers n are not the same. However, it can easily be verified that the difference between the solutions for n = 8 and n = 9 is small. The difference between the MARC solution for n = 9 and the analytical solution is about 0.7%.

Parameters, Options, and Subroutines Summary

Example e4x10.dat:

Parameters	Model Definition Options	History Definition Options
BUCKLE	CONNECTIVITY	BUCKLE
ELEMENTS	COORDINATES	CONTINUE
END	END OPTION	DISP CHANGE
SHELL SECT	FIXED DISP	
SIZING	GEOMETRY	
TITLE	ISOTROPIC	
	POINT LOADS	
	POST	

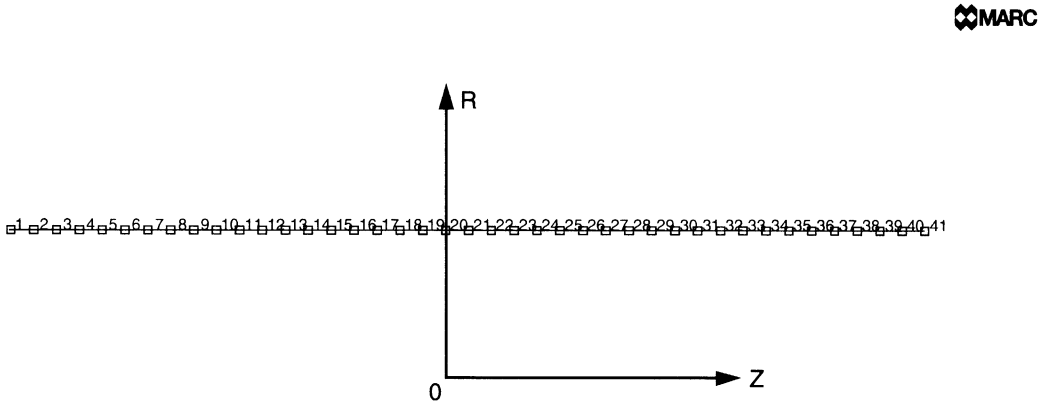

r = 20.0 inches
t = 0.2 inch
L = 20.0 inches

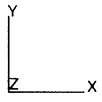

Figure 4.10-1 Mesh

4.11 Geometrically Nonlinear Analysis of a Tapered Plate

A tapered plate is clamped at one edge and loaded by a bending moment at the opposite edge (see Figure 4.11-1). By means of this problems, the capability of a finite element to represent inextensional bending in the geometrically nonlinear regime can be investigated.

Element

Library element type 4 is a 6-node triangular thin shell element. This element allows finite rotational increments so that large load steps can be chosen.

Model

The dimensions of the plate and the finite element mesh are shown in Figure 4.11-1. Based on symmetry considerations, only one-half of the plate is modeled. The mesh is composed of 80 elements and 243 nodes.

Geometry

A uniform thickness of 0.5 mm is assumed. In thickness direction, three layers are chosen using the SHELL SECT parameter. Although initially the mesh consists of flat elements, the coupling between the changes of curvature and the membrane deformations becomes important during the loading process. This means that the default setting for the fifth geometry field must be used.

Material Properties

The material is elastic with a Young's modulus of 2.1×10^5 N/mm^2 and a Poisson's ratio of 0.0.

Loading

The loading consists of a bending moment at the edge opposite to the clamped edge. The magnitude of this bending moment is written as f * 365.284 Nmm, where the maximum value of the scalar multiplier f equals 1.5. The total load is applied in 15 equally sized increments.

Boundary Conditions

Symmetry conditions are imposed on the edge y = 0 ($u_y = 0$, $\varphi = 0$). Clamped conditions are applied to the edge x = 0 ($u_x = 0$, $u_y = 0$, and $\varphi = 0$). Notice that the rotation constraints only apply for the midside nodes.

Results

The final deformed configuration is outlines in Figure 4.11-5. Since this state is reached in 15 equally sized increments, a finite rotation formulation is necessary. The horizontal and vertical tip displacements as a function of the load factor f (notice that this factor corresponds to the time) are given in Figure 4.11-3. An analytical solution for this problem can be found in Y. Ding, *Finite-Rotations-Elements zur geometrisch nichtlinearen Analyse algemeiner*

Flachentragwerke, Thesis Insititut für Statik und Dynamik, Ruhr-Univ Rochum, Germany (1989). The analytical solution for the above mentioned displacements components is given in Figure 4.11-4 and Figure 4.11-5. The finite element and the analytical solutions are in good agreement.

Parameters, Options, and Subroutines Summary

Example e4x11.dat:

Parameters	Model Definition Options	History Definition Options
ALL POINTS	CONNECTIVITY	ACTIVATE
DIST LOADS	COORDINATE	AUTO LOAD
ELEMENTS	DEFINE	CONTINUE
END	END OPTION	DISP CHANGE
LARGE DISP	FIXED DISP	POINT LOAD
SETNAME	GEOMETRY	TIME STEP
SHELL SECT	ISOTROPIC	
SIZING	NO PRINT	
TITLE	OPTIMIZE	
	POST	
	SOLVER	

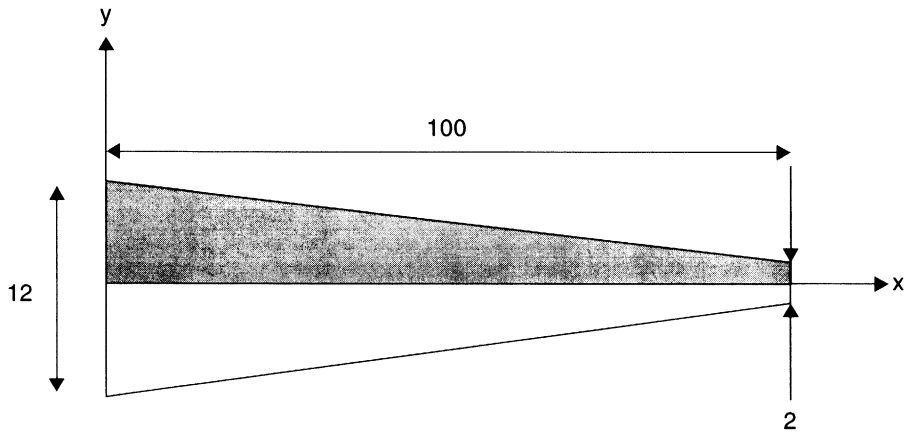

MARC

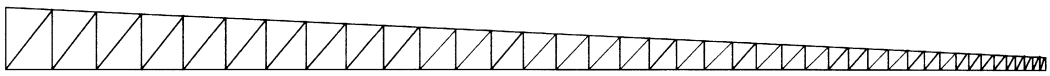

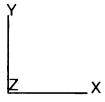

Figure 4.11-1 Clamped Tapered Plate, Geometry, and Finite Element Mesh

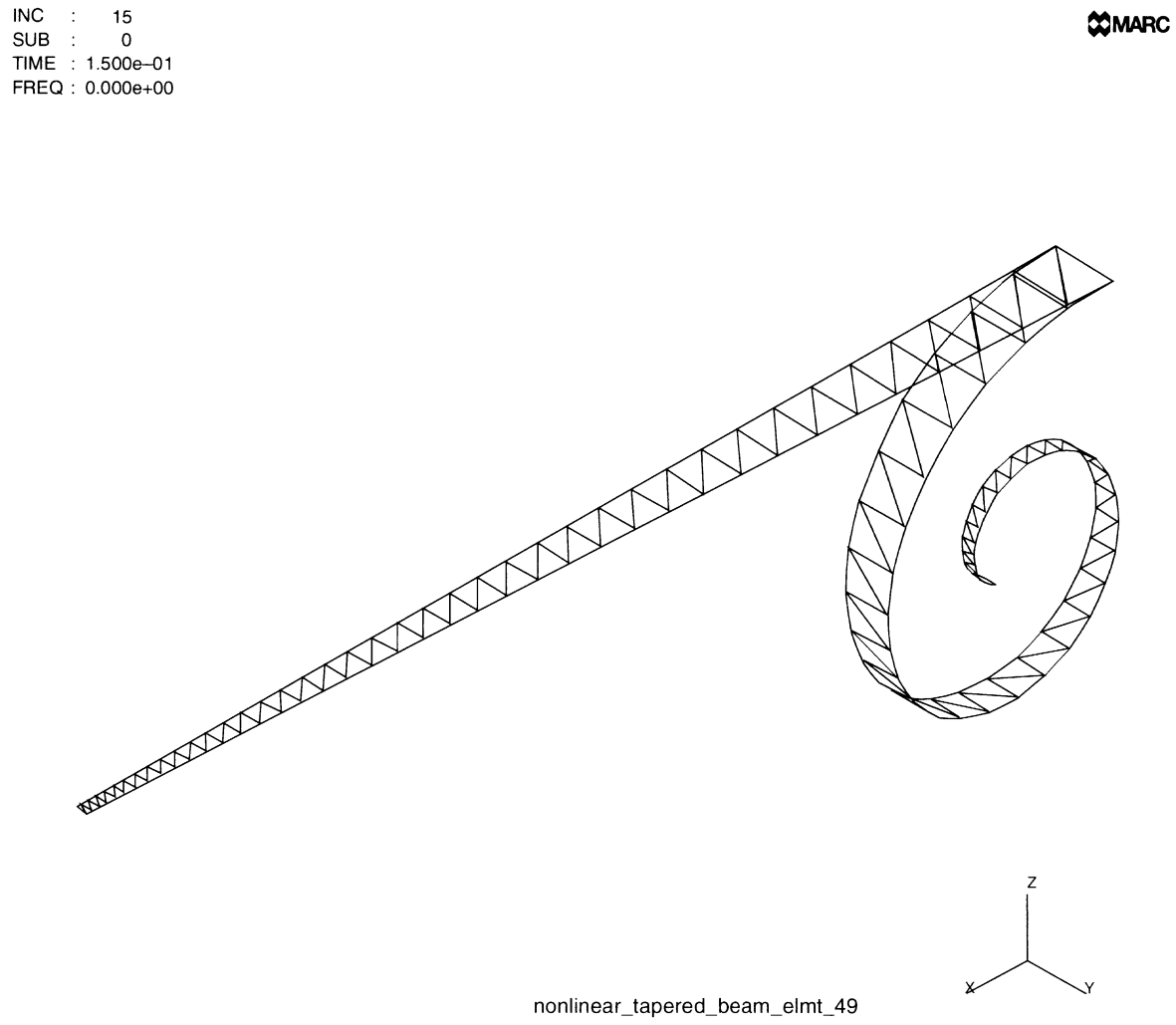

Figure 4.11-2 Undeformed and Final Deformed Configuration

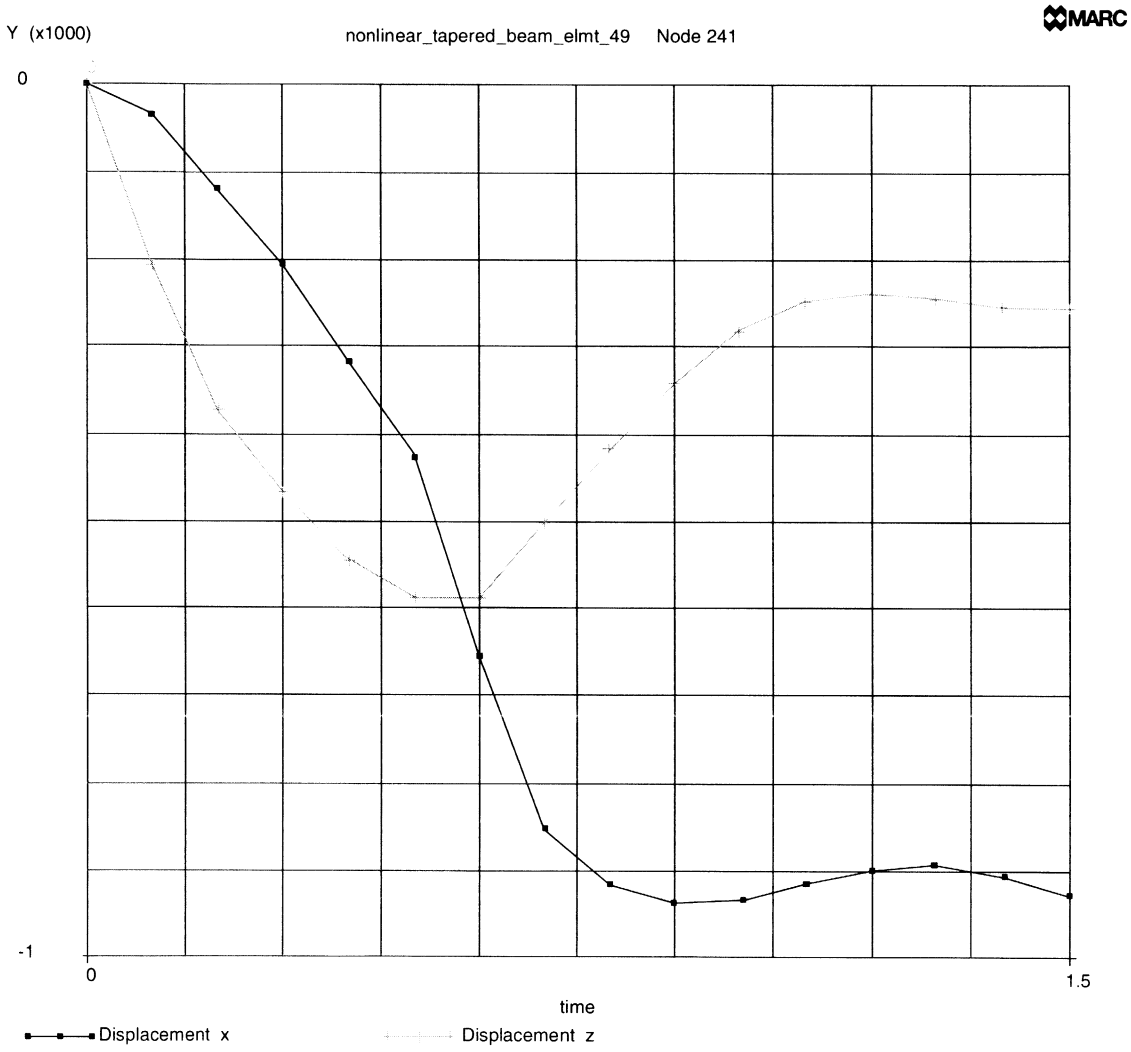

Figure 4.11-3 Finite Element Solution Horizontal and Vertical Tip Displacement

Figure 4.11-4 Reference Solution Tip Deflection

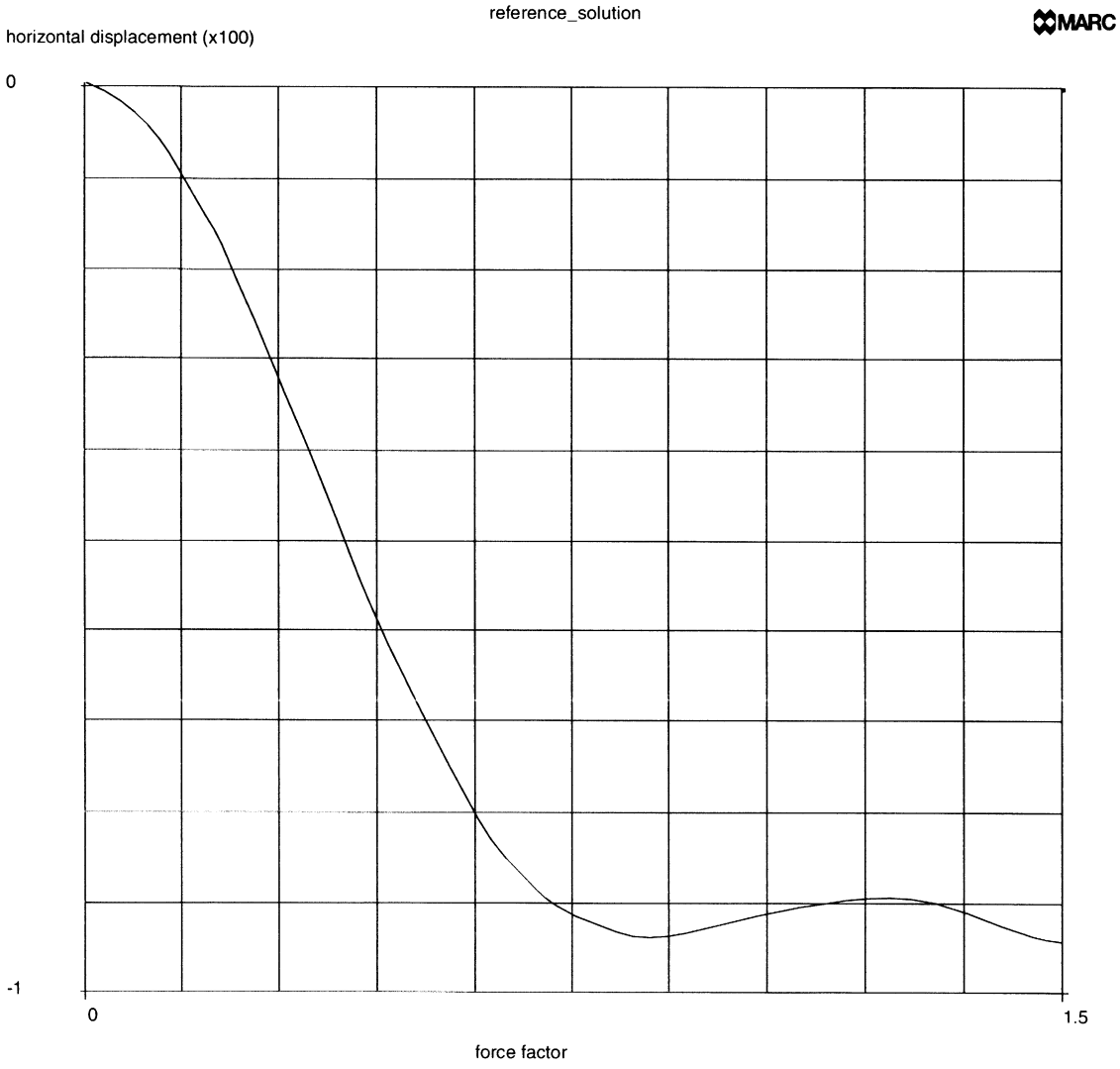

Figure 4.11-5 Reference Solution Horizontal Tip Displacement

4.12 Perturbation Buckling of a Strut

An elastic post buckling analysis is conducted on an initially straight strut. The perturbation buckling technique is demonstrated.

This problem is modeled using the four techniques summarized below.

Data Set	Element Type(s)	Number of Elements	Number of Nodes	Differentiating Features
e4x12a	3	20	42	Peturb to First Mode
e4x12b	3	20	42	Peturb to Second Mode
e4x12c	3	20	42	Buckle Increment
e4x12d	3	20	42	Full Automatic Perturbation

Model/Element

The model consists of 20 plane stress element, type 3, as shown in Figure 4.12-1. The length is 2.0 meters and the width is 0.1.

The LARGE DISP parameter is used to indicate that the total Lagrange large displacement formulation is used. The BUCKLE option indicates how many buckling modes are to be extracted.

Material Properties

The material has a Young's modulus of 1×10^9 N/m^2 and the Poisson's ratio is 0.3.

Geometry

The strut has a uniform thickness of 1 cm.

Boundary Conditions

The bottom of the strut is clamped, and, at the top, no motion is allowed in the x-direction.

Loading

This analysis is performed using four different procedures:

In the first analysis, a load is applied of magnitude 6000 (3000 at nodes 1 and 4) in increment 1, followed by 200. A buckle eigenmode is extracted and then a perturbation is applied, and then a load of 1800 is applied over nine increments. The first perturbation buckling mode is selected through the BUCKLE history definition option.

In the second analysis, a load is applied of magnitude 10,000 in increment 1, followed by 200. A buckle eigenmode is extracted and then a perturbation is applied, and then a load of

9000 is applied over nine increments. The second perturbation buckling mode is selected through the BUCKLE history definition option.

In the third analysis, a load is applied of magnitude 6000, followed by a load of 2000 over ten increments. Hence, the total load is the same as in the first analysis. In this analysis, the BUCKLE INCREMENT mode definition option is used to add the first buckle perturbation mode at the end of increment 2.

The fourth analysis is identical to the third analysis, except that the increment at which the perturbation is applied is automatically determined by the program. The perturbation is applied in the increment after the increment where a nonpositive definite system occurs.

In all problems, the perturbation has a scaled magnitude of 0.001.

Control

The CONTROL option is used to specify that displacement testing is to be performed with a tolerance of one percent. The solution of nonpositive definite systems is forced.

Results

The linear collapse load of this strut is 6050 N. Figure 4.12-2 shows the resultant deformation from the first analysis when the first mode is used. Figure 4.12-3 shows the resultant deformation from the second analysis when the second mode is used. The results of the third analysis are identical to the first analysis. When the fully automatic perturbation procedure is used in the fourth analysis, MARC senses the nonpositive definite system in increment 2, and then automatically extracts the buckle mode. This gives the same results as before. Note that after the perturbation is applied and there is some lateral deflection, you again have a stable physical system and no longer have a nonpositive definite numerical problem.

Parameters, Options, and Subroutines Summary

Examples e4x12a.dat and e4x12b.dat:

Parameters	Model Definition Options	History Definition Options
BUCKLE	CONTROL	AUTO LOAD
ELEMENTS	CONNECTIVITY	BUCKLE
END	COORDINATES	CONTINUE
LARGE DISP	DEFINE	POINT LOAD
SIZING	END OPTION	
	FIXED DISP	
	GEOMETRY	
	ISOTROPIC	
	OPTIMIZE	
	POINT LOAD	
	POST	
	SOLVER	

Examples e4x12c.dat and e4x11d.dat:

Parameters	Model Definition Options	History Definition Options
BUCKLE	BUCKLE INCREMENT	AUTO LOAD
ELEMENTS	CONTROL	CONTINUE
END	CONNECTIVITY	POINT LOAD
LARGE DISP	COORDINATES	
SIZING	DEFINE	
	END OPTION	
	FIXED DISP	
	GEOMETRY	
	ISOTROPIC	
	OPTIMIZE	
	POINT LOAD	
	POST	
	SOLVER	

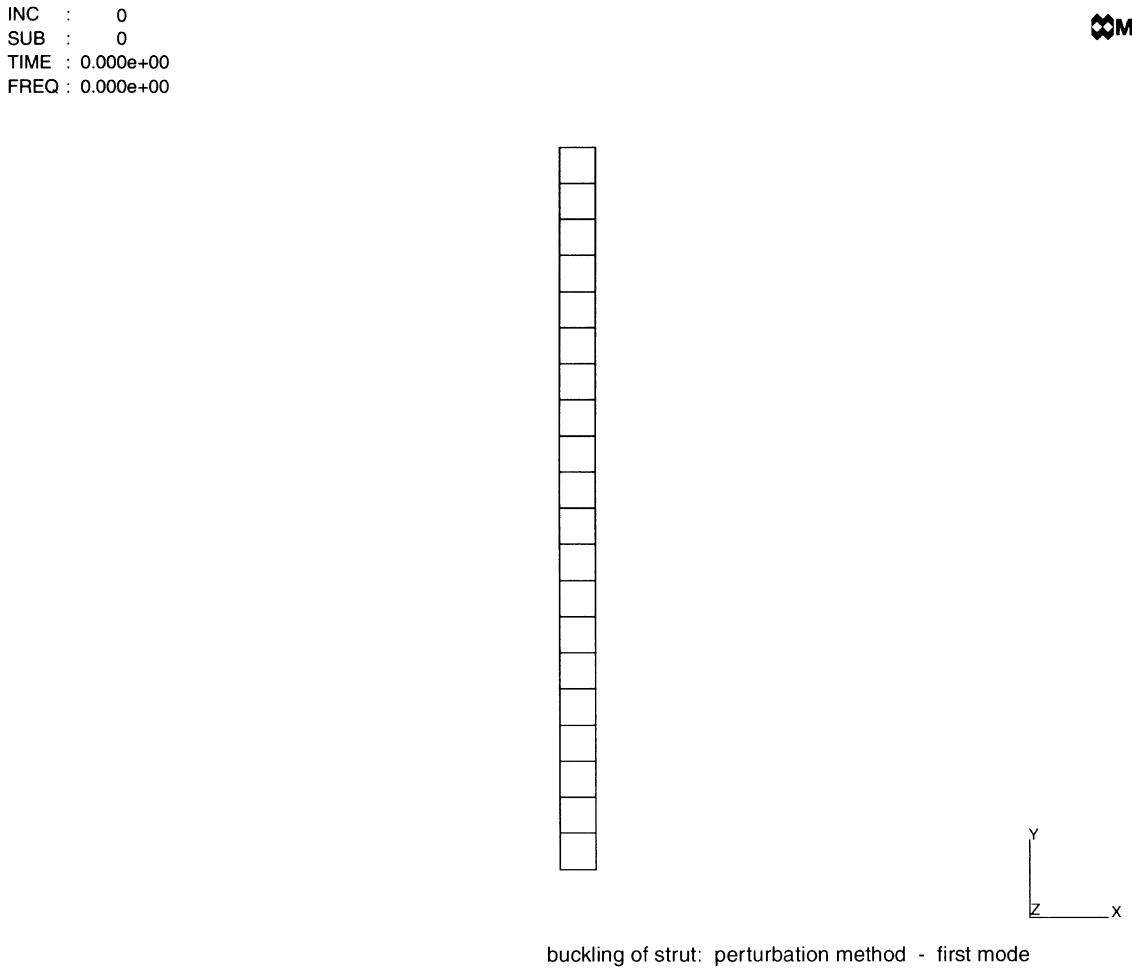

Figure 4.12-1 Mesh of Strut

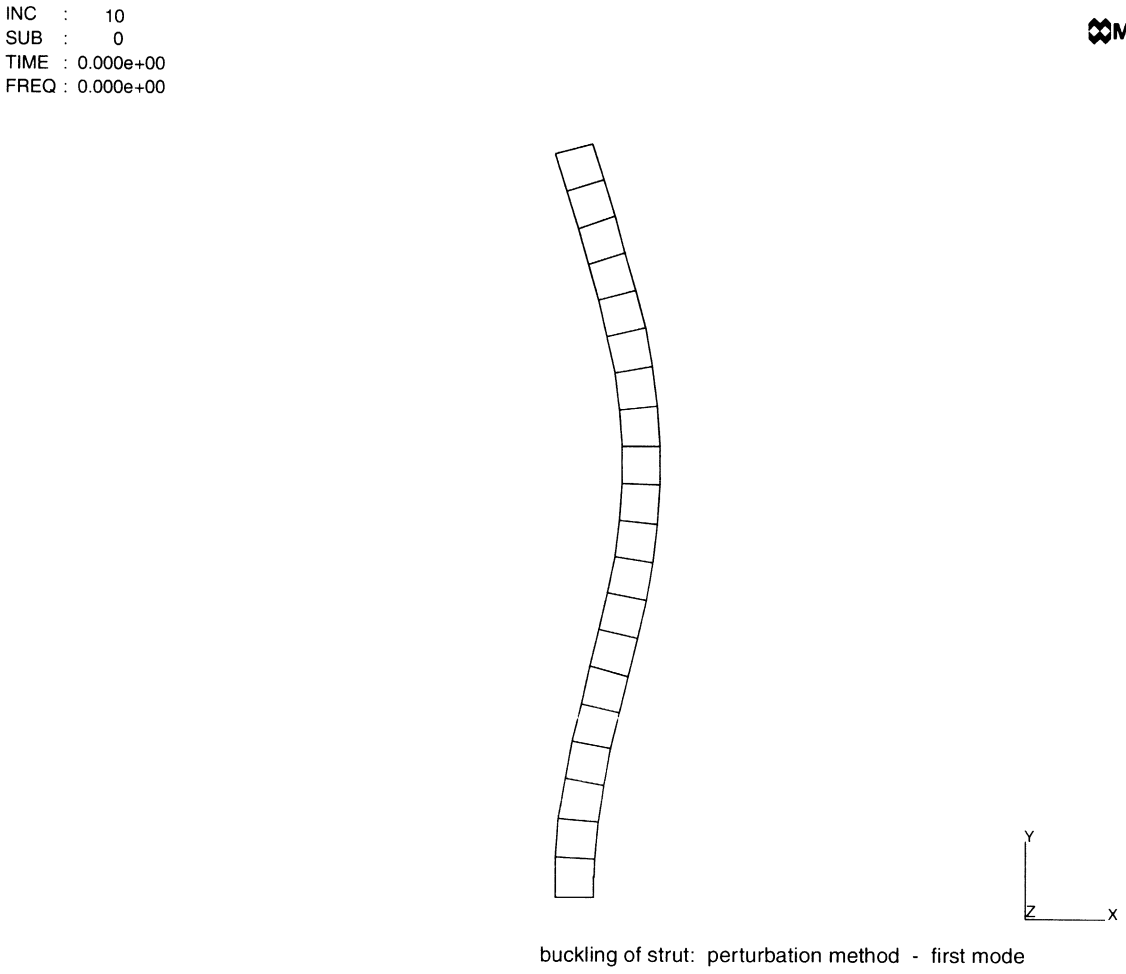

Figure 4.12-2 Displacements Using First Mode

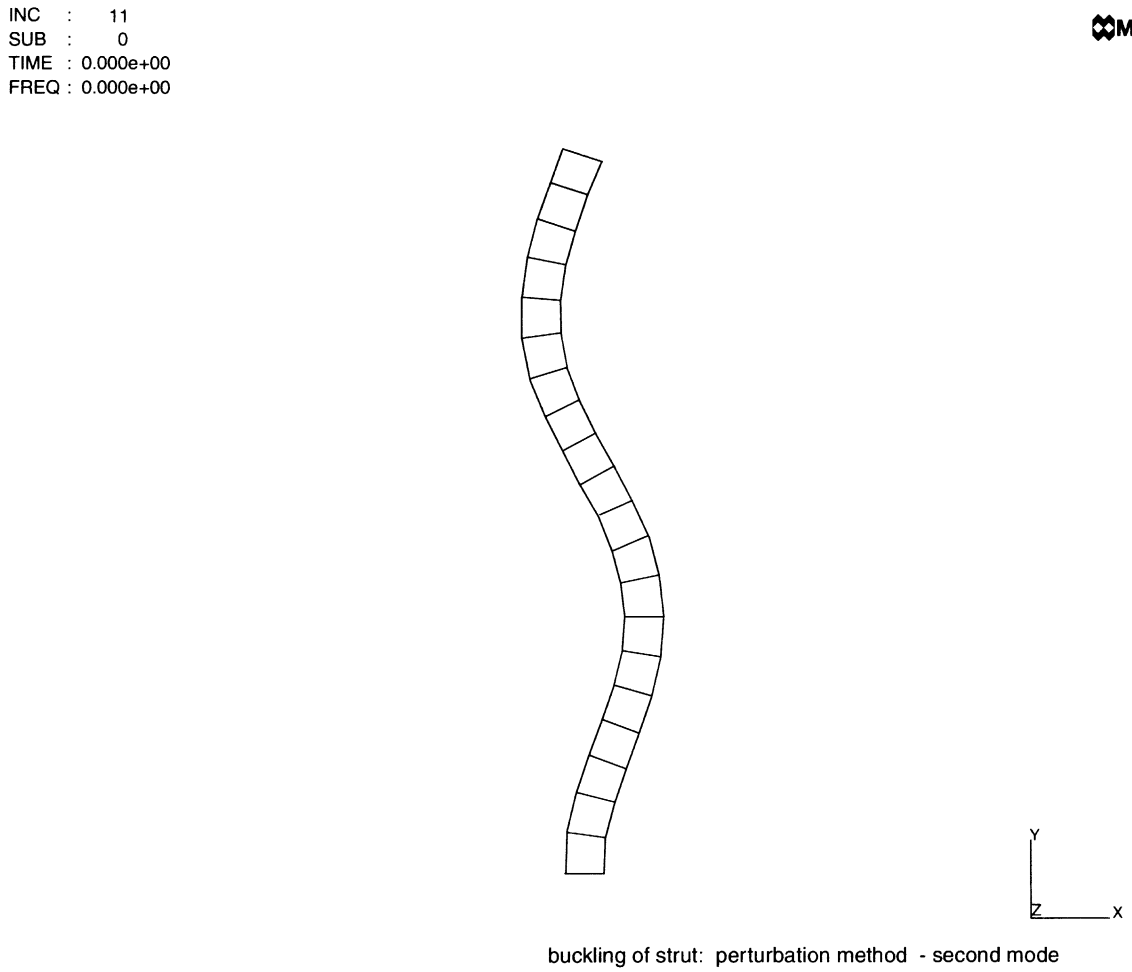

Figure 4.12-3 Displacements Using Second Mode

4.13 Cord-reinforced Thin-wall Cylinder subjected to Inner Pressure using Axisymmetric Elements

As shown in Figure 4.13-1, a thin-wall cylinder, reinforced by two cord layers is subjected to inner pressure. This problem demonstrates the application of axisymmetric rebar elements to cord-reinforced composites at large strains.

This problem is modeled using the three techniques summarized below.

Data Set	Element Type(s)	Number of Elements	Number of Nodes	Differentiating Features
e4x13a	67 & 142	2	8	REBAR
e4x13b	10 & 144	2	4	REBAR
e4x13c	20 & 145	2	4	REBAR

Element

Either element types 67 and 142 (8-node axisymmetric with twist), or element types 10 and 144 (4-node axisymmetric), or element types 20 and 145 (4-node axisymmetric with twist) are used. Elements 142, 144, and 145 are specifically designed to simulate reinforcements in axisymmetric problems. Elements 10, 20, and 67 are used to represent the matrix material in the cord-reinforced composite structure.

Model

The cylinder is modeled by one rebar element and one continuum element as shown in Figure 4.13-2.

Geometry

The radius of the cylinder is 10 inches and the thickness is 0.1 inch.

Material Properties

The Young's modulus is 1500 psi and the Poisson's ratio is 0.3 for the reinforcements. The Young's modulus is 1.5 psi and the Poisson's ratio is 0.3 for the matrix material.

Loading

A uniform distributed inner pressure is applied whose total magnitude is 6.0 psi.

Boundary Conditions

The top and the bottom and fixed in the axial direction.

Rebar Data

The cross-sectional area of each rebar is 0.08 inch^2. The spacing is 1 inch. Therefore, the equivalent thickness is 0.08 inch. The relative position of rebar layer is 0.5. The angle between the axial axis and rebar is ±30. The data is read in via the REBAR option.

Results

The evolution of the radius and the second Piola-Kirchhoff stress due to the inner pressure are given in Figure 4.13-3 and Figure 4.13-4. The agreement between the numerical results and analytical solutions is close. The analytical solution can be derived as:

$$r = r_0\sqrt{1 + \frac{pr_0}{Et_0 Sin^4\alpha_0}}$$

$$S_R = \frac{pr_0}{2t_0 Sin^2\alpha_0}$$

where

r_0 : original cylinder radius

p : pressure

E : Young's modulus

t_0 : ply thickness

α_0 : original rebar angle

S_R : 2nd Piola-Kirchhoff stress

Parameters, Options, and Subroutines Summary

Example e4x13a.dat:

Parameters	Model Definition Options	History Definition Options
ELEMENTS	CONNECTIVITY	AUTO LOAD
END	CONTROL	CONTINUE
FOLLOW FOR	COORDINATES	DIST LOADS
LARGE DISP	DIST LOADS	
SIZING	END OPTION	
TITLE	ISOTROPIC	
	FIXED DISP	
	POST	
	REBAR	

Example e4x13b.dat:

Parameters	Model Definition Options	History Definition Options
ELEMENTS	CONNECTIVITY	AUTO LOAD
END	CONTROL	CONTINUE
FOLLOW FOR	COORDINATES	DIST LOADS
LARGE DISP	DIST LOADS	
SIZING	END OPTION	
TITLE	ISOTROPIC	
	FIXED DISP	
	POST	
	REBAR	

Example e4x13c.dat:

Parameters	Model Definition Options	History Definition Options
ELEMENTS	CONNECTIVITY	AUTO LOAD
END	CONTROL	CONTINUE
FOLLOW FOR	COORDINATES	DIST LOADS
LARGE DISP	DIST LOADS	
SIZING	END OPTION	
TITLE	ISOTROPIC	
	FIXED DISP	
	POST	
	REBAR	

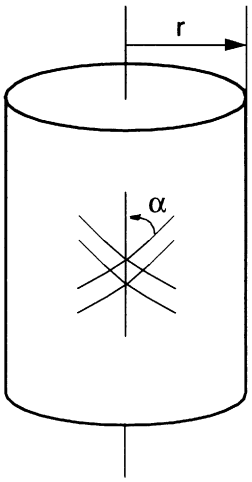

Figure 4.13-1 Cord-reinforced Thin-wall Cylinder subjected to Inner Pressure

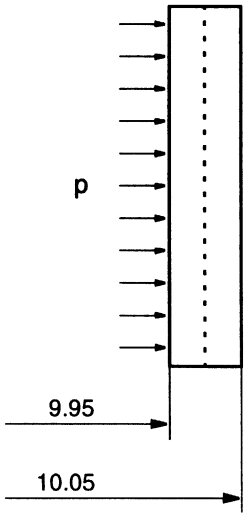

Figure 4.13-2 Finite Element Mesh for Analysis of Cord-reinforced Thin-wall Cylinder subjected to Inner Pressure using Axisymmetric Elements

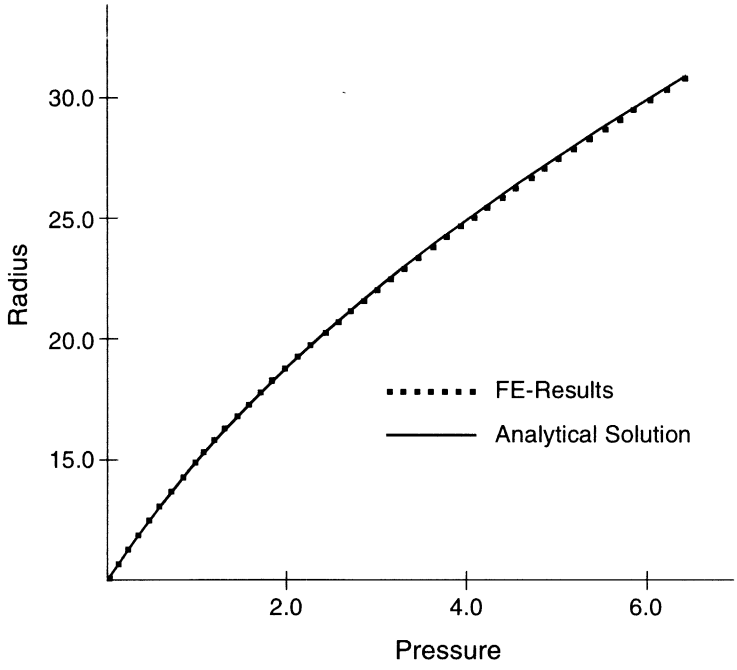

Figure 4.13-3 Radius of the Cylinder subjected to Inner Pressure: Comparison of Numerical Results and Analytical Solutions

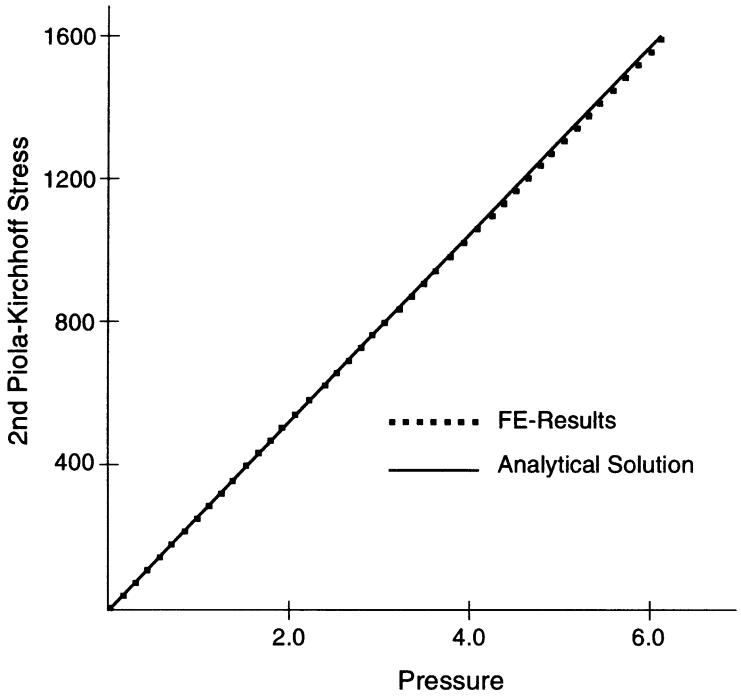

Figure 4.13-4 Second Piola-Kirchhoff Stress of the Cords in the Cylinder subjected to Inner Pressure: Comparison of Numerical Results and Analytical Solutions

4.14 Cord-reinforced Thin-wall Cylinder subjected to Inner Pressure using Membrane Elements

This example is similar to problem 4.13. As shown in Figure 4.13-1, a thin-wall cylinder, reinforced by two cord layers is subjected to inner pressure. The MOONEY option is used in this problem to model the matrix material. This problem demonstrates the application of membrane rebar elements to cord-reinforced rubber composites at large strains.

This problem is modeled using the two techniques summarized below.

Data Set	Element Type(s)	Number of Elements	Number of Nodes	Differentiating Features
e4x14a	18 & 147	20	22	REBAR and MOONEY
e4x14b	30 & 148	20	53	REBAR and MOONEY

Element

Either element types 18 and 147 (4-node membrane elements), or element types 30 and 148 (4-node membrane elements) are used. Elements 147 and 148 are specifically designed to simulate reinforcements in membrane problems. Elements 18 and 30 are used to represent the rubber matrix material in the cord-reinforced rubber composite structure.

Model

The cylinder is modeled by ten rebar elements and ten membrane elements as shown in Figure 4.14-1.

Geometry

For the membrane elements, EGEOM1 is used to input the thickness of the elements. The thickness in this analysis is 1 inch.

Material Properties

The Young's modulus is 1500 psi and the Poisson's ratio is 0.3 for the reinforcements. The Mooney parameters for the rubber matrix material are 1.0 psi and 0.5 psi.

Loading

A uniform distributed inner pressure is applied.

Boundary Conditions

The displacements of all nodes are restricted to radial direction.

Transformation

The user subroutine UTRANS is used to define transformation matrices for all nodes so that the boundary conditions can be easily specified. A model definition block, UTRANFORM, is needed for input of the node numbers to be transformed.

Rebar Data

The cross-sectional area of each rebar is 0.08 inch^2. The spacing is 1 inch. Therefore, the equivalent thickness is 0.08. The angle between the axial axis and rebar is ±30. The data is read in via the REBAR option.

Results

Since the boundary conditions are such that an axisymmetric problem is solved, the results are identical to those in problem 4.13. The evolution of the radius and the second Piola-Kirchhoff stress due to the inner pressure are given in Figure 4.13-3 and Figure 4.13-4. The agreement between the numerical results and analytical solutions is good.

Parameters, Options, and Subroutines Summary

Example e4x14a.dat and e4x14b.dat:

Parameters	Model Definition Options	History Definition Options
ELEMENTS	CONNECTIVITY	AUTO LOAD
END	CONTROL	CONTINUE
FOLLOW FOR	COORDINATES	DIST LOADS
LARGE DISP	DIST LOADS	
SIZING	END OPTION	
TITLE	ISOTROPIC	
	FIXED DISP	
	POST	
	REBAR	

User subroutine in u4x14.f

UTRANS

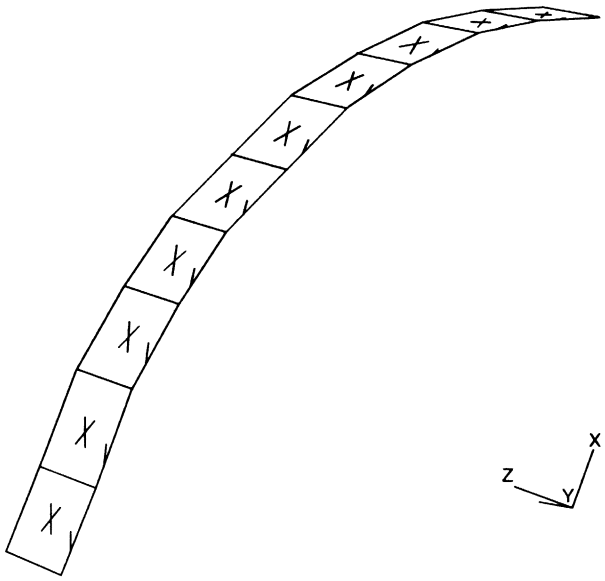

Figure 4.14-1 Finite Element Mesh for Analysis of Cord-reinforced Thin-wall Cylinder subjected to Inner Pressure using Membrane Elements

4.15 Buckling of a Cylinder Tube

The buckling load of a cylinder tube subjected to a lateral load at one end of the tube is calculated using Lanczos procedure. The problem is modeled using element type 75.

Element

Element type 75 is a 4-node bilinear thick shell element with global displacements and rotations as degrees of freedom.

Model

The cylinder tube is modeled using 432 elements and 468 nodes. The finite element meshes shown in Figure 4.15-1. To simulate the lateral load, two additional nodes (469 and 470) are introduced. The two nodes are tied with the nodes on the low end of the cylinder tube using rigid links.

Geometry

The radius and the wall thickness of the cylinder tube are 1 mm and 100 mm, respectively. The length of the tube is 600 mm.

Material Properties

All elements have the same properties. Young's modulus is 3.63E3 N/mm^2. Poisson's ratio is 0.3.

Loading

A point load of 100 N is applied to node 449.

Boundary Conditions

The nodes on the high end of the tube are fixed. The nodes on the low end of the tube are tied with nodes 469 and 470 using rigid links forming a rigid circle.

Results

The MARC solution for the buckling load is given below:

Mode Number	Buckling Load (N)
1	1.786E+01
2	-1.786E+01
3	1.787+01
4	-1.787E+01
5	1.855E+01
6	-1.855E+01

Parameters, Options, and Subroutines Summary

Example e4x15.dat:

Parameters	Model Definition Options	History Definition Options
ALL POINTS	CONNECTIVITY	BUCKLE
BUCKLE	CONTROL	CONTINUE
ELEMENTS	COORDINATES	RECOVER
END	END OPTION	
SETNAME	FIXED DISP	
SIZING	GEOMETRY	
TITLE	ISOTROPIC	
	OPTIMIZE	
	PRINT CHOICE	
	POST	
	POINT LOAD	
	SOLVER	
	TYING	

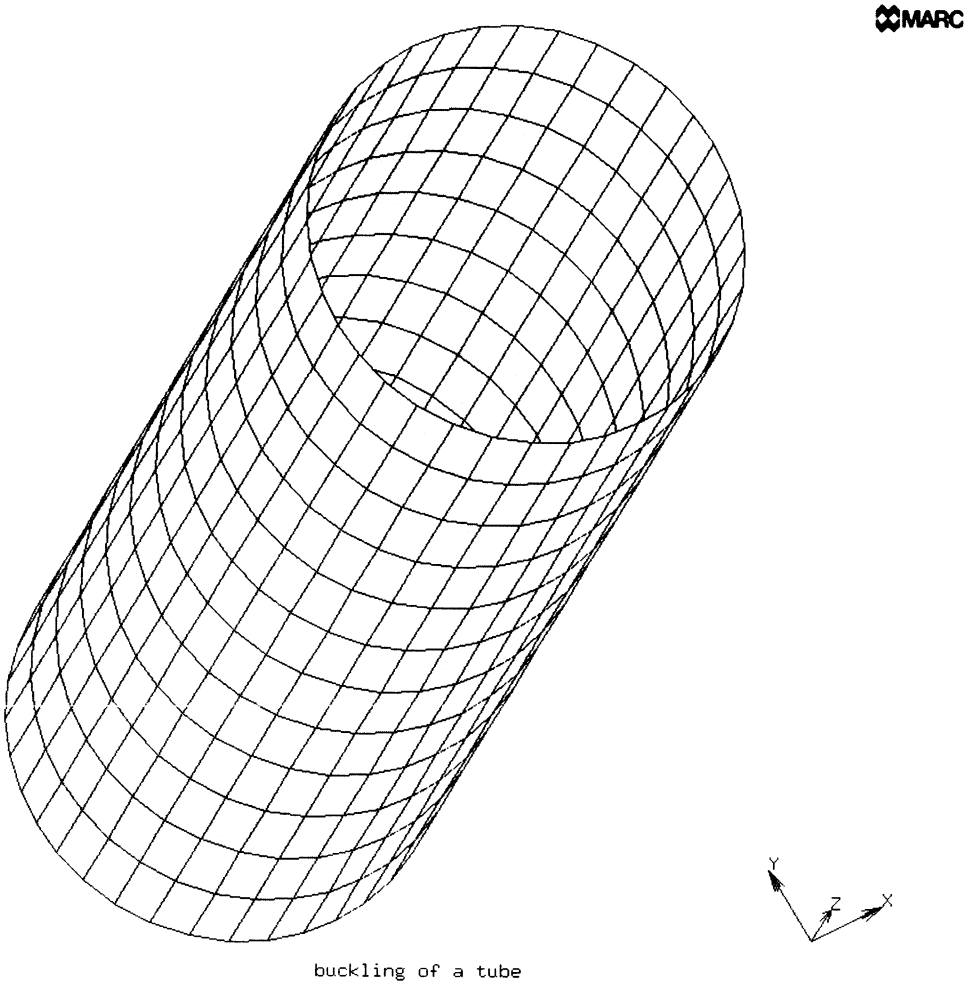

Figure 4.15-1 Finite Element Mesh